Flowering Phenology of Selected Grass Species in Connection with Grass Pollen Dynamics

Carl Alexander Frisk

A thesis submitted in partial fulfilment of the University's requirements for the Degree of Doctor of Philosophy

2021

University of Worcester

Declaration

I hereby declare that the work presented in this thesis has been carried out by myself and does not incorporate any material previously submitted for another degree in any university.

To the best of my knowledge and belief, it does not contain any material previously written or published by another person, except where due reference is made in the text.

I am willing to make the thesis available for photocopy and loan, if it is accepted for the award of the degree.

/ Carl Alexander Frisk /

Abstract

Most of the environments on Earth are occupied by life. The atmospheric environment might seem void of life but it is occupied by many bioaerosols such as bacteria, viruses, plant pollen, fungal spores, arthropods and more. Many of these bioaerosols have negative health impacts on human societies through the allergenicity of the components of their cells.

Perhaps the most allergenic group of bioaerosols are grass pollen. They have been linked with major loss of productivity and quality of life for the grass pollen allergy sufferers. Grass pollen originate from flowering grasses, with differential contribution depending on plant abundance, species biodiversity, pollen production and other biological and environmental factors. Sources and sinks of grass pollen have been identified and quantified, but the connections between sources and sinks are uncertain. The details behind these connections are found in the mechanisms of plant phenology, pollen release and pollen deposition.

To investigate these connections a multidisciplinary research ethos from botany, ecology, environmental and atmospheric sciences, laboratory-based molecular biology, and statistical mathematics was utilized to gain a comprehensive and multispectral view of grass flowering and grass pollen dynamics. Pollen monitoring, atmospheric modelling, flowering phenology, eDNA and metabarcoding were all combined to investigate these connections.

Grass vegetation source areas within the larger Midlands area were important in contributing grass pollen to the Worcester sampling sites. Areas further than 30 km did not contribute significant amount of pollen. Spatially homogeneous stochastic and demographic elements were isolated from detailed observations of eight populations of flowering *Dactylis glomerata* found throughout the larger Worcester region. These elements were utilized to model pollen release scenarios. These scenarios were further confirmed to be representative of atmospheric pollen levels using species-specific eDNA samples that had been processed using DNA metabarcoding and bioinformatics. An isolated population of *Festuca rubra* were shown to contribute only minor levels of pollen eDNA to samplers located 300m away, highlighting the heterogeneity of dispersion distance from pollen source areas to the local environment.

The connection between atmospheric eDNA and flowering phenology have previously been one of the major missing link in current aerobiological knowledge. These findings have contributed new understanding that will be essential in the mechanistic modelling and forecasting of pollen dynamics and to solve the underlying connection with phenology.

Acknowledgements

I would like to thank my Director of Studies Professor Carsten Skjøth for giving me the opportunity to develop as a researcher and as a person, as well as for all the times you provided hope, solutions, knowledge, and laughter when I needed it and for always having your door open.

I would like to thank Dr Beverley Adams-Groom for all the time, knowledge and patience provided to me during the course of my studentship while teaching me the ins and outs of aerobiology and everything related to pollen as well as for just lending an ear and an opinion when I needed it.

I would like to thank Professor Simon Creer and other members of Bangor University for providing valuable enthusiasm throughout my studentship and generously offering their experiences and facilities whilst learning how to lab.

I would also like to thank Dr Mary Hanson for the support, experience and problem solving whilst trying to learn how to approach DNA extraction, PCR, Metabarcoding and associated Bioinformatics.

A special thanks goes out to Dr Geoffrey Petch, without your immense knowledge, experience, support, and dedication to create, run, maintain, and repair all of the field and sampling equipment nothing of this would have been possible.

Lastly I would like to thank my parents, Claes and Camilla, for having always supported me and my decisions regardless of where it took me and for believing that I can accomplish anything that I set my mind to. This thesis and my future motivation as a researcher would not have been possible without them.

Publications and Conference Presentations

Publications

Kurganskiy, A., Creer, S., de Vere, N., Griffith, G. W., … Frisk, C. A., … Skjøth, C. A. (2021). Predicting the severity of the grass pollen season and the effect of climate change in Northwest Europe. *Science Advances* **7** (13). 1-11. Doi: 10.1126/sciadv.abd7658

Rowney, F., Brennan, G. L., Skjøth, C. A., Griffith, G. W., … Frisk, C. A., … Creer, S. (2021). Environmental DNA reveals links between abundance and composition of airborne grass pollen and respiratory health. *Current Biology* **31**. 1-9. Doi: 10.1016/j.cub.2021.02.019

Frisk, C. A., Adams-Groom, B., Skjøth, C. A. (2021). Stochastic flowering phenology in *Dactylis glomerata* populations described by Markov chain modelling. *Aerobiologia*. 1-16. Doi: 10.1007/s10453-020-09685-1

Apangu, G. P., Frisk, C. A., Adams-Groom, B., Satchwell, J., … Skjøth, C. A. (2020). Air mass trajectories and land cover map reveal cereals and oilseed rape as major local sources of *Alternaria* spores in the Midlands, UK. *Atmospheric Pollution Research* **11**. 1668-1679. Doi: 10.1016/j.apr.2020.06.026

Brennan, G. L., Potter, C., de Vere, N., Griffith, G. W., ... Frisk, C. A., ... Creer, S. (2019). Temperate airborne grass pollen defined by spatio-temporal shifts in community composition. *Nature Ecology & Evolution* **3** (5). 750-754. Doi: 10.1038/s41559-019-0849-7

Rojo, J., Oteros, J., Pérez-Badia, R., Cervigón, P., … Frisk, C. A., … Buters, J. (2019). Near-ground effect of height on pollen exposure. *Environmental Research* **174**. 160-169. Doi: 10.1016/j.envres.2019.04.027

Conference Presentations

Frisk, C. A., Apangu, G. P., Petch, G. M., Adams-Groom, B., Skjøth, C. A. (2021). Local and Regional Grass Pollen Distribution Identified using HYSPLIT and Statistical Modelling Approaches. **Conference:** Aerobiology, Climate and Covid-19. 79th International Scientific Conference of the University of Latvia in Riga, Latvia.

Frisk, C. A., Adams-Groom, B., Skjøth, C. A. (2020). Spatial Flowering Patterns in *Dactylis glomerata* Populations. **Conference:** Bioaerosols and Environmental Impacts. 7th European Symposium on Aerobiology (Virtual) in Córdoba, Spain.

Apangu, G. P., Frisk, C. A., Adams-Groom, B., Satchwell, J., … Skjøth, C. A. (2020). Air mass trajectories and land cover map reveal cereal crops as major local source of *Alternaria* spores in Worcester and Leicester, UK. **Conference:** Bioaerosols and Environmental Impacts. 7th European Symposium on Aerobiology (Virtual) in Córdoba, Spain.

Frisk, C. A., Petch, G. M., Skjøth, C. A. (2019). Aerobiology meets Ecology: Development of Low-Cost Passive Gravitational Samplers. **Conference:** Seeds of Knowledge. Postgraduate Research Student Conference in Worcester, United Kingdom.

Apangu, G. P., Frisk C. A., Hanson, M., Petch, G. M., Skjøth, C. A. (2019). A High Abundance of *Alternaria alternata* Fungi Found in Worcestershire, UK. **Conference:** Seeds of Knowledge. Postgraduate Research Student Conference in Worcester, United Kingdom.

Frisk, C. A., Apangu, G. P., Petch, G. M., Adams-Groom, B., Skjøth, C. A. (2018). Spatial and Temporal Variance of Bi-Hourly Grass Pollen Concentrations in the Local Surroundings of Worcester, UK. **Conference:** 11th International Congress on Aerobiology in Parma, Italy.

Apangu, G. P., Frisk, C. A., Petch, G. M., Adams-Groom, B., Skjøth, C. A. (2018). Spatial bi-hourly Variation of *Alternaria* Spore Concentration in Worcester, UK. **Conference:** 11th International Congress on Aerobiology in Parma, Italy.

Rojo, J., Oteros, J., Pérez-Badia, R., Adams-Groom, B., … Frisk, C. A., ... Buters, J. (2018). Effect of Height on Pollen Sampling in Relation to Pollen Exposure at Ground Level. **Conference:** 11th International Congress on Aerobiology in Parma, Italy.

Skjøth, C. A., Petch, G., Ottosen, T., Hanson, M., … Frisk, C. A., … Pope, F. D. (2018). First Experience with Low Cost Optical Particle Counters Reveal Spore Emission in Woodland During Night Time. **Conference:** 11th International Congress on Aerobiology in Parma, Italy.

Frisk, C. A., Adams-Groom, B., Creer, S., Skjøth, C. A. (2017). Pollen Season and Flowering Phenology in *Dactylis glomerata*. **Conference:** Palynology-Aerobiology-Allergy Symposium 2017 in Vienna, Austria.

List of Acronyms

ARL	Air Resources Laboratory
BBCH	Biologische Bundesanstalt Bundessortenamt und Chemische Industrie
Cfb	C (Temperate) f (No dry season) b (Warm summer)
DNA	Deoxyribonucleic Acid
DOY	Day of Year
eDNA	Environmental Deoxyribonucleic Acid
ELISA	Enzyme-Linked Immunosorbent Assay
GDAS	Global Data Analysis System
GFS	Global Forecast System
GLM	Generalized Linear Model
GLMER	Generalized Linear Mixed Effects model in R
GLMM	Generalized Linear Mixed-Model
HYSPLIT	Hybrid Single-Particle Lagrangian Integrated Trajectory
ITCZ	Intertropical Convergence Zone
ITS 1 / 2	Internal Transcribed Spacer 1 / 2
LOESS	Locally Estimated Scatterplot Smoothing
MIDAS	Met Office Integrated Data Archive System
MS	Mass Spectrometry
NPK	Nitrogen Phosphorous Potassium
NS	Non-Significant
OPC	Optical Particle Counter
OTC	Over-The-Counter
PCR	Polymerase Chain Reaction
PR	Pollen Release
PhD	Philosophiae Doctor - Doctor of Philosophy
qPCR	Quantitative Polymerase Chain Reaction
SPIn	Seasonal Pollen Integral
STL	Seasonal and Trend Decomposition using LOESS
TKE	Turbulent Kinetic Energy
VPD	Vapor Pressure Deficit

Table of Contents

1. Background

1.1. Background Interpretation

The following sections of background literature have been specifically compiled to facilitate the interpretation of complex multidisciplinary interactions between traditionally ecological and aerobiological knowledge domains. As such, the reader can gain a comprehensive multifocal lens with which it is possible to properly examine and determine the extent and novel aspects presented in the various sections and chapters of the entire document. The following sections are organized to follow a thread of increasing specificity, originating in allergy, progressing through pollen monitoring, grass pollen dynamics and flowering phenology. This broad scope of inter-connected topics allows for an overarching narrative that leads into the research rationale and associated aims and objectives.

1.2. Grass Pollen and Allergy

Charles Harrison Blackley, the discoverer of the connection between allergic rhinitis and pollen, wrote in 1873:

> *"Even in this country, where the disorder probably had its commencement and where it is still more common than in any other part of Europe, there are medical men to be found who know very little about it; and on the Continent there are still some to be found who have never even heard of the disease. [..] I do not, however, despair of a specific being found for hay-fever, and offer the following pages as a contribution which it is hoped may assist somewhat in the search for the appropriate remedy."*
>
> **Blackley, C. H. *Experimental Researches on the Causes and Nature of Catarrhus Aestivus*. London: Baillère, Tindall & Cox, 1873.**

Blackley might have been the first person to have connected allergic rhinitis and pollen, but he could not have known how important his discovery was and what it might bring in the future. The sensitivity to particles, substances or chemicals that otherwise are benign through antibody or cell-reactions is often referred to as allergy (Johansson et al., 2001). The reaction to the specific compound will range from none to very high, with none being categorized as non-allergenic and low to very high being categorized as allergic (Aalberse, 2000). The intensity of the reaction will depend on the immune-system response and can include a wide range of effects, ranging from irritability to severe immunological anaphylaxis (Wallace et al., 2008) and can in some cases result in death due to asphyxia or cardiac arrest (D'Amato et al., 2016). For airborne particles such as pollen, spores, bacteria etc. the condition is called allergic rhinitis

(Bousquet et al., 2001), from the main interaction between the allergens and the sufferers' nasal cavity (Johansson et al., 2004) with the condition affecting 10 – 20 % of the global population (Akdis and Agache, 2014). For pollen, the phenomenon is specifically called pollinosis and refers to all allergenic connections to pollen (Solomon, 1984), with the common term used being hay-fever. Around 40% of the European population is expected to be suffering from some sort of pollen allergy (D'Amato et al., 2007). The perhaps most common pollen allergy is grass pollen allergy, the allergenic reaction to pollen from the plant family *Poaceae*, or grasses (D'Amato et al., 1998). The effects normally include itching in the eyes and nose, increased nasal secretion and sneezing, but can also indirectly include fatigue, headaches, lack of sleeping and general discomfort brought on by the direct effects (Greiner et al., 2011; Wallace et al., 2008). Allergic rhinitis is not only physically debilitating, it also causes a loss in quality of life (Šaulienė et al., 2016) and a measurable loss of productivity for the entire affected society (Crystal-Peters et al., 2000; Lamb et al., 2006). Interactions between allergy and air pollution further complicates the issues (D'Amato et al., 2010). Traditionally, the pollen from grasses were treated more or less like a monolith, mainly from considering all grass pollen to be equally allergenic (Hyde, 1973, 1972), but for the last few decades this reasoning has been questioned due to differential biochemical composition of different grass species (Suphioglu and Mansur, 2000). If pollen from different grass species behave differently due to some circumstance in terms of allergenicity, then pollen from each species must be investigated in terms of this differentiation.

1.2.1. Grass Species and Allergens

The biochemical differentiation of each grass species creates a wide range of different chemical variants of the same functional product which is mainly seen in lipids, proteins and other compounds in and on the grass pollen grain (Devis et al., 2017). By classifying specific lipids and proteins into categories, investigating the absolute ranges of each biochemical and how each compound itself and in combination with other biochemicals affect grass pollen sufferers it is possible to determine the general allergenicity of each species (Davies, 2014). The grass species which has been investigated most for allergenic compounds and its health effects is the species *Phleum pratense* (e.g. Hatzler et al., 2012; Pilette et al., 2007; Tripodi et al., 2012). Each allergen in this species is named *Phl p*X, with *Phl p* being derived from the genus and species epithet letters, and the X being the allergenic group of the specific allergen, with *Phleum* having at least 13 allergen groups (García-Mozo, 2017). In each group there are also variants of that specific allergen based on local species and genus differences (Mohapatra et al., 2005). Many allergens from different species share commonality within and between allergen groups

based on common evolutionary ancestry, functionality of the compound and amino-acid sequence, which contributes to the cross-reactivity between species seen in pollen sufferers (Pomés et al., 2018; Radauer et al., 2014). However, the species diversity of the pollen contribution will impact in unpredictable ways due to the cross-reactivity of allergens (Aud-In et al., 2019). A primarily allergenic response from the immune-system from the allergens of one dominant species can be strengthened by cross-reactivity from another species flowering at the same time, or perhaps later in the season (D'Amato et al., 1998). This uncertainty makes it difficult to determine which species the sufferer is primarily sensitive towards without extensive immunological investigation. Due to the fundamental complexity of conducting combinatory allergenic experiments on live subjects the general allergenicity of all species has not been established, but the research suggests that some species are indeed more allergenic than others (Abreu et al., 2008). Several allergenic indexes have been suggested from a combinatory approach of plant life-history traits and smaller studies on allergenic compounds (e.g. Cariñanos et al., 2014; Hruska, 2003). These indexes suggest that life-history traits associated with high allergenicity are being perennial, tall, and abundant along with having long-flowering periods and high pollen production. Grasses that fit this description includes species in the genera *Anthoxanthum, Dactylis, Holcus, Lolium, Phleum* and *Poa* among others. Most of the allergenic grass species in Northern Europe (including the genera mentioned) belong to the BOP-clade of Poaceae (Soreng et al., 2017). However, some of the species belong to the PACMAD-clade (e.g. *Molinia* and *Phragmites*). These species tend to flower later in the season when grass pollen concentrations are usually lower (Bastl et al., 2020) and fewer grass pollen allergy symptoms are being reported, this has caused their allergenicity to be under-investigated in temperate regions (Davies, 2014; Nony et al., 2015). The Skin Prick Test (SPT) can give an indication of which species the sufferer is allergic to (Heinzerling et al., 2013), by comparing the reaction from an injection containing a purified allergen or a cocktail of different allergens from a species with a standardized dose of histamine (Burbach et al., 2009; Heinzerling et al., 2009). These indications can be confirmed from a blood analysis by investigating the presence of the species allergen antigens in the blood (Chabre et al., 2010). It is also possible to conduct immunotherapy to a few different grasses based on the results from the above-mentioned tests (Jutel et al., 2005). The immunotherapy can provide some or total immunity for a limited time by injecting the sufferer with a standardized blend of allergens for a certain amount of times until the temporarily immunity is achieved (Andersson and Lidholm, 2003; Mohapatra et al., 2005). These techniques though are not as common as taking antihistamines (Howarth and Holgate, 1984) or other Over-the-counter (OTC) medication (Holgate and Polosa, 2008) for grass pollen inconveniences during the grass pollen season

(Cebrino et al., 2017). For researchers and pollen forecasters alike the simplest way to warn sufferers of the coming (e.g. Kurganskiy et al., 2021) or current grass pollen season is to conduct standard pollen monitoring and to report the results to the public.

1.3. Grass Pollen Monitoring

The monitoring of grass pollen provides valuable information regarding the fluctuations that can be expected in atmospheric grass pollen concentrations (Morrow Brown and Jackson, 1978a). Hourly monitoring provides information of when during the day the grass pollen concentrations is likely to be the highest (Norris-Hill, 1999), which can benefit sufferers by knowing when to stay indoors, but also relay information of when the likeliest time of pollen release will be (Norris-Hill and Emberlin, 1991). However, the diurnal grass pollen concentrations are expected to change between closely located locations (Peel et al., 2014b). Seasonal monitoring provides information of how strong a season is (Galán et al., 1995), and how meteorological patterns can influence both directly (via physical and chemical interactions) (Sabariego et al., 2011) and indirectly (via plant growth) (García-Mozo et al., 2009) the grass pollen concentrations. It also provides data on starting, pre-peak, peak, post-peak and end dates of the season (Fernández-Rodríguez et al., 2015), all of which are important when it comes to the preventative capacity of immunologists and health professionals (Osborne et al., 2017). Yearly monitoring provides information regarding trends and changes in trends for the grass pollen season (Emberlin et al., 1993), which can be used to gain further understanding in climate change scenarios (García de León et al., 2015), long-term weather patterns (Recio et al., 2010) and land-use change (Emberlin et al., 1999). Most nations have their own general pollen monitoring programme (Buters et al., 2018), with examples of prominent ones that also produce new high-impact research in the aerobiological field being the United Kingdom program (e.g. Adams-Groom et al., 2017; Skjøth et al., 2019), the Swiss program (e.g. Crouzy et al., 2016), the Spanish program (e.g. De Linares et al., 2017; Rojo et al., 2019) and the German program (e.g. Oteros et al., 2019a, 2019b). Grass pollen does not exhibit enough morphological differences on a species or genus level to make it possible to determine the taxonomic contribution to anything less than to family level, i.e. grasses (Morgado et al., 2015). It should be noted that there are general size differences between the regularly sized wild grass pollen and larger sized cultivated grass pollen (e.g. cereals) (Joly et al., 2007), but this is not normally of allergenic concern due to the low dispersal rates and pollen loads of cultivated grasses (Damialis and Konstantinou, 2011). The dilemma becomes the disconnect between an uneven allergenicity within the family and the undifferentiability of the contributing pollen. This means that it is impossible to monitor the more allergenic grass species

with regular grass pollen monitoring, the conclusion is therefore to utilize other detection methods for lower taxonomic orders (see section 1.6.). Grass pollen fluctuations, whether it be hourly, daily, seasonally, or yearly will depend on several outside factors with complex interactions that influence the atmospheric concentrations.

1.4. Factors Influencing Atmospheric Grass Pollen Concentrations

Concentrations of aerial grass pollen deviates within and between regions depending on inherent features of the surrounding landscape and interactions with outside influences (Emberlin et al., 2000; Smith et al., 2009). The inherent features of the surrounding area will determine the overall pattern of the annual pollen curve due to the imposing restrictions on plant growth stemming from the habitat (Jantunen et al., 2006), latitude (Devadas et al., 2018) and general meteorological conditions (Valencia-Barrera et al., 2001). Outside influences can shift the annual pollen curve in amplitude and period length, without interfering with the overall pattern. These outside influences can include unusual weather patterns in terms of temperature (heatwave or coldwave), precipitation (wet or draught) (Makra et al., 2012) or long-distance transport (Rousseau et al., 2006). Most influencing factors stem directly or indirectly from the meteorology present in the system, for example directly from precipitation (Zhang et al., 2015) but indirectly from plant health and prosperity (Salisbury, 1939). Five main categories of factors can be identified to have an effect on atmospheric grass pollen concentrations: Meteorological, biological, physical, spatial, and temporal. Many factors intertwine generally by influencing the key features responsible for aerial grass pollen concentrations: plant growth patterns, pollen emission patterns and pollen deposition patterns.

1.4.1. Meteorological Factors

Temperature is arguably one of the most important parameters when it comes to grass pollen concentrations. It has been determined to be important to the grass pollen season overall due to the high correlation with aerial grass pollen concentrations (Myszkowska, 2014), although the correlation is misguided, due to the indirect importance it has on plant growth (Eagles, 1967), plant maturity (Rossignol et al., 2014), anthesis (Emecz, 1962; Liem and Groot, 1973) and anther dehiscence (Keijzer et al., 1996). Increased temperatures are generally positive on the growth progression of most plants. Winter and early spring temperatures will modulate grass emergence and initial growth conditions (Havstad et al., 2004). Spring and early summer temperatures will condition temperature thresholds responsible for grass maturity and inflorescence (with pollen) development (Anslow and Green, 1967). Summer temperatures will further impact anthesis and later anther dehiscence (Khanduri, 2011), which leads into grass pollen emission. Too warm temperatures will however lower transpiration rates (Charles-

Edwards et al., 1971), which in turn decreases photosynthesis and will decrease total energy availability for plant functions along with pollen production. Temperature are also commonly used to forecast future grass pollen concentrations (García-Mozo, 2017; e.g. Smith and Emberlin, 2006).

Precipitation will have an opposite but likewise complex effect on overall grass pollen levels from temperature. Rain will inhibit grass pollen emission by wetting the plant and therefore preventing desiccation of the grass anther. It will at the same time wash pollen out of the air by either hitting the pollen grain directly and increasing its' gravitational deposition rate, or indirectly by enveloping it into condensation and cloud formation, which then precipitates down with the rain (McDonald, 1962; Zhang et al., 2014). The individual grass tiller on the other hand will benefit from optimal water-levels during the primary growth period (Salisbury, 1939), with good water conditions bringing optimal growth in terms of height, stature, tillering (side-shoot production) and amount and size of inflorescence. Increased plant mass will increase the amount of leaves, which in turn will increase absolute photosynthesis (Donald, 1968), which in turn will increase the amount of energy available for pollen production. Optimal water-level is a fine line with either side reducing plant growth (Blair et al., 2014), and by association pollen production (Firon et al., 2012), by either too much or too little water availability. The effects of precipitation will therefore be time-sensitive, with rain during growth but not during anthesis being optimal for pollen production and release, while absence of rain during growth and presence during anthesis being detrimental for the same. A likewise closely related parameter is humidity, which will mainly affect grass pollen emission conditions (Keijzer et al., 1987). High humidity will prevent and/or delay anther dehiscence, while low humidity will have the opposite effect (Keijzer, 1987a). Too high humidity for longer periods will prevent water transpiration and nutrient uptake from the soil, effectively preventing basic plant function (Ford and Thorne, 1974).

Solar radiation will have a general positive impact on grass pollen concentrations, but the interactions between solar radiation and other factors will be complex due to the indirect effects. The direct effects of solar radiation are from photosynthesis potential, which as mentioned above increase the total energy that can be diverted to basic plant functioning (Eagles, 1971) such as growth, inflorescence and pollen production. Too high solar radiation though, as mentioned above, will lower photosynthesis due to the intense increases in temperature (Teramura and Sullivan, 1994). In the rare cases of extreme solar radiation, there could be damage like burning of plant tissue, severely damaging the plant and inhibiting overall plant function (Hollósy, 2002; Rozema et al., 1997). Other direct effects of solar radiation will be the

desiccation of anthers, in which the anther dries, bursts and releases the grass pollen within (van Hout et al., 2008; Viner et al., 2010; Viner and Arritt, 2012). This effect is directional, with increased solar radiation will increase anther desiccation. However, this effect only applies when anthers have been extruded from mature flowers. If the flowers have not yet matured, and increased solar radiation applied without proper water-potential the inflorescence may instead dry-out, which would cause a complete stop in any further pollen production. Solar radiation will also indirectly cause updrafts of air due to the rising effect of warm air (convection) (Talman, 1922), which increases the potential for pollen to disperse further from the emitting plant.

The complex meteorological interaction of temperature, precipitation and solar radiation will give rise to regional differences within these parameters. These regional differences will create high- and low-pressure areas, and as an atmospheric consequence, air will move from high pressure areas to low pressure areas, causing wind (Smith et al., 2005). Wind will move air and the grass pollen content directionally from one place to another, and often from source area to sink area (Maya-Manzano et al., 2017). The air movement will also cause temperature and humidity to fluctuate based on the surrounding air, with both short-term and long-term consequences to nearby plants caused by this depending on the new equilibrium. Sheltered and open areas will be disproportionally affected, with open areas experiencing more fluctuations caused by the movement of air (Cleugh, 1998). This will partly be responsible for the lower pollen concentrations in coastal regions (Morrow Brown and Jackson, 1978b). Pollen will always travel with the wind due to the light-weight nature of the bioaerosol. Stronger winds are also expected to cause the pollen to travel further, although weaker winds are more likely to deposit the pollen grain. Long-distance transport of pollen can cause high pollen concentration events even if the local vegetation is not mature enough to release any pollen grains (Estrella et al., 2006).

The connection between the varied meteorological parameters and the seasonal grass pollen load is clouded due to the complex interactions both within and between variables (Jones and Harrison, 2004; Romero-Morte et al., 2020). The interactions are expected to be overall general due to the mechanism involved, but the exact dynamic is still unknown. Complex grass pollen forecasting has been utilized using combinations of all above-mentioned factors along with multiple computer intelligence (CI) algorithms (e.g. Voukantsis et al., 2010). However, meteorological conditions can only affect grass pollen concentration to a limited degree though since it will all depend on if there are any plants to affect in the first place.

1.4.2. Biological Factors

All grass pollen originate from being released from an inflorescence connected to an individual grass plant. Grass plants however do not exist independently of the surrounding environment, instead, these plants form intricate network and co-dependence with other animate and inanimate objects and circumstances (Wang et al., 2018). Biological factors can be divided between general and specific factors. The general factors include features of the surrounding environment that will directly or indirectly impact the plants themselves on a basic level, such as flowering season (e.g. Munshi, 2000), land-use (e.g. Werchan et al., 2017) and land-management (e.g. Jantunen et al., 2007). The specific factors on the other hand will include features innate to the plant itself and its requirements, such as habitat (e.g. Tng et al., 2010), species abundance (e.g. Zerboni et al., 1991) and species diversity (e.g. Prieto-Baena et al., 2003).

1.4.2.1. General Biological Factors

All grass species have innated nutritional, temperature, solar and water requirements that initiate phenological stages gained through evolutionary development. These requirements and/or thresholds are specific for each species and will diverge based on other local conditions (Emecz, 1962). The implications from these requirements create species-specific flowering seasons, this results in that many species overlap to a strong degree during the season of optimal growth conditions (Cebrino et al., 2016). In the cool temperate parts of Western Europe this season coincide with the late spring to early autumn months of April to September (Adams-Groom et al., 2020), or colloquially, the summer. Species such as *Dactylis glomerata* flowers during the early to middle part of the season (Tormo-Molina et al., 2015), while species such as *Phleum pratense* flowers during the latter pater of the season (Cope and Gray, 2009). The species *Lolium perenne* is one of the species that flowers throughout the entire season (Kmenta et al., 2016). There are exceptions to this rule, with species such as the small annual *Poa annua* that remains in flower for most of the year (Johnson and White, 1998). Implications of a mostly sequential flowering progression within the local species assemblage will be divergent temporal contributions to the annual pollen load of different species-specific grass pollen (Romero-Morte et al., 2018).

Land-use will determine how much of a given space can be colonized by and/or planted with grass plants. The grass dominance will be very low in the concrete landscape of urban areas, with only the hardiest species being able to survive and flower in rare areas of soil or cracked concrete. However, the presence of non-concreted areas within the urban matrix, such as parks, verges etc. will be expected to contain many different species (Hruška, 2000). The grass

dominance will be expected to increase in areas with increased soil content and openness absent in other vegetation, reaching the optimal conditions in grass dominated land-types such as meadows, pastures and some agricultural areas (McInnes et al., 2017). Land-use however is far from the most important factor that determines the potential for grasses to flower and release pollen. Land-management is one of the strongest contenders for the most important factor when it comes to grass pollen concentrations (Skjøth et al., 2013). If all plants in an area are kept from reaching flowering potential, caused by either grazing, mowing, cutting or removal of plant material, then there can be no pollen contribution even if the entire area is technically covered by productive grass plants of particularly species of high allergenicity. The management condition is especially strong when it comes to meadows and pastures, areas that because of the placement of animals can be either completely grazed down, or fully grown with pollen producing and emitting inflorescences (Smith et al., 2000). Without proper and relevant information regarding management, the correlation between land-use and pollen contribution is at best a cautionary guesswork (Maya Manzano et al., 2017). Even with land-use and land-management information, the total grass pollen contribution can be uncertain, mainly caused by the differential pollen production potential of each specific species (Aboulaich et al., 2009), and the accompanied species' abundances (Zerboni et al., 1991).

1.4.2.2. Specific Biological Factors

Grass species have specific ecological niches, with varying requirements for establishment and optimal longevity. This differential creates assemblages of species more likely to be found in specific climates and habitats (Hirzel and Le Lay, 2008; Shoko et al., 2016). One main distinction between grass species is their photosynthetic carbon fixating pathway, either C3 or C4 (Pau et al., 2013). C3-species are classified as cool season grasses while C4-species are classified as warm season grasses. C4-species dominate the tropics due to their ability to survive and photosynthesize more effectively in warmer and dryer climates while C3-grasses dominate elsewhere (Edwards and Still, 2008; Taylor et al., 2010). Some species have strict requirements both in nutrition and in management and can only be found within their optimized habitat, for example calcareous grasslands (e.g. Bąba, 2004) or coastal salt marshes (e.g. Penk et al., 2020). These species would be rarer due to the low total area of these specific habitats (Holdaway et al., 2012) and would not likely contribute much to the overall annual pollen load. Other species have less strict requirements in nutrients but more in management and will mainly be found in meadows primarily used for silage or grazed pastures (Cope and Gray, 2009). Depending on the management of these habitats the contribution to the annual pollen load can vary drastically. Other species are hardier and can survive better in the shaded understory of forest trees. The

pollen contribution here can be expected to be lower, due to the protective nature of the forests against wind (Boudreault et al., 2017; Papaik and Canham, 2006), which would discourage pollen dispersal. Many species however have low requirements in nutrition and management and will grow anywhere their seeds happens to fall (Linder et al., 2018). These are the species that are most likely to contribute to the annual pollen load due to their competitive ability, and success breeds success, which would further encourage spreading and increase their prevalence and dominance.

The abundance of the species is related and will depend on how much the current habitat matches their requirements, along with innate features of their life-history (Danielson, 1991). There are also instances of species adapting their physiology to better adapt to specific habitats or ecological conditions (e.g. Stapledon, 1928, and a discussion about *Dactylis* ecotypes). Species with low requirements and fast life-histories will have an advantage in spreading and flowering, increasing their overall abundance (Koons et al., 2016). Management is a key factor here, due to the differential of grass species to disturbance tolerance (Brock et al., 1996). Some species will be able to survive and even go into flower after heavy disturbance from grazing, cutting or mowing, while others will not (Wang et al., 2018). This further narrows down the number of species capable of surviving and being prosperous throughout the landscape. A disproportionally high abundance of a few grass species will increase their overall role in the grass pollen contribution, making it in a way easier to determine which species that are important in terms of the total contribution (Romero-Morte et al., 2018). High abundances of a few grasses are also likely to increase each species' relative peak within the season, potentially giving rise to stronger pollen concentrations temporarily during peak pollen emission (Kmenta et al., 2016). Additionally, increased species diversity within a region is likely to increase the length of the pollen season, due to the sequential flowering pattern of grass species (Kmenta et al., 2017). Each species will also have a different pollen production capacity (Prieto-Baena et al., 2003), with similar ranges for each individual and flower within a specific species (Aboulaich et al., 2009). This means that some species will produce more pollen, and some will produce less, a factor that will vary depending on the developmental factors and conditions of each species and site (Khanduri, 2011). The abundance of flowering grasses in each location are therefore likely to contribute to the grass pollen season, but it is uncertain to what extent different areas contribute based on the present abundance and diversity. However, each pollen grain will also have physical restrictions that governs atmospheric movements.

1.4.3. Physical Factors

The aerodynamic nature of grass pollen allows them to be moved efficiently by the wind (Cresswell et al., 2010). For grass pollen grains to be moved by the atmosphere there must first be release from the flower. Pollen release can only happen when the male part of the flower, the anther, is mature and extruded from the flower (Zanotti and Puppi, 2000). The plant tissue of the anther must be desiccated enough to break; this will release the pollen inside (Wilson et al., 2011). The dehiscence is encouraged by low humidity, increased temperature and wind speed: all factors that favour the evaporation of water (Viner et al., 2010). For the pollen to become airborne, a gust of wind needs to capture the freshly released pollen either during the moment of release, or while it is still in the recently broken anther (Friedman and Harder, 2004). While airborne, pollen can be transported great distances during optimal atmospheric conditions as seen from studies on long-distance transport (Nathan et al., 2003), this in turn can allow the transfer of genetic material otherwise inaccessible and impact sensitive sufferers (Van de Water et al., 2000). The transportation distance will also depend on the gravitational settling velocity of the grass pollen grain (Jarosz et al., 2003), which in turn is determined by the weight, volume and shape of the grain (Borrell, 2012). All grass pollen grains will have the same spheroidal-ovoid shape (Morgado et al., 2015) but will vary in weight and volume, and thereby density, with higher density increasing the settling velocity (Durham, 1943). The weight and volume will vary depending on the hydration levels of the pollen grain. The hydration levels will depend on meteorological conditions currently applied to the grain (harmomegathy), with relative humidity and solar radiation being the major determinants of this balance (Wodehouse, 1935). Desiccation will decrease the weight and volume of the pollen grain, effectively lowering the density and settling velocity. Hydration will increase the weight and volume of the pollen grain, effectively increasing the density and settling velocity. This deposition is generally referred to as dry deposition and is caused by gravity and air-pressure differential caused by the density of the grain (Kreissl et al., 1991; Lin et al., 1994). Pollen will also deposit from wet deposition, as mentioned in the section about precipitation. The physical size of the pollen grain will vary both within (Ghitarrini et al., 2017a; Takahashi et al., 1995) and between species (Joly et al., 2007), likely causing differential deposition patterns. Tangentially, the physical size of the pollen grain will also influence the symptoms of each hay-fever sufferer. The reasoning is due to smaller airborne objects being capable of traveling further down the throat, potentially causing more adverse effects (Driessen and Quanjer Ph., 1991). However, it is mainly water-soluble allergens that travels further down the respiratory tract after being released from the pollen grain when coming in contact with moist human tissue (Dahl, 2018; Darquenne, 2012). Atmospheric conditions will determine the four-dimensional movement of

the grain, by having the capacity to move the pollen in three spatial dimensions, but also from moving the pollen in the temporal dimension. The temporal movement of pollen grain will be a balance between deposition and resuspension (Dupont et al., 2006). The causes of resuspension are both from updrafts associated with uneven wind movement and turbulence, mainly from collision with other objects but also from warm air rising, as mentioned before (Wu and Russell, 1992). Pollen being able to remain in the atmosphere caused by resuspension can have a long atmospheric lifespan, contributing to the aforementioned long-distance transport and deposition during times when no natural pollen release is occurring. The difference in size and the change in density of grass pollen will be fundamental in its transportation capacity, but it is still uncertain to what degree these changes impact the grass pollen season. Although all the above-mentioned factors are general, there are also differences in the atmospheric grass pollen concentrations between locations and throughout time.

1.4.4. Spatial Factors

The spatial variation is mainly caused by the divergence of the above-mentioned categories through space and can be divided for simplicity in three levels: regional, national, and global. Regional features mainly apply to geography, land-use and surrounding habitats, all of which are fundamentally connected (Somantri and Nandi, 2018). The geography of a landscape will dictate what land-use is possible (Kladnik et al., 2019). Flat areas will be more likely to contain urbanized areas and other anthropogenic activity such as agriculture and manufacturing. Areas that are not flat will be more likely to contain less anthropogenic influenced areas, for example forests, heathlands, and meadows but also smaller settlements. Land-use in combination with geography will ultimately determine which habitats are possible to exists in each location (Guisan and Zimmermann, 2000). Each habitat will then be inhabited by a set of species based on inert preferences along with chance colonization of surrounding areas (Ortiz-Rodríguez et al., 2019). The summation of all these factors will determine which species that are likely to be present in the region and capable of contributing to the atmospheric grass pollen load (Cebrino et al., 2018). The divergent distribution of species will unequally contribute to the entire region, with highly urbanized areas further from source areas being less likely to experience high pollen concentrations (Rodríguez-Rajo et al., 2010). This is mainly due to the effect of distance, with increased chance of pollen deposition closer to the source (Morrow Brown and Jackson, 1978c). These three above-mentioned regional features will also influence the spread of bioaerosols by influencing how wind moves in the landscape. Geological features such as gorges or canyons will inherently funnel the wind and the captured grass pollen within (Schroeder, 1961; Zhang et al., 2020). Anthropogenic features such as city landscapes will act in similar ways, with long

streets surrounded by high buildings experiencing similar effects (Johnson and Hunter, 1999; Peel et al., 2014a). Other features such as forests and mountains (but also buildings) can block the wind, causing similar effects as rain-shadows, but for pollen (Auer et al., 2016).

National features mainly apply to plant growth parameters and species distributions, these too are connected. The spatial scales associated with a national level are larger than regional scales. The increase in scale will allow for divergent meteorological gradients caused mainly by differential in latitude and altitude (Montgomery, 2006; Wang et al., 2011). Higher latitudes will have overall decreased solar radiation compared to lower latitudes (Yilmaz, 2011). Higher latitudes are also more affected by seasonality, with larger difference between the summer and winter months. Plants in higher altitudes will receive more solar radiation during the day, while being exposed to different water and nutritional conditions (Tranquillini, 1963). This will favour certain species over others, with the most discerning factor being the tree line, the altitude and latitude where above this line no trees will survive (Danby and Hik, 2007). Other meteorological features will also impact on a national level, such as distance to the ocean (continentality), which will impact the overall climate and prevalence of rainfall (Andrade and Corte-Real, 2017). Areas closer to the ocean tend to have milder climates with increased rainfall than areas further inland (Mikolaskova, 2009). All of these factors will ultimately cause a divergence in species distributions based on individual species preference and survivability. The differential in plant growth from meteorological parameters on a national level is usually actualized by initial flowering in lower latitudes and at lower altitudes (Lo et al., 2019; Rossignol et al., 2014). The differentiated flowering progression will lead to grass pollen release from mature grasses in some areas while the grasses might not have produced an inflorescence yet in other areas. From this aspect grass pollen can be transported to areas without any currently active flowering.

Global features mainly apply to climate and plant evolution. The spatial scales associated with a global level are larger than both regional and national scales. Climatological differences apply at this scale, with differentiated seasonality of higher and lower latitudes (Donohoe et al., 2020). The seasonality of higher latitudes consists of winter and summer seasons caused by the Earths axial tilt (obliquity) (Ferreira et al., 2014), while the seasonality of lower latitudes consists of dry and wet seasons caused by the Intertropical Convergence Zone (ITCZ) (Gadgil, 2003). These factors are in-turn affected and/or caused by global water-current (Dohan, 2017) and atmospheric circulation (Harrington and Oliver, 2000), causing the presence of differentiated biomes at a global scale (Kottek et al., 2006). The difference in seasonality over biomes will have massive consequences on plant physiology and ecology, which causes selection pressure

and evolutionary dynamics to be high (Mucina, 2019). Because of this there are many genera of grasses that are specific to certain biomes, with plant diversity and plant abundance being specific to each habitat in each ecosystem in each biome (Bouchenak-Khelladi et al., 2010; Clayton et al., 2002). Each genera and species will have a different ecological niche, physiology, and biochemistry, this will cause major variations in flowering seasonality, pollen production, pollen release patterns and allergenicity. Atmospheric grass pollen concentrations will therefore ultimately be affected by global biogeography.

1.4.5. Temporal Factors

The temporal variation is mainly caused by the divergence of the above-mentioned categories through time and include intra-annual (within season) and inter-annual (between seasons) features. Grass pollen can only be released during times when mature grasses are flowering, with differential pollen release patterns being species-specific and caused by local conditions (Bhattacharya and Datta, 1992; Subba Reddi et al., 1988). Mature grasses only flower (in ambient outdoor conditions) during their growing season, which normally coincide with the warmer and sunnier season in the location (Tooke and Battey, 2010). The season is normally considered to be around April to September in the Northern hemisphere (Adams-Groom et al., 2020) and around October to March in the Southern hemisphere (Beggs et al., 2015). Outside of the season atmospheric grass pollen concentrations tend to be low. Pre-seasonal meteorological conditions and off-season growth will be a major determinant to the seasonal health of grasses (Förster et al., 2018). However, the definition of what constitutes 'pre-seasonal' is uncertain, with some studies speculating that the few proceeding months being the most important (e.g. Brown et al., 2019), while other studies speculating that the entire time from the last season will be important (e.g. Hurtado-Uria et al., 2013). The continual growth will further depend on the balance of temperature and water conditions (see above section on the general biology). Growth stimuli from meteorology will impact grasses based on a positive skewed normal distribution in each taxonomic sub-unit (genus, species, population and individual) (Poorter and Garnier, 1996). This will create a distribution of emergence in which some plants emerge quickly, most plants emerge at a 'normal speed' and some plants emerge slowly. This pattern will also be seen in the maturity and other life-history traits, such as flowering (Heide, 1994, 1990). The divergence showcases the pattern on temporal delay between first flowering and the peak or full flowering of each taxonomic unit at each location (León-Ruiz et al., 2012). The divergence is fully illustrated in the seasonal atmospheric pollen load, mainly from the initial slow increase in pollen concentrations caused by plants that have started to flower early, but then further accelerated when the main proportion of plants starts to

flower (Kmenta et al., 2015). Taxonomic units that flower later in the grass pollen season (when the main proportion has finished flowering) will contribute to the end-tail of the seasonal pollen load (Bastl et al., 2020).

Based on the strength of the connection between plant growth and optimal meteorological conditions each season will vary in strength with regards to the amount of grass pollen grains released and captured for pollen monitoring (Karatzas et al., 2019). The monitoring of pollen can create an absolute value of the amount of pollen captured, along with dates relevant in terms of start, peak and end of the season (Emberlin et al., 1994; García-Mozo et al., 2010a). The use of these data enables yearly (or seasonal) comparisons, that can inform the presence of long-term trends (e.g. Besancenot et al., 2019; Ruiz-Valenzuela and Aguilera, 2018). Variations to the long-term trend can indicate changes to the grass flowering equilibrium of the location. These changes can have many different causes, with the most common ones being climate change (Ghitarrini et al., 2017b), extreme weather events (Alba-Sánchez et al., 2010) and land-use change (Emberlin et al., 1999). Climate change have so far mainly contributed to increased average global temperatures (Hansen et al., 2006), a factor which will cause earlier plant emergence and maturity (Park and Schwartz, 2015). Earlier maturity will cause earlier flowering (Park, 2014) that will cause earlier pollen release. Future climate change scenarios have suggested further increases in average global temperatures along with altered precipitation patterns (Alexander et al., 2006), which will further change the grass growth dynamics. Climate change is also suggested to be the cause of more extreme weather events (Easterling et al., 2000) (divergence from normal meteorological norms), causing unpredictable consequences in terms of plant and pollen dynamics (Jentsch et al., 2009). Additionally, climate change is predicted to increase grass pollen season severity by increasing grass pollen production, caused by increased temperatures and CO_2 (Kurganskiy et al., 2021). Although these factors are likely irreversible, land-use change is mostly reversible (Drummond et al., 2015). The change in land-use can cause alterations to the long-term trend depending on the altered abundance of grass pollen source areas (Theuerkauf et al., 2015). Simply, increases in source areas are likely to increase the pollen contribution while decrease in source areas are likely to decrease the contribution. Source areas here is strictly translated as areas where grass plants are present in a notable abundance and contributes meaningfully to the atmospheric pollen load. Speculatively, the long-term change in management of source areas is here of comparable importance, with change in management being potentially more important than the increase or decrease in total area (see above section on general biology). To draw definitive conclusions about the

atmospheric pollen contribution of each source area it is important to also include the life-history progression for the species present: their phenology.

1.5. Grass Phenology

The life-history of an organism is the sequential developmental patterns and features it utilizes during its lifecycle from birth to death, such as dispersal, longevity, growth and reproduction (Beckman et al., 2018). Different strategies are utilized by different organisms and have primarily been caused by and improved upon by evolutionary pressures (Adier et al., 2014). The temporal aspect of life-history development is called phenology (Fenner, 1998). Plant phenology is the study of periodicity in plant growth, with identifiable stages present throughout the development (e.g. Cornelius et al., 2014, 2011). Each plant taxa will have specific identifiable phenological stages, each with specific requirements and growth factors to initiate and progress to the next stage (Meier et al., 2009). For angiosperms (flowering plants) the common identifiable phenological stages include germination, leaf development, shoot development, flowering, fruit development and senescence. The phenological progression of grasses can be described in the same way (e.g. Hong et al., 2011), due to their status as angiosperms. Here, the developmental rate of each stage will depend on above-mentioned meteorological factors such as temperature, solar radiation, precipitation, humidity, soil nutrients etc. (Li et al., 2018; Nord and Lynch, 2009), with a fine balance determining how quickly each stage is reached within each plant. The description of plant phenology is normally straight forward due to the identification of predefined events in plant development (e.g. Meier, 2018; Puppi and Zanotti, 2011), at least when investigation one easily distinguishable plant individual. While one grass plant is the emerging plant from one germinated seed the physical limitations of one plant becomes uncertain due each plant being able to produce many shoots. Each shoot is called a tiller, with all tillers being connected to the same plant (Cope and Gray, 2009). The plant can also produce side-shoots (tillering), which can create the appearance of a new plant, while being connected above or below ground in a network-like structure (Jewiss, 1972). This behaviour can create large patches of grass-covered surfaces with only a few numbers of actual plants or individuals. Another inherent feature that is key to their ecology and to a plant's phenology is the lifespan. Grasses can either be annuals (completing their life-history in one season) or perennial (completing their life-history in more than one season). About 18% of all grass species are considered annuals while the majority, 82%, are considered as perennials (Clayton et al., 2002). The lifespan of a grass will have fundamental implications to its ecology and phenology, due to perennials being able to survive several seasons while annuals cannot. Perennials can therefore accumulate resources between seasons, produce

additional side-shoots and colonize larger areas than annuals, all features that will increase their survivability (Friedman and Rubin, 2015). However, annuals have higher growth rates and would be the favoured life-strategy in unpredictable environments (Garnier, 1992). The inherent difficulty of observing phenological development of individuals (due to the abovementioned reasons) means that only specific tillers can adequately be monitored for phenological progression. Most studies have therefore focused on describing the phenology of individual tillers (e.g. León-Ruiz et al., 2011; Rojo et al., 2017). The phenological stage of interest will depend on the focus of the study, with germination of seeds might be important to some and seed maturity being more important to others. While every single phenological stage contributes to the overall dynamic of how the grass pollen season progresses due to plant growth, only the flowering stage will directly contribute to releasing pollen (e.g. Tormo et al., 2011).

1.5.1. Flowering Phenology

The progression of flowering phenology in grasses is broadly defined as the duration and events present between the creation of an inflorescence and seed set (Smith, 1944). Normally, the grass flowering commences with the extrusion of the first visible anther from the male-part of the flower (anthesis). This event is defined as the first flowering in a tiller, plant, population or species for a specific area and year. Anthesis is distinct from heading (the appearance of the first flowering head) and pollen release/dispersal (the release of pollen from the anther). Each event depend on the previous in a specific sequence: heading first, anthesis secondly and pollen dispersal last. One flowering individual is not noteworthy in terms of generalization of an entire population or area; however, the addition of several locations and years can reveal underlying trends in plant ecology (Estrella et al., 2006; Kožnarová et al., 2011). First flowering showcases that enough growth stimuli have been accumulated in at least one plant within one area to start the flowering (Liem, 1980). First flowering is a standard comparative measure when it comes to comparing the phenology between years and regions (Oteros et al., 2015). It is also used to investigate the effects of climate change (Bertin, 2015). The first flowering is the first tail-end of the normal distribution of plant responses within a population, with increasing amount of plants starting to flower as time moves on in the flowering season (Clark and Thompson, 2011). The flowering continues with more anthers extruding from the inflorescence. The continual emergence is normally classified as the progression of flowering, with some studies categorizing the progression as low, medium and high flowering based on the percentage of anthers extruded for each tiller (e.g. Cebrino et al., 2016). The current general level of flowering in each population can be assessed by averaging the progression of a set of individual observed

tillers, with the set used by most studies being around 25 tillers per species and site (e.g. Frenguelli et al., 2010; Rojo et al., 2017). By using this sampling strategy of sampling (a small subset of the larger population), you can gain an adequate representation of the larger population (Jochner et al., 2012). This approach has been used by several studies to describe the sequential flowering progression of many local grass species (e.g. Kmenta et al., 2015; Rojo et al., 2017). Conclusions gained from these studies will fundamentally depend on the methodology utilized. Increased observation frequency will reveal more about the temporal pattern present between visits (e.g. Grégori et al., 2019). Increased number of individuals observed will increase the representability of the population and reduce the general margin of error (Fox and Kendall, 2002; Koons et al., 2016). Increased number of locations investigated will reveal potential spatial patterns in the flowering progression over larger areas (Cebrino et al., 2018). Probably the most important methodological parameter is the compartmentalization of the flowering progression. By dividing the phenological progression in smaller separate sections more information can potentially be gained. The published literature on flowering phenology in relationship to the aerobiological contribution range the observed phenological phases between one and seven (e.g. one in Bartošová et al., 2015; seven in Ghitarrini et al., 2017a). One phase is commonly used when the interest is mainly on first flowering (e.g. García-Mozo et al., 2010b). Progressively more phases are utilized based on the interest in specific changes within the population, such as first flowering, full flowering and senescence (e.g. Frenguelli et al., 2010; Grégori et al., 2019). The highest number of phases are utilized when there is a suspected differentiation in the effects of each phase, such as with pollen release (e.g. Ghitarrini et al., 2017a). The main rationale is that increased amount of mature and extruded anthers will theoretically increase the amount of grass pollen that can be released, with the peak flowering being the potentially most active section of the phenological progression in that regard (Liem and Groot, 1973). This amount will thereafter decrease due to pollen depletion of the plant (Viner et al., 2010), while absolutely reached at anther fall-off, grass seed maturity or senescence. The exact temporal pattern of when and how much pollen are dispersed from the inflorescences is currently unknown due the missing connection between flowering and species pollen release. The pollen release however happens to all species, which creates a sequential species pollen release profile, which unfortunately is inaccessible through light-microscopy due to the morphological similarity in grass pollen grains, as stated earlier. Instead, the sequential flowering progression of many species is usually correlated with the general atmospheric grass pollen concentration (e.g. Kmenta et al., 2017). This approach can suggest which species that are likely to be mostly responsible for the pattern seen in the general season (Munshi, 2000). The drawback with this approach is that it lacks species-specificity, and without specificity it

is less useful for medical practitioners, the general suffering public, and researchers alike. Instead, to discern the species-specific grass pollen contribution other more advanced detection methods can be utilized.

1.6. Molecular approaches using eDNA

Several methods can be utilized to detect the distribution of species-specific pollen. The most common methods are through identifying specific sections of DNA present in each pollen grain (Montserrat Gutierrez-Bustillo et al., 2016). The samples collected directly from the environment are called environmental DNA (eDNA) and are mostly referred to unspecific samples collected from the atmosphere, water or soil (Creer et al., 2016). First, the pollen is collected from the atmosphere using atmospheric samplers (or simply harvested from inflorescences), then the DNA is extracted for further analytical methods (Núñez et al., 2016). The methods utilized to analyse these samples are called metagenomics, and it includes the genetic study of non-specifically collected samples often containing many genomes (Bohmann et al., 2014). These methods include (but are not limited to) Polymerase Chain Reaction (PCR) (e.g. Kraaijeveld et al., 2015), quantitative PCR (qPCR) (e.g. Teng et al., 2016), shotgun sequencing (e.g. Parducci et al., 2019) and DNA metabarcoding (e.g. Leontidou et al., 2018). PCR and qPCR (and similar methods) form one bulk-section of genomic techniques since they rely on species-specific probes and primers and can only detect one species at a time (Longhi et al., 2009). PCR can detect the presence/absence of the DNA of a species, while qPCR can detect the amount of DNA of the species (Fröhlich-Nowoisky et al., 2016). The advantage of using these methods is their relative simplicity (Bustin et al., 2005; Garibyan and Avashia, 2013). The disadvantage is that they are species-specific and prior knowledge of the targeted organism is required. They also require pre-developed species-specific probes or primers, which might be difficult to design (Bustin and Huggett, 2017) or not be commercially available for the required species. This might therefore require the investment of time and resources for development. One study as of date has utilized the potential to use qPCR methods to explore the species-specific grass pollen season in Perugia, Italy (Ghitarrini et al., 2018). Shotgun sequencing and DNA metabarcoding (and many other similar methods) form another bulk-section of genomic techniques. These techniques use sequences, the order of the DNA nucleotides, to determine to which species the DNA belong (Bell et al., 2016; de Vere et al., 2012). Shotgun sequencing uses long sequences (Núñez et al., 2016) while DNA metabarcoding normally uses shorter sequences (Aguayo et al., 2018). Note that other additional features distinguish these methods from each other. The advantage of these techniques includes non-specificity since they will equally sequence all the DNA present (Fazekas et al., 2008). The

potential disadvantages are that the techniques are more complex and are only semi-quantitative. The semi-quantitativity is reflected in the fact that the methods showcase relative abundance of each sequence and species in the samples but not absolute abundance (Dormontt et al., 2018). The methods also require supplemental data to generate species-specific information. This information is called bioinformatics and include methods and approaches to interpret large and complex datasets of biological molecular data (Diniz and Canduri, 2017; Saeys et al., 2007). Each interpretation of samples also requires a pipeline. The pipeline is a set of pre-processing steps required to format, align and quality control all sequences before being interpretable (Bik et al., 2012). The use of a bioinformatics pipeline and database is fundamental in interpreting the sequences and to connect them to specific species (Creer et al., 2010). One study as of date has investigated the species-specific grass pollen season from several locations in the UK using DNA metabarcoding (Brennan et al., 2019). No single study has yet connected the species-specific pollen concentrations with the same-species flowering progression.

The atmosphere also contains other species-specific derivates originating from pollen grains, with allergens being the main example (e.g. Buters et al., 2012). Allergens can be analysed directly by several techniques, with two prominent examples being through enzyme-linked immunosorbent assay (ELISA) (Pilette et al., 2007) and mass spectrometry (MS) (Schenk et al., 2010). Both methods are considered analytical chemistry methods (Stenken and Poschenrieder, 2015). The ELISA methods use specific antibodies that can detect specific allergens (e.g. Buters et al., 2008; Tripodi et al., 2012). Some antibodies are specific to one specific allergen while other antibodies can detect multiple allergens both within and without chemically similar allergenic groups (Fahlbusch et al., 1993). While there is possibility to determine the concentrations of atmospheric allergens using this approach, there is a lack of studies connecting the allergen concentrations with both grass pollen concentrations and flowering (see Plaza et al. (2016) and Ščevková et al. (2020) regarding the disconnect between grass pollen concentrations and the grass allergen *Phl p5*). Mass spectrometry on the other hand compares the mass-to-charge ratio of ions and displays it as a mass spectrum of present chemical components, for example allergens (e.g. Chabre et al., 2010; Fenaille et al., 2009). By analysing the mass spectrum data and comparing it to a known database it is possible to determine which chemicals are present in the sample (Aebersold and Mann, 2003).

2. Rationale

This chapter presents the rationale for the following research chapters. It contains the general knowledge gaps as identified from the background literature and focus associated with this PhD project. Key studies are presented and summarized as the current knowledge and progression within the selected and relevant interconnected research fields. Furthermore, the specific knowledge gaps stemming directly from the key studies are discussed, with the connected aims and objectives forming the backbone of this PhD project.

2.1. General Knowledge Gaps and Project Focus

Several gaps in current knowledge regarding grass phenology, grass pollen and grass pollen allergies and connections between them could be identified from the background (**Figure 1.**).

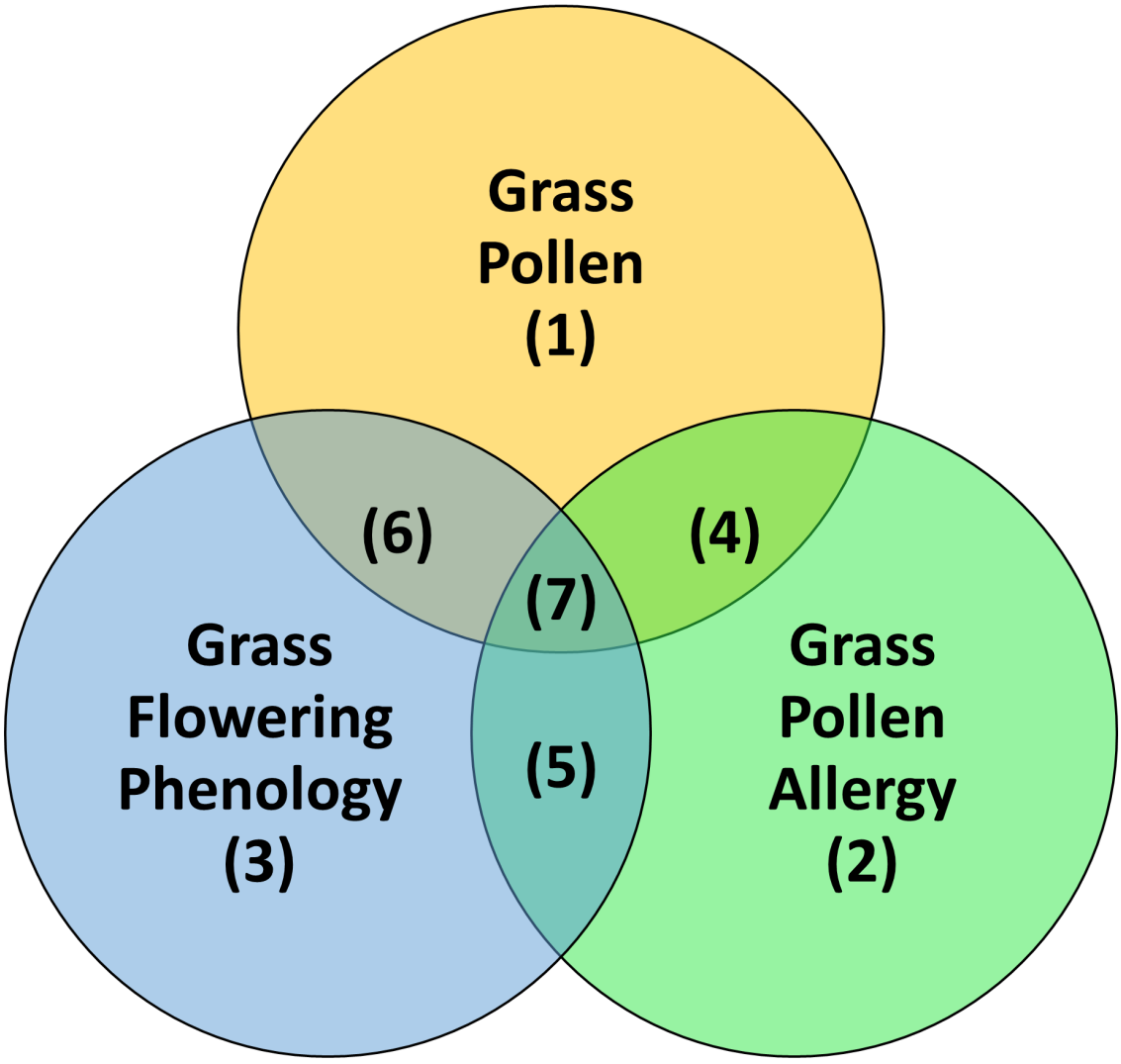

Figure 1. Venn diagram over the seven identified knowledge gap areas within grass pollen allergic research.

Grass Pollen (1): The definitive causative factors of spatial and temporal grass pollen fluctuations and how much each factor contributes to the fluctuations. Predictive modelling approaches that can be adapted to all biogeographical regions and pollen of all grass species.

Grass Pollen Allergy (2): Biochemical interactions and cross-reactivity between all grass pollen allergens. Optimal mixes of grass pollen allergens used in immunotherapy. Identified biochemical functions and potential homology between all grass pollen allergens.

Grass Flowering (3): Variations in spatial and temporal patterns of species-specific grass flowering phenology and detailed biogeographic distribution associated with these species. Modelling of demographic, stochastic, meteorological, and biogeographical processes to predict species-specific grass establishment, growth, and flowering.

Grass Pollen in connection with Grass Allergy (4): Identification of most to least allergenic grass species based on biochemical and immunological analysis of grass pollen. Demographic immunological distributions of most to least common grass pollen allergy within global, regional, and local human populations.

Grass Flowering in connection with Grass Allergy (5): Quantification of aerosolization of plant-parts of grass flowers (excluded grass pollen) and the allergenicity of these plant-parts. Identification of the transportation pathways and distances of these plant-parts.

Grass Pollen in connection with Grass Flowering (6): Predictive modelling of species-specific grass pollen release, with focus on how, when, and how much pollen is released. Predictive modelling of anthesis dates within individual grasses, populations and species based on meteorological, biogeographical, and genetic factors. Identification of causes and quantification of the temporal delays between anthesis and pollen release.

Connection between Grass Pollen, Grass Pollen Allergy and Grass Flowering (7): Identification of a unified theory and a predictive spatial and temporal pathway that can backtrack an immunological response in patient caused by a grass pollen allergen back to the anther it originated and all intermediate steps caused by plant maturity, pollen release, atmospheric transport, biochemical interaction, and immunological pathway.

2.1.1. Project Focus

The overall focus of the PhD project is to investigate the mechanistic connection between spatial and temporal trends in atmospheric grass pollen distributions and the flowering process of allergenically relevant model grass species. The extent of this focus can be isolated from the Venn diagram above (Intersecting areas **1, 3** and **6** in **Figure 1.**).

2.2. Key Studies

A limited number of studies have been published in association with the interconnected focus illustrated in the three intersecting areas mentioned above (**1, 3** and **6**). The focus of these studies was to ascertain the connection between flowering grass species and the observed pattern of grass pollen dynamics, and to what extent individual species could be held responsible for the observed trends. Prior to 2010 only one study can truly be considered to connect grass flowering phenology with atmospheric grass pollen dynamics. Ickovic *et al*. (1989) compared in 1989 the length of the flowering period of multiple grass species in France in connection with atmospheric grass pollen measurements. They concluded that many grass species starts flowering weeks before the first peak in the pollen curve is observed, suggesting a temporal disconnect between the two.

Three studies were published in 2010-2011, all suggesting that phenological information of local grass species can provide increased understanding of aerobiological data (Frenguelli et al., 2010; León-Ruiz et al., 2011; Tormo et al., 2011). Tormo *et al*. (2011) investigated the connection between 24 species of pollen shedding grasses and the seasonal pollen curves for three separate years in Spain, and concluded similarly to Ickovic *et al.* (1989) that there is a substantial disconnect between the two. However, they suggested that likely reasons for the discrepancy included delays between pollen release and appearance of pollen in the atmospheric record. They concluded that likely causes for this was the dissimilar sampling frequency between weekly species phenology and atmospheric pollen loads. In addition, the large number of species made the differentiation of contributing species difficult. Frenguelli *et al.* (2010) collected phase-specific flowering data every ten days in ten species from three regions in Italy and connected this data with the seasonal pollen curve. The phase-specific data was collected to represent times when each species would release pollen. The study concluded that grass species likely release pollen differentially due to flowering periods, and that all species likely contributes to the annual pollen curve although not equally. León-Ruiz *et al.* (2011) investigated weekly phase-specific phenology in 33 species, from 10 locations during three years to gain comprehensive phenological timeseries, and then used statistical correlations to connect each species and year with pollen data. From combining these correlations with pollen production estimates they concluded that four species were more likely to be important to the annual pollen curve around Córdoba, Spain, than others: *Dactylis glomerata, Lolium perenne, Vulpia geniculata* and *Trisetaria panicea*. These three early studies highlight that the connection between species-specific flowering and the seasonal pollen curve is complex, mainly due to the

overlap of sequentially flowering species, each with long flowering periods that is clouding the overall connection.

Further six focus-oriented studies were published between 2016-2018, plus one in 2020 (totalling seven studies). Although slightly different in specific methodologies all seven follow in the footsteps of the previous three, with a species-specific community-structure of flowering grasses that is connected with observed trends in the seasonal pollen curve (Cebrino et al., 2016; Ghitarrini et al., 2017a; Kmenta et al., 2017, 2016; Rojo et al., 2017; Romero-Morte et al., 2020, 2018). What sets these studies apart from the previous three is the integration of other additional estimates of connection between phenology and the pollen curves. Cebrino *et al*. (2016) showed in Spain, using a similar approach to León-Ruiz *et al.* (2011), in which Cebrino *et al.* investigated fewer species (13 instead of 33) but a longer time-series (10 years instead of 3), that there is large yearly variation within the weekly species-specific flowering dynamics, the seasonal grass pollen curve and between habitats. They concluded through the overarching trends in phenology and pollen curves that some species reached full flowering more often during times of atmospheric pollen peaks, suggesting that these species were more likely to be connected with these peaks. Four species were suggested to be more connected with these peaks: *Dactylis glomerata, Lolium rigidum, Trisetaria panicea* and *Vulpia geniculata.* Kmenta *et al*. showed through a pilot study in Austria (2016) and an international study in Austria, Finland and Germany (2017) that the combination of grass pollen dynamics, twice-weekly community-phenology and species-specific allergy-symptoms could shed new multidisciplinary-light on the overall connection. They found that the same species that reached full flowering during the highest peaks of the seasonal pollen curve also caused strong allergenic symptoms in exposed subjects. The five taxa considered most likely to drive these effects were *Dactylis glomerata, Lolium perenne, Poa pratensis, Arrhenatherum elatius* and *Festuca sp.* These studies highlight that it is possible to narrow down the likely candidate species responsible for major parts of the seasonal pollen curve by using longer time-series and immunological effects.

Another option of discerning potential species-specific importance to the seasonal pollen curve is to create an index that is based on factors likely to influence the overall pollen contribution, an approach adopted by two of the seven studies (Ghitarrini et al., 2017a; Romero-Morte et al., 2018). Ghitarrini *et al.* (2017) used a bi-weekly score-based seven-phased phenological method to measure flowering progression in Italy and combined this progression with life-cycle characteristics and regional abundances to create an index that varies between species. This index was then used to compare both the general and species-specific contribution to the

seasonal pollen curve. Four species were found to contribute the most to the overall index: *Dactylis glomerata, Lolium perenne, Poa pratensis* and *Cynodon dactylon*. However, the flowering periods of all four grasses, and their respective indices, all overlapped, making it difficult to assess their individual importance. Romero-Morte *et al.* (2018) combined weekly phenological progression, pollen production, pollen grain-size and relative habitat-abundance in Spain to create each species-specific index. They then deconstructed two years of seasonal pollen curves (2013 and 2015) to be able to model the overall seasonal pollen trends. These trends were then modelled using a Principal Component Analysis (PCA) to determine which species and factors contributing to the index were the most predictive of the pollen trends. They found that species-specific phenology and pollen production were the most predictive factors, with the species most predictive of the pollen trends being *Dactylis glomerata, Lolium rigidum, Trisetum paniceum* and *Arrhenatherum album*. They also concluded that a small number of species were likely to be responsible for the majority of the seasonal pollen curve. These studies highlight that species-specific factors, which are likely to contribute to the absolute number of pollen being released in a specific area, will have a considerable impact on the seasonal pollen curve.

The two last studies utilized statistical modelling approaches by modelling both pollen trends meteorological trends (Rojo et al., 2017; Romero-Morte et al., 2020) and connecting these trends with the species-specific flowering to identify species likely responsible for the seasonal pollen pattern. Romero-Morte *et al.* (2020) modelled a general seasonal pollen trend in Spain from five years of data and isolated four species (*Bromus rubens, Hordeum leporinum, Trisetaria panicea* and *Dactylis glomerata*) that overlapped in flowering period with the pollen peaks. The trends in meteorological conditions (heat units, sunshine hours, and precipitation) were modelled and compared with the yearly phenological progression (sampled weekly) of the four species. They concluded that meteorological conditions likely impacted the variation seen in phenological progression of these species while the overall trends in sequential flowering remained the same between years. This suggests that the same species are likely responsible between years for the seasonal pattern, even if this pattern shifts by a varied meteorology. Rojo *et al.* (2017) used a STL decomposition trend analysis to simplify and model eight years of seasonal pollen trends in Spain. They then collected weekly phenological progression data on 25 species from 10 sites, and used factor analysis to simplify the species-specific phenological data from all sites. By comparing the observed seasonal pollen curve with the modelled seasonal trend they could identify that the residual removed trend was better at identifying the species most likely to contribute to the seasonal pollen curve. Later flowering

species such as *Aegilopsis spp., Dactylis glomerata, Lolium rigidum* and *Trisetum paniceum* were key species for modelling the seasonal pollen trend. They suggested that future research would benefit from investigating species-specific pollen emission, pollen production and pollen dispersal capacity.

2.3. Specific Knowledge Gaps

Although the studies summarized above have suggested flowering in species likely responsible for majority parts of the seasonal atmospheric pollen curve there has been no direct quantification or mechanistic connection to any particular species or subgroup. The disconnect here is four-fold: I) The use of a general taxonomically-limited grass pollen morphology. II) A correlation between cause and effect without any specific reason or mechanism. III) The use of many species causes conflicting effects and residual noise. And IV) Each species metric is treated monolithically with an average response. Each of these disconnects can be modified to allow for the connection between grass phenology and atmospheric grass pollen levels to be clarified, and will lead directly to a substantial contribution to knowledge within the aerobiological community. The identified gaps in knowledge are therefore:

I) The disconnect in a general atmospheric grass pollen pool that cannot be properly reconciled with species-specific flowering. This is due to the fact that these flowers produce and release species-specific pollen, which cannot be measured and quantified using the standard microscopy approach. Pollen production has in previous studies been used as a proxy-measurement of the species-specific pollen contribution, but without any absolute confirmation. The use of quantitative measures of species-specific atmospheric pollen will aid in the closing of this knowledge gap.

II) The disconnect between the cause and effect of grass pollen. Grass anthers is the cause while the atmospheric grass pollen concentrations is the effect. The connection between these two is pollen release/dispersal, and without this connection the correlation and modelling between flowering and grass pollen levels is at best a cautionary guesswork, and at worst misunderstood and misrepresented. Examination of the release/dispersal process will likely be more accurate in describing this connection. The quantification of pollen release and/or pollen dispersal will aid in the closing of this knowledge gap.

III) The disconnect is the use of a multitude of species with overlapping flowering times. While the use of many species makes it possible to theoretically include or discount many species at once it also makes finding relevant patterns more difficult. It obscures the overall connection, which makes it difficult to find the few species that contributes the most to the study system. The difficulty comes from introducing potentially conflicting effects and increase the overall residual noise of any model. Single-species methodologies can directly quantify the contribution of one species, hence being also able to exclude it from the general effect. The development of single-species methodologies will aid in the closing of this knowledge gap.

IV) The disconnect is treating species phenology as a monolith with one average and one response. In reality each species likely exist as a statistical distribution of different responses and phases, causing variation and a varied response based on the sampling methodology. This disconnect exists both in time and in space. The temporal disconnect is that the mean sampling interval represents every stage in-between, which is not likely to be true. The spatial disconnect is that the finite number of measured individuals in the species represents the species as a whole, which is also not likely to be true. The methodologies utilized in sampling can therefore be adapted to account for the distributional response of species metrics instead of assuming that one mean value of the metric is representative. The use of population dynamic approaches with measured and quantified spatial and temporal variation will aid in the closing of this knowledge gap.

2.4. Aims and Objectives

2.4.1. Aims

The first aim of this PhD project was to identify and model representative sources for atmospheric grass pollen using both remote sensing and field-based observations of phenology. The second aim was to identify and model how pollen release and pollen dispersal in species-specific populations can be utilized to connect phenology and atmospheric grass pollen on both a spatial and temporal scale.

2.4.2. Objectives

The objectives had to fully encompass the research area and specific knowledge gaps in order to fully investigate the connection between atmospheric grass pollen and grass flowering. This meant including many different aspects in both ecology and aerobiology: botany, plant ecology,

pollen dynamics, atmospheric transportation, and meteorology. These aspects were fused using several distinct methods: pollen monitoring, phenological surveying, statistical modelling, weather modelling, atmospheric transportation modelling and molecular approaches. In addition, the use of representative model species that had been identified from the literature as highly allergenic, biogeographically widespread, ecologically common, and high pollen producing would be able to address the knowledge gaps presented above. *Dactylis glomerata* was chosen as a species capable of filling all criteria. The aims of the PhD project was divided into the following four connected objectives that were specifically designed to optimally address the aforementioned specific knowledge gaps:

1) Investigate local to regional spatial and temporal trends in atmospheric grass pollen concentrations in relation to grass vegetation source maps and meteorology using atmospheric and statistical modelling approaches. The investigation can be found in Chapter 4.
2) Investigate spatial and temporal trends in the flowering process of the grass species *Dactylis glomerata* and identify demographic and stochastic elements that can explain the process. The investigation can be found in Chapter 5.
3) Investigate spatial and temporal trends in grass pollen emission processes in the grass species *Dactylis glomerata* by modelling demographic and stochastic elements and combining it with meteorology and species-specific grass pollen levels using molecular approaches. The investigation can be found in Chapter 6.
4) Investigate small-scale grass pollen emission processes in multiple grass species using flowering phenology, grass pollen concentrations, meteorology, wind conditions, particle counters and species-specific grass pollen levels using molecular approaches. The investigation can be found in Chapter 7.

The thesis also contains a background section (Chapter 1), a material and methods section (Chapter 3), a summary section (Chapter 8) and a future works section (Chapter 9).

3. Material and Methods

3.1. Overview of Experimental Designs

Four sets of experimental designs were created to encompass each objective described above.

3.1.1. Experimental Design Objective 1

Grass pollen monitoring was conducted during four years (2016-2019) in two locations (St Johns and Lakeside) to investigate the spatial and temporal variation in grass pollen dynamics. The pollen monitoring data for the latter two years were additionally used to model the likely origin of the grass pollen using the atmospheric transportation model HYSPLIT and grass vegetation source maps. The model results were further combined with local meteorology and modelled with a generalized linear mixed-model to identify if this had an effect on the overall grass pollen levels.

3.1.2. Experimental Design Objective 2

Phenological observations of *Dactylis glomerata* populations with focus on flowering were carried out during the course of two years (2017-2018) to observe if demographic trends and stochastic elements could be identified and if so, how these variables varied. The flowering phenology was focused on the progression of the extrusion of anthers. Daily flowering progression was investigated in 2017 for one population while bi-daily and ten times seasonally progression was investigated in 2018 for a total of eight populations.

3.1.3. Experimental Design Objective 3

The identified demographic trends and stochastic elements from above were utilized to model general flowering populations of *Dactylis glomerata* using Markov Chain modelling approaches. Pollen release estimates were then modelled using assumptions of equivalent pollen release in these modelled populations. The pollen release estimates were then connected with species-specific eDNA analysed through molecular metabarcoding methods and modelled to estimate how well the modelled pollen release estimates represented reality via the collected eDNA.

3.1.4. Experimental Design Objective 4

Local-scale grass pollen monitoring was conducted in three rural sites with distances between the sites of about 300m to investigate how grass pollen varied spatially and temporally on a local scale. Species-specific flowering phenology was also observed in a managed area surrounding one of the monitoring stations. eDNA was collected (and processed using DNA metabarcoding) in all three sites to investigate the relationship between flowering phenology in

the managed area and potential grass pollen dispersion between sites. Meteorology and wind conditions were also modelled to investigate how these factors influence the local grass pollen dynamics.

3.2. Pollen Monitoring

The section below contains all materials utilized and methods used in relation to the pollen monitoring of grass pollen employed during the entirety of this doctoral study. It also contains descriptions of the sampling locations, information about the generated pollen data and descriptions of the particle counter methods and equipment used. All pollen-monitoring methods in this section are established methods developed and expanded upon by previous research.

3.2.1. Monitoring Methods used for Optical Recognition of Pollen Grains

The section below contains information regarding the air-samplers used, how the sampling drums are prepared, how the microscopy slides are prepared, the features used to identify grass pollen and the counting methodology applied. The below mentioned methods are the standardized methods of pollen monitoring utilized by the National Pollen and Aerobiological Research Unit (University of Worcester) and the United Kingdom pollen-monitoring network (e.g. Emberlin et al., 2007, 1994; Pashley et al., 2009; Skjøth et al., 2015). All training in aerobiological sampling procedures, pollen monitoring, pollen identification, and microscopy counting methods were undertaken in the Basic Aerobiological Course in Gothenburg during the summer of 2017 and in the University of Worcester's internal pollen training during the summer and autumn of 2017.

3.2.1.1. Sampling Equipment

The Seven-day Volumetric Spore Trap of Hirst design (Hirst, 1952) was used to conduct air sampling for all the below mentioned pollen monitoring datasets. Burkard Manufacturing Co Ltd. manufactures the set of samplers currently being used by University of Worcester. All references to the Volumetric Spore Trap will onward be referred to as Burkard trap (**Supplementary Figure S1.**). The sampler collects bio-aerosols and other particulates in the air by active-sampling using a pump-system that sucks 10 litres of air per minute (nominal rate) (Henningson and Ahlberg, 1994). The actual sampling rate has recently been questioned by the wider aerobiological community due to observed differences in flow rate between samplers (Oteros et al., 2017). However, this concern is likely minimal due to the regular calibration and flow rate tests conducted between the University of Worcester samplers. The air is sucked over a rotating collection surface commonly referred to as a pollen drum, on which the airborne

particles impact and stick (Galán and Domínguez-Vilches, 1997). The pollen drum rotates with a speed of 2 mm per hour and can sample a total period of 7 days (168h). Additionally, the height of the pollen sampler have been shown to play a role in the interpretation of the collected pollen analysis and results (Rojo et al., 2019). The reasoning is that sampling should be done elevated from the terrain and that the typical recommendation being about 10m, while lower elevations can be justified based on the circumstance (Hugg et al., 2020). However, one study has demonstrated that there is no significant difference in *Poaceae* pollen concentrations between sampling at ground levels in contrast to altitude of 16m (Fernández-Rodríguez et al., 2014).

3.2.1.2. Pollen Drum Preparation

Each aluminium pollen drum is prepared by first cleaning the outer area with 70% ethanol to remove potential residues or contaminants from previous sampling periods. The drum is then loaded onto a stationary platform for stability. A sticky double-sided tape is then placed on the outer area to hold one drum-rotation of 'Melinex'-tape. The drum is then placed on a portable heater and heated until the top of the drum is almost too hot to touch. A thin layer of warm adhesive medium made of petroleum jelly and Vaseline is then added with a brush over the 'Melinex'-tape. The drum is then spun on the stationary platform to allow for the mixture to spread evenly and to encourage the mixture to cool. The prepared drum is then stored in room temperature in a clean storage box to prevent contaminants before being used for air sampling in combination with the Burkard trap (for detailed protocol, see Lacey and Allitt, 1995). A few different adhesive materials can be used (e.g. Silicone) but they all have generally the same sampling efficiency (Galán and Domínguez-Vilches, 1997; Maya-Manzano et al., 2018).

3.2.1.3. Microscopy Slide Preparation

When each drum has sampled for its specified period it is stored in a 4-degree fridge to prevent sample-degradation until microscopy slide preparation. To prepare the slides the tape is removed carefully from the drum and placed face up on a mounting block. Each marking on the mounting block corresponds to a 24h period, and this is utilized by using the markers as guides and cutting the tape into seven sections, each corresponding to one day. Each piece of tape is placed on pre-marked microscopy glass slides with a few drops of water already on the slide to facilitate adhesiveness. A few drops of warm 'Basic fuchsine pollen mountant' are placed on a cover glass slip, and then quickly placed on the microscopy slide containing the tape. The fuchsin pollen mountant is a deep magenta colour and works by binding to the outer pollen wall, making it easy to distinguish pollen during microscopy. Each slide is then left to cool to allow the mountant liquid to harden. When cool, each slide is sealed with varnish to

prevent content to leak and dry out, contaminants to get in and for long-term storage (**Supplementary Figure S2.**) (for detailed protocol, see 'Use of the Burkard Spore Trap' by Dr. Estelle Levetin (Levetin, 2013))

3.2.1.4. Counting Methods

There are three main counting methods employed by the aerobiological community in regards to pollen monitoring: the 'Transverse transects method' (e.g. Peel et al., 2014), the 'Longitudinal transects method' (e.g. Bilińska et al., 2019), and the 'Random field method' (e.g. Käpylä and Penttinen, 1981), with the two former ones being the most commonly used (Cariñanos et al., 2000; Galán et al., 2014). The method used by these studies and by the University of Worcester and the UK network is the Transverse transects method, but studies have shown that the methods are comparable with the assumption that similar areas of the slide are being counted and extrapolated from to derive at the daily concentrations (Galán et al., 2014). The Transverse transects method works by observing one transect every 4mm of the slide, resulting in 12 transects in an average placed slide (Comtois et al., 1999). Both random and systematic errors have to be taken into account before counting each slide (Oteros et al., 2013). All pollen found in each transect are counted, resulting in 12 bi-hourly values for each slide. These values are then summed and multiplied with a correction factor (a fractional number from 0 to 1), based on the number of transects and specific to each microscope (based on the area of the field of view) (Comtois et al., 1999). The correction factor itself is based on the area of the slide counted and the total volume of air collected by the sampler for the slide. The final number is expressed as a concentration of grains of pollen per cubic meter of air (p/m^3) averaged for the duration of the slides' sampling period (24h) (Galán et al., 2017). The bi-hourly pollen concentrations can be isolated using the 12 bi-hourly values and multiplying it with 6.12, a factor that will also vary based on the number of transects counted. The sampling period can vary depending on the equipment and methodology utilized, but the standard trap utilizes a 24h periodicity per slide. All microscopy slides were counted using a Nikon Eclipse E400 microscope in x400 magnification, hence eliminating the uncertainty with the use of multiple microscopes or magnifications.

3.2.1.5. Pollen Identification

Grass pollen are characterized by their monoporate and spheroidal/ovoid shaped grains (Jan et al., 2015). The normal size range is between 25μm and 40μm, with grains from agricultural species (such as wheat, oats etc.) being noticeably larger than 40μm (Joly et al., 2007). Two key defining features are the finely granular exine and a single circular pore with an operculum (Morgado et al., 2015). When stained with Basic fuchsine (see section 3.2.1.3.) proteins in the

grass pollen grain outer wall turns pink, with the depth and shade ranging from light pink to dark magenta dependent on the amount of staining and the amount and colour of the protein (**Figure 2.**). Unstained pollen will maintain their natural yellow, slightly green colouring (**Figure 3.**).

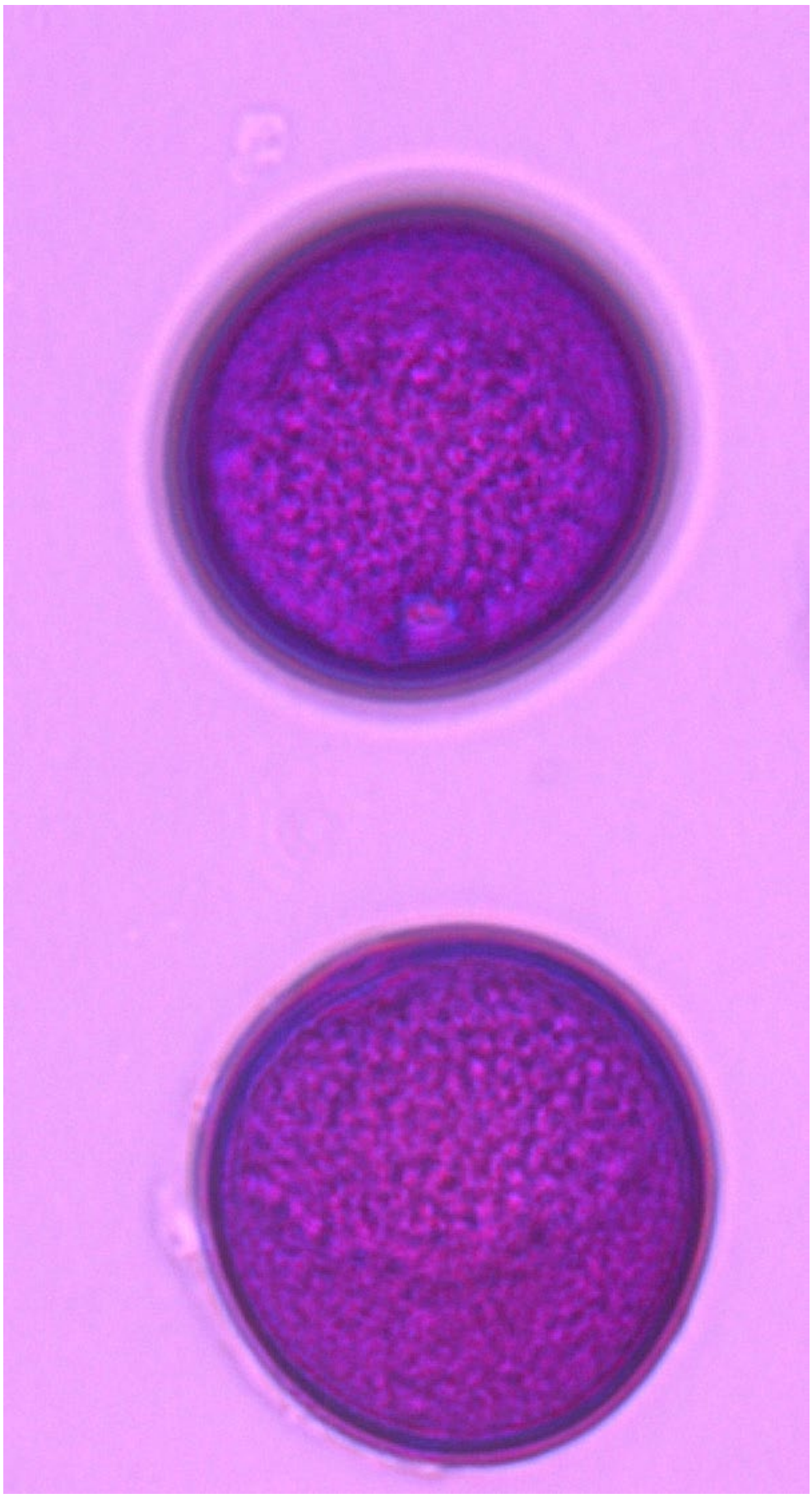

Figure 2. Microscopy photograph of stained grass pollen.

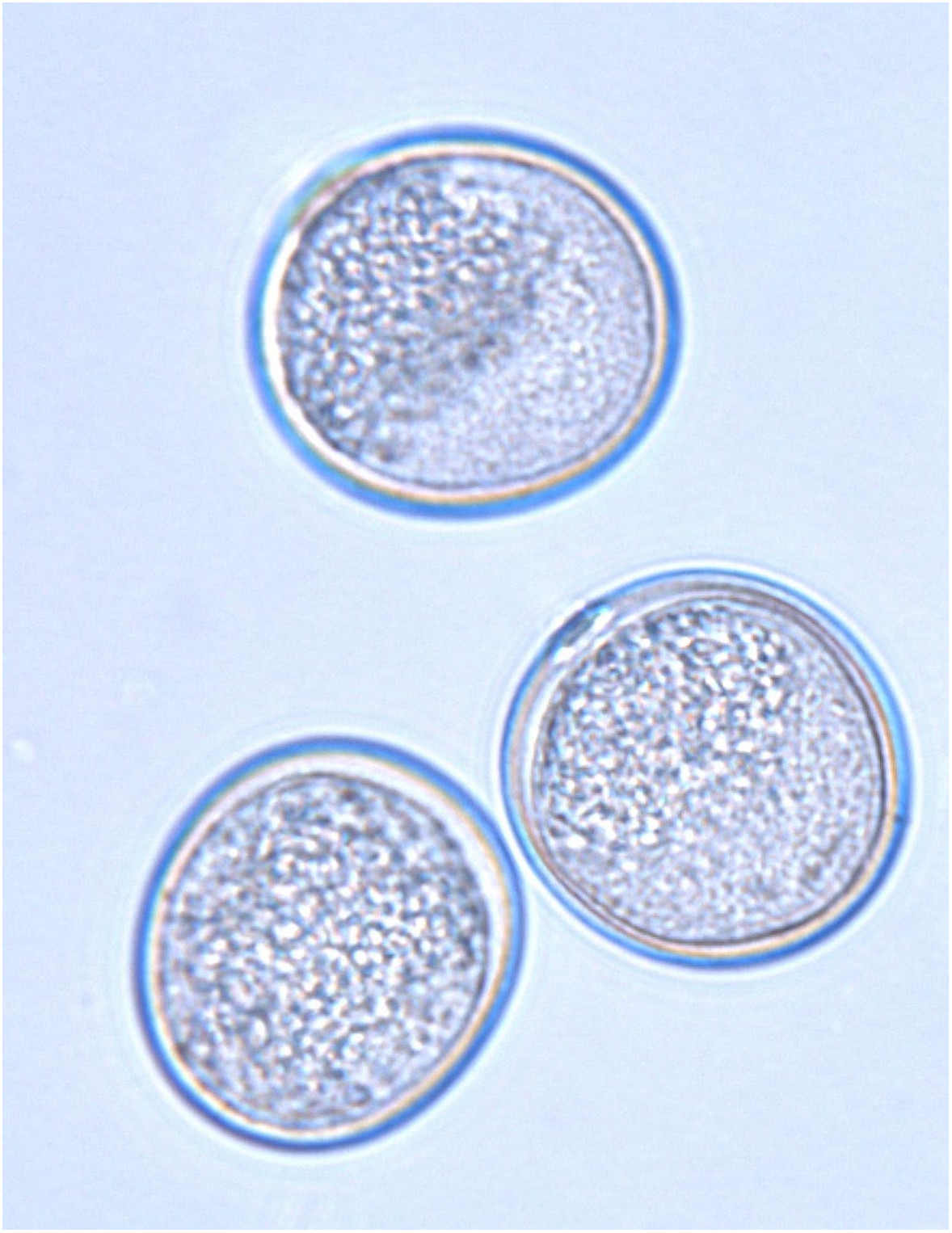

Figure 3. Microscopy photograph of unstained grass pollen.

3.2.2. Sampling Locations

Pollen monitoring equipment was placed at two locations in Worcestershire, both locations belonging to the University of Worcester: St Johns Campus and Lakeside Campus. The information regarding the details of each sampling location along with their surrounding ecosystems and usage can be found below (see sections 3.2.2.3. and 3.2.2.4.). The equipment of both locations consisted of Burkard Traps, Burkard Multi-Vial Cyclone Samplers (see section 3.5.1.1. for more detail), Campbell Scientific logger stations with various meteorological sensors (**Supplementary Figure S3.**) and associated electrical and power equipment. There are also other local and regional meteorological weather stations with associated meteorological sensors that are included within the data framework.

3.2.2.1. Worcestershire Climate

The Worcestershire climate is characterized according to the Köppen-Geiger climate classification as a part of the sub-group oceanic/maritime climate, along with the rest of the United Kingdom (Kottek et al., 2006). The specific climate classification for the UK is **Cfb**, or temperate oceanic climate, and is characterized for its mild wet winters, despite the high latitude, and warm wet summers (Peel et al., 2007). Worcestershire experiences an annual mean temperature of 9.5 degrees, with about 670mm of rain (baseline) (Cavan, 2004). Weather conditions tend to be very changeable from day to day.

3.2.2.2. Main Meteorological Information

The meteorological information to be used in the modelling sections was acquired from five different meteorological loggers based on the year and location due to missing data and the limited data-series length of recently installed loggers (**Table 1.**). Two loggers were used to represent the St Johns location: The St Johns Campbell logger and the Davis logger. They are located 13 meters apart. For 2016 the Davis logger was used alone, for 2017 both loggers were used, while for 2018 and 2019 the Campbell logger was used alone. Three loggers were used to represent Lakeside location: The Lakeside Campbell logger, the Skye logger and the Pershore weather logger. The distance between the Campbell and Skye logger is around 700 meters, while the distance to the Pershore weather logger is around 19 km. For 2016 both the Skye logger and Pershore logger was used, for 2017 all three loggers were used, while for 2018 and 2019 the Campbell logger was used alone. The Campbell's, Davis and Skye loggers are all managed by the University of Worcester and accessed and quality controlled accordingly. The Pershore logger was accessed from the 'Met Office Integrated Data Archive System' (MIDAS) co-opted by The Centre for Environmental Data Analysis (CEDA), the National Centre for Atmospheric Science (NCAS) and the National Centre for Earth Observations (NCEO). The

meteorological weather information was acquired from the station located in Pershore, Worcestershire, UK, maintained by Pershore College. The reason to use several loggers for the years 2016 and 2017 was due to the two recently installed Campbell loggers were installed in the middle of July 2017, while meteorological data was required from the 1st of May 2017 and the entire season of 2016. The Pershore logger was chosen to represent the weather for the Lakeside's missing data period due to its relative proximity to the location, its' use in the standardized network utilized by the UK Met Office and its' long-term reliable usage. The rationale and statistical investigation of the fusion of meteorological data sets in 2016 and 2017 are available elsewhere (see section 3.8.1.). The total datasets consists of many different weather and meteorological measurements, however only a subset of these were collected and processed further. Six variables were isolated (temperature, precipitation, relative humidity, wind-speed, wind direction and solar radiation) due to their common use in modelling pollen dynamics (e.g. Gioulekas et al., 2004; Jung and Choi, 2013; Recio et al., 2010; Ribeiro et al., 2003; Sánchez-Mesa et al., 2002), with these being available at 30min intervals.

Table 1

Breakdown of the percentual contribution of each weather logger to the bi-hourly meteorological data of the season (1st of May to 1st of September) in each year (2016-2019) and location (St Johns and Lakeside).

Location	Logger	Coordinates	2016 Variable		2017 Variable		2018 Variable		2019 Variable	
			Temperature	Precipitation	Temperature	Precipitation	Temperature	Precipitation	Temperature	Precipitation
St Johns	Campbell (St Johns)	52.197N, -2.242E	0.00%	0.00%	31.56%	18.52%	100.00%	100.00%	100.00%	100.00%
	Davis	52.197N, -2.242E	100.00%	100.00%	68.44%	81.48%	0.00%	0.00%	0.00%	0.00%
	Pershore	52.148N, -2.041E	0.00%	0.00%	0.00%	0.00%	0.00%	0.00%	0.00%	0.00%
			100.00%	100.00%	100.00%	100.00%	100.00%	100.00%	100.00%	100.00%
Lakeside	Campbell (Lakeside)	52.251N, -2.253E	0.00%	0.00%	39.72%	26.79%	100.00%	100.00%	100.00%	100.00%
	Skye	52.258N, -2.257E	99.99%	99.99%	54.15%	67.08%	0.00%	0.00%	0.00%	0.00%
	Pershore	52.148N, -2.041E	0.01%	0.01%	6.13%	6.13%	0.00%	0.00%	0.00%	0.00%
			100.00%	100.00%	100.00%	100.00%	100.00%	100.00%	100.00%	100.00%

3.2.2.3. St Johns Campus

The location St Johns Campus is the main campus for the University of Worcester in Worcester, Worcestershire, UK (*52.193N, -2.221E*). The surroundings (< 200m) are mainly comprised of residential houses with associated garden vegetation and various university buildings with associated park landscapes, with a smaller part of public infrastructure such as roads, hedges, and lawns. All the sampling equipment is located 10m above ground on a stationary metallic rail structure on the large roof of the Edward Elgar building, with a central placement of the samplers to avoid edge effects and air updrafts caused by the building. This pollen sampler is part of the University of Worcester pollen-monitoring program and has been active for pollen collection since 1996 (Emberlin et al., 2007).

3.2.2.4. Lakeside Campus

The location Lakeside Campus is a secondary campus for the University of Worcester (*52.254N, -2.254E*), located 6.4 km NNW of St Johns Campus in Worcester, Worcestershire, UK. The surroundings (< 200m) are mainly comprised of well-maintained grass areas, lakes, agricultural fields, and pastures, with a smaller part of university buildings and outdoor storage. Two sets of sampling equipment are located at Lakeside, one set for comparative sampling and one set used as an experimental set-up. The comparative sampler has been moved between three different close-by locations (< 300m) due to unforeseen circumstances: location 1 in year 2016, location 2 in years 2017 and 2018 and both location 2 and location 3 in year 2019. Placement for location 1 (*52.253N, -2.253E*) was 4 metres above ground on top of a framework of wooden poles south of the main building, previously (and subsequently) used in climbing and adventure-related activities. Placement for location 2 (*52.254N, -2.253E*) was 4 metres above ground on top of a large portable container north of the main building, previously used as a sports-laboratory. Placement for location 3 (*52.253N, -2.257E*) was 2.5 metres above ground on a cross-arm connected to a portable mast in the shape of a metallic tri-pod structure west of the main building. The 2.5 metres mentioned above was chosen to compare the below mentioned experimental sampler, situated at the same height. The field surrounding placement 3 was regularly cut by a large, motorized lawnmower while the vegetation inside the placement itself was regularly cut using a handheld mower. The vegetation was cut to avoid the localized effect of vegetation, and instead promote the regional profile. Note that both location 2 and location 3 consisted of two separate samplers, active during the same time in 2019, for comparability. The experimental sampler (*52.251N, -2.253E*) is located 2.5 metres above ground on a crass-arm connected to a 10m stationary mast SSW of the main building in a large grass-field (see section 3.3.4.1 for more details). The reasoning behind selecting a sampling height of 2.5 metres

is the assumption that a factor of 10 difference between height and radius of the sampling area (25 metres radius of the sampling circular sampling area) is representative for pollen sampling. See Lakeside sampling locations 2, 3 and 4 in Figure 51 in Chapter 7.

3.2.3. Pollen Monitoring Data

The total grass pollen database utilized in these studies is comprised of daily and bi-hourly grass pollen concentrations that has been summarized from **1229** microscopy slides (**Table 2.**). The Worcester St Johns pollen monitoring station contributed with all slides from 1st of May to 1st of September 2016 to 2019: **492** slides. The Lakeside placement 1 and placement 2 pollen monitoring station contributed with all slides from 29th of June to 1st of September 2016, 22nd of June to 1st of September 2017, 1st of May to 1st of September 2018 and 1st of May to 1st of September 2019: **381** slides. The Lakeside placement 3 pollen monitoring station contributed with all slides from 18th of May to 1st of September 2019: **110** slides. The Lakeside Field (see section 3.3.4.1 for more details) pollen monitoring station contributed with all slides from 1st of May to 1st of September 2018 to 2019: **246** slides.

Table 2

Total number of daily Burkard samples collected and microscopy slides created during the pollen monitoring for all locations.

Dates		**Locations**					**Totals**
Years	Months	St Johns	Lakeside P1	Lakeside P2	Lakeside P3	Lakeside Field	
2016	May	31					31
	June	30	2				32
	July	31	31				62
	August	31	31				62
2017	May	31					31
	June	30		9			39
	July	31		31			62
	August	31		31			62
2018	May	31		31		31	93
	June	30		30		30	90
	July	31		31		31	93
	August	31		31		31	93
2019	May	31		31	18	31	111
	June	30		30	30	30	120
	July	31		31	31	31	124
	August	31		31	31	31	124
Totals		492	64	317	110	246	1229

3.2.3.1. Data Series Formats

The total grass pollen database described above was available in the following formats: Daily pollen concentrations, Bi-hourly pollen concentrations and Bi-hourly pollen counts. The time it takes to replace drums after each sampling-period, and the time to travel to the next site, will create a temporal-difference between the slides/drums of each site. Due to this time-difference, the data points have been shifted to assure temporal comparability.

3.2.4. Particle Counter Equipment

Grass-pollen can be considered as generic particles occupying a certain size-range (Šauliene et al., 2019). The AlphaSense OPC-N2 has previously been used to measure PM1, PM2.5 and PM10 for atmospheric air-monitoring (e.g. Crilley et al., 2018). By using modified AlphaSense OPC-N2 Optical Particle Counters (adapted for a higher size-range) airborne grass-pollen can be monitored with high temporal resolution (10s) (**Supplementary Figure S4.**). The particle counter works by active-sampling using a pump-system that sucks 1.2 litres of air per minute (AlphaSense OPC-N2 Specifications Manual). The particles are then measured with the help of two lasers. The measurement is then placed within one of sixteen size-bins, with the smallest one being Bin00 (0.75μm - 1.46μm) and the biggest one being Bin15 (39μm - 40μm). Most grass pollen has a diameter range between 25μm and 40μm, taking small species-specific differences into account. High temporal resolution grass-pollen monitoring results could potentially be used as a proxy for grass-pollen emission due to the particle counters proximity to the source area (< 1m). The particle counters are controlled using small and portable computers, Raspberry Pi's, developed by the company of the same name. The particle counter, Raspberry Pi's and accompanying electronic equipment are placed together and connected within a weatherproof container and connected to the power-system of the site. The equipment is operated wirelessly through Linux-based software.

3.2.4.1. OPC Method

During the summer of 2019, two boxes of particle counter equipment were placed on Lakeside Campus in a large grass-field (see section 3.3.4.1 for more details) to monitor grass-pollen emission. Ideally, the boxes would have been placed to face the major wind-direction, which was SW for the site. However, there was also a need to place the second sampler in the opposite direction to measure the difference, but NE was the direction with the least wind for the location. Instead, the samplers were placed facing NW and SE, the two second-most common wind-directions. The boxes were placed in the field facing outwards, 10m from the stationary mast (**Supplementary Figure S5.**). A third box of particle counter equipment was placed at location 3 for the comparative sampler location, this particle counter was to be used as a reference to the other two, due to there being no vegetation surrounding this location (**Supplementary Figure S6.**). All boxes were placed to allow for a vertical distance of 50cm between the inlet of the sampler and the canopy of the underlying vegetation, based on experience from previous studies (Šikoparija et al., 2018). This means that the height of the inlet of the two grass-fields counters were 120cm and for the reference counter was 50cm.

3.3. Phenological Observations

The section below contains all methods used in relation to the phenological observations in relation to Poaceae (Grasses) species employed during the entirety of this doctoral study. It also contains descriptions of the phenological observation locations and the importance of each set of the phenological observations. The phenological observation methods (mainly the BBCH-scale (see below)) have been developed and expanded upon by previous research studies. Methods that have been altered or developed for this thesis report will state this (mainly argumentative reasoning in the Population phenological section 3.3.1.1.).

3.3.1. Phenological Method

All phenological observations are modelled after the '**B**iologische **B**undesanstalt, Bundessortenamt und **CH**emische Industrie' system, also referred to as BBCH-scale (Meier, 2018). The system was developed by and for agricultural practitioners, for them to be able to discern and record phenological development of a wide range of possible crops. Each developmental stage is expressed as a two-digit code, corresponding to a primary growth stage and a secondary growth stage within the primary one (Meier et al., 2009). Not all stages are present within all crops, due to developmental differences inherent to each crop. The primary stages utilized by the classification are the following:

0. Germination, sprouting, bud development
1. Leaf Development
2. Formation of Side shoots, tillering
3. Stem elongation or rosette growth, shoot development
4. Development of harvestable vegetative plant parts, bolting
5. Inflorescence emergence, heading
6. Flowering
7. Development of Fruit
8. Ripening or maturity of fruit and seed
9. Senescence, beginning of dormancy

The secondary growth stages are then expressed either as a percentage of the primary stage (for **6.** Flowering it can be the percentage of open flower based on the total possible flower amount), or as secondary observable events within each primary growth stage (for **1.** Leaf development it can be the number of leaves before **2.**). The only primary stage recorded within all the phenological observations employed by these studies is **6.** Flowering and secondary growth stages within this primary developmental stage. For the classification to be accurate to the

species selected (Poaceae) the crop type 'Cereals' was chosen to model flowering phenological development. The secondary stages utilized by the classification are the following:

61. Beginning of flowering: first anthers visible
65. Full flowering: 50 % of anthers mature
69. End of flowering: all spikelets have completed flowering but some dehydrated anthers may remain

Several other studies have utilized the same methodological approach (e.g. Cebrino et al., 2018; Kmenta et al., 2017; Rojo et al., 2017; Romero-Morte et al., 2018). The methodology from two studies that have utilized a similar approach (Léon-Ruiz et al. (2011) and Kmenta et al. (2016)) have been modified for the phenological observations.

Their adaptation of the flowering phenological classification is similar but slightly different. Leon-Ruiz et al. (2011) used the following set-up:

60. Period of time between plant emergence and the start of flowering Phase 0
61. Start of flowering phase – begins with the first open florets and ends with 25% open florets Phase 1
66. Full flowering phase – time period in which between 25% and 75% of the florets are open Phase 2
68. End of flowering phase – starts when 75% of florets are open and ends when all florets have released their pollen grains Phase 3
69. Fructification phase – starts when all florets have released all their pollen grains. Phase 4

While Kmenta et al. (2016) used the following set-up:

60. Period of time between plant emergence and the start of flowering Phase 0
62. Start of flowering phase – reached when first anthers in 25 % of the observed individuals are extruded Phase 1
65. Full flowering phase – in 50 % or more of the individual's anthers are extruded and fully developed Phase 2
67. Second flowering phase - >50% of the individuals are withered, 25% or more are still in flowering condition Phase 3
69. Fructification phase or end of flowering – starts when all anthers are withered Phase 4

The methodologies from previous studies expressed above have been adopted along with a simplistic yet intuitive approach to make the phenological flowering observations as simple and as replicable as possible using the following set-up (see *Dactylis glomerata* flowering as examples):

60. Period of time between plant emergence and the start of flowering (**Figure 4.**) Phase 0

61. Start of flowering – Between 1% and 25% of the individual's anthers are extruded (**Figure 5.**) Phase 1

63. Upper Start of Flowering – Between 26% and 50% of the individual's anthers are extruded (**Figure 6.**) Phase 2

65. Start of Main Flowering – Between 51% and 75% of the individual's anthers are extruded (**Figure 7.**) Phase 3

68. End of Main Flowering – Between 76% and 100% of the individual's anthers are extruded (**Figure 8.**) Phase 4

69. Fructification or End of Flowering – All anthers of the individual have detached (**Figure 9.**) Phase 5

The main differences between these three set-ups are what is emphasised within the classification. Léon-Ruiz et al. (2011) emphasises the openness of flowers and pollen-release, Kmenta et al. (2016) emphasises the extruded anthers and gradual withering and re-emergence of anthers, while this approach emphasizes the cumulative percentage of extruded anthers. The phases of previous studies are also more open to interpretation, potentially creating confusion in the interpretation of the results. The flexibility of adapting the original BBCH description will create uncertainty in comparability between the above-mentioned studies (along with Cebrino et al. (2016)). Therefore, in this study the focus is on the use of a simple, accurate and easily comparable approach.

Figure 4. *Dactylis glomerata* flowering, phase 0 (No extruded anthers).

Figure 5. *Dactylis glomerata* flowering, phase 1 (Between 1 and 25% extruded anthers).

Figure 6. *Dactylis glomerata* flowering, phase 2 (Between 26 and 50% extruded anthers).

Figure 7. *Dactylis glomerata* flowering, phase 3 (Between 51 and 75% extruded anthers).

Figure 8. *Dactylis glomerata* flowering, phase 4 (Between 76 and 100% extruded anthers).

Figure 9. *Dactylis glomerata* flowering, phase 5 (Senescence, all anthers detached).

3.3.1.1. Population Phenology

This section is mainly the argumentative reasoning why a set of choices were utilized for the phenological observations. This section does not follow previous research in aerobiology, due to the lack of the same, instead it has been adapted from basic ecological understanding of plant population dynamics. The use of the population term and concept is here used to represent all the individuals within a defined space. It does not represent the 'real' biological or statistical population as a whole, that exists as a continuous range over a large distance. Instead each population refers to a sampled spatially-limited subset of the 'real' population. The sporadic emergence and growth patterns of Poaceae species makes many of them unreliable in terms of simple ecological observations (Havstad et al., 2004). The result of this is that the observation strategy must be carefully planned and meticulously executed to account for the natural variation of plant emergence (Hardegree and Van Vactor, 2000). A coarse temporal resolution might miss the flowering patterns of individuals that emerge between observations, thereby missing important features of the population patterns (see similar discussion about birches in Siljamo *et al.* (2008)). Information could be lost concerning the starting date of the individuals flowering if a temporal resolution of one week or similar is utilized, this will be especially noticeable for grasses with short flowering seasons. Sampling frequency has previously been shown to have impacts on the observed distributions of flowering phenology (Miller-Rushing

et al., 2008). The same applies to spatial resolution, due to the more resource demanding practice of increasing spatial resolution during fieldwork. An increase in spatial resolution will ultimately decrease temporal resolution when there is only a limited amount of resources to dedicate to phenological observations. A population approach to the phenological flowering observations was employed to gain as much temporal resolution as possible. The key consideration here is to reduce the impact of stochastic variation on the observation of species demographic development (Fox and Kendall, 2002; Kendall and Fox, 2002). By observing all the individuals within one plot or section prior to the start of flowering it is possible to consider both early and late flowering individuals while trying to determine the populations' full range of flowering dynamics for that location. Additionally, the use of a population-based approach is likely the only way to be able to predict species responses to their environment (Forrest and Miller-Rushing, 2010), which is a crucial step in assessing the impact of climate change on future pollen scenarios (García de León et al., 2015). The alternative to utilizing a population approach would be to select a limited number of individuals at a larger number of plots and only looking at these. The issue here is that by selecting a set of individuals only in a certain time-period it will not be possible to gain information regarding individuals yet to emerge (Fox, 1998). Another alternative is to observe new individuals each visit, a randomized design, but then the information regarding each individual's flowering progression is lost (Siljamo et al., 2008). There is also the chance of selecting individuals by random chance that do not represent the population as a whole, which will skew the data. To avoid a skew, a stratified design would be required, which could possibly skew the population in another way by selectively picking which flowers that will represent the population. A full population approach on a smaller spatial scale was considered to be more informative regarding the species as a whole, due to the entire spectrum of flowering development being observed. This has previously been suggested to be essential in gaining full understanding about a species' phenology (Visser et al., 2010). It should be noted here that the size of the plot or section would reflect the detail of the phenological observation, with smaller plots granting more detail to more individuals, and larger plots granting less phenological detail but higher spatial resolution, all due to resource management. It should also be noted that one tiller is referred to as 'one individual', and that no distinction is made between tillers that may or may not be belowground connected together to form one plant (Derner et al., 2012; Jewiss, 1972). In addition, that 'one sub-population' refers to all individuals located within the perimeter of each plot, while 'one population' refers to all sub-populations/all plots within one location.

3.3.1.2. Identification

For the observations where individuals' flowering progression was relevant, a marking strategy was employed over all the plots. At the start of each season and initiation of a new plot all of the individual grasses with a flowering head were marked by placing a piece of tape around the lower section of the stem, containing a permanent marker ID number (**Figure 10.**). By utilizing this identification method, it was possible to get individual progressions of all the individuals present in each plot. During each visit to the plot, each newly heading individual was given an ID number. All individuals were then retroactively marked in the protocol as non-flowering using their ID number until the sign of first flowering.

Figure 10. ID-tag identification during the *Dactylis glomerata* flowering.

3.3.2. *Dactylis*: Pilot Study

During the summer of 2017, a phenological pilot study was conducted on the ground belonging to St Johns; University of Worcester (*52.196N, -2.241E*). The pilot study was inspired by the research of León-Ruiz *et al.* (2011) but with a substantial increase in the number of tillers observed. A large patch of natural grassland-like vegetation was left uncut to allow flowering of containing species (see **Supplementary Figure S7.** for photograph). Four patches with the area of 2.25 m^2 (1.5m x 1.5m) were marked with corner posts to avoid the plots being trampled or otherwise disturbed. All individuals of *Dactylis glomerata* in each patch were then successively marked throughout the season with the above-mentioned method to allow both individual flowering progression information but also a population based flowering progression to be monitored. The current phenological state of each *D. glomerata* individual was monitored every day from the start of flowering of the first individual to the end of flowering of the last individual for that season.

3.3.3. *Dactylis*: Main Study

During the summer of 2018, the main phenological study focused on *D. glomerata* was conducted over eight sites (see map for all locations in **Figure 11.**): two main sites (see maps for the two main locations in **Supplementary Figures** S**8 - S9**.) and six secondary sites (see maps for all secondary locations in **Supplementary Figures S10 – S15.**) (see section 3.4.7. for the creation of the maps). The two below sections will focus on the information and proceedings of the main sites and the secondary sites.

Figure 11. All eight (8) locations utilized during the *Dactylis glomerata* 2018 sampling campaign with associated locations in the United Kingdom. The black grass icons represent the main locations, while the white grass icons represent the secondary locations (see section 3.3.3.2. for more information).

3.3.3.1. Main Sites

The two main sites selected were St Johns Campus, University of Worcester, and Lakeside Campus, University of Worcester. These main sites were selected based on the monitoring equipment already present at the locations, easy and quick access due to both locations being part of the University, along with the presence of areas occupied by *Dactylis*. Another contributing factor was that the St Johns location was selected based on it being the location for the pilot study. To allow for higher spatial resolution during the main study the temporal resolution for the main populations was lowered from one to two days. Both locations were visited on the same days. The plots within each location were chosen at random within a confined area of each field. For St Johns, the entire field was fenced off using fencing pins to avoid the field being disturbed (see **Supplementary Figure S16.** for photograph). Three plots measuring at 2.25 m^2 (1.5m x 1.5m) were then marked with small posts in each corner and all individuals marked with the above-mentioned method throughout the season. The reason for selecting three plots instead of four as in the pilot was that the number of individuals were more numerous during the main study and three plots were found sufficient to monitor the population. For Lakeside, the plots were located within a bigger field, and hence only the plots themselves were marked with posts of each corner (see **Supplementary Figure S17.** for photograph). Two plots measuring 2.25 m^2 (1.5m x 1.5m) were selected, however the first one of these plots contained a huge number of individuals, and hence only two plots were selected to represent the population. After selecting the plots all individuals were marked with the above-mentioned method throughout the season. The current phenological state of each individual *D. glomerata* was then monitored every second day from the start of flowering of the first individual to the end of flowering of the last individual for that season for both locations.

3.3.3.2. Secondary Sites

The secondary sites were utilized to increase the spatial resolution of the phenological observations in the aspect of population dynamics. The six secondary sites selected were given informal names, and from North to South are referred to as Lower Lakeside, Football Field, Upper Bridge, West Field, Lower Field and Lower Bridge (see **Supplementary Figures S18 – S23.** for photographs of each location). The criteria of selecting the secondary fields were the following: Not a roadside verge, more than 100 *Dactylis* individuals in total for the site, easily accessible and located within the perimeter of Worcester. The reason to avoid roadside verges were twofold: most roadside verges are regularly cut and are exposed to other environmental factors than fields. More than 100 *Dactylis* individuals were used as a way of ensuring a reasonable population size, with smaller population sizes giving rise to higher uncertainties

regarding the representability. Easy accessibility was needed to allow the observations to continue smoothly during the season. Location within Worcester was to allow a gradient in spatial locations but still ensure the species' growth and flowering patterns stay consistent. Due to these sites being secondary sites, none of the individual grasses was marked with IDs, and only the population progression as a whole was considered. For the sites with lower density of individuals (Lower Lakeside and Football Field) all individuals were monitored at each visit. For the sites with moderate density of individuals (Upper Bridge and Lower Bridge) all individuals within four plots measuring 2.25 m^2 (1.5m x 1.5m) were monitored at each visit. For the sites with high density of individuals (West Field and Lower Field) all individuals within three plots measuring 2.25 m^2 (1.5m x 1.5m) were monitored at each visit. The visiting frequency for the secondary sites varied during the season, with every plot being visited at least once a week and sometimes twice. The observations ended when each sampling location had been visited ten times, which also coincided with the majority of the flowers having reached phenological phase 5 (end of flowering).

3.3.4. Complex of Grass Species

During the summer of 2019, phenological studies were conducted with a focus on grass species other than *Dactylis*. The study was conducted using three nearby areas on Lakeside Campus. The below sections focus on the information and proceedings of this Lakeside field study.

3.3.4.1. Managed Field Study

During the summer of 2018, a circle with a radius of 25m was fenced off in the middle of a field on Lakeside Campus (*52.251N, -2.253E*). A fertilizer recommendation from ADAS of 80kg N per hectare was applied due to the concern for low productivity, caused mainly by the porous and stony soil (Mueller et al., 2010) along with the lack of nutrient-rich clay and silt components. This information was categorized from a low-nutrient status grassland recommendation (Rollett et al., 2015). Four standard mix (15:10:10 NPK) bag of 25kg each were acquired from BHGS Ltd. The recommendation above was used, which resulted in just below 16 kg N for the circles area of just below 0.2 hectare, and most of the four bags were spread evenly over the area. All vegetation outside of the circle was regularly cut while the vegetation inside the circle was preserved to allow grassland vegetation to grow naturally, specifically grasses (**Figures 12 – 13.**). A path from the outside to the middle of the circle (where other sampling equipment was located) was created and fenced off, to prevent trampling and general destruction of the vegetation within the circle. During the season of 2018, a botanical inventory was conducted within the circle to determine the species present along with a rough estimate of abundance (**Supplementary Table S1.**). An updated version of the

botanical survey along with the abundance was created during the season of 2019. It was found in both surveys that the main grasses occupying the circle were *Lolium perenne, Festuca rubra, Poa annua* and *Poa trivialis*. The field circle is the only place in the Lakeside surroundings where the grass *F. rubra* occurs. The grasses selected for phenological observations for the summer of 2019 were based on the previous inventory and abundances, with the selected species being *L. perenne* (**Figures 14 – 15.**) and *F. rubra* (**Figures 16 – 17.**) due to their higher abundance, while *P. annua* and *P. trivialis* were excluded. The reasoning to exclude the latter mentioned species was due to their uneven distribution and low flowering rate. The phenological observations were conducted every third day using 50 random individuals from within the circle of each of the two species using the phenological method mentioned above. The reason for selecting 50 individuals were the same as with the secondary sites for the main *Dactylis* observations. The absolute amounts however were changed from 100 to 50, following the assumption that 50 individuals would be a reasonable sample-size to determine population patterns in the smaller, more concentrated, circle. Phenological observations could only be conducted from the outside of the circle, from the path leading to the inside and from the inner part of the circle, due to the desire to not disturb the vegetation more than necessary by walking around in the field. The prime condition of the vegetation inside the circle was essential due to the data collection related to the grasses from the other monitoring equipment. Note a 10m meteorological mast with a Campbell weather monitoring station was positioned at the centre of the circle along with other monitoring equipment.

Figure 12. Managed circle/Field with cut/uncut dichotomy.

Figure 13. Managed circle/Field with cut/uncut dichotomy.

Figure 14. *Lolium perenne*, phase 0 (No extruded anthers).

Figure 15. *Lolium perenne*, phase 4 (Between 76 and 100% extruded anthers).

Figure 16. *Festuca rubra*, phase 0 (No extruded anthers).

Figure 17. *Festuca rubra*, phase 4 (Between 76 and 100% extruded anthers).

3.4. Atmospheric Modelling

The section below contains all the methods, databases and processing used to create all the atmospheric modelling elements developed and used during the entirety of this doctoral study. It also contains the description of the HYSPLIT modelling, meteorological information, grass maps, spatial fusion, and satellite images. All atmospheric modelling methods were developed and expanded upon by previous research, sections that have been altered or developed for this thesis report will state this.

3.4.1. Motivation of year selection

Two of the four years of available bi-hourly grass pollen concentrations were used in the atmospheric modelling investigation. The years 2016 and 2017 were excluded due to limited overlap in pollen data of each season between the two locations (St Johns and Lakeside) and meteorological data unsuitable for local small-scale differentiation gained from multiple weather loggers (see sections 3.2.2.2. and 3.8.1.1.). The years 2018 and 2019 were included due to full overlap in bi-hourly grass pollen concentrations and reliable local meteorology from the same model of weather logging system.

3.4.2. HYSPLIT

Air-mass transport can reveal connections between the likely origin of particles (such as grass-pollen (e.g. Viner and Arritt, 2012)) and its' final deposition location (caught in a Burkard sampler) (Stein et al., 2015). To investigate if the grass pollen collected in St Johns Campus and Lakeside Campus differed in origin the HYbrid Single Particle Lagrangian Integrated Trajectory (HYSPLIT) model (Draxler et al., 2016) was used. The model utilizes meteorological data in the HYSPLIT ARL format to calculate the movement of air masses or 'air-parcels' (Draxler and Hess, 1998). This dataset is available from the year 2016 and onwards from the HYSPLIT ftp server (ftp://arlftp.arlhq.noaa.gov/archives/gfs0p25/). The model is capable of running both forward (e.g. Van de Water et al., 2000) and backwards (e.g. Skjøth et al., 2012; Su et al., 2015) in both trajectory (e.g. Izquierdo et al., 2011; Rousseau et al., 2006) and particle mode (e.g. Veriankaitė et al., 2010), enabling many specific features for specific circumstances. The backwards trajectory model was chosen to investigate the possible origin of the grass-pollen. Parameters used: HYSPLIT ARL with 0.25 x 0.25-degree resolution, 55 hybrid sigma-pressure levels, 2-h temporal resolution (due to the nature of the bi-hourly pollen counts) and a 500m receptor height. The model was restricted to 12 hours to exclude potential long-distance transport (the opposite of the approach and interval used by Rousseau et al. (2008)). The reasoning being that grass pollen are relatively heavy bioaerosols, increasing their

settling velocity, and make them fall out comparatively quicker from the atmosphere than lighter bioaerosols (Gregory, 1961).

3.4.2.1. HYSPLIT Data Processing

All even hours between 1st of May and the 1st of September for two (2018 and 2019) of the four years (not 2016 and 2017) and two locations (St Johns and Lakeside) acted as data points. Each data point acts as a spatial and temporal origin for one trajectory, with the model calculating the backwards movement by one hour per time step (for 12 hours) for the air mass connected to that origin. Each trajectory is essentially twelve points with its' own spatial and temporal value backwards in time, with the points being theoretically connected to form a trajectory. All modelling was computed using a custom-made script to accommodate the number of trajectories needed to be calculated. The GFS-archive was used to calculate all trajectories bar three days (2nd of June to 4th of June 2019) due to missing data in the archive. For these three days, the GDAS-archive was used instead. The main difference between the two archives is the resolution (0.25 x 0.25 for GFS, 0.5 x 0.5 for GDAS). The calculated trajectory dataset containing all the data points for the two years was then imported into ArcGIS ver. 10.7 to be processed further. For each year and location, all points were connected back to their original trajectory, creating four datasets of trajectories (two locations per two years). All trajectories were then filtered to exclude those where there were no corresponding pollen measurements, this also applies to situations where a pollen measurement was present only for one of the sites but not for the other. This was done to avoid skewing the results based on the lack of comparative measurements. By combining all the calculated trajectories for each location, it was possible to determine the likely total catchment area for the grass-pollen for each area during the specific sampling season (Plaza et al., 2016). It should also be noted that pollen are more likely to originate from areas closer to the pollen traps even if the catchment area is large due to the depository nature of (heavier) bioaerosols such as pollen (Adams-Groom et al., 2017).

3.4.3. Meteorological Data Processing

The two entire temperature and precipitation datasets for the years 2018 and 2019 were compiled into one dataset (see section 3.2.2.2. and 3.8.1.1.). The dataset was then filtered and processed to allow for easy access to the relevant period corresponding to the available bi-hourly data points described in 3.4.2.1. Two meteorological sub-sets were then created. The first sub-set corresponding to the timing of the bi-hourly data point (1200, 1400, 1600 etc.), essentially ignoring every odd hour and measurement between the bi-hourly points. The second sub-set also corresponds to the timing of the bi-hourly data point but also considers the odd

hour between the data points, with temperature being averaged for the data-points' time and the previous hour, and with precipitation being summed for the data-points' time and the previous hour. The second sub-set proved to be more accurate in explaining the overall conditions during the transportation of the bioaerosols that corresponds to each data-point and was thus used going forward.

3.4.4. Mapping Grids

To allow for a generalized approach and simplicity while mapping, a grid-system was utilized. The grid-system is composed of a circular grid using a square grid definition and a gridcell resolution of 100 x 100 m. The standard simulated pollen dispersal distance is 30 km (e.g. Avolio et al., 2008; Katelaris et al., 2004; Pashley et al., 2009), which means that one circular grid with a radius of 30 km per location was recommended. A larger than recommended circular grid with a radius of 50 km per location was utilized to investigate and confirm the likely distance for pollen dispersal. The dispersal distance was chosen due to the unlikelihood of grasses outside of this radius contributing noteworthy pollen loads. To simplify the grids, a point was selected with equal distance between the two locations, and a new grid was created at that point to encompass both locations within 50 km (possible using a grid with a radius of 53 km). The new grid had a gridcell count of almost 885k cells. To further narrow down the likely pollen dispersal distance the large grid was divided into smaller ones based on earlier atmospheric scale-definitions proposed by Orlanski (1975) and set into context by Smith et al. (2013). By including concentric circles of increasing radius around central circles of each location each new dispersal distance can be accounted for, this has previously been shown to identify likely pollen dispersal distance (Oteros et al., 2015). Eight circular grids and concentric circular grids were created in total. Two micro-scale grids (0 – 2 km) were created for each location. Two small meso-gamma grids (2 – 10 km) were then added for each location (excluding the current location but including the other locations micro-scale grid). One larger meso-gamma grid (10 – 20 km) and three meso-beta grids (20 – 30, 30 – 40, 40 – 50 km) in the form of concentric circles were then added. All spatial maps were created by combining the circular grids with projected features. All map features were created using the software ArcGIS ver. 10.7.

3.4.5. Grass Maps

The air-masses that comprised the trajectories must travel through areas where grasses are available and able to pick up released grass pollen successively for the trajectory to contain any measurable amounts of grass pollen. Theoretically, the more grasslands the air-masses travel through, the more grass pollen the air-masses should acquire. To determine the amount of

grasslands the trajectories travelled through a rough grass map was created. The grass map was created using the 2017 version of the 'CEH Land Cover Plus®: Crop' dataset, developed by the Centre for Ecology and Hydrology (CEH). This is a UK-wide dataset containing a wide range of agricultural crops and improved grass fields down to the field specific level. The dataset was created using both Sentinel-1 and Sentinel-2 remote sensing data (Sentinel-2 from 2016) and has a kappa statistics accuracy of 0.82. A recent study has questioned the validity of the use of kappa statistics in the image classification of maps (Foody, 2020). The format of the dataset is shapefiles and consists of polygons. The main identifying feature of the polygons being the type of vegetation present in each polygon: either a specific agricultural crop, or improved grass. The grass field accuracy is >94% (CEH Land Cover plus Crop Map: Quality Assurance). The above-mentioned dataset does not however include features that are smaller than the map-resolution, such as road-verges, house-hold lawns, and similar features. This introduces an uncertainty regarding the grass contributions of areas not included in the dataset. Management is also excluded, which introduces uncertainty regarding equal temporal contribution.

3.4.5.1. Grass Maps Data Processing

To create the grass-map the full dataset was imported into ArcGIS. Due to the size of it, the dataset was spatially cut down to only incorporate the area within the larger grid. Then all grass areas were selected, discarding the agricultural crop areas, and combined with the grid. At that point, each gridcell contained the class 'grass fields', and the class 'other', which was essentially the remainder of the gridcell unoccupied by grass fields. The amount of grass field in each gridcell was then converted to the percentage of grass field per gridcell, effectively removing all areas unoccupied by grass fields. This provides the percentage of grass fields per gridcell. The percent of grass field in each gridcell was then graphically represented by using a green natural colour ramp using 32 natural Jenks, to provide distinction between low and high amounts of grass fields in the map. This was done for all eight circular and concentric circular grids.

3.4.6. Spatial Fusion

The main reason to develop separate grass maps was to measure how much grasslands each trajectory travels through until it approaches each of the sampling locations (St Johns or Lakeside). The fusion of grass maps and trajectories allows for spatially dynamic comparison with potential grass pollen concentration contribution on a bi-hourly temporal resolution. This method creates 24 separate trajectory-grass map data-sets (six grass maps per location, two locations and two years).

3.4.6.1. Spatial Fusion Data Processing

All trajectories for each year and location were spatially joined and summed with each grass map, allowing each trajectory to acquire the amount of gridcells it travels through within the grid. By acquiring all the gridcells, it also acquires the summed value of the percent of grass fields, i.e. the amount of grass fields each trajectory passes from start to finish from within the grid. All trajectories for each year and location were then summed over the larger grid (50 km) using a lower grid resolution (1 x 1 km), providing each gridcell with all the values for all the intersecting trajectories. Gridcells where few trajectories intersect will generally gain lower values while gridcells where many trajectories intersect will generally gain higher values. Each grid now represent the distribution of trajectories over each year and location. The two grids (2018 and 2019) per location were then added together based on gridcell ID to represent the distribution and densities of trajectories for each location. As in the grass map, the graphical representation of each variable was done with the help of natural Jenks; however, the natural Jenks were changed in order to allow for comparability between variables and sites. The new Jenks were taken from the variable with the highest variation of values between gridcells and changed into percent of the total value of all the gridcells, with each gridcell ranging from a value of 0.001% to 1.230% of the total. This was done for demonstrative purposes only to showcase the distribution of trajectories.

3.4.7. Satellite Images and Other General Mapping Features

The maps only meant to represent the relative distance between geographical locations used in the pollen monitoring or flowering phenological observations satellite images were used. Images obtained from Google Earth Pro (Google Earth Pro, 2019) were used for this purpose. Google Earth Pro is a service that can provide satellite images with high resolution, and only utilized to provide geographical context to the research, without providing data utilized for any other purpose or analysis. Both the over-arching regional images and context location specific images were utilized. Location and equipment specific map-icons were also created and utilized. World countries boundaries (2019) were acquired from ESRI under the licencing of ArcWorld Supplement. UK counties boundaries (2016) were acquired from the Office of National Statistics (ONS) and Ordnance Survey (OS) under the licencing of Open Government Licence v3.0.

3.5. eDNA Molecular Approaches

The section below contains all materials and methods utilized for the molecular experiments and lab-work employed during the entirety of this doctoral study. It also contains descriptions of the environmental DNA (eDNA) sampling equipment, pollen approaches, DNA extraction and protocols, DNA metabarcoding experiments and protocols and bioinformatics. This entire section is based on previous research conducted in the field of molecular ecology and genomic methods.

3.5.1. eDNA Collection and General Approach

All the molecular approaches are centred around sampling environmental DNA from the air, in the form of particles, extracting the DNA and conducting subsequent analysis to answer specific questions. The particles sampled for molecular approaches can be sampled in several different ways, while the distinction is usually made between active and passive sampling. Active sampling comprised methods in which pumps and similar air-movement systems are engaged to actively move air over a filter or other collection container or surface. Common active sampling methods include Multi-Vials using Cyclones (Brennan et al., 2019; West and Kimber, 2015), Burkard traps using tape (e.g. Grinn-Gofroń et al., 2016; Kraaijeveld et al., 2015) and ChemVol® samplers using filters (e.g. Buters et al., 2012). The pump-systems allow the samplers to collect more particles due to the high volume of air processed. Passive sampling comprised methods in which the wind is usually deflected in different ways, to ensure that the gravitational force on the particle is making them fall into some sort of collection container or surface. Available passive sampling methods include Gravimetric Samplers (e.g. Werchan et al., 2017) and Sigma-2 Samplers (e.g. Guéguen et al., 2012). Passive methods are more dependent on wind-speed; thus, the efficiency of such methods is inherently lower, and less particles are collected overall. Passive methods have certain advantages overactive methods. They are normally cheaper to produce and manage, more adaptable and does not require electricity. This can enable higher spatial sampling resolution, especially in remote areas. In these studies, active sampling through the Multi-Vial Cyclones was utilized, mainly due to the higher volumetric sampling capacity.

3.5.1.1. Multi-Vial Cyclones

For active sampling of eDNA, Multi-Vial Cyclones constructed by Burkard (**Supplementary Figures S24 – S25.**) were used. The core of the sampler is the Cyclone unit and the active pump-system. Air is pumped into the sampler using an active suction system, which is then funnelled into the Cyclone unit. A miniature cyclone is formed within the specially constructed unit, with the air circling in the cyclone before escaping again, while particles fall into a below

situated Eppendorf tube (West and Kimber, 2015). The carousel-housing is automatically rotated every 24-h to allow for a new Eppendorf tube to collect the next sample. The Multi-Vial Cyclone collects 16.6 litres of air per minute. One fully loaded Multi-Vial Cyclone sample can hold 8 tubes, effectively sampling 7-days per load, due to the overlap of timing in the change of tubes. All tubes were before sampling marked with date, sampling location and index based on the current number of samples.

3.5.1.2. eDNA Samples

Several sets of eDNA samples were collected. In 2018 two sets of samples were collected and utilized, one from St Johns and one from location 2 in Lakeside. The St Johns samples utilized include 34 days, ranging from the 8th of June to the 11th of July. The Lakeside samples include 48 days, ranging from the 25th of May to the 11th of July. The 14 days overlap missing is accounted for elsewhere (see section 3.5.2.2.). In 2019 three sets of samples were collected and utilized, one from each of the currently active Lakeside locations. The samples include 42 days per location, ranging from the 24th of May to the 4th of July.

3.5.1.3. Storage

After each 7-day load of Eppendorf Tubes have been sampled, they were collected and temporarily stored in Eppendorf Storage boxes until transported back to the laboratory. While back at the laboratory, they were sorted according to date and placed with a larger storage box in a -20 °C freezer for temporary storage. If the period extends above temporary storage, the samples were instead transferred to the -80 °C freezer for any potential future use. All results reported in this thesis constituted samples that were temporarily stored.

3.5.2. Pollen eDNA Approach

The main area of interest in this study is the spatial and temporal distribution of species-specific grass pollen (e.g. Brennan et al., 2019; Ghitarrini et al., 2018; Rowney et al., 2021). By sampling pollen using the above-mentioned technique, it is possible by molecular methods (for example DNA metabarcoding) to identify semi-quantitative relative abundance of pollen that originates from each taxon (Núñez et al., 2016). The relative distribution of species can be identified by utilizing DNA extraction and DNA metabarcoding methods with the correct associated primers and protocols. The creation of specific primers developed to connect with certain plant genes (such rbcL (mostly genera), ITS1 or ITS2 (mostly species)) will enable the identification of species-specific plants and pollen through molecular DNA metabarcoding approaches (e.g. Galimberti et al., 2014). The sequence reads generated from the DNA metabarcoding can be sorted and processed using bioinformatics, genomic databases and relevant pipelines (e.g. Kraaijeveld et al., 2015).

3.5.2.1. DNA Extraction Protocols and Sample Pooling Strategy

Two different DNA extraction kits and protocols were used depending on the sets of samples extracted. The eDNA samples collected in 2018 were extracted using the MP Biomedicals™ FastDNA™ SPIN Kit. The motivation for using the MP Bio kit was to allow for the extension of a previous DNA metabarcoding series (see section 3.5.2.2.). Samples were initially pooled during the lysis-step of the protocol by alternating four and three consecutive days, with Monday-Thursday being one alternative and Friday-Sunday being the other alternative. Prepared lysis buffer was added to each daily sample, vortexed, micro-centrifuged and then transferred into a new tube to create the pooling strategy above. This pooling resulted in 10 extracted samples for St Johns and 14 extracted samples for Lakeside. The accompanied suggested protocol was utilized during the extraction process. The homogenizer step utilized a MP Biomedicals FastPrep-24™ Classic Instrument homogenizer. The recommended program for pollen-samples were utilized, with a speed 6.0m/s and a duration of 40s.

The eDNA samples collected in 2019 were extracted using the QIAGEN DNeasy Plant Mini Kit. The motivation for using the QIAGEN kit was to follow specific and grass pollen adapted DNA extraction protocols (minus the specific beads and homogenizer/TissueLyser) utilized by Brennan et al. (2019) with the same modification to the protocol as utilized by Hawkins et al. (2015). Samples were initially pooled during the lysis-step of the protocol by three consecutive days, resulting in 14 extracted samples per location. Prepared lysis buffer was added to each daily sample, vortexed, micro-centrifuged and then transferred into a new tube to create the pooling strategy above. The same MP Biomedicals homogenizer and settings were used as in the above-mentioned protocol. Garnet sand of varying size-fraction was used to aid in the homogenizer step. The DNA was eluted twice using the same 60µl elution buffer. A small fraction of each extracted sample from each site was then pooled to form three entire-season samples, resulting in one sample for each location to use for downstream applications. The DNA concentrations from all 2018 and 2019 samples were determined using a Thermo Fisher Scientific NanoDrop™ spectrophotometer with a blank buffer measure between each real measurement.

3.5.2.2. DNA Metabarcoding

The relative species-specific grass pollen amounts were investigated using DNA metabarcoding approaches using some of the samples mentioned above. The samples were investigated using the universal (plant and fungal) spacer DNA genes ITS1 and ITS2 (White et al., 1990). These genes have the potential to differentiate (by using bioinformatics) sequence-reads from different species (e.g. Op De Beeck et al., 2014; Toju et al., 2012; Yang et al., 2018), with both regions

being able to distinguish Poaceae species (Grebenstein et al., 1998; Hsiao et al., 1995; Rodionov et al., 2017). The company Eurofins Scientific was chosen to produce the sequence-reads using their expertise knowledge and advanced laboratory resources. Twenty-seven samples in total were sent to Eurofins. Twelve samples were sent from the 2018 sample-set: the first four of the St Johns series and the first eight of the Lakeside series. Three samples were sent from the 2019 sample-set: one from each Lakeside location containing the combined seasonal eDNA contribution. One sample was a negative control only containing buffer from the MP Bio DNA extraction kit. One sample was a positive control containing a pre-defined DNA mock community of different species normally found in atmospheric samples: grass species, tree species and fungal species (see an example of the distribution of a bioaerosol diversity range in Ezike et al. (2016)). The negative and positive control are essential in keeping reproducibility and certainty high in disciplines involving genomic and molecular research (Hornung et al., 2019). The remaining ten samples were sent from another project.

The DNA metabarcoding series from 2018 utilized sections from a previous DNA metabarcoding series processed by Dr Maria Grundström (unpublished data) and Eurofins. The series also investigated the ITS1 and ITS2 genes, with samples originating from the St Johns sampling station between April to June the same year. The same sampling, pooling and extraction protocol were shared between the two series along with the same company (Eurofins) processing, hence the two series can be fused and extended without methodological complications. Although there is a small potential for bias due to the DNA extractions themselves being conducted at two different times.

3.5.2.3. Bioinformatics

The returned sequence reads from Eurofins were processed using the software R and the R packages *DADA2* (Callahan et al., 2016) and *phyloseq* (McMurdie and Holmes, 2013). The sequences reads were delivered pre-trimmed and pre-merged, hence that step of the pre-processing was skipped. The package *DADA2* was used to assign taxonomy to the sequence reads based on a filtered custom-made PLANiTS reference database. The PLANiTS reference databases were created to be Viridiplantae (green plant) specific (Banchi et al., 2020). The original PLANiTS ITS1 and ITS2 reference databases were filtered using a UK-exclusive grass species list compiled by the Botanical Society of Britain and Ireland (BSBI) in 2009 (Cope and Gray, 2009). This was done to avoid very similar sequence references from species that are not present within the United Kingdom, similar to Brennan et al. (2019). All reference sequences that matched the species and subspecies present within the UK grass species list were imported into the new filtered custom reference database. The taxonomical classification method is based

around a Bayesian approach that randomly selects eight consecutive nucleotides (kmer = 8) from each sequence and tries to match it to one of the taxonomical reference sequences (Wang et al., 2007). The method matches each sequence 100 times (100 bootstrap replicates), with the default cut-off point being 50 matches for the same reference sequence to correctly assign taxonomy. All samples are then post-processed and interpreted using the package *phyloseq*. This package can be used to showcase relative abundances of taxonomical units found along with sub-section using taxonomical units or other variables. The relative proportion of the Poaceae-section of the processed samples were further used in all eDNA bioinformatics statistical analyses.

3.6. Markov Chain Modelling

The section below contains all the materials utilized and methods used in relation to the Markov Chain modelling during the entirety of this doctoral study. It also contains descriptions of the general modelling approach, the creation of general populations, the modelling of pollen release and data processing of all above-mentioned aspects. The Markov Chain modelling approaches are established methods developed and expanded upon by previous research. The use of the methods to estimate general population phase distributions and to model pollen release have been suggested and developed by this doctoral study.

3.6.1. General Modelling Approach

The Markov Chain model estimates the change in possible event sequences (or phase/status) of an object over time (Meyn and Tweedie, 1993). In this case it has been estimating the change in flowering phenology in specific tillers over time. This can shed light on differential development between individuals or within specific flowering stages of the population. It can also indicate if the presence of external stimuli, such as water availability, temperature and solar radiation is sufficient for additional development. The modelling approach is made possible for the three main populations due to the continuous observation protocol and the following of each tiller as separate units via ID-tagging (see section 3.3.1.2.). Dynamics of the phase-shift will depend on the possible transitions between phases. Not all phase-shifts are possible in the case of grass flowering dynamics due to the specific directional way that flowers progress from pre-flowering to senescence (Calder, 1964a). This means that phase-shifts going to previous flowering phases are not possible, neither directly from pre-flowering (Phase 0) to senescence (Phase 5), since it does not meet the requirement of starting to flower. Once the flowering progression had been determined for each tiller the model creates a transitional matrix for each possible transition within the population at large, that essentially estimates the likelihood of

phases transitioning between each other (see Grinstead and Snell (1997) for examples and progressions concerning transitional matrix dynamics).

3.6.1.1. General Modelling Data Processing

To investigate how the dynamics of tiller-specific development is reflected in each of the three main populations a summation formula was used. The formula works by incorporating the temporal phase-shift for each tiller for each observation point (see **Equation 1.**). All phase-shifts are then summed in a six-by-six matrix.

Eq. 1: $for\ (t\ in\ 1{:}\ (length(x)\ -\ 1))\ p[x[t], x[t\ +\ 1]]\ <-\ p[x[t], x[t\ +\ 1]]\ +\ 1$

$$for\ (i\ in\ 1{:}6)\ p[i,]\ <-\ p[i,]\ /\ sum(p[i,])$$

p is the six-by-six matrix. t is each phase-observation. i is the index-term in the algorithm. x is the dataset containing all phases-observations. This algorithm creates a six-by-six transitional matrix, which describes the likelihood of each tiller within the population to transition between phases based on all available tiller-specific data points for the entire temporal dataset. The transitional matrix is then put into a Markov Chain object using the R package *markovchain* (Spedicato, 2017). The package and associated functions allow for further processing using Markov Chain methods.

3.6.2. Creating General Populations

To further process the information gained from the real observed populations it is essential to create modelled general populations from that information. By doing this is it possible to gain understanding into the general flowering processes within each population (see similar approach in Tseng et al. (2020)). The above-mentioned method depends on the temporal aspect of the transitional matrix. The temporal aspect can vary depending on the purpose. For example, there could be one transitional matrix that models the overall change within one population over an entire season. There could also be one transitional matrix that models the change over one week, allowing for as many transitional matrices as there are weeks observed. An entire season matrix is the mean of all the transitions over the season and cannot account for the change in transitional strength likely seen between sections of the season. The use of several matrices, each modelling a specific sub-section of the season can therefore be used to gain a more representative general population.

3.6.2.1. Markov Chain Data Processing

The same approach as seen above is utilized, but instead of one seasonal transitional matrix many day-to-day transitional matrices are created (from the day-to-day observations of the main

populations) instead and put into a list of matrices. Each transitional matrix from the list is then put into its own Markov Chain object, creating as many Markov Chain objects as there are matrices in the list. Different combinations of Markov Chain objects can thereafter be utilized together in Markov Chain lists, essentially a vector where each element in the vector is one specific Markov Chain object. Within each Markov Chain list there are a set number of elements, each representing one time-step (the change in phenology from one day to the next) of the modelled population. Individual tiller count was set to 5000 to represent the general population in each Markov Chain list. Each tiller starts in Phase 0 (non-flowering). For each time-step each tiller is randomly sampled based on the transitional probabilities of that element (transitional matrix/Markov Chain object), representing the natural phenological progression likely to happen during that timeframe. For the next time-step the newly changed population of 5000 individual tillers are randomly sampled again based on the new transition probabilities. This continues until all elements in the Markov Chain list have been progressed through, which represent the natural progression of flowering tillers from non-flowering to senescence. The differences between the different Markov Chain lists are how many elements (time-steps) are present and which Markov Chain objects that have been chosen to represent each element. The probabilistic behaviour of the Markov Chain list creates general populations of flowering tillers based on the observational data from the three real populations (One for St Johns 2017, one for St Johns 2018 and one for Lakeside 2018).

3.6.3. Modelling Pollen Release

Only the two general populations from 2018 were utilized for the pollen release modelling due to the presence of DNA metabarcoding grass pollen bioinformatics for comparison in 2018 but not in 2017. The phenological development of a flowering grass tiller will depend on the percentage of anthers extruded, as defined above with specific phase progressions. Each extruded anther of each tiller is expected to release grass pollen with a specific rate. This rate can either be static based on the pollen release mechanics of the anther (Keijzer, 1987b), or dynamic, depending on meteorological factors involved (such as temperature, solar radiation, humidity, precipitation, windspeed etc.) (Bhattacharya and Datta, 1992) or both. The true pollen release rate and how much different factors influence it is still largely unknown. The static rate would be the same for the species throughout the flowering process, while the dynamic rate would change throughout depending on the weather preferential to pollen release parameters. Extruded anthers might not be able to release pollen instantly after being extruded, creating a potential delay between anthesis and pollen release (anther dehiscence) (Wilson et al., 2011). Regardless, the rate will vary between 0 and 1, with the pollen release depending on the

flowering phase (percentage of extruded anthers), the status (how much pollen has been released) of earlier extruded anthers and a potential delay. The pollen release profile of each tiller can therefore be calculated as a combination of its flowering progression, the rate in which the pollen is released and the delay. The pollen release profile of the entire population will be the mean of all the tillers within the population and their pollen release profiles. The differences between the different pollen release profiles of the population are the type of pollen release rate (static or dynamic), what the rate will be (low, strong, or meteorological dependent) and how long the delay is between anthesis and pollen release.

3.6.3.1. Pollen Release Data Processing

The flowering progression of the modelled general populations are here used to discern the general pollen release scenarios. The amount of pollen in each tiller will be directly related to the percent of extruded anthers (definition of each phase), with Phase 1 having 25 percent pollen release potential, Phase 2 having 50 percent pollen release potential etc. For each additional increase in phase 25 percent of additional pollen release potential is added. The reasoning was that each anther would have an approximate equal amount of pollen to release (Prieto-Baena et al., 2003). The maximum pollen release potential of a tiller is reached for a tiller progressing from Phase 0 (non-flowering) to Phase 4 (full flowering) between two observation dates, with a 100 percent increase in pollen release potential. The decrease in pollen release potential (the actual pollen being released) will then depend on the specific pollen release rate mentioned above along with the delay seen in anther dehiscence. This method creates pollen release profiles for all the modelled tillers. The population release profile is then calculated as the mean pollen release profile of all modelled tillers. One population pollen release profile is modelled for each pollen release rate scenario and anther dehiscence delay. The total pollen release for each tiller will be equally divided between all anthers, which assumed that the pollen release rate will be the same within each scenario and that the pollen production in each tiller and anther will be constant. The delay between anther dehiscence delay was assumed to be nominal, based on previous research (Keijzer et al., 1996; Wilson et al., 2011).

3.7. Lakeside Field Study

The section below contains all materials utilized and methods used in relation to the lakeside field study during the entirety of this doctoral study. It also contains descriptions of the general information regarding this study, information about the TKE experiments and wind direction monitoring.

3.7.1. General Information

This section represents the spatial and temporal analysis pertaining to the causes, movement and dynamics of grass pollen dataset collected at the three placements in Lakeside campus in 2019. Two main pieces of methodologies are presented below: the measurement of wind speed and turbulence within the air and the wind direction. These two categories of information are directly related to the movement of grass pollen within this location. Both factors were monitored using the data from the WindMaster 3D Ultrasonic Anemometer developed by Gill Instruments. The instrument (from now on referred to as an Ultrasonic) is located in the middle in the managed circle (see section 3.3.4.1.) at a height of 10m and connected to the Campbell weather logger located at the bottom of the mast. This section is also directly related to the phenological investigation of the managed field study (see section 3.3.4.1.) and the DNA metabarcoding results from the year 2019 (see section 3.5.2.2.).

3.7.2. Wind speed and TKE

The ultrasonic works by sending sound-signals between receivers, with the delay between sending and receiving the signal being attributed to the speed of the wind (Zhang et al., 2020). The device can measure the wind at 10hz, meaning it can measure the speed of the wind 10 times per second. It also has three sets of receivers, making it possible to measure the wind in three directions at once: X (north-south), Y (west-east) and Z (up-down). The benefit of the high-speed three directional measurements is that it can determine how strong the wind is, in which wind-direction it travels and if there are presences of upwards or downwards drafts. Combinations of the high depositional velocity of grass pollen and the strength of the wind speed can suggest if the grass pollen originated from a local or regional source (Ciani et al., 2020). A higher wind speed can transport the pollen grain further from the source while a low wind speed cannot (Damialis et al., 2005). The presence of upwards or downwards draft can suggest if the underlying field acted as a source or sink for the grass pollen (Chamecki et al., 2009). An upwards draft can suggest that the pollen came from beneath before getting sampled (source) while a downwards draft can suggest that the pollen came from above before getting sampled (sink). By combining the strength of the three wind directions it is possible to calculate Turbulence Kinetic Energy (TKE). TKE is a measure of how turbulent the wind is, and it is suggested to be a contributing factor in how likely pollen can be released from the flowering anther (Šikoparija et al., 2018), with higher turbulence potentially being more likely to contribute to pollen release.

3.7.2.1. Wind and TKE Data Processing

Ultrasonic data was collected to overlap completely with the presence of phenological data (see section 3.3.4.1.) and DNA metabarcoding data (see section 3.5.2.2.). Included dates are between 13th of May to 6th of July, which constitutes 47.520.000 datapoints per direction. The equation of calculating TKE is the half the sum of the variances of the three directional measurements (see **Equation 2.**).

Eq. 2: $$TKE = \frac{1}{2}\left(\left(\sqrt{\frac{\sum(X-\bar{X})^2}{N-1}}\right) + \left(\sqrt{\frac{\sum(Y-\bar{Y})^2}{N-1}}\right) + \left(\sqrt{\frac{\sum(Z-\bar{Z})^2}{N-1}}\right)\right)$$

$[X, Y, Z]$ is the wind measurement per direction in each 1/10s. $[\bar{X}, \bar{Y}, \bar{Z}]$ is the mean wind measurement per direction for all 10-consecutive measurement. N is the number of consecutive measurements; in this instance it is 10. The variance was calculated using each 10 consecutive wind measurement, effectively creating a mean TKE per second. To narrow down the TKE data for it to fit the bi-hourly grass pollen measurements from the monitoring a min, mean and max TKE for each 120 min was created (using 7200 TKE points per 120 min). The mean wind speed in each three directions is also calculated per 120 min.

3.7.3. Wind Direction

The wind direction will be fundamental in understanding the spatial movement of grass pollen in the surrounding area (Peel et al., 2013). Higher pollen contribution from specific directions can help in the determination of potential local source areas (Maya-Manzano et al., 2017). Although not investigated in this study, the distribution of windbreaks in the local landscape can further help to determine the local movement of grass pollen (Auer et al., 2016). Wind direction is based on geometry and the radius of a circle, with the direction being between 0-359° (or 1-360°, with 0° and 360° being the same value). Colloquially, 0° or 360° is North, 90° is East, 180° is South and 270° is West, with the direction being origin of the current wind flow.

3.7.3.1. Wind Direction Data Processing

The wind direction was calculated from the same data as the TKE calculations (see section 3.7.2.1.). The calculations use an equation that translates the positive and negative value of two of the three directional measurements: The X direction (positive being North, negative being South) and the Y direction (positive being West, negative being East). The equation uses radius circle geometry (See **Equation 3.**).

Eq. 3: $$Wind\ Degrees = 180 + \left(\left(\frac{180}{\pi}\right) * atan2(-Y, -X)\right)$$

The mean wind degrees for every 10 consecutive measurements is calculated. From that the mean wind degree is calculated for every 120 min for the same reason as explained above. The wind direction is then calculated by isolating eight separate intervals of 45° (NNE is 0° to 45°, ENE is 45° to 90° etc.). From these eight intervals the wind directions NE, SE, SW and NW can be isolated by combining two consecutive intervals.

3.8. Statistical Analyses

The section below contains all the statistical analysis utilized to evaluate and analyse data during the entirety of this doctoral study. It also contains descriptions of the analysis pertaining to Meteorological Datasets, Spatial and Temporal Variation, Population Dynamics, Markov Chain calibrations, Pollen Release parameters and the Lakeside Field Experiment.

3.8.1. Meteorological Dataset Investigations

This section represents the statistical investigation and rationale of fusing meteorological datasets for the years 2016 and 2017 due to missing sections of meteorological data from the associated weather loggers. The St Johns datasets in 2017 were fused using the St Johns Campbell logger and the Davis logger. The Lakeside datasets in 2016 were fused using the Skye logger and the Pershore weather station. The Lakeside datasets in 2017 were fused using the Lakeside Campbell logger, the Skye logger and the Pershore weather station (see section 3.2.2.2. for the general meteorological information). The datasets were investigated using Pearson correlation and R^2 values of a linear model.

3.8.1.1. Comparison and Rationale

The two Campbell loggers at each location were chosen to be the primary meteorological dataset for all years (including 2017 but not for 2016) due to the improved methodology and technology of these recently acquired weather loggers. The meteorological data from these loggers were available from the 11th of July 2017, meaning that data from previous dates (1st of May to 10th of July) had to be augmented by other weather loggers. To determine which loggers were most suited for this purpose a correlation of the entire available dataset for that year shared between loggers were investigated. All available datapoints (hourly temperature and precipitation measurements) were collated into one dataset per variable and correlated using Pearson's product-moment correlation (see Sedgwick, 2012) between loggers. A linear model between the datasets were also fitted to help with this determination. The distance, correlation coefficient and R^2 value between datasets was used to determine the best dataset to use for the augmentation (**Table 3.**). For Lakeside in 2016 only two hourly datapoints had to be augmented using the Pershore weather station. For St Johns in 2017, the Davis logger was chosen to

augment the beginning of the 2017 season. For Lakeside in 2017, the Skye logger was chosen to augment the beginning of the 2017 season. A section of the Lakeside dataset had to be further augmented due to missing sections of the Skye dataset (26th of June to 3rd of July). The Pershore weather station was chosen for this missing section due to its reliability and long use, even if the correlations could have been better. This was due to the need of having full meteorological data series.

Table 3

Comparison of different hourly meteorological data sets for both locations (St Johns and Lakeside) in 2017 for the period of available overlapping data in St Johns (11th of July to 31st of December) and Lakeside (11th of July to 7th of November).

Location	Variable	Logger1	Logger2	Data points	Distance (m)	Statistics	
				Comparison		Pearson Correlation	R^2
St Johns	Temperature	Campbell	Davis	3850	13m	0.995	0.990
	Temperature	Campbell	Pershore	3848	14.802m	0.985	0.970
	Temperature	Davis	Pershore	4158	14.791m	0.979	0.959
	Precipitation	Campbell	Davis	3467	13m	0.489	0.240
	Precipitation	Campbell	Pershore	3467	14.802m	0.460	0.211
	Precipitation	Davis	Pershore	4159	14.791m	0.605	0.366
Lakeside	Temperature	Campbell	Skye	2783	720m	0.982	0.964
	Temperature	Campbell	Pershore	2781	18.569m	0.977	0.955
	Temperature	Skye	Pershore	2853	19.168m	0.965	0.932
	Precipitation	Campbell	Skye	2401	720m	0.810	0.655
	Precipitation	Campbell	Pershore	2401	18.569m	0.339	0.115
	Precipitation	Skye	Pershore	2854	19.168m	0.307	0.094

3.8.2. Spatial and Temporal Variation

This section represents the spatial and temporal analyses conducted on the cohesive 2016, 2017, 2018 and 2019 grass pollen monitoring datasets obtained from the St Johns and Lakeside pollen monitoring stations (for the analysis concerning the 2019 grass pollen monitoring dataset collected from the three Lakeside locations, see section 3.8.5.). Five main pieces of analysis are presented below. The first one is the standardization of the grass pollen seasonal data. The second one is a STL Decomposition analysis of the grass pollen seasonal data. The third one is Spearman's correlations and Breusch-Godfrey analysis of the full data and the STL components. The fourth one is a Spearman's correlation and Wilcoxon Signed-Rank test analyses of meteorological data. The fifth one is a generalized linear mixed modelling approach using the variables constructed in the Atmospheric modelling section and weather variables, note that the 2016 and 2017 grass pollen dataset is not included in this specific section. One potential issue with using these analyses for the data is the questionable independence when

comparing data timeseries (pollen and weather) of nearby locations, an assumption of the statistical analyses. While these types of issues has been reported elsewhere the solution to the problem is not obvious since this is currently the most straightforward approach to compare this type of data. Therefore, the decision was made to follow the methods of previous publications (e.g. Fernández-Rodríguez et al., 2014; Kasprzyk, 2006; Maya Manzano et al., 2017; Pashley et al., 2009) until a better solution and standard practice has been developed by the statistical community. Potential future solutions could include additional development and adaptations of other timeseries analyses such as AutoRegressive Integrated Moving Average (ARIMA) approaches, however this is outside of the scope of this thesis.

3.8.2.1. Standardization

For each year (2016, 2017, 2018 and 2019) and location (St Johns and Lakeside) there is a grass pollen monitoring dataset (see sections 3.2.3 for details). The 95% pollen method was used to standardize the season within each year (e.g. Myszkowska, 2014; Smith et al., 2009). The method consists of discarding all dates in which below 2.5% and above 97.5% of the total seasons' pollen load falls. This is done to avoid long tails of low grass pollen concentrations at either end of the season. Both locations contributed equally to this method by summing and averaging each cumulative sum of grass pollen, and then distinguishing the 2.5% and 97.5% limits, as one grass pollen sum. Both standardized datasets for each year were tested for non-normality using the Shapiro non-normality test (Shapiro and Wilk, 1965), in which all datasets showed non-normality. The Seasonal Pollen Integral (SPIn) was calculated for available overlapping data in the grass pollen seasons (1st of May to 1st of September) for all years and locations using the standardized method (Galán et al., 2017). This was done to investigate the abundance of grass pollen captured within each location and to identify underlying patterns of grass pollen collection. Here, it was calculated by summing the average daily grass pollen concentration for each overlapping season. The SPIn Ratio was calculated as the ratio between St Johns to Lakeside (St Johns:Lakeside).

3.8.2.2. STL Decomposition

The grass pollen time-series were investigated using a Seasonal Decomposition of Time Series by LOESS (STL Decomposition) analysis (Cleveland et al., 1990), in which the LOESS stands for LOcally Estimated Scatterplot Smoothing (Cleveland, 1979). This time-series analysis decomposes each grass pollen season to its core components: seasonal, trend and remainders. A time-series reoccurrence frequency of 12 creates a daily-seasonality of the sample. The seasonal component highlights the varying intensity within the season. The trend component highlights the average peaks and dips present throughout the season. The remainder highlights

the components of the grass pollen season not explained by the seasonal intensity and the average trend. The remainder-component can be likened to the residual-component in other statistical models. The seasonal and trend components can be compared between location in the overlapping season to find inherent similarities, while the remainder component can be utilized to investigate autocorrelations between locations.

3.8.2.3. Pollen Correlations (Spearman and Breusch-Godfrey)

Both standardized grass pollen datasets for each year were statistically analysed using Spearman's correlation to investigate the spatial correlation between each location for the four years, an approach similar to Skjøth et al. (2013). Spearman's correlation was used due to the non-normality of the grass pollen data from all seasons, as tested with the Shapiro-Wilks test (Shapiro and Wilk, 1965). The seasonal and trend components of the STL Decomposition of each season was also investigated using Spearman's correlation to investigate potential commonalities in seasonality and trend between the two locations. The third component of the STL Decomposition, the remainder, was utilized to test for potential autocorrelation between the two locations for all years. The test was issued to determine if the pollen data captured is one signal with time delay, or two independent signals. The Breusch-Godfrey test was used for this purpose (Breusch, 1978; Godfrey, 1978). The test was performed using all time-delays between one data points (2 hours delay) and one hundred data points (16 days delay) to investigate the pattern of the potential autocorrelation. This test is distinct from the Breusch-Pagan, which tests for heteroskedasticity in the residuals of linear models (Breusch and Pagan, 1979).

3.8.2.4. Meteorological Correlations (Spearman and Wilcoxon)

The bi-hourly temperature and precipitation datasets from both locations (St Johns and Lakeside) for both the years' seasons (2018 and 2019) were statistically analysed using Spearman's correlation to investigate the similarities between the two locations. Spearman's correlation was used due to the non-normality of the meteorological data from all seasons, as tested with the Shapiro-Wilks test (Shapiro and Wilk, 1965). Wilcoxon Signed-Rank test was utilized to test for any general differences in the meteorology of the locations. The test was used due to the non-normality expressed by the data and the paired connection between the measurements of each timestep (Wilcoxon, 1945).

3.8.2.5. Generalized Linear Mixed-Effects Modelling

In this section, the variables created during the Atmospheric Modelling section (trajectory-grass maps) along with weather variables (temperature and precipitation) were used to investigate the contribution to the bi-hourly grass pollen concentrations collected in St Johns and Lakeside

respectively. To investigate each variables' contribution to the grass pollen concentrations, a GLMER (Generalized Linear Mixed Effects models in R) approach was utilized. The GLMER utilized is a adapted version of the overarching GLMM (Generalized Linear Mixed Model) class of models (Breslow and Clayton, 1993). The R package *lme4* (Bates et al., 2015) was used to create the model. The model works by building a generalized linear regression using random and fixed variables to calculate parameters and minimize residuals in the generalized linear relationship. The GLMER approach (being similar to a GLM (Generalized Linear Model) (McCulloch, 2001)) incorporate a family object, which instructs in how the model is fitted. The family object utilized in this model is the Gamma family with a link-log function used to fit exponential models. To utilize this model the grass pollen concentration variables had to be increased by 1, since using the natural logarithm on a zero-values is not possible, a common approach in ecological statistics (Fletcher et al., 2005). The use of random variables can account for additional model variation otherwise overlooked. In this model three temporal variables were used to represent the random variation: DOY (Day of Year), the time of day (every second hour as measured by the bi-hourly pollen concentrations) and the year (2018 or 2019). By accounting for these temporal variables, a general contribution of each fixed variable can be gained without considering how they might vary temporally. For example, the fixed effect of temperature might be skewed due to some years being warmer on average. Another example is that pollen concentrations tend to be higher during the days than during the nights. Eight fixed variables were included: six trajectory-grass variables (two unique per location and four shared) along with temperature and precipitation. All variables were taken from the abovementioned sections. The trajectory-grass maps variables were transformed using the natural logarithm (ln), as common practice while using variables with large natural variation. The model then summarizes the total contribution of each variable to the bi-hourly grass pollen concentrations for each location. The model t – values are interpreted using Satterthwaite's method by the R package *lmerTest* (Kuznetsova et al., 2017) into p – values. The coefficients of determination (R^2) of the generalized linear mixed-models were determined using the R package *MuMIn* (Barton, 2020). The more conservative Trigamma R^2 estimate was used instead of the Delta or Lognormal estimates (Nakagawa et al., 2017). The predicted grass pollen concentrations were back-transformed from natural logarithm to real numbers using the base of the natural logarithm (*e,* Eulers number) in order to facilitate a comparison on the same scale. While the R^2 estimate provides a general model performance metric the predicted grass pollen concentrations showcases how the model performs in relation to low and high pollen concentrations separately.

3.8.3. *Dactylis* Population Phenological Dynamics

All *Dactylis* populations were compared statistically to evaluate spatial and temporal inter- and intra-variation trends. Two main pieces of analysis are presented below. The first one is collation of the temporal general phenological phase of each of the nine populations in and between years in order to create a general phenological development per year. The second one is the use of a Markov Chain approach to incorporate a systematic method to compare tiller-specific development between the three main populations.

3.8.3.1. General Flowering Progression Data Processing

It is possible to create an average phenological phase of each population by summing and averaging the phase of each tiller in each time-step. This average phenological phase represents how far in development each population is in relation to each standardized phase (Phase 0 to Phase 5). The processing was achieved by taking all the available average phases during each date and averaging them, to obtain a general phenological development of all populations in each year. For 2017 there was only one population and data points available each day, hence there was no standard error or missing data points. In 2018, however, there were eight populations, with varying degrees of observations each day, with some days completely missing data points due to the observation protocol utilized. All available population averages were averaged for each day, creating a few gaps. Each gap was filled with the average general phase of the two surrounding days for model and comparative necessity. The 2018 data set also contains a standard error present in each date due to the potential of having several averaged populations observed during the same date with varying degree of population development.

3.8.3.2. General Flowering Progression Correlation

The datasets comprised of one year each were then investigated for normality using the Shapiro non-normality test (Shapiro and Wilk, 1965). Both datasets expressed non-normality and hence the non-parametric Spearman rho correlation (Spearman, 1904) was utilized to test for correlation between the two data sets. By using a Spearman rho correlation, it is possible to investigate yearly temporal trends in the general *Dactylis* flowering progression. Significance testing was omitted due to the strong autocorrelation present in the comparison of accumulated time series.

3.8.3.3. Markov Chain Matrix Correlation

Three seasonal transitional matrices from the general Markov Chain approach (see section 3.6.1.) compiled from each observed population (St Johns 2018, St Johns 2019, and Lakeside 2019) were investigated using matrix correlation coefficients. The matrix correlation coefficients were utilized from the R package *MatrixCorrelation* (Indahl et al., 2018). Three

different matrix correlation coefficients were used in order to avoid potential bias using only one. The three matrix coefficients used were: RV (Robert and Escoufier, 1976), RV2 (Smilde et al., 2009) and Adjusted RV (Mayer et al., 2011). All possible combinations were tested for in order to investigate trends based on spatial and temporal differentiation. The three combinations were the following: St Johns 2017 vs St Johns 2018 (investigating temporal trends), St Johns 2018 vs Lakeside 2018 (investigating spatial trends) and St Johns 2017 vs Lakeside 2018 (investigating both temporal and spatial trends).

3.8.3.4. Markov Chain Diagrams

Each matrix can be expressed as a transitional likelihood between phases. It is possible to create graphical interphases from the matrices, increasing the interpretation and overview significantly to the viewer using Markov Chain Diagrams. Each diagram is simply the directional phase-shift, expressed with arrows of comparative thickness dependant on the likelihood of transition, i.e. a thin arrow represents a low likelihood, and a thick arrow represents a high likelihood. Each arrow is also accompanied by the strength of the likelihood in absolute percentage.

3.8.4. Markov Chain Optimization and Pollen Release Dynamics

This section represents the statistical analyses pertaining to the Markov Chain general population modelling approaches using the observed *Dactylis glomerata* populations and the selection and comparison of optimized models. Three main pieces of analysis are presented below. The first one is the correlation of the Markov Chain lists: how many elements that are optimal to include and which Markov Chain objects that can produce the most accurate modelled population for each of the two main population in 2018 (St Johns and Lakeside). The second one is the investigation into the correlations between the pollen release scenarios created from the above-mentioned general populations and the DNA metabarcoding results obtained from the proximity of the observed populations. The third one is the investigation into the correlations between the DNA metabarcoding results and the meteorological measurements taken from the Campbell weather loggers in proximity to the observed populations. This was done to determine the most important weather variables likely responsible for the grass pollen release.

3.8.4.1. Optimization of the Modelled General Populations

Each modelled general population was created from a unique Markov Chain vector-list (see section 3.6.2.1.). Each modelled general population was then compared to the observed population of the associated location (St Johns or Lakeside). The second day of each modelled general population was extracted to match with the observation dates of the observed populations, this was done to facilitate exact comparison. The comparisons were made using

Kendall rank correlations (Kendall, 1938). Reasonings of utilizing Kendall rank correlations were two-fold: both populations expressed non-normally distributed data due to being converging time-series, and the narrower confidence interval that the method provides (Puth et al., 2015). Phases were compared i) independently (singularly) between populations to illustrate how the modelled population behaves per phase, and ii) in together (combined) between populations to illustrate how the modelled population behaves as a whole. The combined approach would be more accurate to measure the true similarity between each observed and modelled population pair.

3.8.4.2. Pollen Release – DNA Metabarcoding Bioinformatics Correlations

Ten pollen release scenarios were modelled based on the most accurate modelled general population from the section above. The ten static pollen release scenarios were modelled with each scenario being intervals of 10 (10% per day, 20% per day etc.) for each tiller and combined for each population (see section 3.6.2.1.). Each pollen release curve were then compared to the DNA metabarcoding bioinformatics ITS1 and ITS2 time-series of *Dactylis glomerata* using Spearman rho correlation. Each pollen release time-series were condensed to match the 3 - 4 days pooling strategy of the sampled eDNA. The condensed pollen release scenarios and DNA metabarcoding results were compared for each location and ITS-region, but also combined for both regions per location and for both locations combined. The motivation of combining ITS-regions and locations was due to the low number of data points utilized to test for the same mechanism: the connection between flowering and pollen release. The fusion of datasets was therefore justified due to same mechanism being investigated.

3.8.4.3. Weather Conditions – DNA Metabarcoding Bioinformatics Correlations

Location-specific meteorological conditions were measured using the Campbell weather loggers during the same period as the eDNA collection. Five meteorological variables were compared with the DNA metabarcoding bioinformatics: solar radiation, temperature, relative humidity, precipitation, and wind speed. All weather variables were averaged to daily values expect for precipitation, which was summed to daily values. All variables were further condensed to match the 3 – 4 days pooling strategy mentioned above. The condensed meteorological variables were then compared to the DNA metabarcoding bioinformatics using Spearman rho correlation. This was done for consistency with the pollen release scenarios in order for equal comparison between all datasets. The combined ITS-regions for both locations were utilized for the correlation with location-specific weather conditions, due to the low number of data points utilized and the same mechanism investigated.

3.8.5. Lakeside Field Experiments

This section contains the statistical analysis pertaining to the statistical analysis of grass pollen dynamics and emission parameters of *Festuca rubra* within three local locations in Lakeside 2019. Two main pieces of analyses are presented below. The first one is the correlations between varying grass pollen concentration intervals from the different Lakeside locations. The second one is the generalized linear modelling (GLM) of the bi-hourly grass pollen concentrations from each location and a wide range of meteorological variables and potential emission parameters. The analyses are further validated and enhanced using *F. rubra* pollen eDNA bioinformatics and population flowering phenology. *F. rubra* was the dominant grass species present within the Lakeside field circle, and it only occurred there. The other selected grass species, *Lolium perenne*, was excluded from the analysis due to uncertain bioinformatics classification.

3.8.5.1. Grass Pollen Correlations

Both bi-hourly and daily grass pollen concentration datasets from all three Lakeside locations in 2019 were used to test for correlations between the locations. All datapoints between 15th of May to 6th of July were included in the analysis. All datasets were investigated for normality using the Shapiro non-normality test. All datasets expressed statistical normality hence the parametric Pearson's product-moment correlation was utilized for the correlation testing.

3.8.5.2. Generalized Linear Modelling

To test the influence of local meteorological variables on localized bi-hourly grass pollen a Generalized linear modelling (GLM) approach were utilized. All bi-hourly grass pollen concentration datapoints below 61.2 grains/m^3 (10 grains per bi-hourly microscopy slide transect) were excluded from the analysis due to the general uncertainty of using low grass pollen concentrations in modelling approaches. The GLM-approach creates one model per location (bi-hourly grass pollen concentration dataset) with meteorological variables collected from the Campbell meteorological station located in the middle of the Lakeside Field location. Bi-hourly meteorological variables accounted for are the following: temperature, precipitation, relative humidity, solar radiation, wind direction, wind speed and Turbulent Kinetic Energy (TKE). Wind speed were accounted from three directions (N-S, W-E and Up-Down). All variables are accounted for as bi-hourly means except precipitation which is bi-hourly sums. TKE were accounted for as minimum, mean, and maximum per bi-hourly timepoint. The particle datasets collected from the AlphaSense particle counters within the same locations were excluded from the analysis due to hardware malfunction.

4. Local Spatial and Temporal Variation in Grass Pollen Distribution

4.1. Introduction

In-depth exploration of the spatial and temporal variation of grass pollen distributions and how it varies on a localized scale will increase the fundamental understanding necessary for the development of future mechanistic and pollen forecasting models (see section 1.4.). The sections below presents results related to the spatial and temporal variation divided into annual sections based on bi-hourly pollen concentrations alone in the spirit of traditional aerobiological research. It also includes a modelling of bi-hourly pollen concentrations based on a generalized linear mixed modelling approach that incorporates both fixed (temperature, precipitation, atmospheric wind movement and grass area landcover) and random (DOY, Time of day and Year) variables to predict grass pollen concentrations. Discussion surrounding the comparison of location-specific grass pollen seasons and model results based on the locations round off the chapter.

4.2. Results

4.2.1. Result Summary – Chapter 4

This chapter sought to explore how the spatial and temporal trends in grass pollen concentrations varied between years for two locations and how these trends could be identified using source maps and meteorological and atmospheric modelling. It was found that there were highly significant correlations in the grass pollen concentrations between the two locations but with substantial residual variation after trend elements were removed. Potential grass pollen source areas were identified using the Crop map from CEH. The atmospheric modelling approaches using HYSPLIT identified that there was differential origin of the grass pollen found in each location. Grass pollen collected in urban site were likely to have originated between 20 and 30 km away, while for the rural site areas between 2 and 10 km away were likely to have contributed pollen.

4.2.2. Seasonal Spatial and Temporal Pollen Variation

The section below presents the results of the seasonal comparisons of bi-hourly grass pollen concentrations within and between the location St Johns and Lakeside for all of the sampling years (2016-2019). For a graphical overview of the daily grass pollen concentrations, see supplementary information (**Supplementary Figures S26 – S29.**).

4.2.2.1. Spatial and Temporal Pollen Variation during 2016

The full grass pollen seasonal data from the St Johns pollen monitoring station was collated between the 1st of May and the 1st of September (**Figure 18.**). By applying the 95% method, the general grass pollen season during 2016 was estimated to have started on the 25th of May and ended on the 18th of August, discarding the first and last 2.5% of the total season load. The first high phase of the season lasted between the 4th and 12th of June, with the first big peak being observed on the 6th of June. The levels then decreased for about 5 days, until the second phase of June began, lasting from the 15th of June and onwards, with the season peak being on the 23rd of June. During the 2016 grass pollen seasons overlapping data between the locations St Johns and Lakeside existed between the 29th of June and 1st of September, which was the primary focus of the spatial and temporal comparison. During the 29th of June a peak was reached at Lakeside while being almost absent in St Johns. For the rest of July, the peaks coincided in timing, with the peaks in Lakeside usually being slightly stronger. This was noticeable during the second largest peak of the season, on the 3rd of July with the peak reaching both locations within four hours. The last big peak of the season occurred on the 14th of July, with both locations experiencing this peak at the same time. The grass pollen concentrations will from this point remained low, except for a few low local peaks in St Johns during the middle of August. When accounting for the overlapping season using the 95% method, the overlapping general season was estimated to have statistically started on the 29th of June and ended on the 21st of August. Spearman correlation was used to test for a statistical relationship due to the non-normality expressed in the pollen seasons from both locations as investigated by the Shapiro-Wilks test ($p < 0.001$ x2). The Spearman's correlation on the standardized 95% overlap bi-hourly grass pollen concentration series for this period estimated that there was a correlation of 0.590 ($p < 0.001$) between the two locations (**Table 4.**). This indicated that there was a spatial relationship of moderate strength between the locations during the overlapping period of this year. The STL Decompositions indicated that there was a strong correlation in the seasonal and trend components between locations, 0.858 ($p < 0.001$) and 0.737 ($p < 0.001$) respectively. Breusch-Godfrey test of the model residuals from the remainder concluded that there was autocorrelation between the two locations for up to 16 days' time-lags (**Supplementary Figure S30.** and **Figure S31.**, **Supplementary Table S2.**). The Seasonal Pollen Integral (SPIn) for the overlapping period in 2016 was 1994 (pollen*day/m^3) for St Johns, and 1831 (pollen*day/m^3) for Lakeside. The SPIn ratio for 2016 St Johns:Lakeside was close to 1:1.09.

4.2.2.2. Spatial and Temporal Pollen Variation during 2017

The full grass pollen seasonal data from the St Johns pollen monitoring station was collated between the 1st of May and the 1st of September (**Figure 19.**). By applying the 95% method, the general grass pollen season during 2017 was estimated to have started on the 24th of May and ended on the 1st of August, discarding the first and last 2.5% of the total season load. The season started slowly with small peaks from the start to the middle of June, with the first larger peak being on the 14th of June. The season continued to intensify with the first large peak and the seasons second largest peak being on the 17th of June, with two medium sized peaks occurring during the following few days. During the 2017 grass pollen seasons overlapping data between the locations St Johns and Lakeside existed between the 22nd of June and 1st of September, which was the primary focus of the spatial and temporal comparison. The overlapping period at the end of June was marked by mainly overlapping medium-sized peaks with the Lakeside pollen concentrations being noticeably higher than the St Johns peaks. The main peak of the seasons was observed on the 1st of July, with both the strength and timing being the same between the locations. The continuation of July was marked by smaller peaks, with incremental increases in the ratio between St Johns and Lakeside, with the last big peak being on the 8th of July. The rest of the season was mainly characterized by low grass pollen concentrations. When accounting for the overlapping season using the 95% method, the overlapping general season was estimated to have statistically started on the 23rd of June and ended on the 17th of August. Spearman correlation was used to test for a statistical relationship due to the non-normality expressed in the pollen seasons from both locations as investigated by the Shapiro-Wilks test ($p < 0.001$ x2). The Spearman's correlation on the standardized 95% overlap bi-hourly grass pollen concentration series for this period estimated that there was a correlation of 0.513 ($p < 0.001$) between the two locations (**Table 4.**). This indicated that there was a spatial relationship of moderate strength between the locations during the overlapping period of this year. The STL Decompositions indicated that there was a moderate correlation in the seasonal and a strong correlation in the trend components between locations, 0.634 ($p < 0.001$) and 0.715 ($p < 0.001$) respectively. Breusch-Godfrey test of the model residuals from the remainder concluded that there was autocorrelation between the two for up to 16 days' time-lags (**Supplementary Figures S32 - S33.**, **Supplementary Table S2.**). The Seasonal Pollen Integral (SPIn) for the overlapping period in 2017 was 1360 (pollen*day/m^3) for St Johns, and 1267 (pollen*day/m^3) for Lakeside. The SPIn ratio for 2017 St Johns:Lakeside was close to 1:1.07.

4.2.2.3. Spatial and Temporal Pollen Variation during 2018

The full grass pollen seasonal data from both locations (St Johns and Lakeside) were collated between the 1st of May and the 1st of September (**Figure 20.**). By applying the 95% method, the general grass pollen season during 2018 was estimated to have started on the 21st of May and ended on the 20th of July, discarding the first and last 2.5% of the total season load. Most of May was characterized by low pollen concentrations for both locations, until the first high peak hit simultaneously during the 31st of May. The following week was characterized by several high peaks, occurring in both locations at the same time, with higher intensity seen in Lakeside. The seasons' highest peak occurred during this week, on the 3rd of June, with a similar higher intensity seen in Lakeside. This was the highest grass pollen concentration observed during the three years. The pollen concentrations for the following week was lower for Lakeside, but increased for St Johns, with the seasons' second highest peak present in St Johns, but mostly absent for Lakeside. The period between 3rd of June to 18th of June was mainly characterized of high peaks with varying intensity ratio between St Johns and Lakeside, indicating a partial overlap in timing but not in uniform strength. The continuation of June highlighted a general lowering of Lakeside pollen concentrations with St Johns still experienced high pollen concentrations in daily intervals. This trend continued with the decline of the seasons into July, with levels reached low background concentrations around the 15th of July. The rest of July and August was characterized by low pollen concentrations. When accounting for the overlapping season using the 95% method, the overlapping general season was estimated to have statistically started on the 21st of May and ended on the 20th of July. Spearman correlation was used to test for a statistical relationship due to the non-normality expressed in the pollen seasons from both locations as investigated by the Shapiro-Wilks test ($p < 0.001$ x2). The Spearman's correlation on the standardized 95% overlap bi-hourly grass pollen concentration series for this period estimated that there was a correlation of 0.683 ($p < 0.001$) between the two locations (**Table 4.**). This indicated that there was a spatial relationship of moderate strength between the locations during the overlapping period of this year. The STL Decompositions indicated that there was a strong correlation in the seasonal and trend components between locations, 0.843 ($p < 0.001$) and 0.841 ($p < 0.001$) respectively. Breusch-Godfrey test of the model residuals from the remainder concluded that there was autocorrelation between the two locations for up to 16 days' time-lags (**Supplementary Figures S34 - S35.**, **Supplementary Table S2.**). The Seasonal Pollen Integral (SPIn) for the overlapping period in 2018 was 5941 (pollen*day/m^3) for St Johns, and 4423 (pollen*day/m^3) for Lakeside. The SPIn ratio for 2018 St Johns:Lakeside was close to 1:1.34.

4.2.2.4. Spatial and Temporal Pollen Variation during 2019

The full grass pollen seasonal data from both locations (St Johns and Lakeside) were collated between the 1st of May and the 1st of September (**Figure 21.**). By applying the 95% method, the general grass pollen season during 2019 was estimated to have started on the 1st of June and ended on the 5th of August, discarding the first and last 2.5% of the total season load. The entire May period was characterized by low pollen concentrations levels both at St Johns and Lakeside. The first peak was visible during the 1st of June, with it being noticeably higher in Lakeside. The first half of June was visibly lower in grass pollen concentration intensity, until the second peak of the season hit both locations during the 15-16th of June. A few days of low concentrations was followed by four days of high concentrations, 21-24th of June, with the general levels being higher in St Johns while the peak was larger in Lakeside. The two highest seasonal peak sections hit during the 27-29th of June and 3-5th of July. Peaks located in St Johns had equal strength while the Lakeside peaks had stronger and weaker peaks interchangeably. The overarching pattern of both locations had up-until this point been markedly similar in the trend of the grass pollen season. The continuation of July was marked by successively smaller localized peaks with decreasing intensity, with St Johns having localized stronger concentrations than Lakeside. The pollen curve was marked with lower background concentrations from the 22nd of July and onwards to the start of September. When accounting for the overlapping season using the 95% method, the overlapping general season was estimated to have statistically started on the 1st of June and ended on the 5th of August. Spearman correlation was used to test for a statistical relationship due to the non-normality expressed in the pollen seasons from both locations as investigated by the Shapiro-Wilks test ($p < 0.001$ x2). The Spearman's correlation on the standardized 95% overlap bi-hourly grass pollen concentration series for this period estimated that there was a correlation of 0.781 ($p < 0.001$) between the two locations (**Table 4.**). This indicated that there was a spatial relationship of strong strength between the locations during the overlapping period of this year. The STL Decompositions indicated that there was a strong correlation in the seasonal and trend components between locations, 0.773 ($p < 0.001$) and 0.936 ($p < 0.001$) respectively. Breusch-Godfrey test of the model residuals from the remainder concluded that there was autocorrelation between the two locations for up to 16 days' time-lags (**Supplementary Figures S36 – S37.**, **Supplementary Table S2.**). The Seasonal Pollen Integral (SPIn) for the overlapping period in 2019 was 4905 (pollen*day/m^3) for St Johns, and 4164 (pollen*day/m^3) for Lakeside. The SPIn ratio for 2019 St Johns:Lakeside was close to 1:1.18.

Table 4

Spearman ρ (r_s) correlations for the STL Decompositions for the 95% seasonal Bi-hourly grass pollen concentration overlap between St Johns and Lakeside for the years 2016-2019.

STL Decompositions	Spearman ρ (r_s)				P-Value			
	2016	2017	2018	2019	2016	2017	2018	2019
Full Pollen Series	0.590	0.513	0.683	0.781	< 0.001	< 0.001	< 0.001	< 0.001
Seasonal	0.858	0.634	0.843	0.773	< 0.001	< 0.001	< 0.001	< 0.001
Trend	0.737	0.715	0.841	0.936	< 0.001	< 0.001	< 0.001	< 0.001
Remainder	0.494	0.288	0.492	0.514	< 0.001	< 0.001	< 0.001	< 0.001

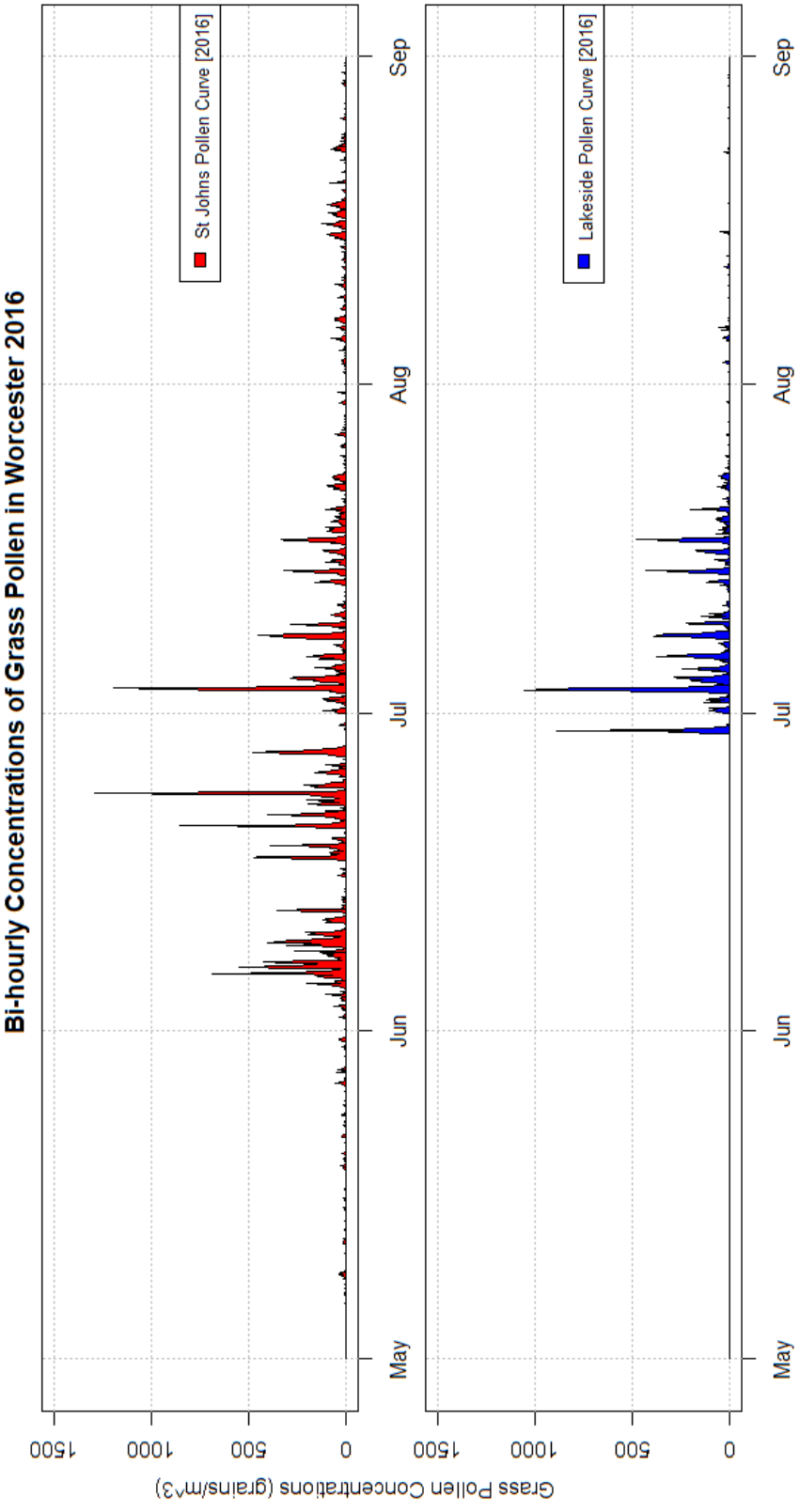

Figure 18. Bi-hourly concentrations of grass pollen from two locations (St Johns and Lakeside) during the 2016 season in Worcester. Note that overlapping data in 2016 is available from the 29th of June.

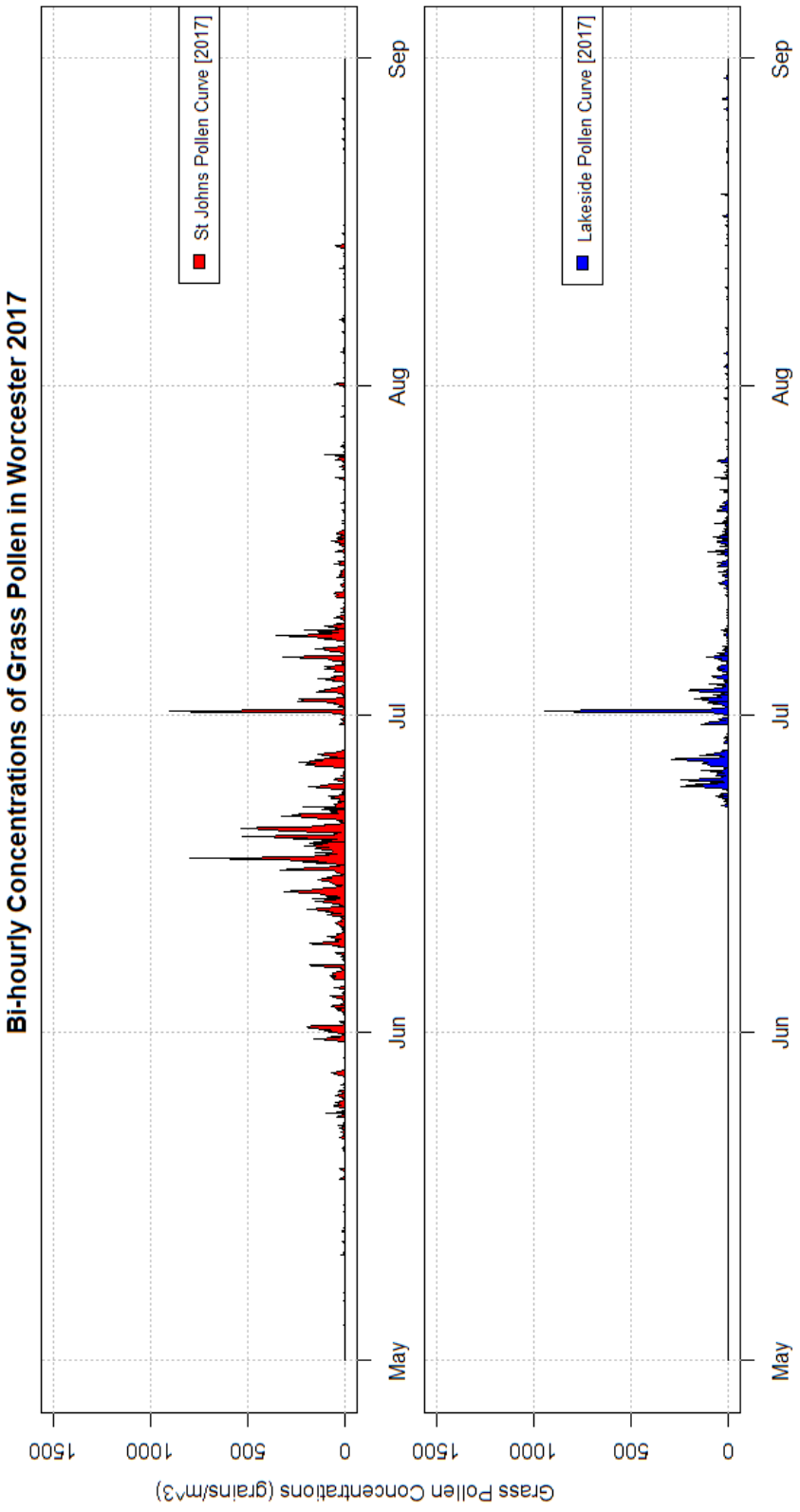

Figure 19. Bi-hourly concentrations of grass pollen from two locations (St Johns and Lakeside) during the 2017 season in Worcester. Note that overlapping data in 2017 is available from the 22nd of June.

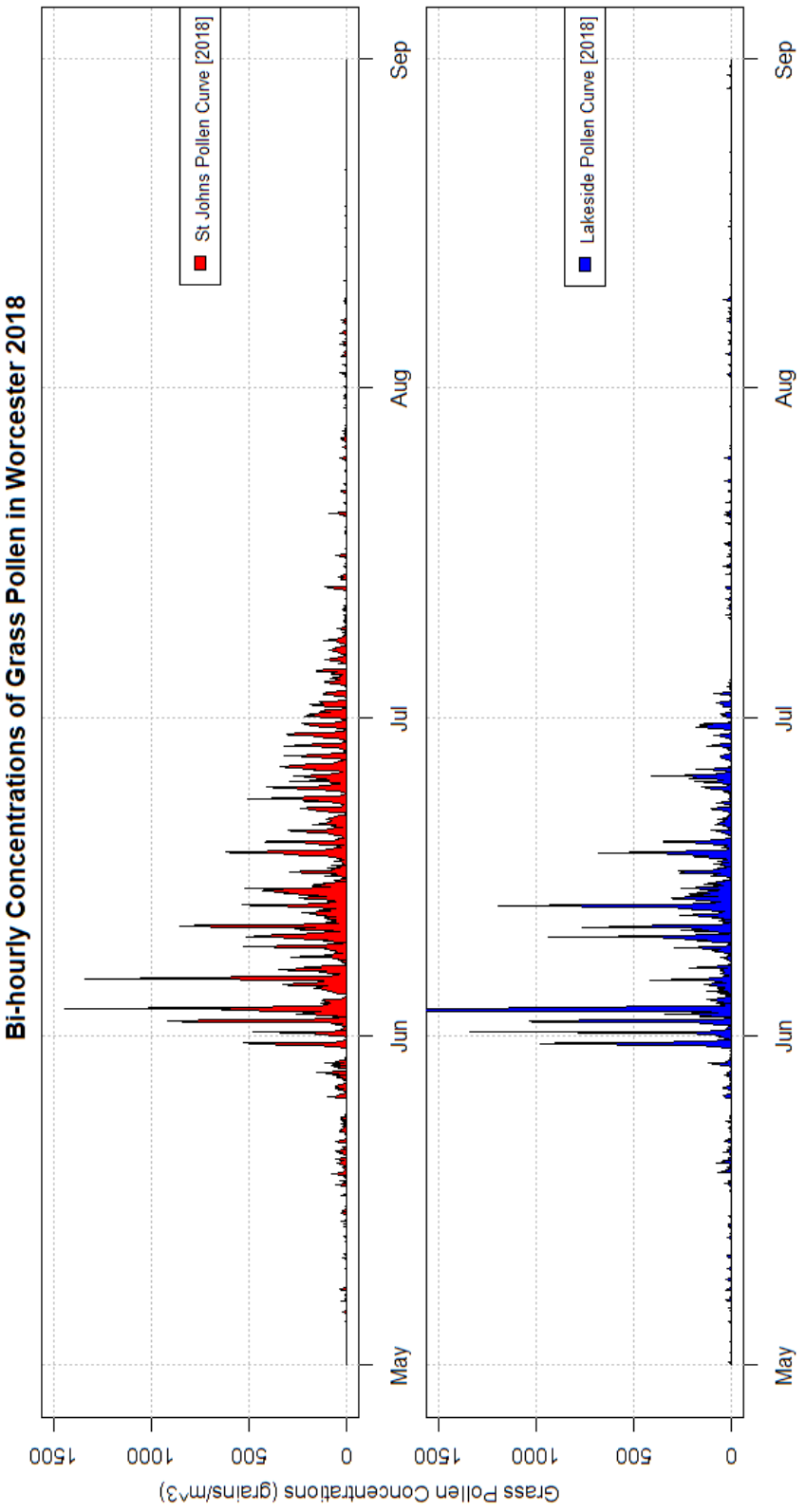

Figure 20. Bi-hourly concentrations of grass pollen from two locations (St Johns and Lakeside) during the 2018 season in Worcester. Note that the top peak of the season (3359 grains/m^3) exceeds the y-axis maximum.

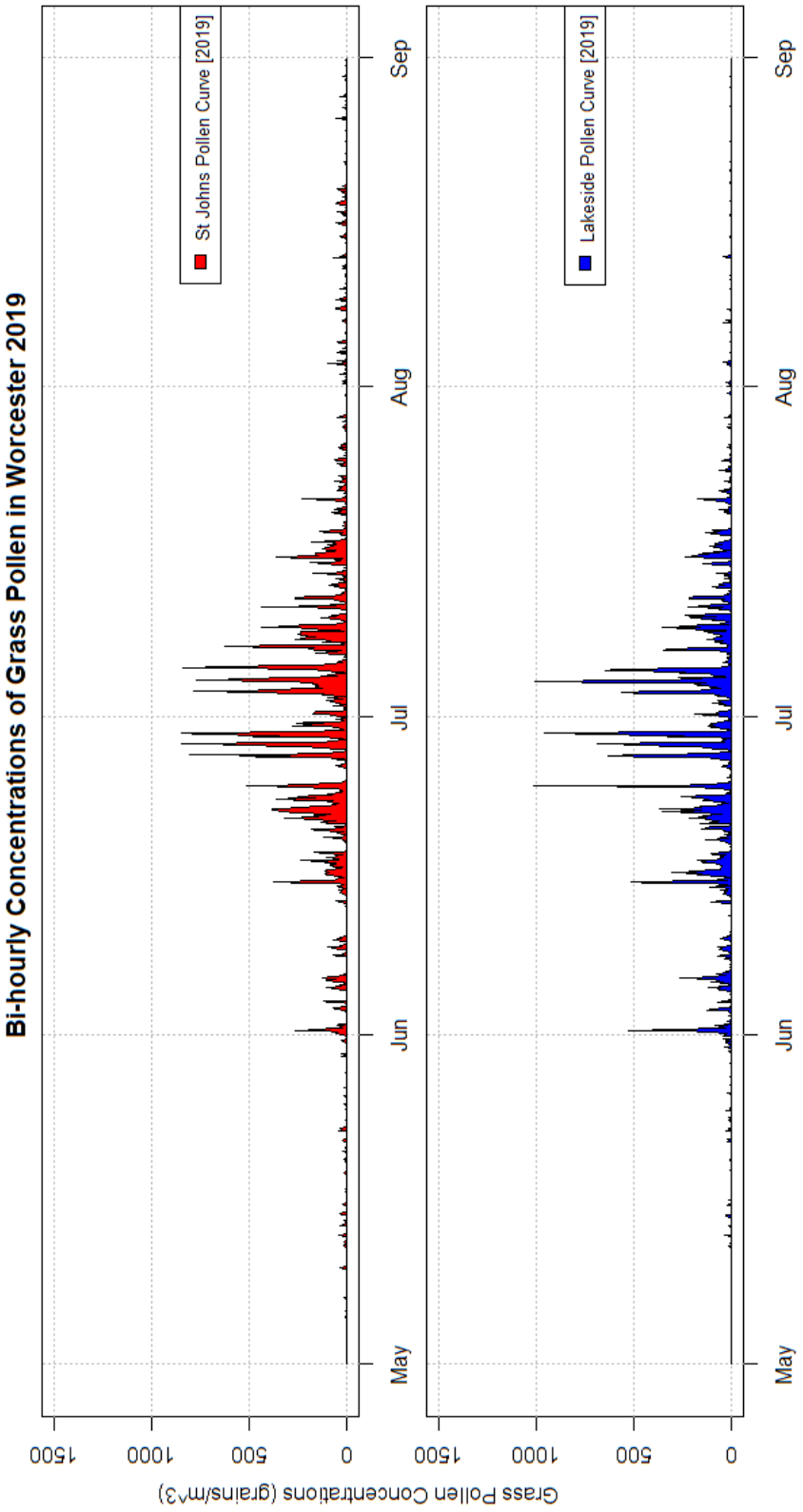

Figure 21. Bi-hourly concentrations of grass pollen from two locations (St Johns and Lakeside) during the 2019 season in Worcester.

4.2.3. Potential Source Areas

The potential main areas contributing grass pollen in the Worcestershire area were estimated from the 'CEH Land Cover Plus ®: Crop' dataset. The eight grass maps included seven counties in the Midlands area of the United Kingdom: Worcestershire, Gloucestershire, Herefordshire, Shropshire, Staffordshire, West Midlands, and Warwickshire (**Figure 22.**). The source map highlighted the lower absolute presence of pollen contributing areas within the major city hubs around the Midlands area (**Figure 23.**). Reasoning for this was that most grass pollen contributing areas had been replaced with urban infrastructure in the recent past. Several prominent cities could be located due to the lack of grass pollen contributing areas. Examples include several cities in Worcestershire: Worcester in the middle of the map, Kidderminster/Stourport-on-Severn city-complex to the north and Redditch to the east. Other notable examples include Gloucester/Cheltenham city-complex in the middle of Gloucestershire and the Telford city-complex in the east of Shropshire. It was especially pronounced in the West Midlands, where the second biggest settlement in the UK is located: the Birmingham metro area and the connecting urban areas. It is however important to remember that features with as road-verges, home gardens and similar features are not incorporated in the above dataset due to the higher resolution needed to account for these features. This will lower the absolute number of grass pollen contributing areas in major city hubs, even if the presence of parks and similar large features still remain. The source map also highlighted places where the potential pollen source areas were more highly concentrated than the general matrix. These places included areas in eastern Herefordshire, central Shropshire, north-western Warwickshire, and northern Gloucestershire. There were also many local areas that had high amounts of grass areas in the form of potential source areas, but that had surrounding areas that were low in grass areas, potentially obscuring their regional importance.

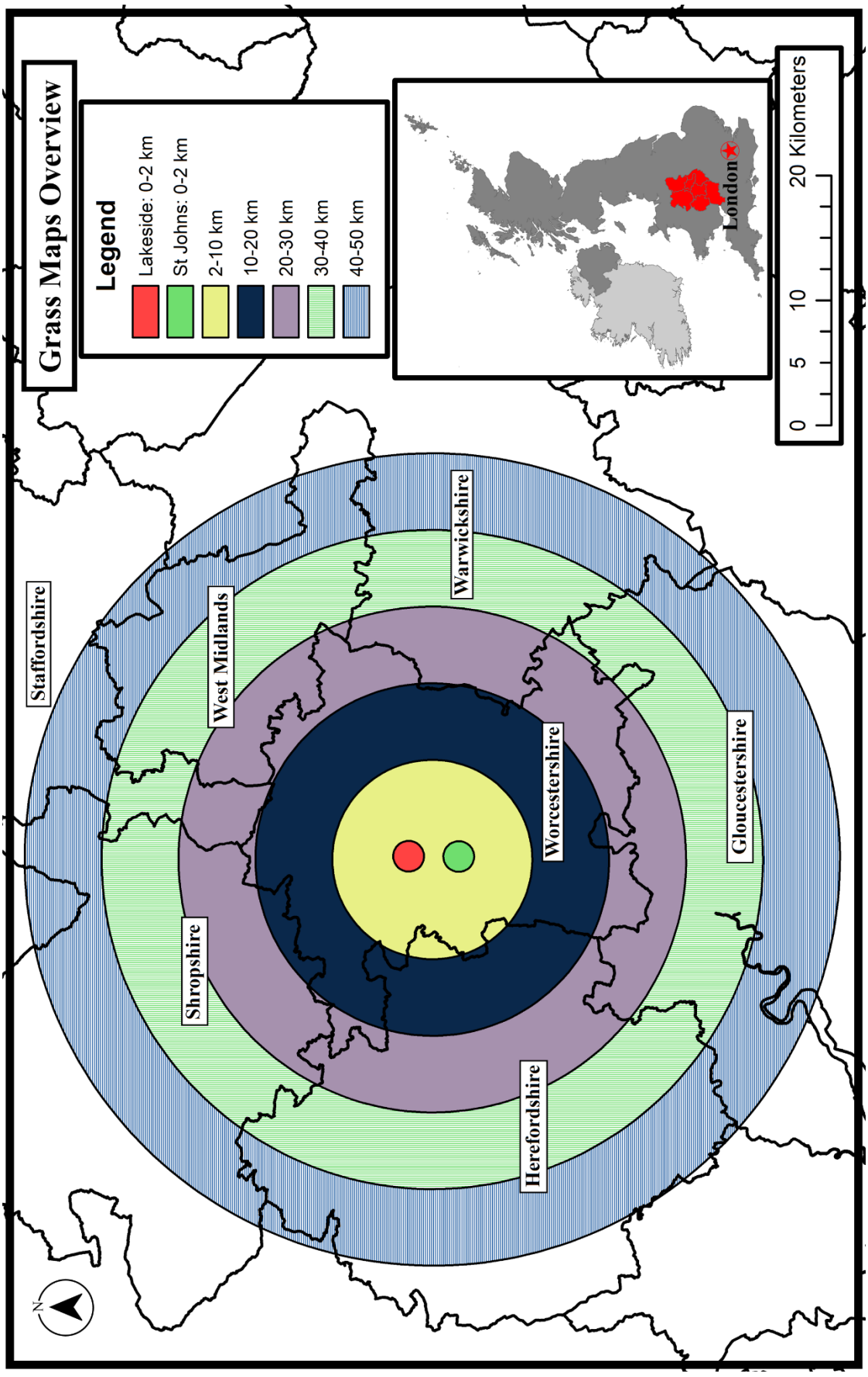

Figure 22. Overview of the circular and concentric circular grass maps within the surrounding counties created for the grass pollen investigation of the locations St Johns and Lakeside. The overlapping counties can be found in the United Kingdom overview map.

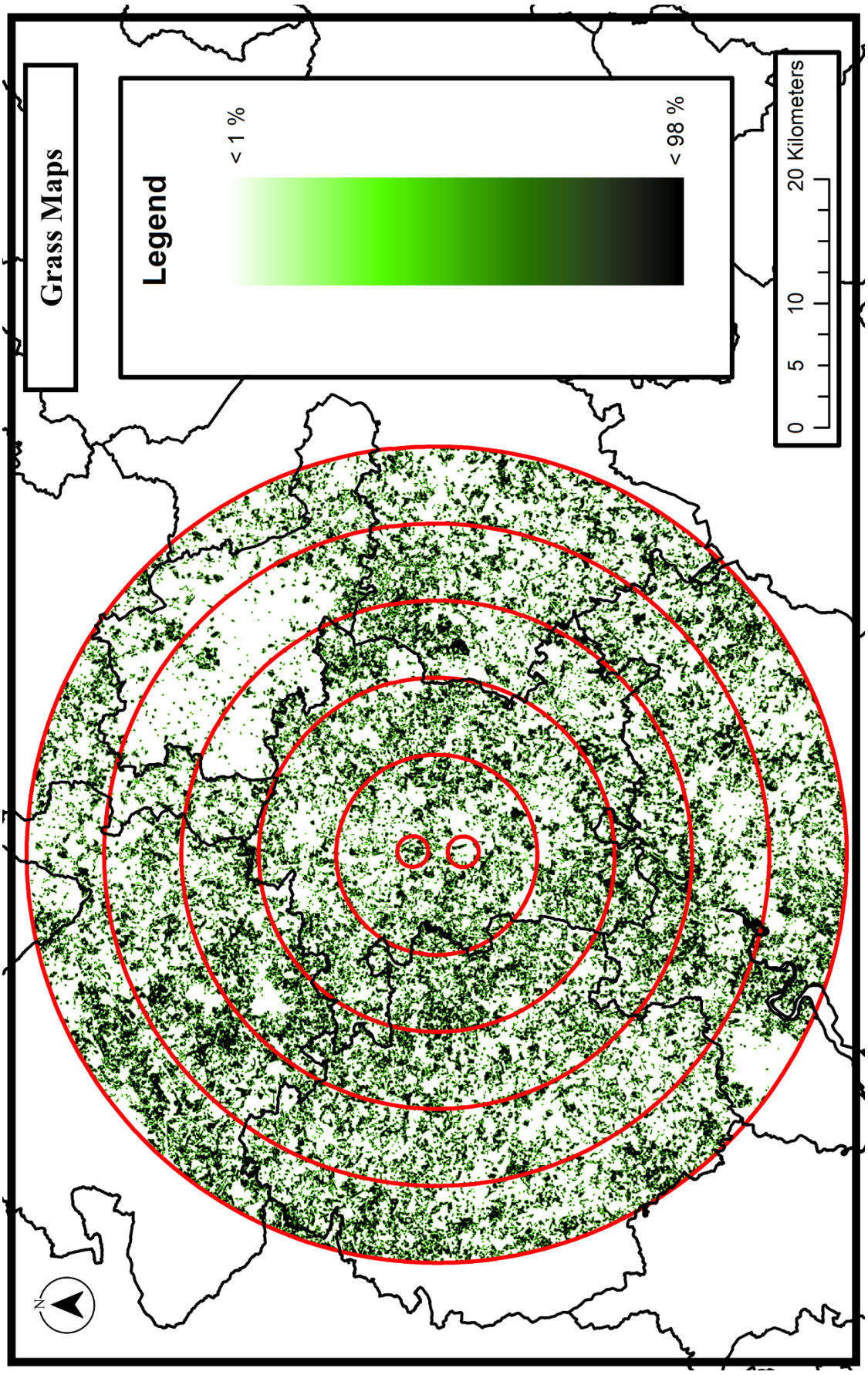

Figure 23. The circular and concentric circular grass maps within the surrounding counties created for the grass pollen investigation of the locations St Johns and Lakeside. The gridcell resolution is 100 x 100 m. The legend specifies how much of each gridcell is covered by grass areas.

4.2.4. Atmospheric Wind Movement Distribution

This section presents all the calculated HYSPLIT trajectories. The trajectories were calculated for each site during the periods with overlapping data for the years 2018 and 2019. Trajectories from the year 2016 and 2017 were not included due to unreliable meteorological data. All trajectories for the two years were overlaid one grid and calculated based on densities of the full sample values.

4.2.4.1. St Johns

All trajectories corresponding to the timing of the bi-hourly pollen measurements for the 1st of May to 1st of September 2018 and 1st of May to 1st of September 2019 were summed into one dataset to estimate atmospheric transport to the St Johns pollen monitoring station (**Figure 24.**). Most transects intersected in gridcells close to the origin in St Johns, with a higher concentration originating from south-western directions. There was a clear emphasis on trajectories originating from a western direction and an eastern direction, as showed by the higher intensity horizontal line in Figure 24. Trajectories were also generally more likely to originate from the western regions than eastern regions, with a few exceptions towards the northeast. Trajectories tended to be less likely to originate from south-eastern areas.

4.2.4.2. Lakeside

All trajectories corresponding to the timing of the bi-hourly pollen measurements for the 1st of May to 1st of September 2018 and 1st of May to 1st of September 2019 were summed into one dataset to estimate atmospheric transport to the Lakeside pollen monitoring station (**Figure 25.**). The general atmospheric transport patterns were like the relative pattern from St Johns, with similar regional directional movement. While the relative patterns were the same, the absolute patterns were different. This was due to the slightly divergent areas the wind travelled through on the way to the Lakeside, caused by the underlaying wind data. Areas in central Worcestershire and eastern Herefordshire overlapped, but the Lakeside trajectories also included areas of northern Worcestershire and Herefordshire.

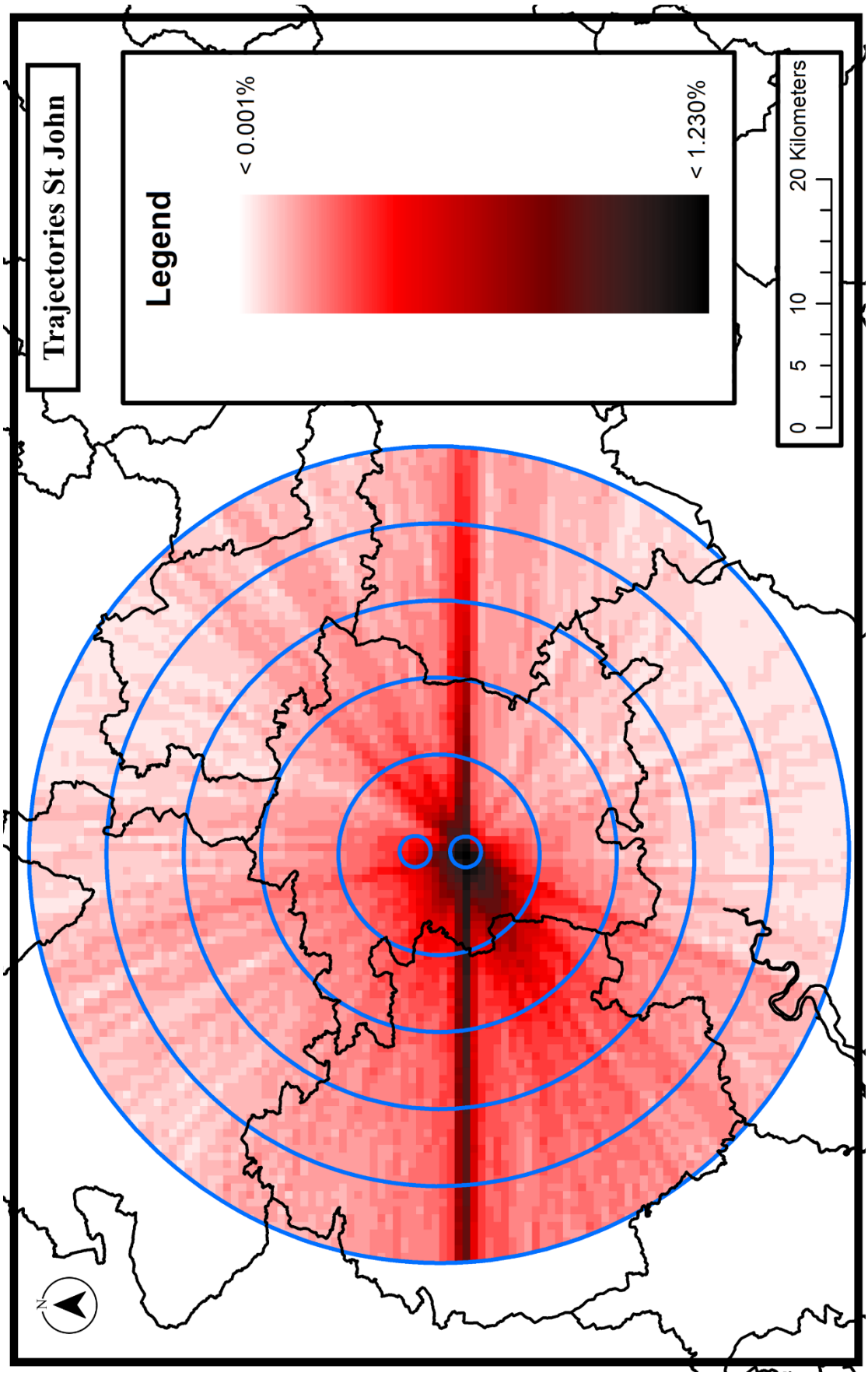

Figure 24. Densities of the atmospheric trajectories passing St Johns within the grass pollen seasons during the years 2018 and 2019. The shown gridcell resolution is 1 x 1 km. The legend specifies the contribution of each colour to the total number of trajectories.

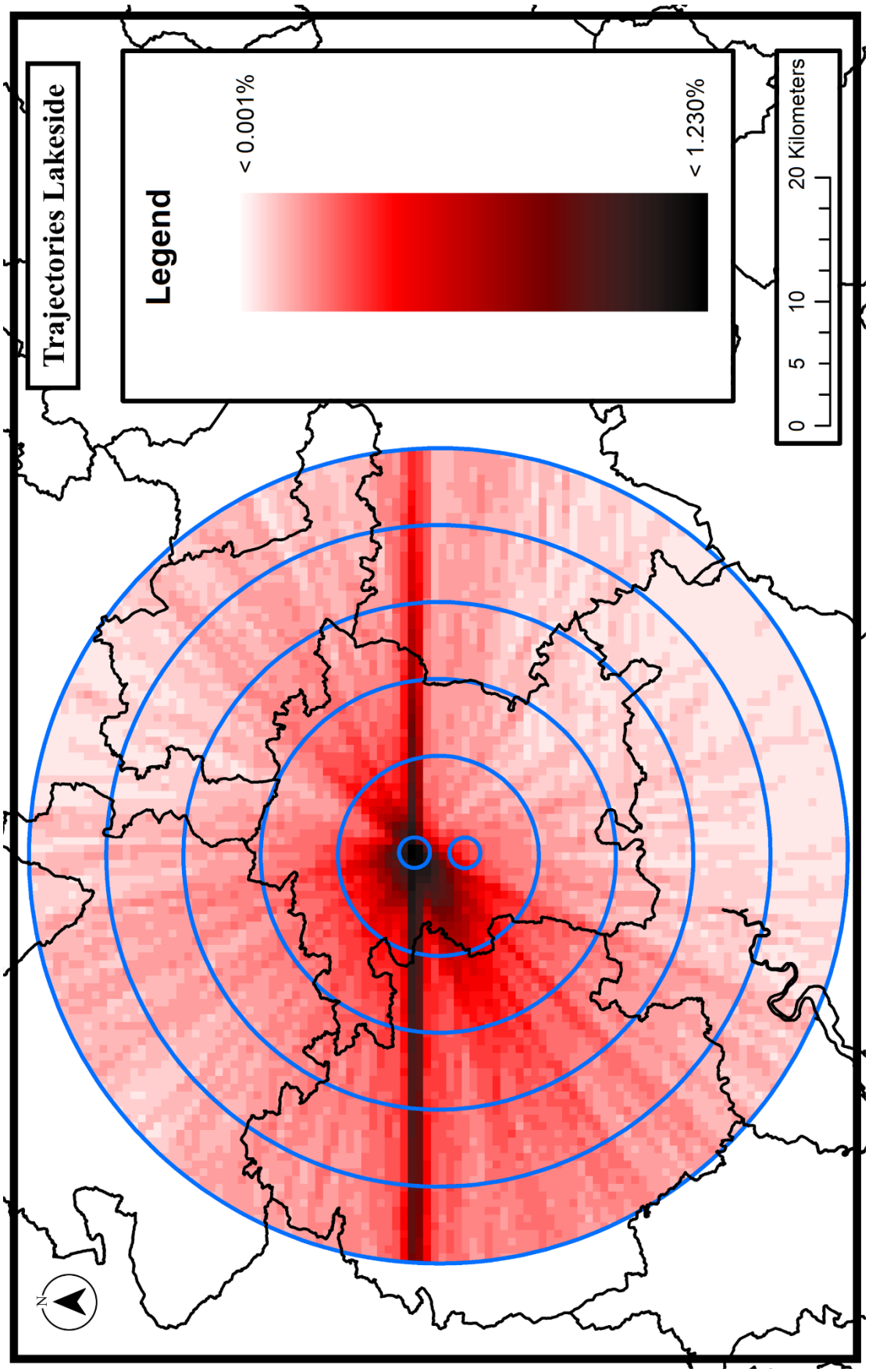

Figure 25. Densities of the atmospheric trajectories passing Lakeside within the grass pollen seasons during the years 2018 and 2019. The shown gridcell resolution is 1 x 1 km. The legend specifies the contribution of each colour to the total number of trajectories.

4.2.5. Meteorological Comparison

This section presents the meteorological comparison between St Johns and Lakeside for the overlapping seasons between May and September for the years 2018 and 2019. The meteorological variables compared were temperature and precipitation. Both variables were bi-hourly measurements/estimates. Temperature is presented as the average temperature between hour t and hour t-1 (previous hour). Precipitation is presented as the sum of the precipitation for hour t and hour t-1 (previous hour). Non-parametric statistical testing was used to compare both years and locations due to both data-series expressed non-normality measured in the Shapiro-test ($p < 0.001$ for both years and locations).

4.2.5.1. Temperature

The warmest months of the overlapping period in 2018 sorted from warmest to coldest were July, June, August, and May (**Figure 26.**). The temperature in St Johns for 2018 ranged between 5 and 30°C while it ranged from 4 to 30 °C for Lakeside of the same year. The Spearman rho correlation demonstrated that there was a strong correlation between the temperature datasets of 2018 (Spearman $r_s=0.99$, $p < 0.001$ (***)) (**Table 5.**). The mean temperature for St Johns in 2018 was 17.5°C while it was 17.0°C for Lakeside of the same year. The Wilcoxon Signed-Rank Test demonstrated that there was a significant difference between the two locations ($p < 0.001$ (***)). St Johns was on average 0.48°C warmer than Lakeside during the overlapping months of 2018.

The warmest months of the overlapping period in 2019 sorted from warmest to coldest were July, August, June, and May (**Figure 26.**). The temperature in St Johns for 2019 ranged between 3 and 33°C while it ranged from 1 to 33 °C for Lakeside of the same year. The Spearman rho correlation demonstrated that there was a strong correlation between the temperature datasets of 2019 (Spearman $r_s=0.99$, $p < 0.001$ (***)) (**Table 5.**). The mean temperature for St Johns in 2019 was 16.0°C while it was 15.5°C for Lakeside of the same year. The Wilcoxon Signed-Rank Test demonstrated that there was a significant difference between the two locations ($p < 0.001$ (***)). St Johns was on average 0.51°C warmer than Lakeside during the overlapping months of 2019.

4.2.5.2. Precipitation

The wettest months of the overlapping period in 2018 sorted from wettest to driest were May, August, July, and June (**Figure 27.**). St Johns received a total of 185.4 mm of rain in 2018 while Lakeside received 160.2 mm during the same period. The Spearman rho correlation demonstrated that there was a strong correlation between the precipitation datasets of 2018 (Spearman r_s=0.75, $p < 0.001$ (***)) (**Table 5.**). The Wilcoxon Signed-Rank Test demonstrated that there was no significant difference between the two locations ($p = 0.10$ (NS)).

The wettest months of the overlapping period in 2019 sorted from wettest to driest were June, August, July, and May (**Figure 27.**). St Johns received a total of 291.0 mm of rain in 2019 while Lakeside received 282.2 mm during the same period. The Spearman rho correlation demonstrated that there was a strong correlation between the precipitation datasets of 2019 (Spearman r_s=0.76, $p < 0.001$ (***)) (**Table 5.**). The Wilcoxon Signed-Rank Test demonstrated that there was no significant difference between the two locations ($p = 0.12$ (NS)).

Table 5

Model statistics and significance levels for the comparison of bi-hourly temperature and precipitation for the locations St Johns and Lakeside for the combined years of 2018 and 2019.

Varible	Year	Model Statistics						
		Spearman Rank Correlation				Wilcoxon Signed-Rank Test		
		S	rho	P - value	Significance	V	P - value	Significance
Temperature	2018	4105414	0.992	< 0.001	***	1000781	< 0.001	***
	2019	3955388	0.993	< 0.001	***	1020509	< 0.001	***
Precipitation	2018	135514067	0.747	< 0.001	***	3728	0.100	NS
	2019	129536855	0.758	< 0.001	***	12566	0.117	NS

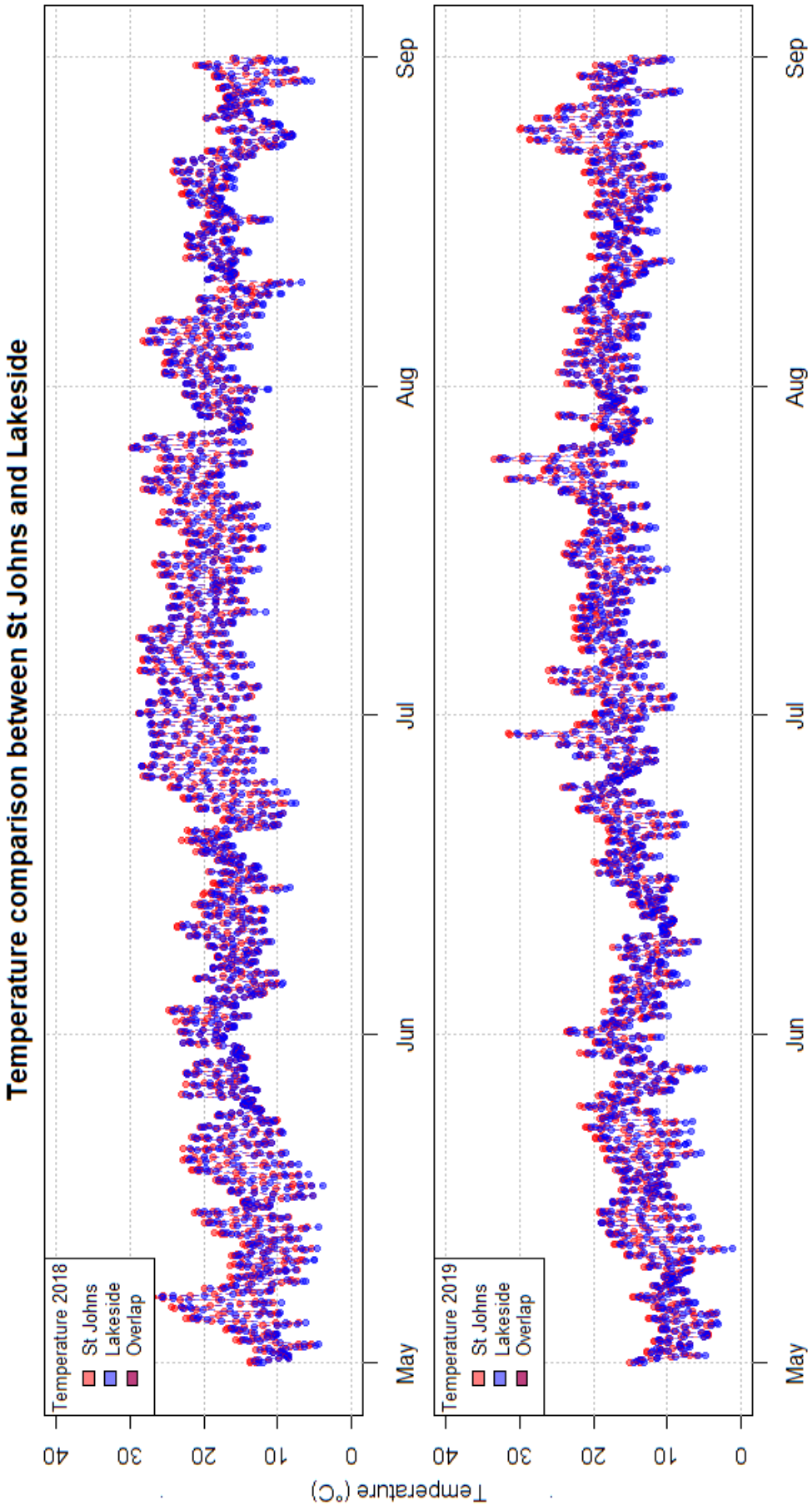

Figure 26. Comparison of bi-hourly measurements of temperature from two locations (St Johns and Lakeside) for the years 2018 and 2019.

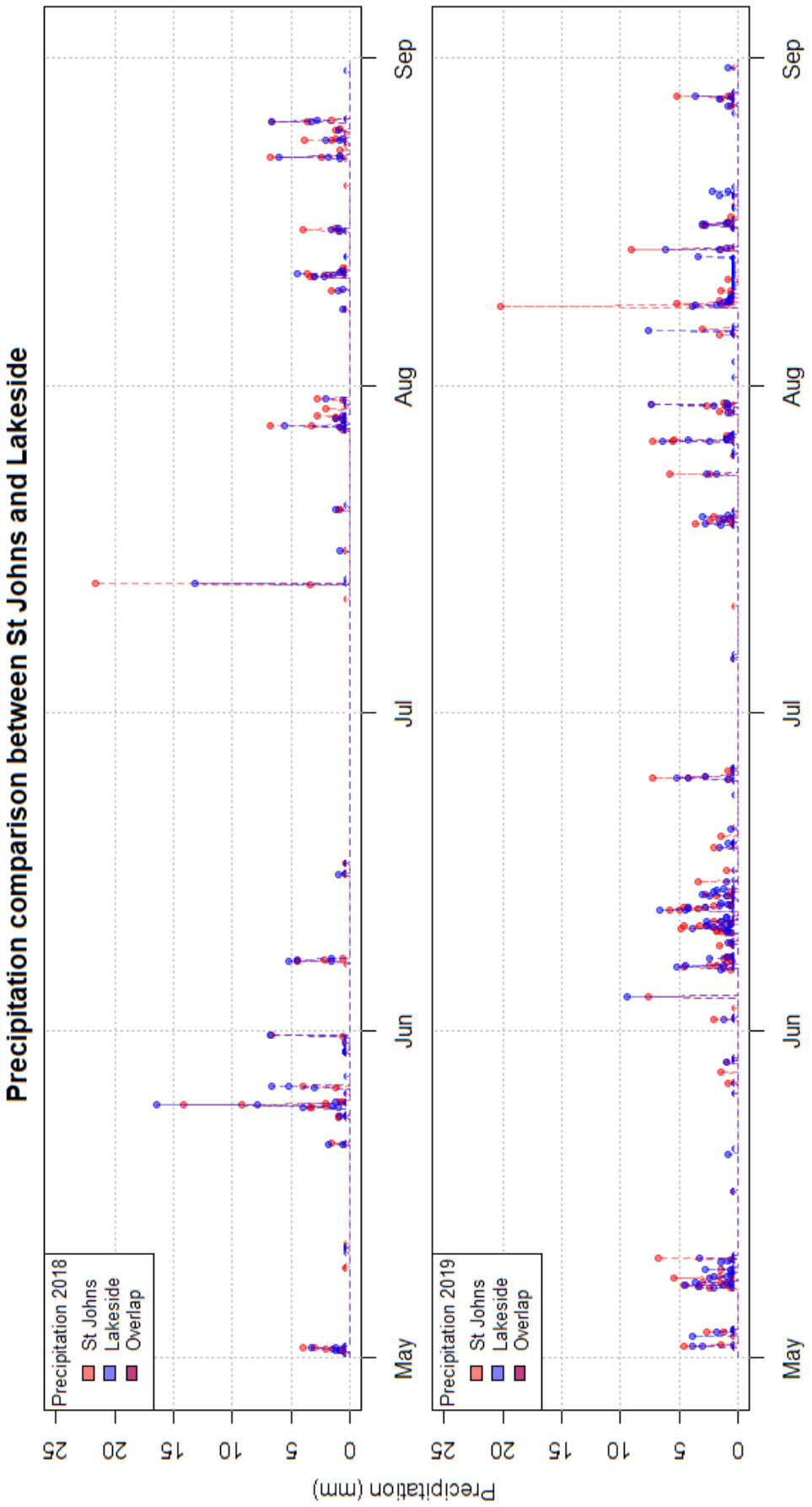

Figure 27. Comparison of bi-hourly measurements of precipitation from two locations (St Johns and Lakeside) for the years 2018 and 2019.

4.2.6. Generalized Linear Mixed-Modelling

This section presents the results of the generalized linear mixed-modelling (GLMER) approach. The generalized linear mixed-modelling approach included both fixed and random effects. The model accounted for the fixed effects: grass pollen concentrations, trajectory-grass maps and weather and calculated a linear regression model based on one response and several explanatory variables. The response variable in this model being grass pollen concentrations, while the explanatory variables being the trajectory-grass maps both unique and shared between locations, temperature, and precipitation. The model also accounted for variables causing temporal variation: DOY, time of day and year (as described in the methods chapter section 3.8.2.4.). Grass pollen concentrations larger than 30 times the mean value of the variable were considered as outliers and removed: which resulted in the removal of two data points from St Johns (35 and 37 times larger) and one data points from Lakeside (108 times larger). This model was then run for both locations with separate sets of local variables. The model results were primarily expressed as effective estimates, t – values and p – values for each variable in the generalized linear regression and R^2-values for the entire generalized linear regression model. The comparison between observed and predicted bi-hourly grass pollen concentrations for both locations is also showcased.

4.2.6.1. St Johns

The model statistics showed that the variables had differential effect on the number of grass pollen collected at the St Johns location (**Table 6a.**). The weather variable temperature had a positive very significant effect on bi-hourly grass pollen concentrations ($p < 0.001$ (***)). Meanwhile, the weather variable precipitation had no significant effect on the same ($p = 0.292$ (NS)). The micro-scale (0 – 2 km) grass map had a positive significant effect on bi-hourly grass pollen concentrations ($p < 0.05$ (*)) as did the small meso-gamma (2 – 10 km) grass map ($p < 0.05$ (*)). The large meso-gamma (10 – 20 km) grass maps on the other hand had no significant effect ($p = 0.344$ (NS)). The first meso-beta (20 – 30 km) grass map had a positive very significant effect on bi-hourly grass pollen concentrations ($p < 0.001$ (***)). Meanwhile, the second meso-beta (30 – 40 km) grass map had a negative very significant effect on the same ($p < 0.001$ (***)). The third meso-beta (40 – 50 km) had no significant effect on bi-hourly grass pollen concentrations, although a positive trend was present ($p = 0.087$ (·)). The full model has a R^2 value of 49.9%. DOY has larger variation in relation to the grass pollen concentrations than Time of day, and in the same way in regarding Time of day than Year (**Supplementary Figures S38 – S40.**). The model predicted 74% of bi-hourly grass pollen concentrations to within 30 grains/m^3 in comparison to the observed values (**Figure 28.**). Only 10% of the

predicted values had a difference of above 90 grains/m^3. Absolute differences in predicted and observed bi-hourly grass pollen concentrations can be found in the supplementary material (**Supplementary Figure S41.**).

4.2.6.2. Lakeside

The model statistics showed that the variables had differential effect on the number of grass pollen collected at the Lakeside location (**Table 6b.**). The weather variable temperature had a positive very significant effect on bi-hourly grass pollen concentrations ($p < 0.001$ (***)). Additionally, the weather variable precipitation had a negative significant effect on the same ($p < 0.05$ (*)). The micro-scale (0 – 2 km) grass map had no significant effect on bi-hourly grass pollen concentrations ($p = 0.392$ (NS)). The small meso-gamma (2 – 10 km) had a positive significant effect on bi-hourly grass pollen concentrations ($p < 0.05$ (*)), while the larger meso-gamma (10 – 20 km) had no significant effect ($p = 0.874$ (NS)). The first meso-beta (20 – 30 km) grass map had no significant effect on bi-hourly grass pollen concentrations, although a positive trend was present ($p = 0.058$ (·)). Meanwhile, the second and third meso-beta (30 – 40, 40 – 50 km) grass maps had no significant effects ($p = 0.150$ (NS) & $p = 0.591$ (NS) respectively). The full model has a R^2 value of 50.3%. DOY has larger variation in relation to the grass pollen concentrations than Time of day, and in the same way in regarding Time of day than Year (**Supplementary Figures S38 – S40.**). The model predicted 79% of bi-hourly grass pollen concentrations to within 30 grains/m^3 in comparison to the observed values (**Figure 29.**). Only 7% of the predicted values had a difference of above 90 grains/m^3. Absolute differences in predicted and observed bi-hourly grass pollen concentrations can be found in the supplementary material (**Supplementary Figure S42.**).

Table 6a

Model statistics and significance levels for the Generalized Linear Mixed-Model (GLMER) in regards to the Bi-hourly Grass Pollen concentrations for the location St Johns for the combined years of 2018 and 2019.

Abbreviations: GM - Grass Map, **SJ** - St Johns, **DOY** - Day of Year, **N/A** - Not Applicable

Location	**Variables**	**Effect**	**Model Statistics**						
		Type	Estimate	Variance	Std. Error	Std. Dev.	t - value	P - value	Significance
St Johns									
	Intercept	Fixed	-2.251	N/A	0.581	N/A	-3.874	< 0.001	***
	Temperature	Fixed	0.133	N/A	0.009	N/A	14.268	< 0.001	***
	Precipitation	Fixed	0.021	N/A	0.020	N/A	1.054	0.292	NS
SJ Specific GM	GM1 [0 - 2 km]	Fixed	0.034	N/A	0.015	N/A	2.227	< 0.05	*
SJ Specific GM	GM3 [2 - 10 km]	Fixed	0.145	N/A	0.065	N/A	2.225	< 0.05	*
	GM5 [10 - 20 km]	Fixed	-0.048	N/A	0.051	N/A	-0.946	0.344	NS
	GM6 [20 - 30 km]	Fixed	0.331	N/A	0.038	N/A	8.783	< 0.001	***
	GM7 [30 - 40 km]	Fixed	-0.158	N/A	0.028	N/A	-5.722	< 0.001	***
	GM8 [40 - 50 km]	Fixed	0.031	N/A	0.018	N/A	1.709	0.087	.
	DOY [121 - 244]	Random	N/A	2.484	N/A	1.576	N/A	N/A	N/A
	Time [00, 02, etc]	Random	N/A	0.173	N/A	0.415	N/A	N/A	N/A
	Year [-17, -18, -19]	Random	N/A	0.000	N/A	0.000	N/A	N/A	N/A
	Residuals	Random	N/A	1.512	N/A	1.230	N/A	N/A	N/A

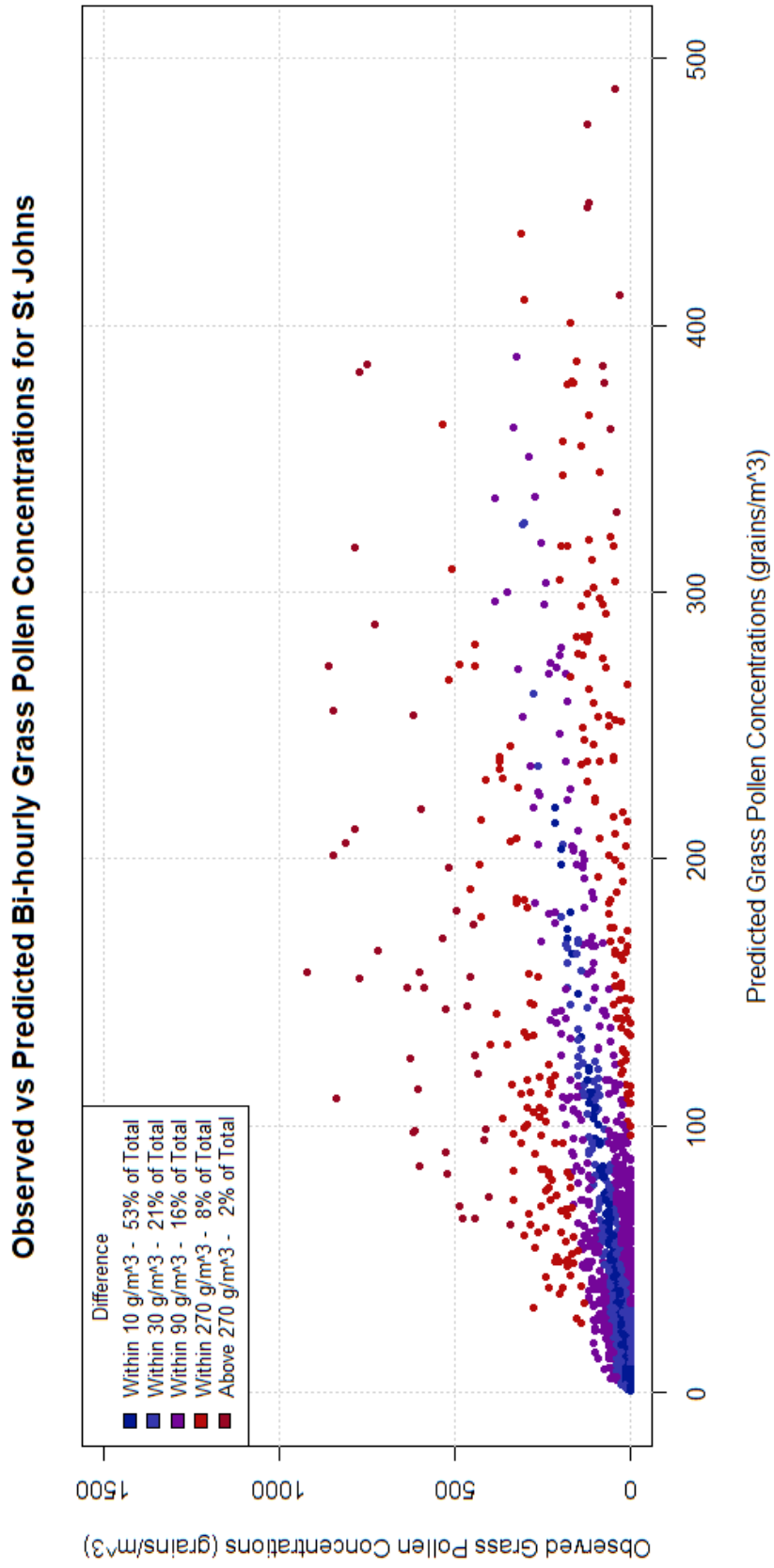

Figure 28. Observed vs Predicted Bi-hourly grass pollen concentrations for St Johns. Modelled using the Generalized Linear Mixed-Model with variables explored in Table 6a.

Table 6b

Model statistics and significance levels for the Generalized Linear Mixed-Model (GLMER) in regards to the Bi-hourly Grass Pollen concentrations for the location Lakeside for the combined years of 2018 and 2019.

Abbreviations: GM - Grass Map, **LS** - Lakeside, **DOY** - Day of Year, **N/A** - Not Applicable

Location	**Variables**	**Effect**	**Model Statistics**						
		Type	Estimate	Variance	Std. Error	Std. Dev.	t - value	P - value	Significance
Lakeside									
	Intercept	Fixed	-0.554	N/A	0.627	N/A	-0.884	0.377	NS
	Temperature	Fixed	0.117	N/A	0.010	N/A	12.003	< 0.001	***
	Precipitation	Fixed	-0.062	N/A	0.024	N/A	-2.552	0.011	*
LS Specific GM	GM2 [0 - 2 km]	Fixed	-0.054	N/A	0.063	N/A	-0.856	0.392	NS
LS Specific GM	GM4 [2 - 10 km]	Fixed	0.118	N/A	0.047	N/A	2.521	0.012	*
	GM5 [10 - 20 km]	Fixed	-0.009	N/A	0.054	N/A	-0.159	0.874	NS
	GM6 [20 - 30 km]	Fixed	0.081	N/A	0.043	N/A	1.898	0.058	.
	GM7 [30 - 40 km]	Fixed	-0.034	N/A	0.024	N/A	-1.439	0.150	NS
	GM8 [40 - 50 km]	Fixed	0.010	N/A	0.018	N/A	0.538	0.591	NS
	DOY [121 - 244]	Random	N/A	2.870	N/A	1.694	N/A	N/A	N/A
	Time [00, 02, etc]	Random	N/A	0.189	N/A	0.434	N/A	N/A	N/A
	Year [-17, -18, -19]	Random	N/A	0.008	N/A	0.087	N/A	N/A	N/A
	Residuals	Random	N/A	1.581	N/A	1.258	N/A	N/A	N/A

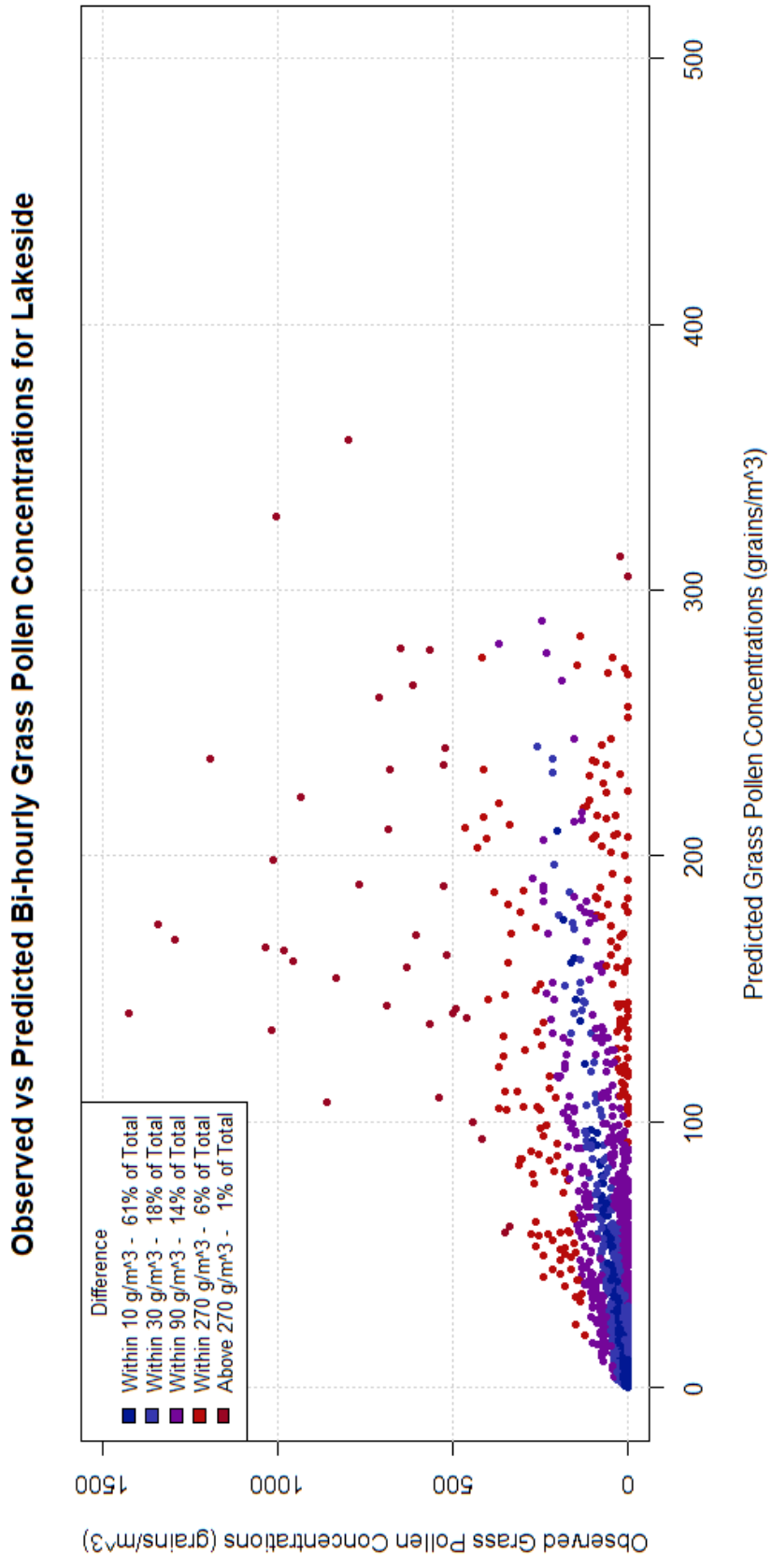

Figure 29. Observed vs Predicted Bi-hourly grass pollen concentrations for Lakeside. Modelled using the Generalized Linear Mixed-Model with variables explored in Table 6b.

4.3. Discussion

This research has shown that grass pollen concentrations can vary substantially between years and between locations that are located closely together. This is at least partly due to the fact that urban and rural areas receive grass pollen from different sources depending on distance. Rural areas receive pollen from areas located 2-10 km away while urban areas from areas < 30 km away. Source areas of grass pollen within 30 km will be the most important regardless of urbanisation. Pollen forecasters can therefore provide a much more accurate grass pollen forecast to sufferers by only accounting for the grasses flowering within 30 km. The inclusion of this information will also be critical in the development of future grass pollen forecasting models. This original research represents a significant contribution to aerobiological knowledge by demonstrating relevant distances of atmospheric grass pollen transportation.

4.3.1. Grass Pollen Variation

The spatial and temporal variation in bi-hourly grass pollen concentrations within Worcestershire showcased differences between closely located pollen sampling stations. Correlations within the full seasonal grass pollen series ranged between 0.513 and 0.781, indicating that there are pronounced differences in grass pollen concentrations on a two-hour basis within a six km range between years. Seasonal intensities (Seasonal) and seasonal trends (Trends) correlations vary between 0.634 and 0.858 and 0.715 and 0.936 respectively, with higher correlations than between the full seasonal grass pollen series. However, the remainder correlations range between 0.288 and 0.514, indicating that the main differences between the locations are in the unknown variation not included in seasonal intensities or trends that nonetheless vary between years. The spatial autocorrelation suggests up to 16 days of time lags within the bi-hourly grass pollen. This is highly unlikely due to the short distance between the locations and is more likely caused by the common occurrence of low pollen concentrations and temporal effects of pollen sampling, as spatial autocorrelations are common features of ecological research (Dale and Fortin, 2002). The main difference therefore is likely to be caused by temporal factors which vary within and between years. This is substantiated by the higher SPIn in St Johns compared to Lakeside. Overlapping periods of SPIn range from 1360-5941 (mean 3550) for St Johns and 1267-4423 (mean 2921) for Lakeside. Grass pollen SPIn vary naturally between years, as shown previously for 2008-2016 in Mexico (1465-2375 (mean 1793)) (Calderon-Ezquerro et al., 2018) and for 1989-2018 in France (~3600-~6000) (Besancenot et al., 2019). The SPIn ratio between St Johns:Lakeside range between 1:1.07 and 1:1.34 (mean 1:1.17). The lower ratio of the first two years can be due to the lower overlapping data availability, and that the grass pollen concentration becomes more similar later on in the

season, this however is not collaborated upon while viewing the late season data of 2018 and 2019. The similarity in the SPIn ratio suggests that there are conditions that apply to closely located locations that keep the ratio low, to provide similar total grass pollen concentration ratios over the season. This has been shown to be the case in northern Spain, with grass pollen SPIn ratios between six locations ranging from 1:0.53 to 1:2.06 (Majeed et al., 2018). The SPIn of a location however can only provide information regarding the overall strength of the seasons (Lo et al., 2019), without including inter-seasonal dynamics, and can thusly not convey enough information to evaluate spatial connectivity or detailed ecological relationships. Investigations into meteorology and the transportation of grass pollen are likely to shed light on the variation caused by spatial and temporal factors.

4.3.2. Representation of Source Areas

The 100 x 100 m resolution grass maps created from the 2017 Crop Map highlights the heterogeneity of potential grass pollen source areas within the greater West Midlands landscape. It has recently been shown to identify local source areas of *Alternaria* spores within both the West and East Midlands areas of the United Kingdom (Apangu et al., 2020). Additionally, a previous iteration of the same map has been shown to produce reliable grass maps over the United Kingdom using 1 x 1 km resolution (McInnes et al., 2017). This resolution is the standard for the creation of grass vegetation maps (e.g. Khwarahm et al., 2017; Zerboni et al., 1991), although some studies have used lower resolutions (e.g. 500 x 500 m) (Devadas et al., 2018). This resolution however disregards features smaller than the resolution, for example road-verges, home gardens and similar, which are known to be sources of grassland vegetation (Jantunen et al., 2007, 2006). This has previously been suggested to have potential impacts on localized grass pollen concentrations by using very high resolution grass maps (0.6 x 0.6 m) from a study conducted in urban parts of Denmark (Skjøth et al., 2013). The use of a higher resolution grass maps (100 x 100 m) is likely to give a more detailed understanding of source dynamics compared to the standard resolution (1 x 1 km). This resolution is likely to suffice in investigating source dynamics until the contributions of smaller source areas have been thoroughly quantified and higher resolution satellite images and public vegetation dataset have been made publicly available.

4.3.3. Temporal Effects

The temporal variation accounted for by the GLMER model highlighted that daily variation caused by the progression of the season (DOY) is higher than diurnal variation or yearly variation. Natural temporal variation has shown to be a major cause of the variation in grass pollen concentrations seen during grass pollen seasons (García-Mozo, 2017; Núñez et al.,

2016). Grass pollen concentrations tend to be low during the start of the season, slowly increase, quickly reach peak levels and then slowly decrease down again to background levels (Galán et al., 1995; Norris-Hill, 1995; Plaza et al., 2016; Sabariego et al., 2011). The variation in DOY confirms this general pattern, and is further substantiated by regional grass pollen calendars (Adams-Groom et al., 2020). Grass pollen concentrations were found to be low during the night and early mornings, whilst increasing during mid-day and reaching highest levels around 6 pm, this is confirmed by previous studies from both UK, Denmark and Germany (Hyde and Williams, 1945; Norris-Hill, 1999; Peel et al., 2014b; Simoleit et al., 2016). This is in contrast to other studies from Spain and Poland, which has suggested that concentrations tend to be high during major parts of the day, and perhaps highest during mid-mornings around 9-11 AM, while reducing during evenings to early mornings (Cariñanos et al., 1999; Kasprzyk, 2006; Latałowa et al., 2005). The yearly mean bi-hourly grass pollen concentration show that there are small differences between the years, but it is uncertain how large these differences are due to only two years being included. Previous studies have concluded that yearly differences in grass pollen concentrations are common, but that it will depend on the locations and the sampling duration to which magnitude the difference is expressed (Emberlin et al., 1999; Ghitarrini et al., 2017b; Karatzas et al., 2019; Sabariego et al., 2011; Smith et al., 2014).

4.3.4. Fixed Effects

The inclusion of temporal variables as random variation within the model accounts for the temporal trends within the pollen variables. This simplifies the interpretation of the model variables since it includes the variation naturally caused by fluctuating highs and lows. The modelling results indicate a differential contribution of source areas depending on the distance to the sampling location and its surroundings. Grass sources within meso-gamma distance (> 30 km) were important in determining grass pollen concentrations for St Johns while both lower meso-beta (2 – 10 km) and meso-gamma (20 – 30 km) distances were important for Lakeside. Temperature was found to be important for both locations, while precipitation was important for Lakeside but not for St Johns. The larger meso-gamma scale (10 - 20 km) grass sources were found to not be an important factor for either location.

The first meso-gamma distance (20 – 30 km) had a strong positive influence on grass pollen concentrations for St Johns, while the second meso-gamma distance (30 – 40) had a negative influence. This suggest that grass pollen are likely to be transported within a 20 – 30 km distance from high grass pollen source areas. Meanwhile, high grass pollen source areas from within 30 – 40 km does not increase grass pollen concentrations to the sampling location, suggesting that the grass pollen transported from these areas are not able to travel the entire distance to the

sampler, but settle sometime before then. Source areas within 30 km of St Johns have significant effects on grass pollen concentrations. This contrasts with Lakeside, in which more localized grass pollen source areas are important (2 – 10 km) along with source areas within 20 – 30 km, although not as strongly as for St Johns. Both locations are in agreement with other dispersal studies suggesting that local vegetation is likely responsible for the observed bioaerosol patterns (Apangu et al., 2020; Avolio et al., 2008; Katelaris et al., 2004; Oteros et al., 2015; Pashley et al., 2009; Skjøth et al., 2009), although this is not always the case (e.g. de Weger et al., 2016; Izquierdo et al., 2011; Skjøth et al., 2007). However, the definition of 'local source' is up to debate since micro-scale grass sources (< 2 km) did not have a measurable effect for Lakeside, even if it did for St Johns. Oteros et al. (2015) have suggested this to be due the absence of local sources close to sampling stations (which normally are located within urban centres). This is strange in relation to Lakeside since source areas are immediate upon the sampling station. This is in agreement of previous studies from Germany and Poland, that has shown that the presence of an urban-rural gradient in pollen concentrations caused by differential source area allocation (Rodríguez-Rajo et al., 2010; Werchan et al., 2017). The accounting for temporal variation is here likely to be causing the discrepancy for Lakeside. If grass pollen sources within Lakeside are dominated by few grass species that flowers intensely closely together during a narrow section of the season then the grass pollen contribution will be intensive but temporally short. This has been shown to be the case when investigating grass pollen concentrations in relation to flowering phenology (Cebrino et al., 2016; Rojo et al., 2017). This can potentially dampen the signal of the local vegetation as a whole over the seasons. Vegetation over a regional-sized area however are likely to contain a wide-range of grass species dispersing pollen during diverse times due to differential flowering times (Cebrino et al., 2018), localized micro-climatic factors (Jackson, 1966) and differential management regimes (Theuerkauf et al., 2015). This would be able to explain the importance of meso-gamma distance (2 – 10 km) grass sources and the absence of effects from micro-scale sources for Lakeside.

Another potential reason for the lack of pollen contributions from local sources (within 10-20 for both sites) could be attributed to the wind-movement patterns present during these years (Smith et al., 2005). Unequal contribution from local source areas due to differential atmospheric transport and wind conditions has previously been shown be a major factor of the difference in atmospheric pollen concentrations at closely located pollen sampling locations (Alan et al., 2018; Bilińska et al., 2019; Maya-Manzano et al., 2017; Maya Manzano et al., 2017; Van De Water and Levetin, 2001). The distribution of source areas therefore is only important if transport of pollen from these sources is present (Šikoparija et al., 2018) and to

what extent the transportation is relevant (Adams-Groom et al., 2017). One previous study has also suggested that the resolution and quality of the input data will be important in determining the contribution of pollen sources (Hernández-Ceballos et al., 2014). In this paper they concluded that going from HYSPLIT default input to WRF generated input data while increasing data resolution improved trajectory calculations, which was used to resolve the effects from the landscape relief. Future research should incorporate these approaches to confirm the regional effects of grass pollen source areas.

Temperature and precipitation have previously been shown to have strong effects on grass pollen concentrations, which has been showcased in many studies (e.g. García-Mozo et al., 2010, 2009; García de León et al., 2015; Khwarahm et al., 2014; Makra et al., 2012; Recio et al., 2010; Sánchez-Mesa et al., 2002). The 0.5°C temperature discrepancy displayed between St Johns and Lakeside likely stems, at least partly, from the Urban Heat Island (UHI)-effect (Kim, 1992), which previously have shown to have a measurable effect on grass pollen concentrations (Ríos et al., 2016). The likely reason why temperature was shown to have a strong significant effect on grass pollen concentrations is not only due to the direct (although complicated) effect on grass pollen concentrations (Jung et al., 2021; Myszkowska, 2014; Norris-Hill, 1997), but also from the indirect effect through plant growth, maturity, anthesis and anther dehiscence (Charles-Edwards et al., 1971; Liem and Groot, 1973). All of these factors have their own complex relationships to pollen release and atmospheric pollen concentrations (Viner et al., 2010). The weak (and for St Johns, lacking) effect of precipitation on grass pollen concentrations is likely obscured due to the presence of many low counts of grass pollen during the seasons regardless of high or low measures of precipitation, this might lessen the overall effect in the model estimate. Previous studies have suggested that the relationship between precipitation and pollen concentrations can be complicated, and rely on other factors than just the presence and abundance of precipitation, such as rain intensities and wind conditions (Kluska et al., 2020; Norris-Hill and Emberlin, 1993; Pérez et al., 2009). The nonsignificant influence on grass pollen concentrations for St Johns is likely to be a false negative due to the generally lower intensities of precipitation (< 5mm/h), which are not likely to effect the pollen concentrations to any large extent (Kluska et al., 2020). Therefore, the presence of rain during generally higher atmospheric pollen concentrations is interpreted by the model as not having an influence because the rain is not intensive enough to reduce the concentrations.

4.4. Conclusion

Clear differences in bi-hourly gras pollen concentrations between closely located pollen sampling stations were found for the duration of four years (2016 – 2019). These differences were mainly constituted from higher SPIn at St Johns contributed to generally higher pollen concentrations. The use of grass maps with high resolution has been able to distinguish likely source areas containing vegetation that contribute to the seasonal atmospheric grass pollen load for these two locations within the larger West Midlands regional area. The combination of atmospheric wind trajectories and grass maps in a generalized linear modelling approach suggested that source areas further away than 30 km are unlikely to contribute grass pollen to each location. It is likely that there is an urban-rural gradient within these 30 km that affects the source-area distribution and transportation probabilities of grass pollen. This causes an uneven contribution of grass pollen from source areas to each location based on their immediate surroundings. Temperature had a highly significant effect, likely causing both direct and indirect influences on the atmospheric grass pollen concentrations. The importance of precipitation however was uncertain, likely due to confounding factors such as abundance, intensity, and wind conditions. A generalized modelling approach using regional grass vegetation source maps and atmospheric trajectories are highly accurate tools in predicting the fine differences in bi-hourly grass pollen concentrations between closely located pollen sampling stations.

5. Flowering Phenology and Population Development in *Dactylis glomerata*

5.1. Introduction

A population approach to flowering phenology will be able to distinguish features of flowering dynamics otherwise inaccessible by regular randomized sampling methods. The use of full spatial and temporal aspects to the populations, along with categorized phase distributions incorporates the totality of the species flowering potential and development. By observing the development of each specific grass tiller, it is possible to determine the likelihood of tiller transitioning between phases for each population. The sections below presents the spatial and temporal aspects of *Dactylis glomerata* population phenology within three different levels of observational and analytical depth. Discussions surrounding the general flowering patterns, the phase distribution patterns and tiller-specific transition patterns rounds off the chapter.

5.2. Results

5.2.1. Result Summary – Chapter 5

This chapter sought to explore the phenological progression of flowering *Dactylis glomerata* populations and to quantify demographic and stochastic trends in the process. It was found that there was large homogeneity in the flowering process between years and spatially distinct populations, with distributions of flowering phases following the same progression pattern. Key phenological events in the populations, such as start of flowering, full flowering, and peak flowering, varied by at most a few days, with the exception for the senescence, which had larger variation pattern. The three main populations showed a varied pattern in stochastic development between years, with tillers in 2017 being more likely to stay longer in their specific phases, and the opposite seen in 2018, with tillers being more likely to progress quickly to full flowering.

5.2.2. Main Populations

The section below present all the spatial and temporal flowering dynamics of the main *Dactylis glomerata* populations investigated within the study: The 2017 St Johns population, the 2018 St Johns population, and the 2018 Lakeside population.

5.2.2.1. St Johns 2017

The entire main population of St Johns in 2017 consisted of 317 individual tillers split over four 2.25 m^2 plots. The split between the plots were 72 (22.7%) in plot A, 118 (37.2%) in plot B, 24 (7.6%) in plot C and 103 (32.5%) in plot D. The population started flowering in late May (26th of May), where the first few tillers reached p1 and p2 (**Figure 30.**). Over the next two days more tillers reached p1 and p2, with one tiller reaching p3. The next day (29th of May) a big increase in flowering was seen, with almost 40% of the population having started to flower,

with about equal division between p1, p2 and p3, along with the first full flowering tillers reaching p4. Over the next two days incremental increases to the flowering of the tillers occurred, with the ratio between the three lower flowering phases remaining fairly stable, while simultaneously an increase in p4 tillers to 10% occurred. The next day (1st of June) a strong turnover progressed, with 70% of the population started to flower, with 55% of the population having reached full flowering in p4. The next day, the population flowering increased to 80% of flowering tillers, and 70% having reached full flowering in p4. In the coming five days a slow increase in tillers that start flowering (p1) was observed, with a general stability in the population demographics. The next day (9th of June) most of the lower flowering phases reached full flowering, with almost 85% of the population having reached full flowering in p4. This was also the day where the first tillers reached senescence in p5. From this point onward, a linear increase in senescence was observed in the population, along with a linear increase in the last 15% of the non-flowering tillers and low flowering phases reaching full flowering in p4. The balance from a majority full flowering population to a majority senescent population was then reached in the middle-end of June (22nd of June). The last non-flowering tiller finally started to flower (25th of June) with the tillers in population having reached 70% senescence in p5. From this point onward there was a slow decline into p5 for all tillers, with the last tiller reached senescence in p5 in the middle of July (17th of July).

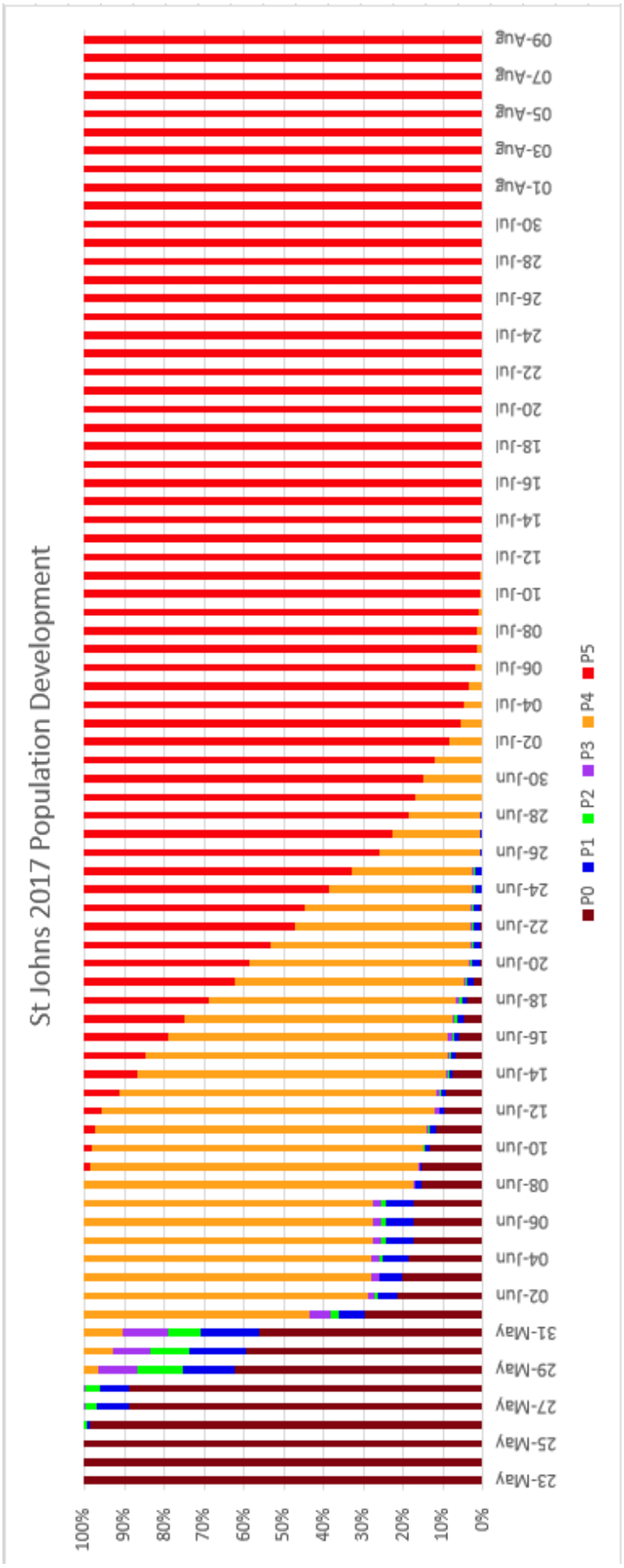

Figure 30. *Dactylis glomerata* population development shown per phase for the St Johns 2017 main population.

5.2.2.2. St Johns 2018

The entire main population of St Johns in 2018 consisted of 355 individual tillers split over three 2.25 m^2 plots. The split between the plots were 86 (24.2%) in plot E, 123 (34.7%) in plot F and 146 (41.1%) in plot G. The population started to flower in late May (29th of May), with the first few tillers (about 5%) reaching p1, p2 and p3 (**Figure 31.**). The flowering proportion of the population increased to 8% the coming two days (31st of May) in the lower flowering phases. The next two days (2nd of June) the population flowering skyrocketed to 75% flowering, with about 65% of the population tillers having reached full flowering in p4. Over the next two days (4th of June), the population reached 85% flowering, with almost all of those tillers being in full flowering in p4, with only a small proportion of lower flowering phases. Incremental increases in tillers starting to flower and reaching full flowering was seen over the next 10 days. The maximum full flowering was then reached (14th of June) with 97% of the population being in full flowering in p4. At the same time, the first tillers reaching senescence in p5 was observed in the population. From this point onward, the tillers in the population continued to experience linear develop into senescence. About 2.5 % of tillers were currently not flowering or in lower flowering phase. The last tiller started to flower 20 days later (2nd of July). The balance from a majority full flowering population to a majority senescent population was reached two days later (4th of July). The last tiller reached senescence more than a month later, in early August (9th of August).

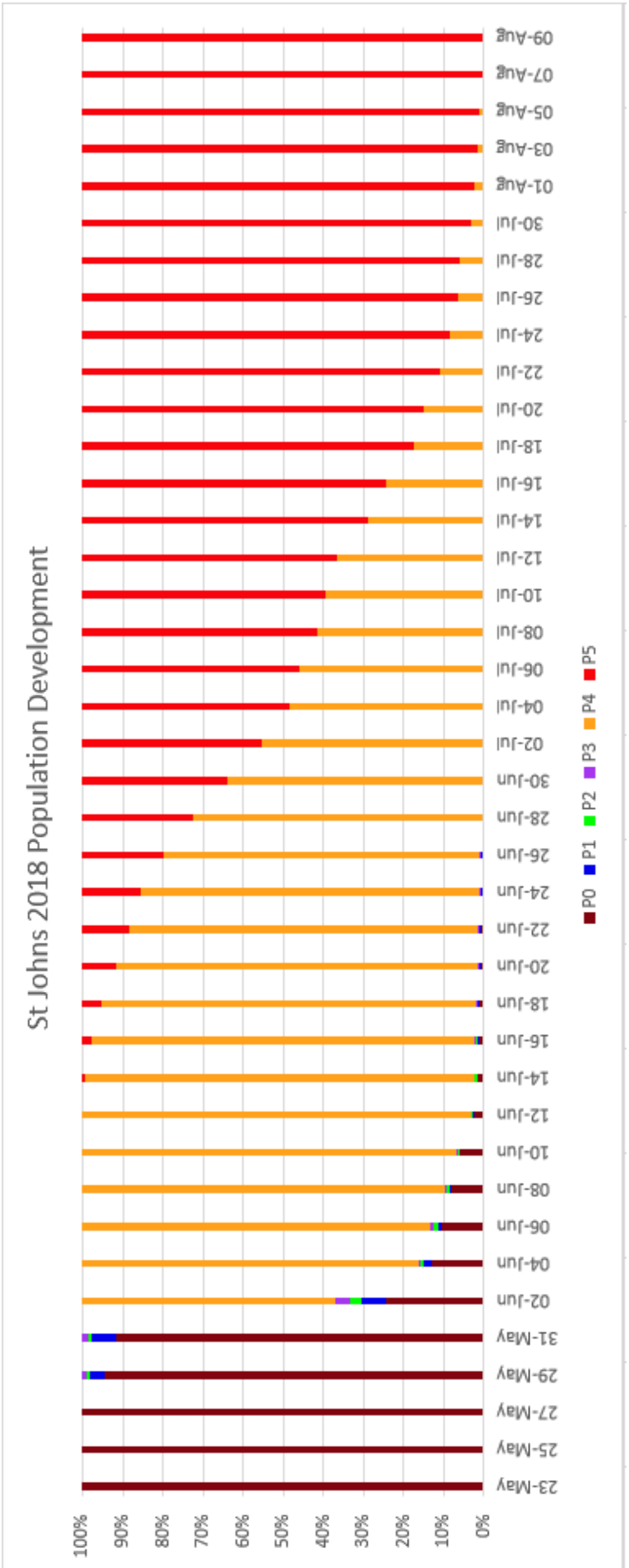

Figure 31. *Dactylis glomerata* population development shown per phase for the St Johns 2018 main population.

5.2.2.3. Lakeside 2018

The entire main population of Lakeside in 2018 consisted of 535 individual tillers split over two 2.25 m^2 plots. The split between the plots are 368 (68.8%) in plot E and 167 (31.2%) in plot F. The population started to flower in late May (29th of May), with the first few tillers (about 2%) reaching p1, p2 and p3 (**Figure 32.**). The population remained stable for the coming two days, with only a single tiller started to flower. The next two days (2nd of June) the population reached its first big flowering development, with almost 50% of the population starting to flower, with about 30% having reached full flowering in p4. The next two days (4th of June) the population reached its second big flowering development, with about 80% of the population having started to flower, with about 60% having reached full flowering in p4. The next two days (6th of June) half of the lower flowering phases reached full flowering, with only a small increase in the total amount of flowering tillers. The next two days (8th of June) almost all of the lower flowering phases reached full flowering, with the population having now reached 85% full flowering, along with a few tillers started to flower. At this time, there were still 15% of the population that had not started to flower yet. Over the next six days (14th of June) 90% of the non-flowering tillers have reached full flowering. Additionally, the population also reached maximum flowering, with 98% of the population being in full flowering along with the first tiller to reach senescence. From this point onward, that the population was observed to have reached senescence in a sigmoid pattern, with initial slow phase, followed by a quickening phase, and then ended with a slow phase. The last tiller started to flower 18 days later (2nd of July). At the same day, the balance from a majority full flowering population to a majority senescent population is reached. The last tillers reaches senescence 22 days later (24th of July).

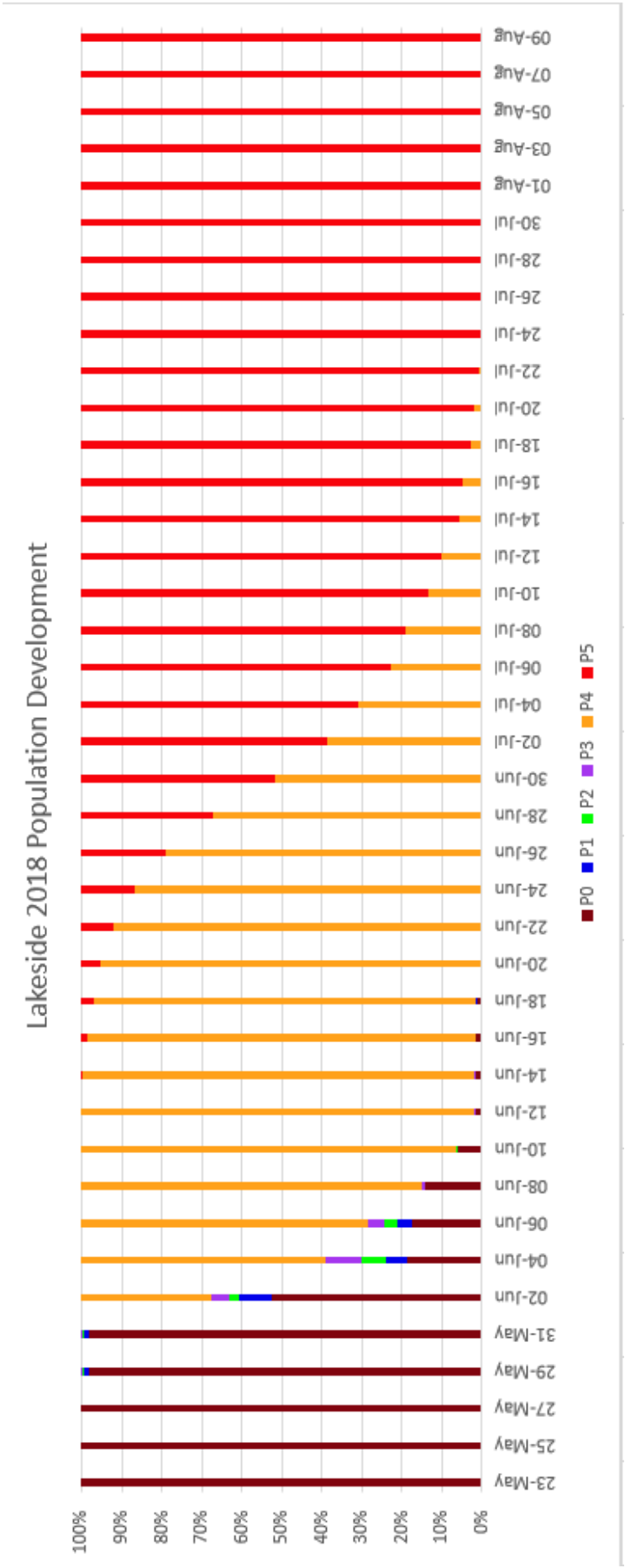

Figure 32. *Dactylis glomerata* population development shown per phase for the Lakeside 2018 main population.

5.2.3. Secondary Populations

The section below present all the spatial and temporal flowering dynamics of the secondary *Dactylis glomerata* populations investigated within the study, with all populations being observed in 2018: Lower Lakeside, Football Field, Upper Bridge, West Field, Lower Field and Lower Bridge.

5.2.3.1. Lower Lakeside

The entire secondary population of Lower Lakeside in 2018 consisted of 210 individual tillers split over the entire sampling location. Lower Lakeside was one of the two locations with an overall lower number of tillers, therefore all tillers in the location were observed. The first observation visit (7th of June) highlighted that the more than 80% of the population was in full flowering in p4, with about 10% still to flower (**Figure 33.**). The next visit (11th of June) the population had reached maximum full flowering at 89%, along with the first tillers having reached senescence. The subsequent visits showcased a smaller proportion of non-flowering tillers, along with an increase in senescence for the population. All non-flowering tillers had started to flower by the beginning of July (5th of July), while at the same time highlighting the shift in the balance of the population from a majority full flowering to a majority senescence. By the late of July (25th of July) only one tiller remained in full flowering. The dynamics of the population could be discerned by a quick and intensive start along with a sigmoid-type senescence pattern.

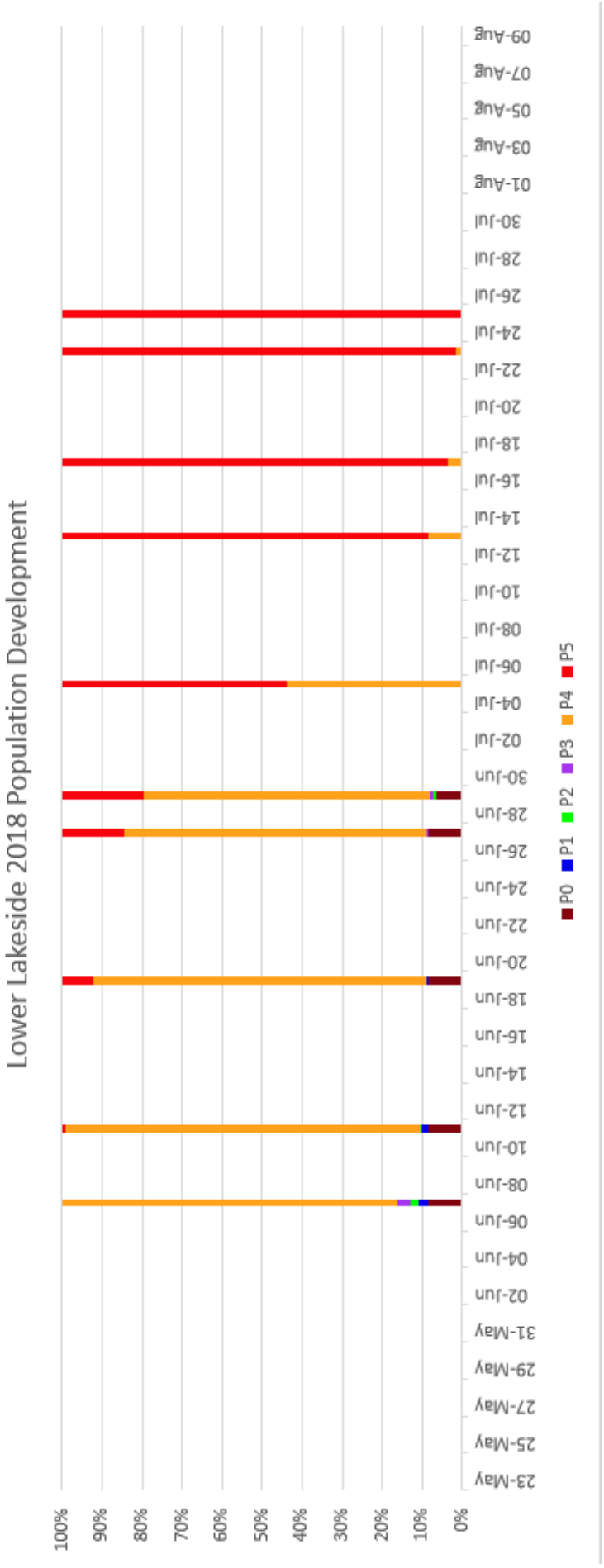

Figure 33. *Dactylis glomerata* population development shown per phase for the Lower Lakeside 2018 secondary population.

5.2.3.2. Football Field

The entire secondary population of Football Field in 2018 consisted of 160 individual tillers split over the entire sampling location. Football Field was one of the two locations with an overall lower number of tillers, therefore all tillers in the location were observed. The first observation visit (1st of June) highlighted that 20% of the population had started to flower, with a smaller proportion having reached full flowering in p4 (**Figure 34.**). At the next visit (5th of June), 70% of the population had started to flower, with about 60% having reached full flowering, with an additional 30% non-flowering tillers. The next visit (11th of June) highlighted the populations maximum flowering with 92% of tiller being in full flower, along with the first tillers having reached senescence. The continuation of the season was characterized by a slow increase in senescence, with the last tiller having started to flower in the beginning of July (5th of July). The next visit (9th of July) highlighted the transition of the population from being majority full flowering to majority senescence, with almost a 50-50 split. During the last visit in the latter half of July (23rd of July) less than 1% of the population remained in full flowering. The dynamics of the population could be discerned by a slow start along with a sigmoid-type senescence pattern.

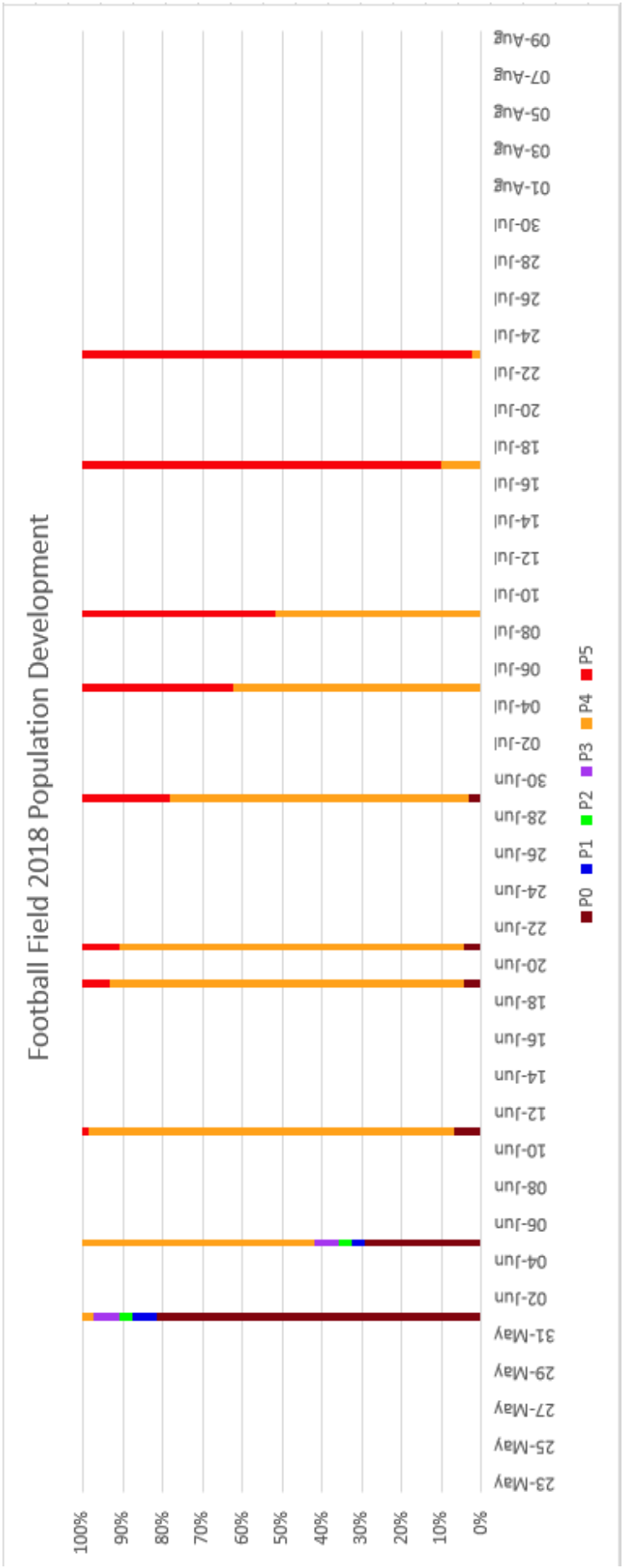

Figure 34. *Dactylis glomerata* population development shown per phase for the Football Field 2018 secondary population.

5.2.3.3. Upper Bridge

The entire secondary population of Upper Bridge in 2018 consisted of 418 individual tillers split over the entire sampling location. Upper Bridge was one of the two locations with an overall higher number of tillers, therefore only individuals occupying three 2.25m^3 plots were observed. The first observation visit (1st of June) highlighted that 50% of the population had started to flower, with 40% having reached full flowering (**Figure 35.**). The next visit (5th of June) 70% of the population had started to flower, with most tillers having reached full flowering in p4. The population reached maximal full flowering in the middle of June (19th of June) with 98% having reached full flowering, this was also when the first senescence in the population was observed. The next visit (29th of June) the senescence in the population was seen to starting to increase, with almost 20% senescence. From this point onward a slow increase in senescence over time was observed, with 40% still remaining in full flowering in the latter end of July (23rd of July). The dynamics of the population could be discerned by a slower start along with a slow linear senescence pattern.

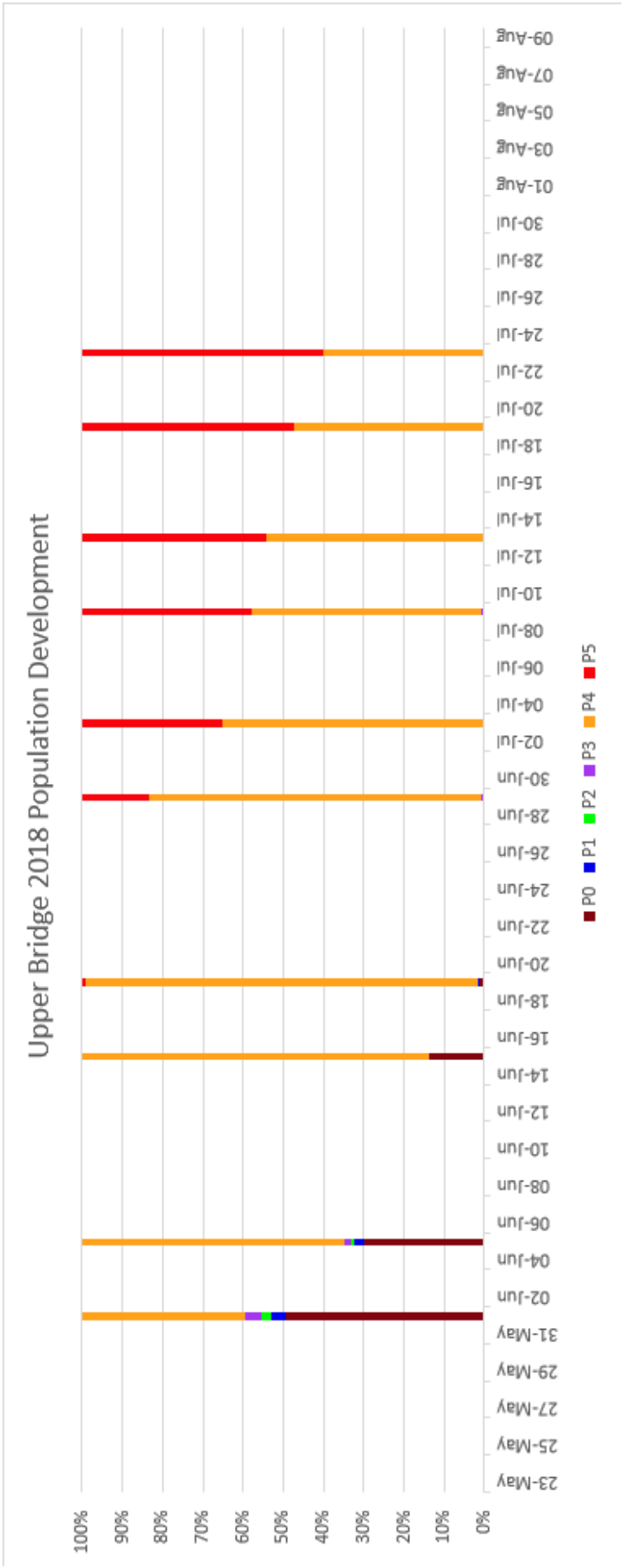

Figure 35. *Dactylis glomerata* population development shown per phase for the Upper Bridge 2018 secondary population.

5.2.3.4. West Field

The entire secondary population of West Field in 2018 consisted of 427 individual tillers split over the entire sampling location. West Field was one of the two locations with an overall higher number of tillers, therefore only individuals occupying three 2.25m^3 plots were observed. The first observation visit (7th of June) highlighted that the population had reached 93% full flowering, which was quicker and more intense than any of the other main and secondary populations (**Figure 36.**). The rest consisted of 5% non-flowering and 2% in lower flowering phases. This balance ratio was consistent until the middle of June (15th of June) when the first tillers reached senescence. This new balance ratio was consistent until the end of June (29th of June) when the senescence in the population increased to 25%. Over the next two weeks (9th of July) senescence increased to 70% with still a few tillers that have not yet started to flower. The next visit (17th July) the population senescence had increased to 95% with a few non-flowering tillers remaining. The next visit (19th of July) the last tillers reached full flowering. The last observation visit (25th of July) 99% of the population had reached senescence. The dynamics of the population could be discerned by a quick and intensive start along with a sigmoid-type senescence pattern.

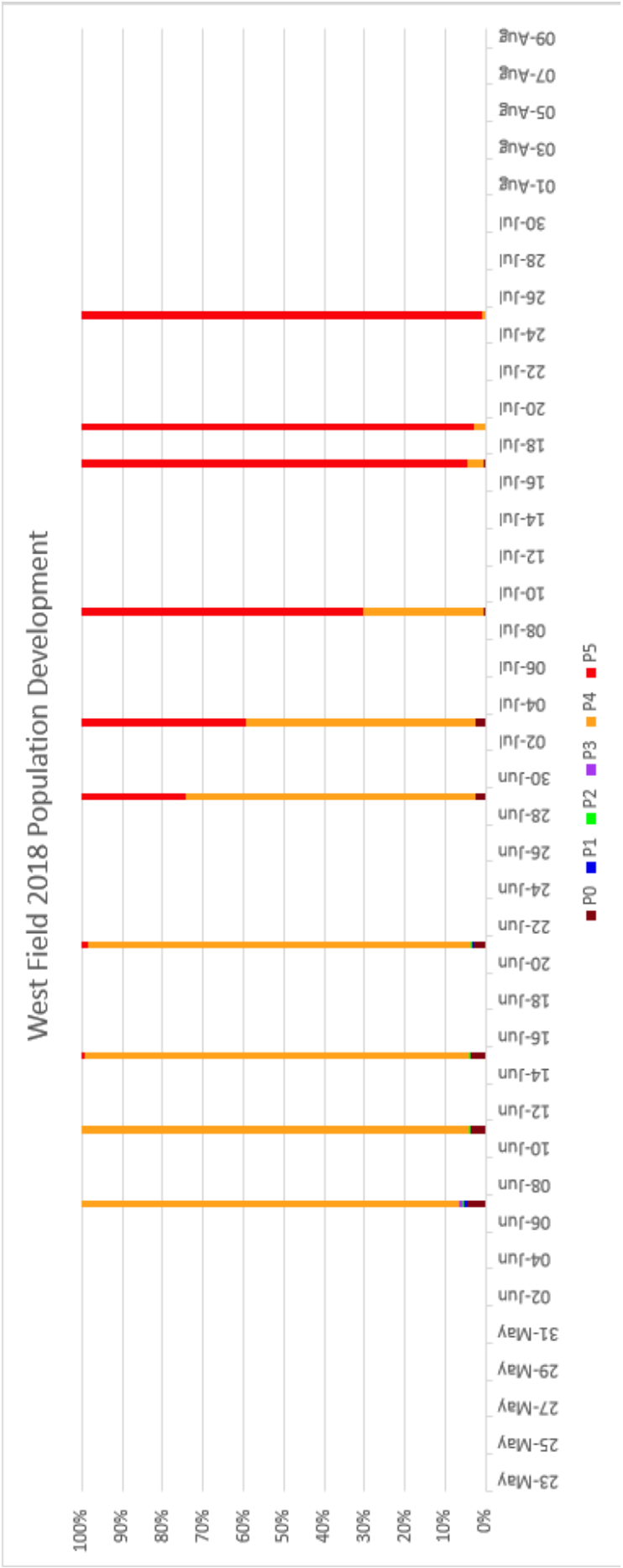

Figure 36. *Dactylis glomerata* population development shown per phase for the West Field 2018 secondary population.

5.2.3.5. Lower Field

The entire secondary population of Lower Field in 2018 consisted of 322 individual tillers split over the entire sampling location. Lower Field was one of the two locations with an overall moderate number of tillers, therefore only individuals occupying four 2.25m^3 plots were observed. The first observation visit (5th of June) highlighted that the 90% of the population had started to flower, with 86% having reached full flowering in p4 (**Figure 37.**). In the next ten days (15 of June) an increase in flowering was observed, with 96% having reached full flowering. The next visit (21st of June) the maximal full flowering at 97% was observed, along with the first tillers reaching senescence. During the last visit (27th of June) an increase in senescence to 10% was observed, along with the last tiller having started to flower (based on the observed tillers up-until that point). In the beginning of July (3rd of July) the location had been cut, and all future information regarding the flowering lost. The dynamics of this location is uncertain due to the unfortunate cut-off during the end of June. The dynamics of the start was discerned by a quick start.

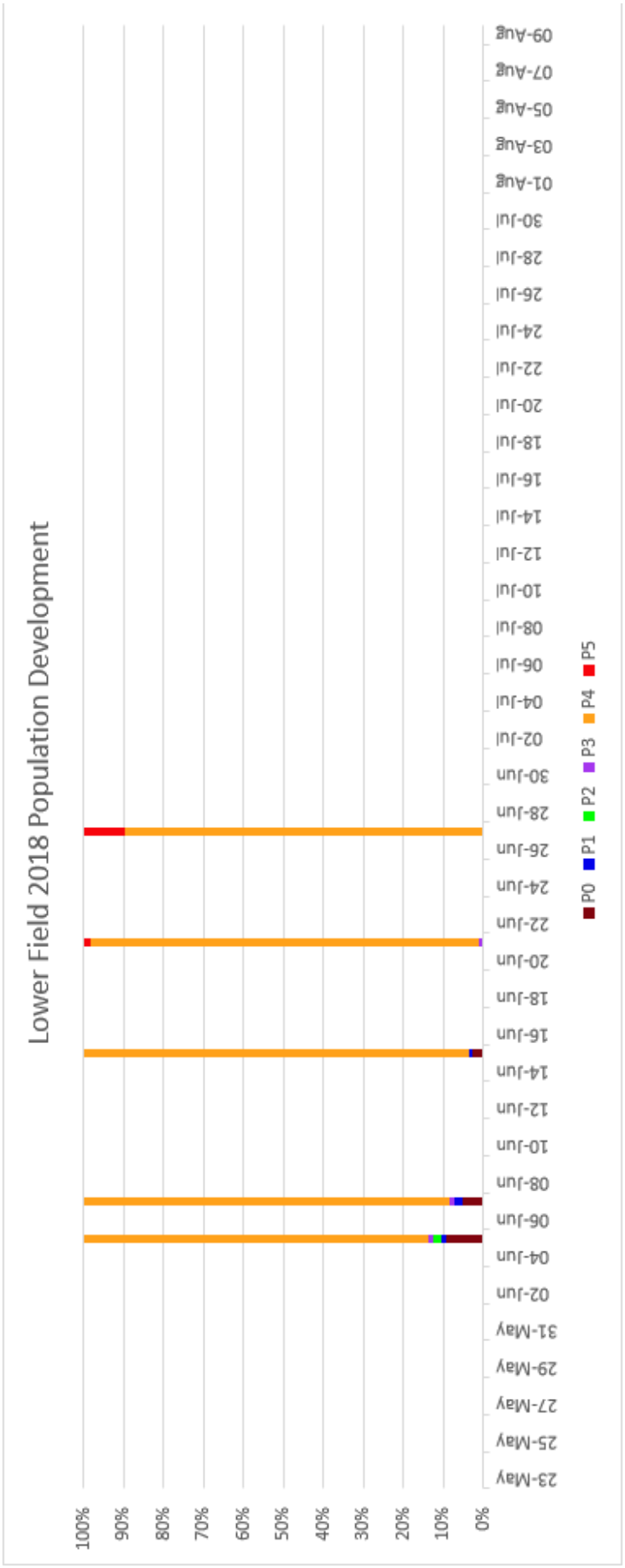

Figure 37. *Dactylis glomerata* population development shown per phase for the Lower Field 2018 secondary population.

5.2.3.6. Lower Bridge

The entire secondary population of Lower Bridge in 2018 consisted of 245 individual tillers split over the entire sampling location. Lower Bridge was one of the two locations with an overall moderate number of tillers, therefore only individuals occupying four 2.25m^3 plots were observed. The first observation visit (5th of June) highlighted that 88% of the population have started to flower, with 78% having reached full flowering in p4 and 10% occupying lower flowering phases (**Figure 38.**). The next visit (7th of June, only 2 days later) showed that the population had quickly gained 17% of full flowering to 95% full flowering. The next visit (15th of June) the population reached maximum full flowering, with almost 99% of tillers being in full flowering in p4. The next visit (19th of July) the first tillers reached senescence, along with the last tillers starting to flower. For the coming two weeks (5th of July) the population continued to senesce, with the balance shifting from majority full flowering to majority senescence. From this point onward the increase in senescence occurred in a linear pattern. During the latter half of July (25th of July) the population had reached 99% senescence. The dynamics of the population could be discerned by a quick and intensive start along with a linear senescence pattern.

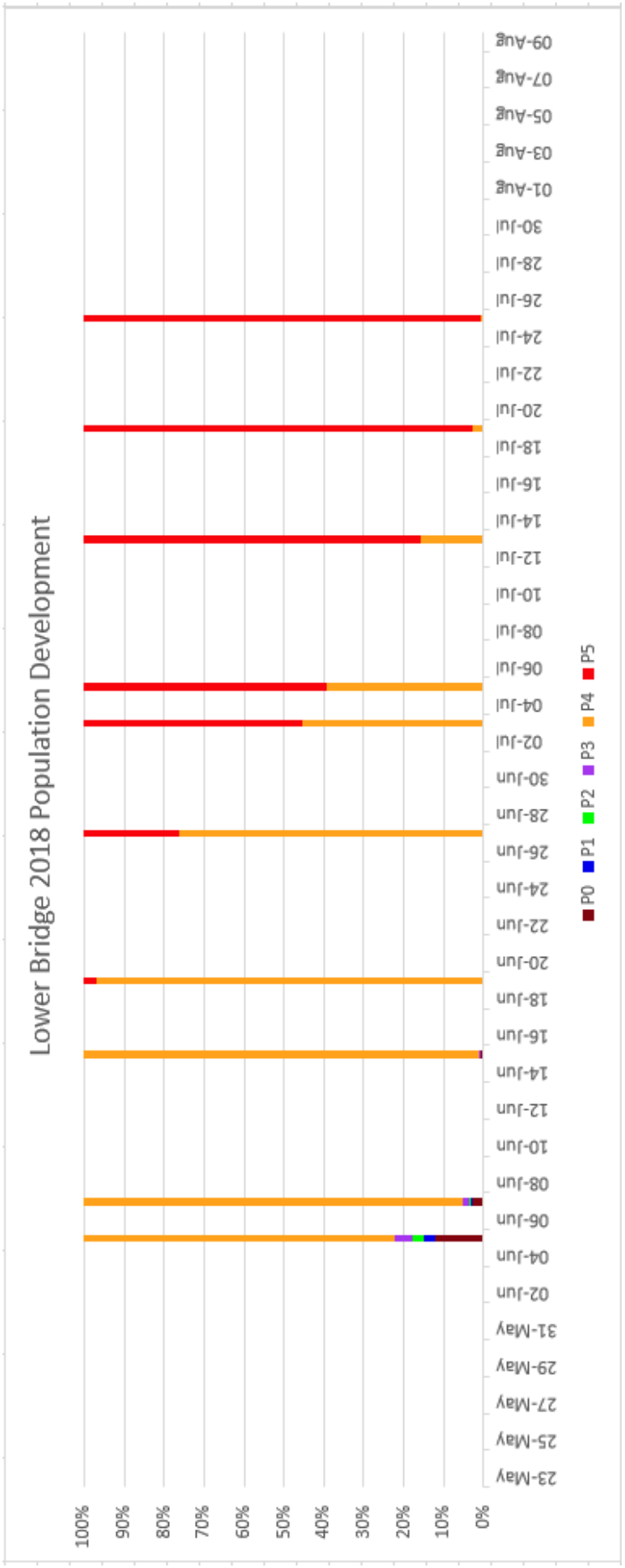

Figure 38. *Dactylis glomerata* population development shown per phase for the Lower Bridge 2018 secondary population.

5.2.4. General Flowering Progression

The section below presents the general flowering progression during 2017 and 2018. The section is divided between the two years, 2017 and 2018. The 2017 general flowering progression is determined from one main population. The 2018 general flowering progression is determined from two main populations, along with six secondary populations.

5.2.4.1. General Flowering Progression 2017

The investigation into the general flowering progression for *Dactylis* in 2017 comprised 317 individuals (14560 observations), and is the same population as found in section 5.2.1.1 (**Figure 30.**). The temporal flowering progression in 2017 ranged from p0 (non-flowering) to p5 (senescence), a development that occurred over the span of 53 days (**Figure 39.**). The flowering started on the 26th of May and finished on the 17th of July. The general population reached the average phenological state pX Y days (t+Y) after the flowering start (t), culminating in p1 at t+6, p2 at t+7, p3 at t+10, p4 at t+24 and p5 at t+53. The population traversed p0 to p1 during the course of 6 days, from the 26th of May to the 1st of June. This was characterized by a slow increase in incrementally higher flowering phases. The population traversed p1 to p2 during the course of one day to another, from 1st of June to the 2nd of June. This was characterized by an intense burst of many both non-flowering and flowering tillers transitioning into full flowering. The population traversed p2 to p3 during the course of 4 days, from the 2nd of June to the 4th of June. This was characterized by a slow increase in flowering individuals. The main reason was due to the general phase on the 2nd of June already being at the theoretical ‘p2.5’ and not p2, which highlight the average developmental phase increase of only 0.5 during 4 days. The population traversed p3 to p4 over the course of 15 days, from the 4th of June to the 18th of June. This was characterized by a slow increase in flowering tillers with a burst increase of full flowering tillers between the 7th and 8th of June, and the start and incremental increase of senescence in the population. At this point, even if the population was in the average phase 4, full flowering, many tillers had still yet to flower, while others had reached senescence. The population traversed p4 to p5 over the course of 30 days, from the 18th of June to the 17th of July. This was characterized by a slow increase in senescence, along with the last tillers in the population starting to flower.

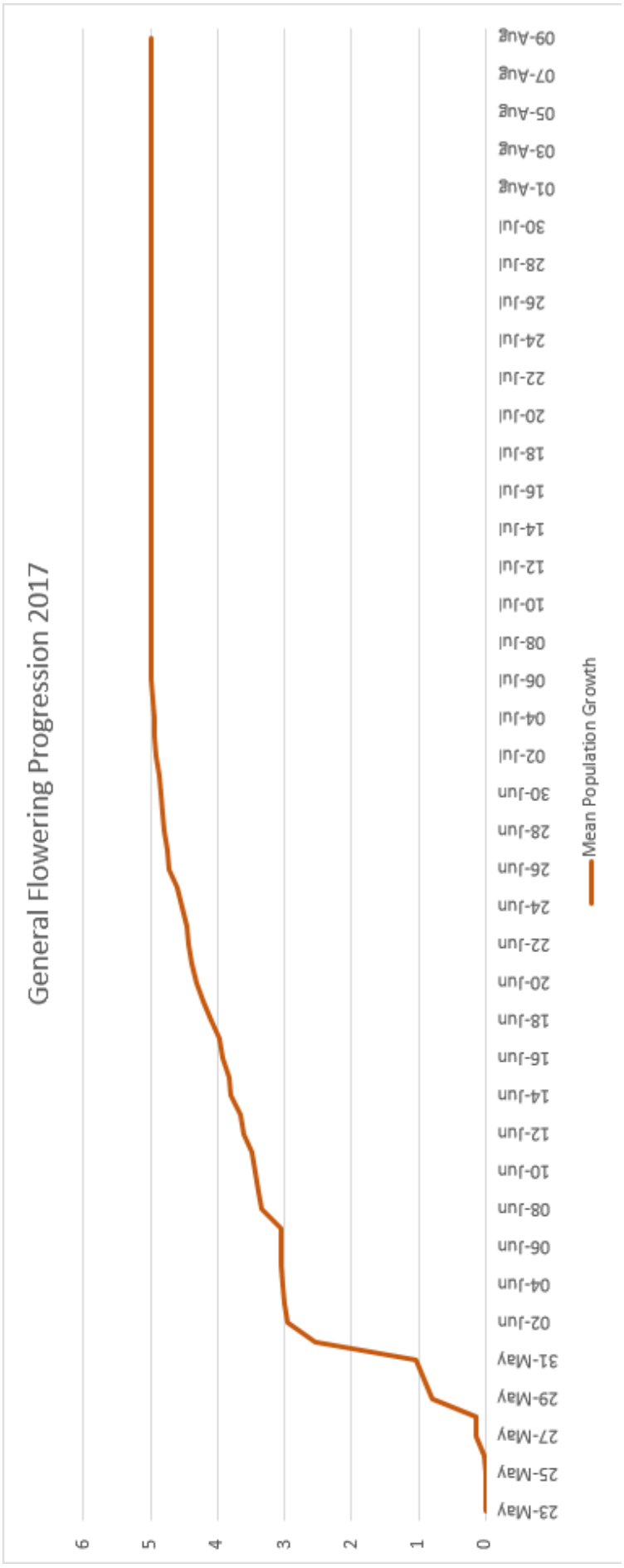

Figure 39. *Dactylis glomerata* general flowering progression for the year 2017, averaged from one population.

5.2.4.2. General Flowering Progression 2018

The investigation into the general flowering progression for *Dactylis* in 2018 comprised 2672 individuals (45662 observations), spread over two main populations, and six secondary populations (see sections 5.2.1 and 5.2.2, minus the 2017 St Johns population). The general flowering progression was the average progression split between all available populations at each observation occasion. Each population contributed equally to the general flowering progression in each time-step (see **Supplementary Figure S43.** for the contribution of each population). The temporal flowering progression in 2018 ranged from p0 (non-flowering) to p5 (senescence), a development that occurred over the span of 73 days (**Figure 40.**). The flowering started on the 29th of May and finished on the 9th of August. The general population reached the average phenological state pX Y days (t+Y) after the flowering start (t), culminating in p1 at t+4, p2 at t+5, p3 at t+7, p4 at t+23 and p5 at t+73. The population traversed p0 to p1 during the course of 4 days, from the 29th of May to the 1st of June. This was characterized by a slow start, with an intense burst between the 31st of May and the 1st of June. The population traversed p1 to p2 during the course of one day to another, from the 1st of June to the 2nd of June. This was characterized by an intense burst of full flowering tillers along with new tillers starting to flower. The population traversed p2 to p3 during the course of 3 days, from the 2nd of June to the 4th of June. This was characterized by a second intense burst of full flowering tillers, with many tillers from the moderate flowering phases and non-flowering tillers reaching full flowering. The population traversed p3 to p4 during the course of 17 days, from the 4th of June to the 20th of June. This was mainly characterized by non-flowering tillers reaching full flowering, but it is also caused by smaller parts of moderate flowering phases reaching full flowering, along with some tillers reaching senescence. The population traversed p4 to p5 during the course of 51 days, from the 20th of June to the 9th of August. This was characterized by a slow increase in senescence, along with a few non-flowering tillers starting to flower and reaching full flowering. The population did reach the theoretical developmental stage ‘p4.9’ after 28 days, on the 17th of July. This means that the last 0.1 developmental points took 24 days. This is mainly caused by a few late-lowering tillers that remained in full flowering for longer.

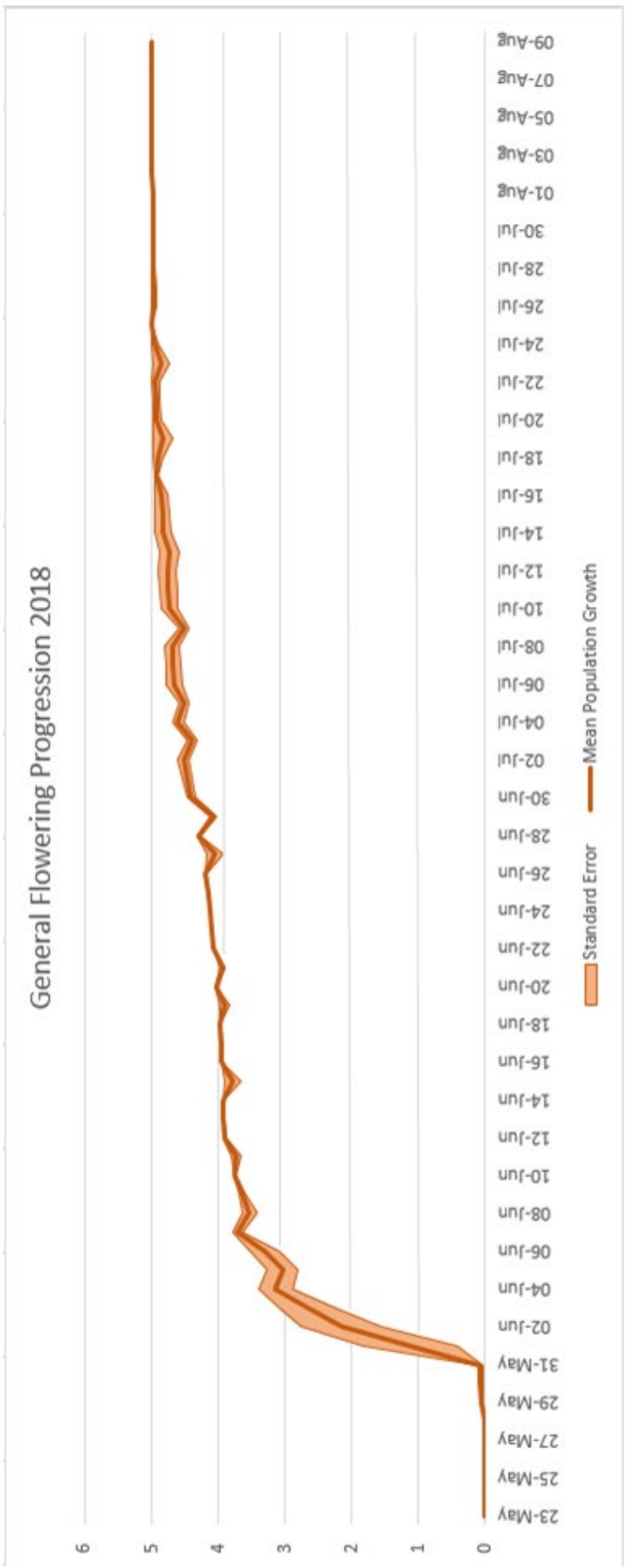

Figure 40. *Dactylis glomerata* general flowering progression for the year 2018, averaged from eight populations.

5.2.4.3. General Flowering Progression Comparison

The average standard deviation between the populations in 2018 for the entire season was 0.08 developmental points (± p0.08 e.g. between phase p1 and the imaginary phase p1.08 or the imaginary phase p0.92). The average difference between the two years (2017 minus 2018) was 0.18 developmental points, with a standard deviation of 0.04. This means that the 2017 general population was on average one fifth phase earlier than the 2018 general population (e.g. difference of phase p1 and the imaginary phase p1.2) (**Figure 41.**). A non-parametric correlation was used to compare the two years due to the non-normality expressed by both populations, as determined by the Shapiro-test ($p < 0.001$ for both years). The Spearman rho correlation suggested that there is a high correlation between the phenological development of the two years ($r_s = 0.98$).

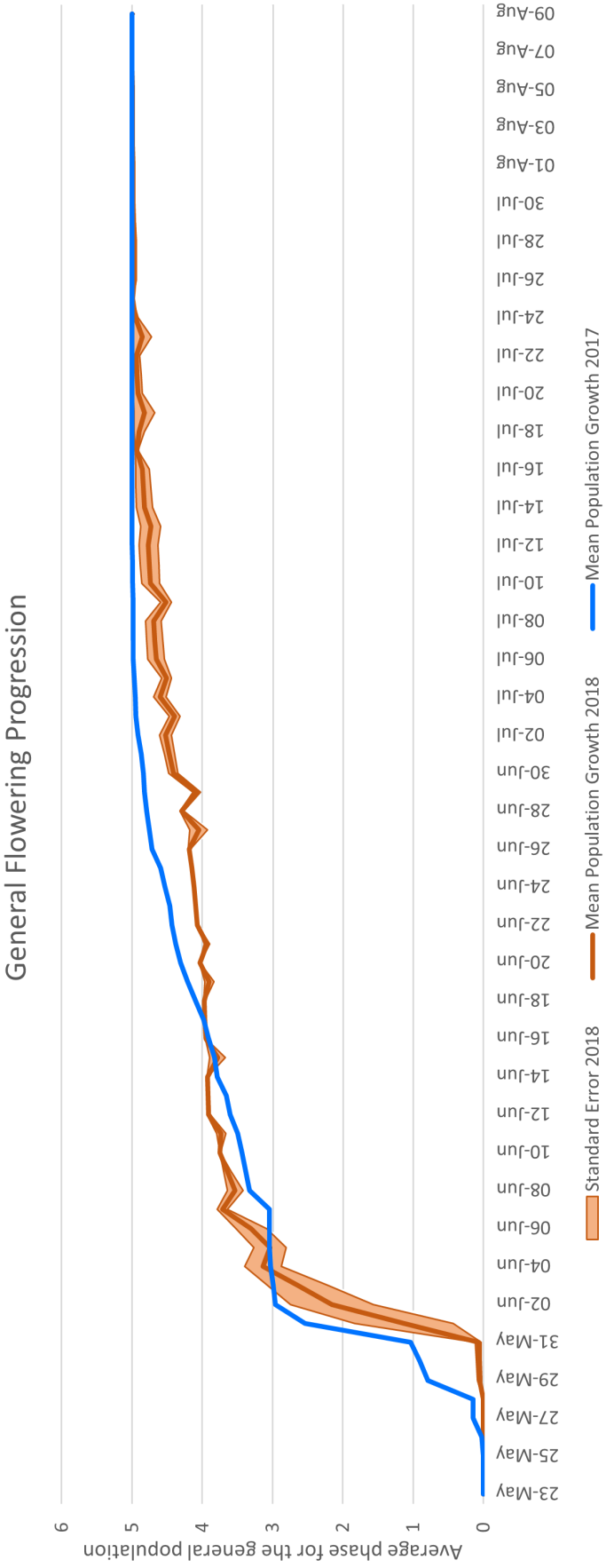

Figure 41. *Dactylis glomerata* general flowering progression of all observed populations for both years.

5.2.5. Tiller Specific Phase Dynamics

The section below presents the tiller specific phase dynamics of each main population as determined by the stochastic Markov Chain approach. The tiller specific phases dynamics of each main population has been translated into Markov Chain diagrams from the total transition matrix of each main population. Each tiller in each phase has a chance between 0 and 1 to transition to all other possible phases, note that not all phase transitions are possible due to the directional nature of flowering development. Also note that these diagrams highlight the total developmental behaviour of the observed populations.

5.2.5.1. St Johns 2017

The tiller specific phase dynamics for the main population St Johns in 2017 highlighted that all kinds of phase transitions occurred during the developmental process (**Figure 42.**). The seasonal dynamics highlighted that tillers that start flowering (p0) were from most to least likely to develop to p1, p4, p2 and p3. Almost 70% of the first flowering tillers reached either low flowering in p1 (41%) or full flowering in p4 (28%) first. Each of the flowering phases (p1, p2, p3 and p4) were most likely to stay in their respective phases (69%, 57%, 51% and 95%) than to transition to one of the subsequent phases in their development. The moderate flowering phases (p1, p2 and p3) had the second most likely transition to full flowering in p4 (22%, 26% and 49%), with p3 being almost twice as likely to transition to full flowering, then the other two phases. Tillers were likely to stay in full flowering p4 (95%), with the likelihood to transition to senescence being low (5%), although eventually all tillers reached senescence. The moderate flowering phases (p1, p2 and p3) had low likelihoods (around 1% each) to transition directly into senescence, meaning that these tillers reached senescence without ever reaching full flowering in p4. The only three transitions not yet talked about are the p1 transition to p2 (4%), the p1 transition to p3 (4%), and p2 transition to p3 (16%). All of these transitions would seem like the likely natural transitions, from one phase to the next, but neither were common in the population (or were not commonly observed using the observational methodology).

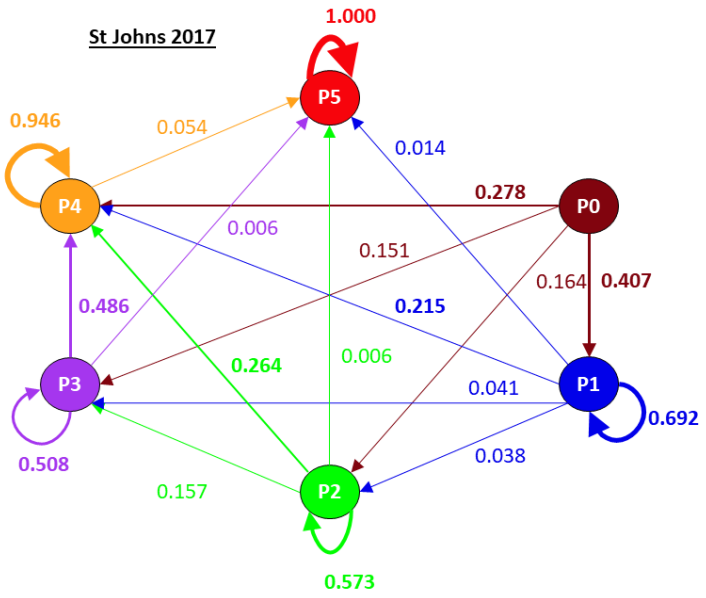

Figure 42. Tiller specific phase dynamics for the St Johns 2017 main population. Arrows indicate the direction of the transition, with all arrows from each phase adding up to 1. The thickness of each arrow is directly associated with the strength of the transition.

5.2.5.2. St Johns 2018

The tiller specific phase dynamics for the main population St Johns in 2018 highlighted that almost all kinds of phase transitions occurred (except for one) during the developmental process (**Figure 43.**). The seasonal dynamics highlighted that tillers that start flowering (p0) were most likely to develop directly to full flowering (79%) with the remaining likelihoods of developing to p1, p2 and p3 (10%, 5% and 6%). Each of the moderate flowering phases (p1, p2 and p3) were most likely to develop to full flowering in p4 (76%, 73% and 73%). The second most likely transition was to stay in their own respective phases (17%, 23% and 24%). This was the opposite as seen in the 2017 St Johns population. Tillers are likely to stay in full flowering p4 (94%), with the likelihood to transition to senescence being slightly higher than in 2017 (6%). Two of the moderate flowering phases (p1 and p3) had low chances (1% and 3%) to transition directly to senescence, without reaching full flowering, this was not observed in p2 during this season. The only three transitions not yet talked about are the p1 transition to p2 (5%), the p1 transition to p3 (2%), and p2 transition to p3 (3%). These transitions were less likely this season than the last one.

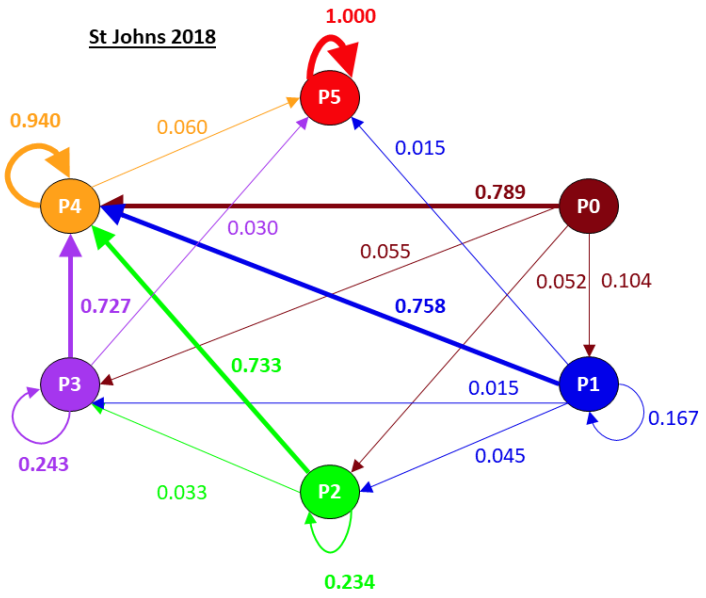

Figure 43. Tiller specific phase dynamics for the St Johns 2018 main population. Arrows indicate the direction of the transition, with all arrows from each phase adding up to 1. The thickness of each arrow is directly associated with the strength of the transition.

5.2.5.3. Lakeside 2018

The tiller specific phase dynamics for the main population Lakeside in 2018 highlighted that most kinds of phase transitions occurred (except for four) during the developmental process (**Figure 44.**). The seasonal dynamics highlighted that tillers that start flowering (p0) were most likely to developed directly from non-flowering to full flowering in p4 (64%) with the remaining likelihood split almost evenly between the moderate flowering phases p1, p2 and p3 (14%, 9% and 13%). This highlighted the difference to the St Johns population of the same year, in which tillers were 15% more likely to go directly into full flowering. The moderate flowering phases (p1, p2 and p3) were here, same as in St Johns, more likely to transition into full flowering in p4 (73%, 76% and 74%). The second most likely transition for the moderate flowering phases (p1, p2 and p3) were to stay in their own respective phase (23%, 24% and 26%), which was the same as seen in the St Johns population of the same year. Tillers were likely to stay in full flowering p4 (93%), with the likelihood to transition to senescence (7%) being slightly higher than the St Johns population of both years. The only phase that transitioned to senescence was p4, which was different from what has been observed for St Johns for both years. The only two transitions not yet talked about are the p1 to p2 (2%) and p1 to p3 (3%), both of which were unlikely transitions in this population. Note that there was not a single tiller that transition from p2 to p3 (between observations).

5.2.5.4. Tiller Specific Phase Dynamics Comparison

The Tiller-specific phase dynamics were investigated using three different RV correlation coefficients. The RV coefficients ranged from 0.824 to 0.999 for all population comparisons (**Table 7.**). The spatial comparison (St Johns 2018 – Lakeside 2018) coefficients ranged from 0.995 to 0.999. The temporal comparison (St Johns 2017 – St Johns 2018) coefficients ranged from 0.824 to 0.932. The spatio-temporal comparison (St Johns 2017 – Lakeside 2018) coefficients ranged from 0.847 to 0.950. See the supplementary material for the transitional matrices of each main population (**Supplementary Table S3.**).

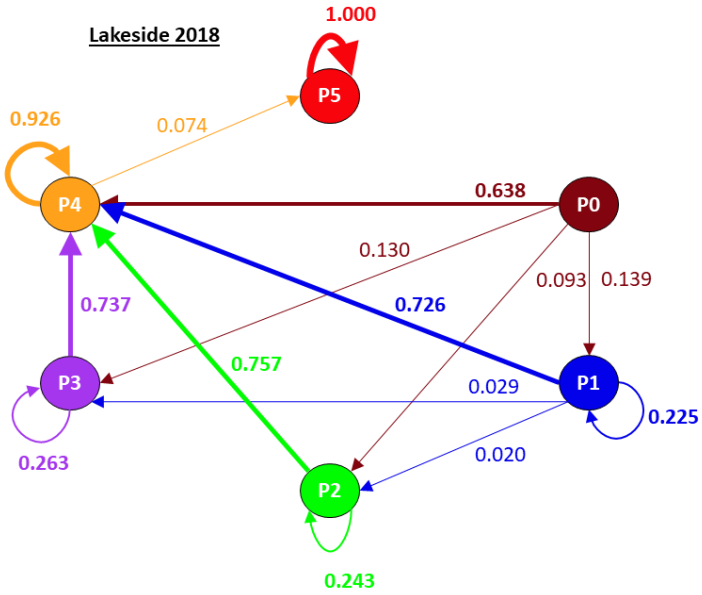

Figure 44. Tiller specific phase dynamics for the Lakeside 2018 main population. Arrows indicate the direction of the transition, with all arrows from each phase adding up to 1. The thickness of each arrow is directly associated with the strength of the transition.

Table 7

RV coefficients between the three main seasonal Markov Chain population matrices calculated from the flowering phenological observations in *Dactylis glomerata*.

Matrix 1	Matrix 2	Correlation Tested	RV Coefficient	RV2 Coefficient	RVadj Coefficient
St Johns 2018	Lakeside 2018	Spatial	0.999	0.995	0.999
St Johns 2017	St Johns 2018	Temporal	0.849	0.932	0.824
St Johns 2017	Lakeside 2018	Temporal and Spatial	0.868	0.950	0.847

5.3. Discussion

This research has shown that the species *Dactylis glomerata* flowers at the same time for an entire region. This has been the first time it has been shown that each population within a larger region develops in the same rate, which would lead to that pollen release likely also happens at the same rate. The process has also been explained to be caused by the same probabilistic mechanism shared between populations. This new knowledge has only been possible by observing the phenology of many individual plants within each population and by doing so every second day. Pollen forecasters can make this information public and recommend sufferers allergic to *Dactylis glomerata* pollen to avoid going out during these days. In addition, this information will be fundamental in developing mechanistic pollen release models in *Dactylis glomerata* and similar grasses.

5.3.1. General Population Flowering Dynamics

The seasonal general flowering trends between the *Dactylis glomerata* populations of the two years were highly correlated, with the 2017 population being on average one fifth of a phase earlier than the 2018 population. The difference in early phase flowering development (p1, p2 and p3) of the two populations (2017 minus 2018) ranged between 0 and -2 days, highlighting that the early phases of the 2017 population was reached either on the same date or at maximum two days earlier than the 2018 population. This suggests that the dates in which specific phases are reached are consistent between years. This is in contrast to findings from a previous study from Spain that concluded that early phases in *Dactylis glomerata* flowering between years within the same habitats were not reached on closely related dates, but could differ for up to several weeks (Cebrino et al., 2016). The length of the early phases (p0 to p1, p1 to p2 and p2 to p3) for the two years ranged between 1 to 6 days, with the total transition time from p0 to p3 never being higher than 10 days. This highlights that the populations of both years' transitions quickly between first flowering and p3. This is in agreement with previous studies from Austria (Kmenta et al., 2017, 2016), but in disagreement with studies from Spain (Cebrino et al., 2016; León-Ruiz et al., 2011), in which the early phases in *Dactylis* transitions over the course of a few weeks instead of a few days. However, the full flowering transition period from p3 to p4 is here observed to be longer, with it occurring over the course of 14 – 16 day (2 weeks), which again agrees with the Austrian studies but not with the Spanish studies, in which this period takes about one week. Physiological discrepancies between *Dactylis* populations from northern and southern locations within Europe have previously been attributed to adaptations to and differentials in photoperiod and temperature (Eagles, 1971, 1967), as demonstrated by varying growth rates and competitive abilities (Eagles, 1972; Eagles and Williams, 1971). It therefore

stands to reason that these differential responses to their immediate surroundings and meteorological influence might also translate into a differential flowering progression pattern, as previously suggested by Heide (1994, 1987). This is further collaborated upon by the generally shorter grass flowering seasons (15 to 30 days) present in Spanish habitats (Cebrino et al., 2018; Tormo-Molina et al., 2015) in contrast to the longer flowering seasons (50 to 73 days) in Worcestershire found in 2017 and 2018. The last transition, from p4 to p5, took 29 days in 2017 and 50 days in 2018, while previous studies have reported this transition to take approximately 7-14 days (Cebrino et al., 2016; León-Ruiz et al., 2011). The discrepancy is likely to originate (at least partly) from the differential in methodology, due to this study being centred around the strict presence of visible anthers, and not on the openness of flowers. However, the averages can only describe so much of the progression process. While an average of p4 suggests full flowering for all, it is more likely to describe most of the population being in full flowering (p4), while some might have reaches senescence (p5) and others not having started to flower yet (p0). A population in which all tillers are in full flowering will act differently than a population that occupy full flowering in name only, caused by an averaged flowering progression. Temporal variation in the phase distribution of the population is needed to explore the detailed population development, since each tiller will behave differently depending on its relative position in the developmental process.

5.3.2. Specific Population Flowering Dynamics

The temporal variation in phase distributions contains six phases, essentially increasing the dimensions six-fold in comparison to the general phenological progression above. The increased dimensionality showcases the uniformity of phase distributions shared between populations and years, with only small differences in daily variation between all populations. The key events of population phenological transitions, such as start of flowering, full flowering, start of senescence and the shift in balance between these stages all overlap in both in time and in space. The main piece of information extracted from the increased dimensionality and balance between stages is the divergent potential pollen release from tillers in different phases of flowering (Ghitarrini et al., 2017a; Tormo et al., 2011). If the absolute abundance of anthers is directly connected with the potential pollen release, then the lower flowering phases (p1, p2 and p3) present in the early season will release lower levels of pollen while the full flowering phase (p4) will release maximum levels of pollen. This has been shown to be the case for *Dactylis* in earlier studies from Spain (Rojo et al., 2017; Romero-Morte et al., 2018). Uniform flowering behaviour, as observed in this study, suggest a synchronistic grass pollen release over the entire study area. This has been suggested to be the case in studies from Austria (e.g. Kmenta

et al., 2017), Italy (e.g. Ghitarrini et al., 2017) and Spain (e.g. Cebrino et al., 2016). The uneven distribution of tillers identified in the average phase p4 from the previous section illustrates that average full flowering does not equate to full flowering for all individual tillers. Peak flowering can here be identified as the day of the season with maximum number of tillers in phase p4 (full flowering). Grass pollen has previously been demonstrated to be released evenly during full flowering (Subba Reddi et al., 1988). Since the phase p4 has been identified as the phase most likely associated with pollen release, then peak flowering can be identified as the day that has the likely maximum pollen release (Frenguelli et al., 2010; Romero-Morte et al., 2018). Therefore, this illustrates that bi-daily phenological observations are needed to showcase the connection between peak flowering and maximum grass pollen release. However, for complete confidence in pollen release estimates the temporal lag that occurs between anthesis and pollen release due to anther drying needs to be accounted for (Keijzer et al., 1987; Liem and Groot, 1973; Wilson et al., 2011). The main differences between the phenological development of the *Dactylis* populations were the senescence rates. Sigmoid and linear drying rates were identified, with the likely reason for the rate and shape differential being external factors relating to the physiological drying response in separate populations. This is modulated by grass evapotranspiration rates, which are regulated by local soil and weather conditions (De Bruin and Stricker, 2000; Hayhoe and Jackson, 1974; Hill, 1976). Previous modelling studies have suggested that increased temperature, solar radiation and windspeed have positive effect on grass drying, while increased rain, humidity and tiller density have negative effects on the same (Atzema, 1992; Khanchi et al., 2018). Even though no meteorology have been included in this section, the yearly differential in temperature and rain (as seen between years 2018 and 2019 in Chapter 4) suggests that this is a distinct possibility to be the cause of the differential in drying rates. Phase distribution gives fundamental understanding in the rates and patterns of flowering development in *Dactylis glomerata* but the mechanistic rules within populations that give rise to these patterns can only be understood by modelling tiller-specific phase changes.

5.3.3. Tiller Specific Developmental Dynamics

The tiller-specific transitions within each population shared core commonalities, with the main differences being visible in the absence/presence of the rarer phase transitions and the switching of most common transitions. The matrix comparisons revealed very high correlations within the phase transition dynamics between the three main populations, suggesting inherent stochastic elements in the *Dactylis glomerata* flowering progression. The spatial correlations were stronger than the spatiotemporal ones, which in turn were stronger than the temporal ones. This implies that there were larger differences in the phase transitions between years, than

between locations. Therefore, these differences were likely caused by regional conditions that varies on a temporal basis. No previous research have been published on the phase transition dynamics of *Dactylis glomerata* or any other similar grass species, but Calder (1964a, 1964b) have performed research into the stage-based development of the species. Calder concluded that the dynamics in stage-based development were directly caused by physiological responses to temperature and photoperiod. Three primary stages of development were identified in these two studies: juvenile (non-receptive to temperature and photoperiod), inductive (receptive to temperature and photoperiod) and post-inductive (receptive to long days). Further research in *Dactylis glomerata* flowering induction confirms the physiological growth stimuli caused by temperature, photoperiod and day-length (Broué and Nicholls, 1973; Cooper and Calder, 1964; Heide, 1987; Wilson and Thomas, 1971). The most common transitions in the 2017 phase changes were for tillers to stay in lower flowering phases, instead of transitioning to full flowering, this is consistent with a lack of growth stimuli from the above-mentioned causes (Calder, 1963; Heide, 1994). This was the opposite of what was observed in 2018, where tillers were most likely to transition directly to full flowering, highlighting the temporal divergences in the most common phase transitions. The stochasticity observed (e.g. through the varied presence of tillers rarely transitioning directly from lower flowering phases to senescence, by skipping full flowering altogether) implies that there were substantial differences in how individual tillers respond to the flowering developmental pathways. This introduces developmental variation into each population. This has previously been noted by Calder, who acknowledges considerable within-population variation (Calder, 1964a), likely stemming from natural genetic diversity within wild populations (Last et al., 2013; Lindner and Garcia, 1997; Peng et al., 2008). Natural genetic diversity in *Dactylis glomerata* populations has previously been shown to cause differential responses to growth stimuli (Garcia and Lindner, 1998), ecosystem adaptations (Trejo-Calzada and O'Connell, 2005) and flowering phenology (Zhao et al., 2017). Differential in growth stimuli and random stochastic variation (caused partly by genetic diversity) are likely possible explanations for the temporal divergence in phase transitions observed in the *Dactylis glomerata* populations.

5.4. Conclusion

Developmental dynamics in the flowering phenological process in *Dactylis glomerata* showed high consistency between years and over the entire study area. The general flowering trends implied only a few days differences in the overarching development between years. This was demonstrated by the general averaged populations reaching average phenological phases at closely related dates between the two years. Phase distribution patterns were uniform throughout the phenological development for all populations and years. This was demonstrated by key phenological events, such as start of flowering, full flowering and start of senescence being reached synchronistically throughout the region, only varying by a few days. This has been the first study to quantify proportional timeseries of intra-population phenology of any grass species, with fundamental applications in aerobiology, ecology, and agriculture. Demographic differences between full flowering and peak flowering suggested that peak flowering of each population was the theoretical period of maximal grass pollen release. This was due to the maximal absolute abundance of extruded anthers on all tillers within each population. The identification of peak flowering can be utilized to enhance the methodology in future studies regarding grass pollen release mechanics. The senescence rate differential between populations were likely caused by a varied response to physiological drying factors, such as temperature and rain. The tiller-specific developmental dynamics indicate the presence of inherent low variation stochastic elements within the species that likely responds to local growth stimuli. The demographic and stochastic elements identified within the study are critical at explaining the detailed and multifaceted flowering development present in *Dactylis glomerata* populations. The quantification of these elements can be used to refine future modelling approaches of grass phenology and grass pollen emission estimates.

6. Pollen Release Modelling in *Dactylis glomerata* Populations

6.1. Introduction

The use of demographic and stochastic elements from observed flowering grass populations can be utilized to model general flowering populations. These general populations can further be used to model grass pollen release scenarios based on the flowering progression and pollen release assumptions. Molecular data isolated from eDNA and processes through the lens of DNA metabarcoding bioinformatics can further be used to strengthen and optimize model performance to gain deeper understanding of fundamental pollen release mechanisms. The sections below presents the modelling of general *Dactylis glomerata* populations and pollen release scenarios connected with these modelled populations. Furthermore, pollen release scenarios are compared with collected *Dactylis glomerata* pollen eDNA. Discussion surrounding the population modelling, the connection between grass flowering and pollen release and implications for grass pollen allergy rounds off the chapter.

6.2. Results

6.2.1. Result Summary – Chapter 6

This chapter sought to explore the grass pollen emission process in *Dactylis glomerata* by modelling general populations based on the results from Chapter 5 and to confirm the modelling results using species-specific eDNA isolated from collected grass pollen. It was found that general populations could be modelled with good correlations to the observed populations using Markov Chain population models. All pollen release scenarios suggested that pollen release likely peaked between 3rd and 6th of June, with total pollen release being 5% or lower by the 11th of June, with almost identical results for both modelled populations. The comparison between pollen release scenarios with collected eDNA suggested that 70% pollen release of current levels showed the highest correlation, with changes to the release by successively ±10 % caused lower and lower correlations.

6.2.2. Modelling of General Populations of Flowering *Dactylis glomerata*

Twenty-one different Markov Chain transitional matrices were utilized to model the general populations of flowering *Dactylis glomerata* tillers (**Table 8.**). The first transitional matrix corresponds to the full transitional probabilities of the entire season (S1). The other twenty transitional matrices (D1 – D20) are subsets of S1 created from the observed population of each location, with the index being the observation day from the start of the flowering observations. Four different Markov Chain transitional lists were created using different combinations of the transitional matrices in Table 9 (**Table 9.**). Each list was utilized to create a modelled population

with all tillers from all corresponding phases depending on the cycling of transitional matrices. The modelled general populations (and the distributions of all six phases) created from each St Johns list can be found in the supplementary material (**Supplementary Figures S44 – S47.**). The Kendall tau-similarity between the phase-combined modelled St Johns populations and the phase-combined observed population ranged from 0.587 to 0.891, with all comparisons being highly significant ($p < 0.001$) (**Table 10.**). List #4 had the highest tau-similarity (0.891) for the modelled St Johns populations. The St Johns independent phase comparisons for each list can be found in supplementary material (**Supplementary Table 4a.**). The modelled general populations (and the distributions of all six phases) created from each Lakeside list can be found in the supplementary material (**Supplementary Figures S48 – S51.**). The Kendall tau-similarity between the phase-combined modelled Lakeside populations and the phase-combined observed population ranged from 0.560 to 0.861, with all comparisons being highly significant ($p < 0.001$) (**Table 10.**). List #4 had the highest tau-similarity (0.861) for the modelled Lakeside populations. The Lakeside independent phase comparisons for each list can be found in supplementary material (**Supplementary Table 4b.**).

Table 8

Description of the different transitional matrices utilized in the population modelling produced from the observed populations in St Johns and Lakeside 2018. **Abbreviations**: **S** - Static, **D** - Dynamic.

Type	Name	Index	Start Date	End Date
Transitional Matrix	S1	N/A	15-May	09-Aug
Transitional Matrix	D1	4	19-May	21-May
Transitional Matrix	D2	6	23-May	25-May
Transitional Matrix	D3	8	27-May	29-May
Transitional Matrix	D4	10	31-May	02-Jun
Transitional Matrix	D5	12	04-Jun	06-Jun
Transitional Matrix	D6	14	08-Jun	10-Jun
Transitional Matrix	D7	16	12-Jun	14-Jun
Transitional Matrix	D8	18	16-Jun	18-Jun
Transitional Matrix	D9	20	20-Jun	22-Jun
Transitional Matrix	D10	22	24-Jun	26-Jun
Transitional Matrix	D11	24	28-Jun	30-Jun
Transitional Matrix	D12	26	02-Jul	04-Jul
Transitional Matrix	D13	28	06-Jul	08-Jul
Transitional Matrix	D14	30	10-Jul	12-Jul
Transitional Matrix	D15	32	14-Jul	16-Jul
Transitional Matrix	D16	34	18-Jul	20-Jul
Transitional Matrix	D17	36	22-Jul	24-Jul
Transitional Matrix	D18	38	26-Jul	28-Jul
Transitional Matrix	D19	40	30-Jul	01-Aug
Transitional Matrix	D20	42	03-Aug	05-Aug

Table 9

The combination of different transition matrices that comprise each phase transition list utilized in the modelling of the generalized *Dactylis glomerata* flowering populations for St Johns and Lakeside 2018. Each list includes a starting condition, which increases the total number of matrices by 1. See **Table 8** for description of each matrix.

Phase Transitions List Combination	**Matrices** Numbers	**Different Matrices** Unique matrices	**Description**
#1	101	1	Only the seasonal matrix used [S1], 100 of them.
#2	101	10	Each even matrix [D2, D4, D6, .. ,D20] used, 10 of each in order.
#3	101	20	Each matrix [D1, D2, D3, .. ,D20] used, 5 of each in order.
#4	121	20	Each matrix [D1, D2, D3, .. ,D20] used, 6 of each in order.

Table 10

Correlations between the combined temporal phase distributions in each modelled *Dactylis glomerata* population and the observed populations in 2018. Each list is unique for the location.

Location	**Phase Transitions** List Combination	**Phases** Combined	**Kendall Rank Correlation** z	tau	P - value	Significance
St Johns	List #1	All Six	12.637	0.587	< 0.001	***
St Johns	List #2	All Six	15.093	0.761	< 0.001	***
St Johns	List #3	All Six	17.188	0.850	< 0.001	***
St Johns	List #4	All Six	18.105	0.891	< 0.001	***
Lakeside	List #1	All Six	11.913	0.560	< 0.001	***
Lakeside	List #2	All Six	14.433	0.747	< 0.001	***
Lakeside	List #3	All Six	16.258	0.840	< 0.001	***
Lakeside	List #4	All Six	16.727	0.861	< 0.001	***

6.2.3. Modelling of Pollen Release Scenarios

The modelled general population created using list #4 was chosen to create the pollen release scenarios due to the higher Kendall tau-similarity for both locations (**Table 10.**). Ten pollen release scenarios ranging from 10% pollen release per day to 100% pollen release per day were created for both locations. Each pollen release scenario corresponds to the amount of pollen released per day based on the currently available pollen amounts while the data below corresponds to the amount of pollen released daily based on the total seasonal pollen amount.

All pollen release scenarios for St Johns show low pollen release during the end of May (**Figure 45.**). Pollen release then quickly peaks (with ranges from 2.5% to 31.2% of total available pollen per day) during the beginning of June (3rd – 6th of June, depending on the scenario). All scenarios decrease to max 5% pollen release of total per day (0.7 % - 4.9 % per day) during the middle of June (11th of June). All scenarios (except the 10% and 20% PR/day) decrease to max 1% pollen release of total per day (0.1 % - 0.9 %) during the latter part of June (20th of June), with the two remaining scenarios having between 2 – 3 % pollen release per day. By the end of June (27th of June) only the 10% PR/day release over 1% pollen per day. This dynamic is illustrated in the modelled cumulative pollen release for St Johns (**Figure 46.**).

All pollen release scenarios for Lakeside show low pollen release during the end of May (**Figure 47.**). Pollen release then quickly peaks (with ranges from 2.6% to 32.6% of total available pollen per day) during the beginning of June (3rd – 6th of June, depending on the scenario). All scenarios decrease to max 5% pollen release of total per day (0.2 % - 4.7 % per day) during the middle of June (12th of June). All scenarios (except the 10% and 20% PR/day) decrease to max 1% pollen release of total per day (< 0.01 % - 0.8 %) during the latter part of June (20th of June), with the two remaining scenarios having between 2 – 3 % pollen release per day. By the end of June (27th of June) only the 10% PR/day release over 1% pollen per day. This dynamic is illustrated in the modelled cumulative pollen release for Lakeside (**Figure 48.**).

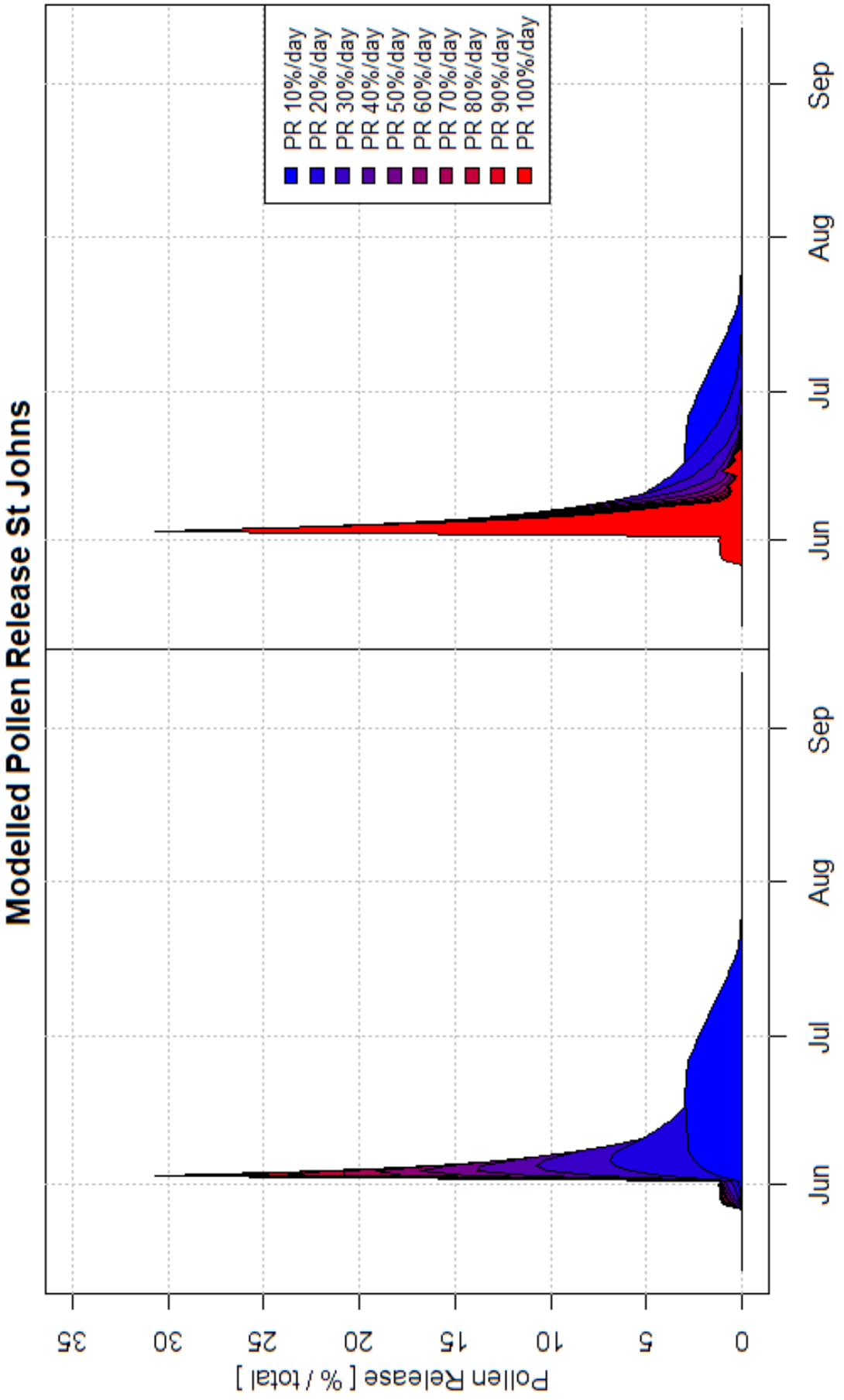

Figure 45. Modelled pollen release of *Dactylis glomerata* pollen for the St Johns population in 2018. Ten pollen release scenarios are displayed, from 10% to 100% pollen release per day. The graphs are the same but with reverse order, to showcase all features of each curve.

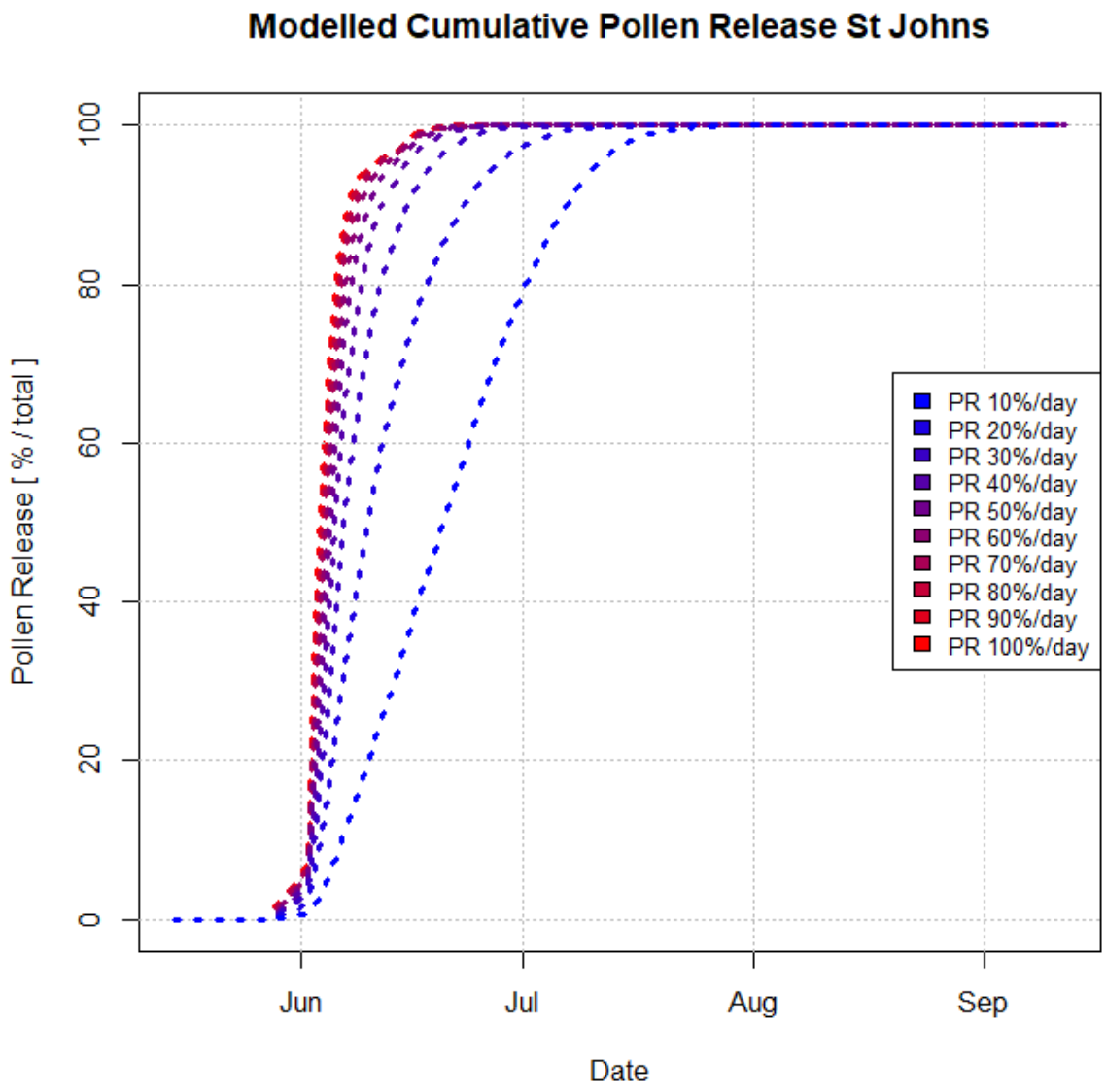

Figure 46. Modelled pollen release of *Dactylis glomerata* pollen for the St Johns population in 2018, cumulative. Ten pollen release scenarios are displayed, from 10% to 100% pollen release per day. This figure presents the same data as **Figure 45**, but in a different format.

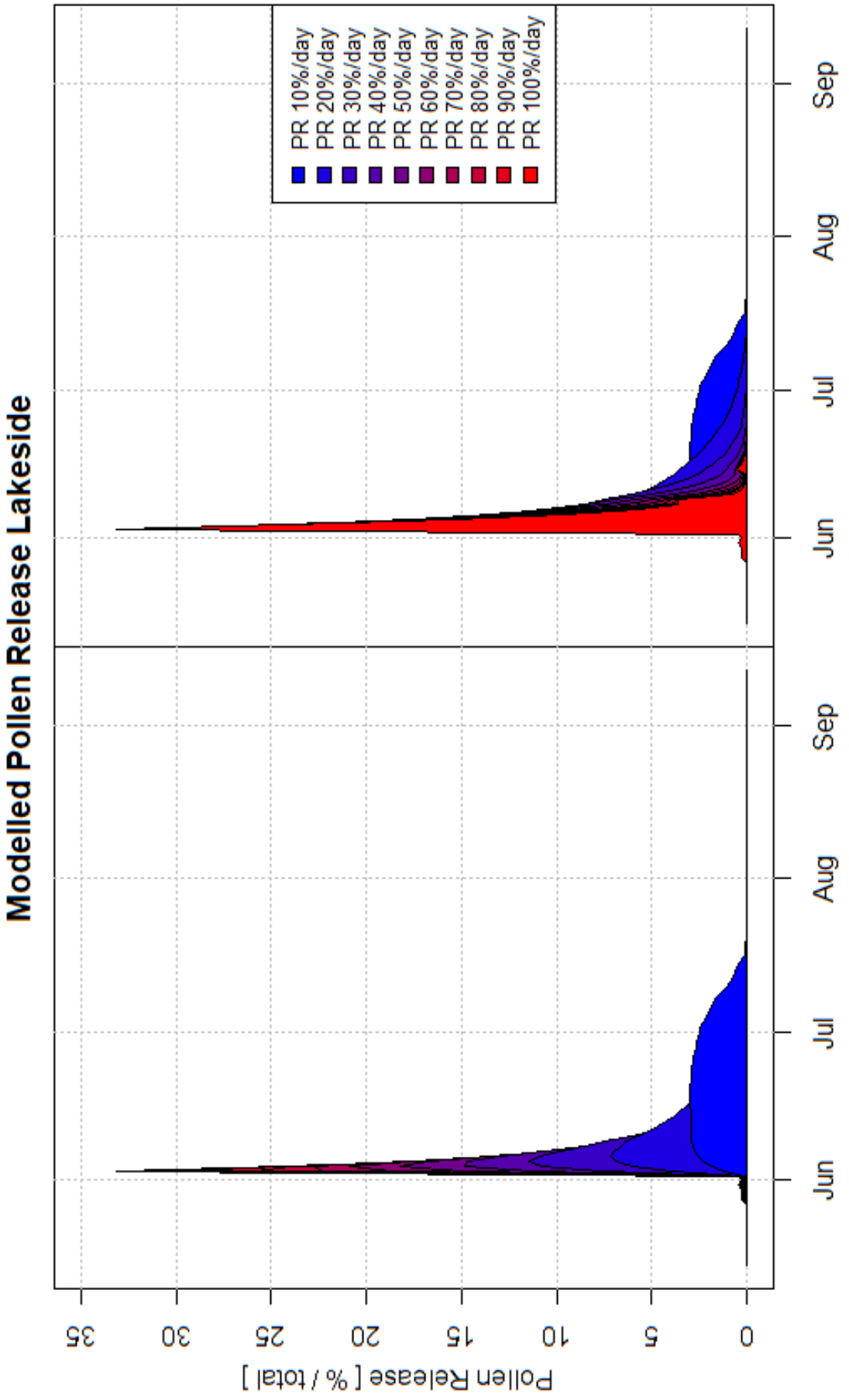

Figure 47. Modelled pollen release of *Dactylis glomerata* pollen for the Lakeside population in 2018. Ten pollen release scenarios are displayed, from 10% to 100% pollen release per day. The graphs are the same but with reverse order, to showcase all features of each curve.

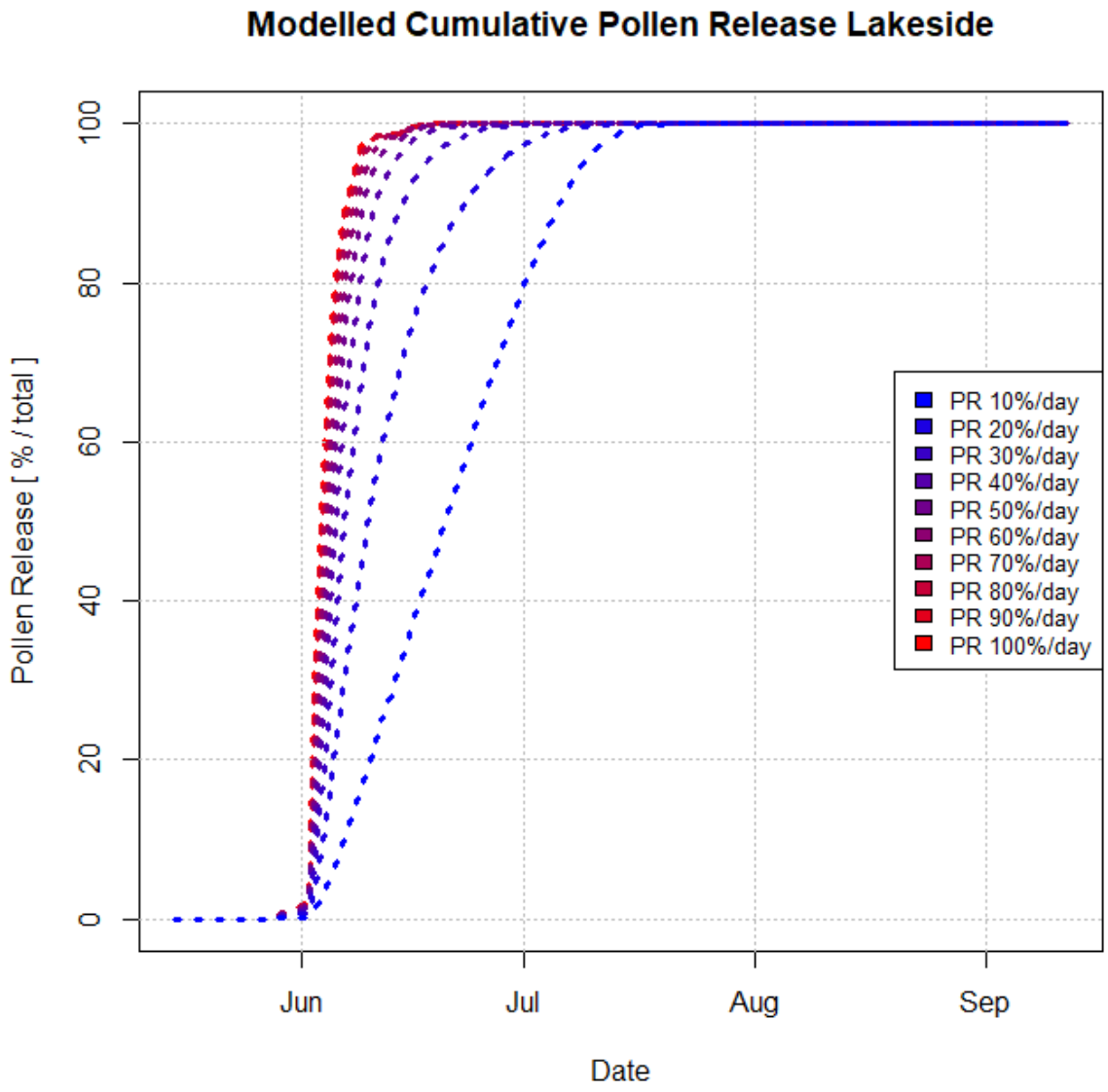

Figure 48. Modelled pollen release of *Dactylis glomerata* pollen for the Lakeside population in 2018, cumulative. Ten pollen release scenarios are displayed, from 10% to 100% pollen release per day. This figure presents the same data as **Figure 47**, but in a different format.

6.2.4. Pollen Release Estimates Estimated via the Metabarcoding Analysis of eDNA

The pollen release estimates above were compared with real species-specific pollen estimates using metabarcoding analysis of eDNA collected at the same location and time as the observed flowering populations in 2018. Here no anther dehiscence delay and fixed pollen release rates were assumed.

The St Johns combined ITS-regions show Spearman rho correlations of between 0.214 and 0.826 with the different pollen release scenarios (**Table 11a.**). Pollen release scenarios of 60 – 70 % per day show high correlations with the combined ITS-regions (rho = 0.826, $p < 0.001$ x2). Six other pollen release scenarios 30 – 50 % and 80 – 100 % show high correlations with the combined ITS-regions (rho = 0.715 – 0.822, $p < 0.01$ x6). The correlations with the individual ITS-regions for St Johns can be found in the supplementary material (**Supplementary Tables S5a – S5b.**). The ITS-regions are showed overlaying the pollen release scenarios (**Figure 49**).

The Lakeside combined ITS-regions show Spearman rho correlations of between 0.058 and 0.668 with the different pollen release scenarios (**Table 11b.**). Pollen release scenarios of 80 – 100 % per day show high correlations with the combined ITS-regions (rho = 0.668, $p < 0.01$ x3). Three other pollen release scenarios 50 – 70 % show high correlations with the combined ITS-regions (rho = 0.510 – 0.617, $p < 0.05$ x3). The correlations with the individual ITS-regions for Lakeside can be found in the supplementary material (**Supplementary Tables S5c – S5d.**). The ITS-regions are showed overlaid the pollen release scenarios (**Figure 50**).

The combined locations and combined ITS-regions show Spearman correlations between 0.072 and 0.700 with the different pollen release scenarios (**Table 12.**). Pollen release scenarios of 40 – 100 % per day show high correlations with the combined ITS-regions (rho = 0.597 – 0.700, $p < 0.001$ x7). Two other pollen release scenarios 20 – 30 % show correlations with the combined ITS-regions (rho = 0.407, $p < 0.05$ and rho = 0.502, $p < 0.01$, respectively). The pollen release scenario of 70% per day shows the smallest S-statistic and the highest Spearman-rho value in relation to the combined ITS-regions.

Table 11a

Correlations between modelled pollen release estimates in the modelled Dactylis glomerata populations and the relative proportion of Dactylis glomerata pollen based on the ITS1 and ITS2 region bioinformatics of collected eDNA in St Johns 2018.

Pollen Release	Pooled Samples	ITS1 Data Points	ITS2 Data Points	Days	Spearman Rank Correlation			
					S	rho	P - value	Significance
100%/day	8	8	4	28	81.391	0.715	< 0.01	**
90%/day	8	8	4	28	61.032	0.787	< 0.01	**
80%/day	8	8	4	28	61.032	0.787	< 0.01	**
70%/day	8	8	4	28	49.834	0.826	< 0.001	***
60%/day	8	8	4	28	49.834	0.826	< 0.001	***
50%/day	8	8	4	28	50.852	0.822	< 0.01	**
40%/day	8	8	4	28	55.942	0.804	< 0.01	**
30%/day	8	8	4	28	64.086	0.776	< 0.01	**
20%/day	8	8	4	28	136.36	0.523	0.08088	.
10%/day	8	8	4	28	224.92	0.214	0.5051	NS

Table 11b

Correlations between modelled pollen release estimates in the modelled Dactylis glomerata populations and the relative proportion of Dactylis glomerata pollen based on the ITS1 and ITS2 region bioinformatics of collected eDNA in Lakeside 2018.

Pollen Release	Pooled Samples	ITS1 Data Points	ITS2 Data Points	Days	Spearman Rank Correlation			
					S	rho	P - value	Significance
100%/day	8	8	8	28	225.54	0.668	< 0.01	**
90%/day	8	8	8	28	225.54	0.668	< 0.01	**
80%/day	8	8	8	28	225.54	0.668	< 0.01	**
70%/day	8	8	8	28	260.66	0.617	< 0.05	*
60%/day	8	8	8	28	332.96	0.510	< 0.05	*
50%/day	8	8	8	28	332.96	0.510	< 0.05	*
40%/day	8	8	8	28	355.68	0.477	0.06177	.
30%/day	8	8	8	28	355.68	0.477	0.06177	.
20%/day	8	8	8	28	479.62	0.295	0.2679	NS
10%/day	8	8	8	28	640.75	0.058	0.8319	NS

Table 12

Correlations between modelled pollen release estimates in the modelled Dactylis glomerata populations and the relative proportion of Dactylis glomerata pollen based on the ITS1 and ITS2 region bioinformatics of collected eDNA in St Johns and Lakeside 2018.

Pollen Release	Pooled Samples	ITS1 Data Points	ITS2 Data Points	Days	Spearman Rank Correlation			
					S	rho	P - value	Significance
100%/day	16	16	12	28	1256.7	0.656	< 0.001	***
90%/day	16	16	12	28	1273.1	0.652	< 0.001	***
80%/day	16	16	12	28	1232.1	0.663	< 0.001	***
70%/day	16	16	12	28	1095.8	0.700	< 0.001	***
60%/day	16	16	12	28	1314.1	0.640	< 0.001	***
50%/day	16	16	12	28	1353.1	0.630	< 0.001	***
40%/day	16	16	12	28	1474	0.597	< 0.001	***
30%/day	16	16	12	28	1821.4	0.502	< 0.01	**
20%/day	16	16	12	28	2165.8	0.407	< 0.05	*
10%/day	16	16	12	28	3389.6	0.072	0.7144	NS

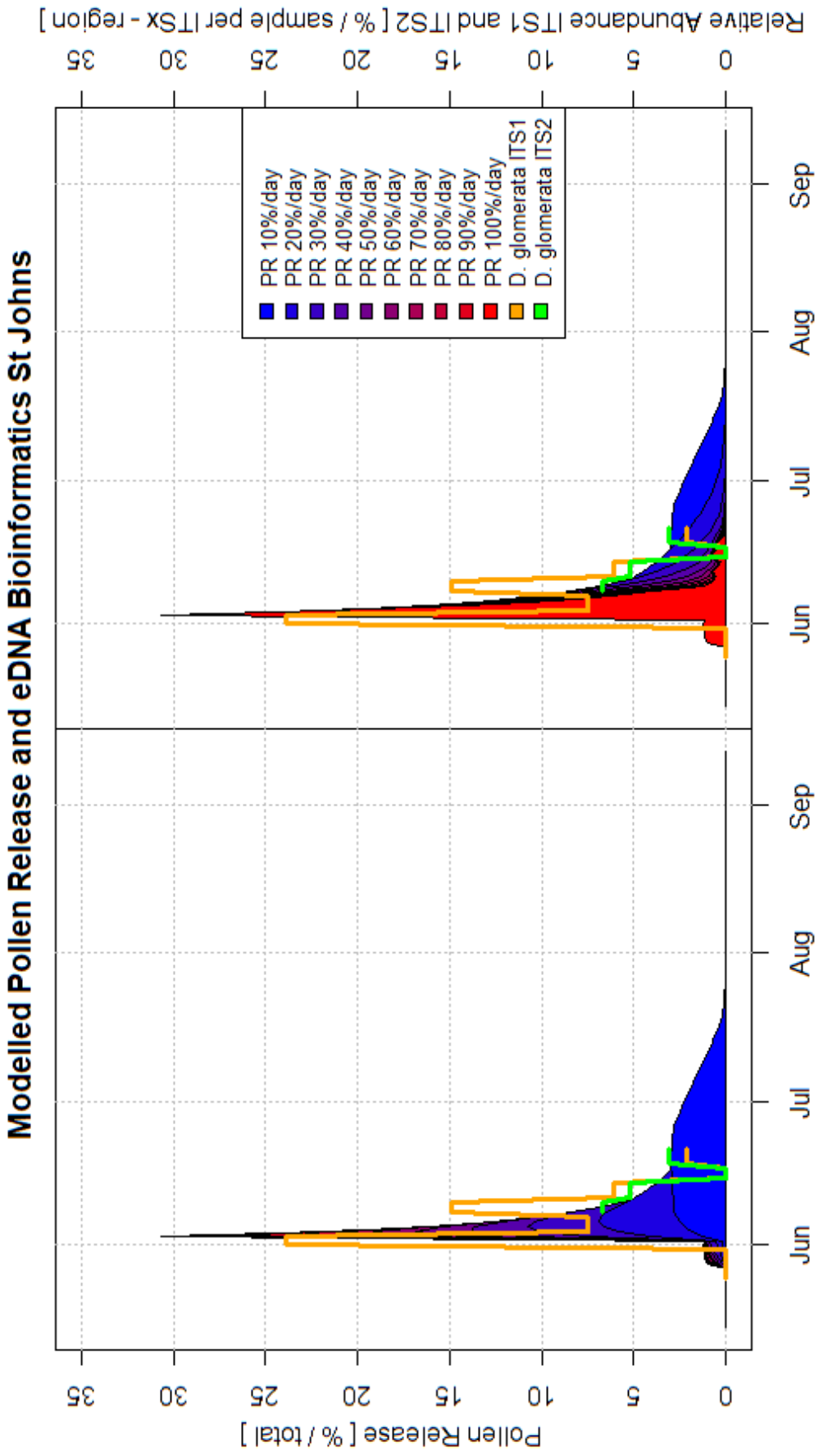

Figure 49. Modelled pollen release of *Dactylis glomerata* pollen for the St Johns population in 2018. The graph also includes relative abundance of *Dactylis glomerata* pollen isolated from eDNA samples from the location. Ten pollen release scenarios are displayed, from 10% to 100% pollen release per day. The graphs are the same but with reverse order, to showcase all features of each curve.

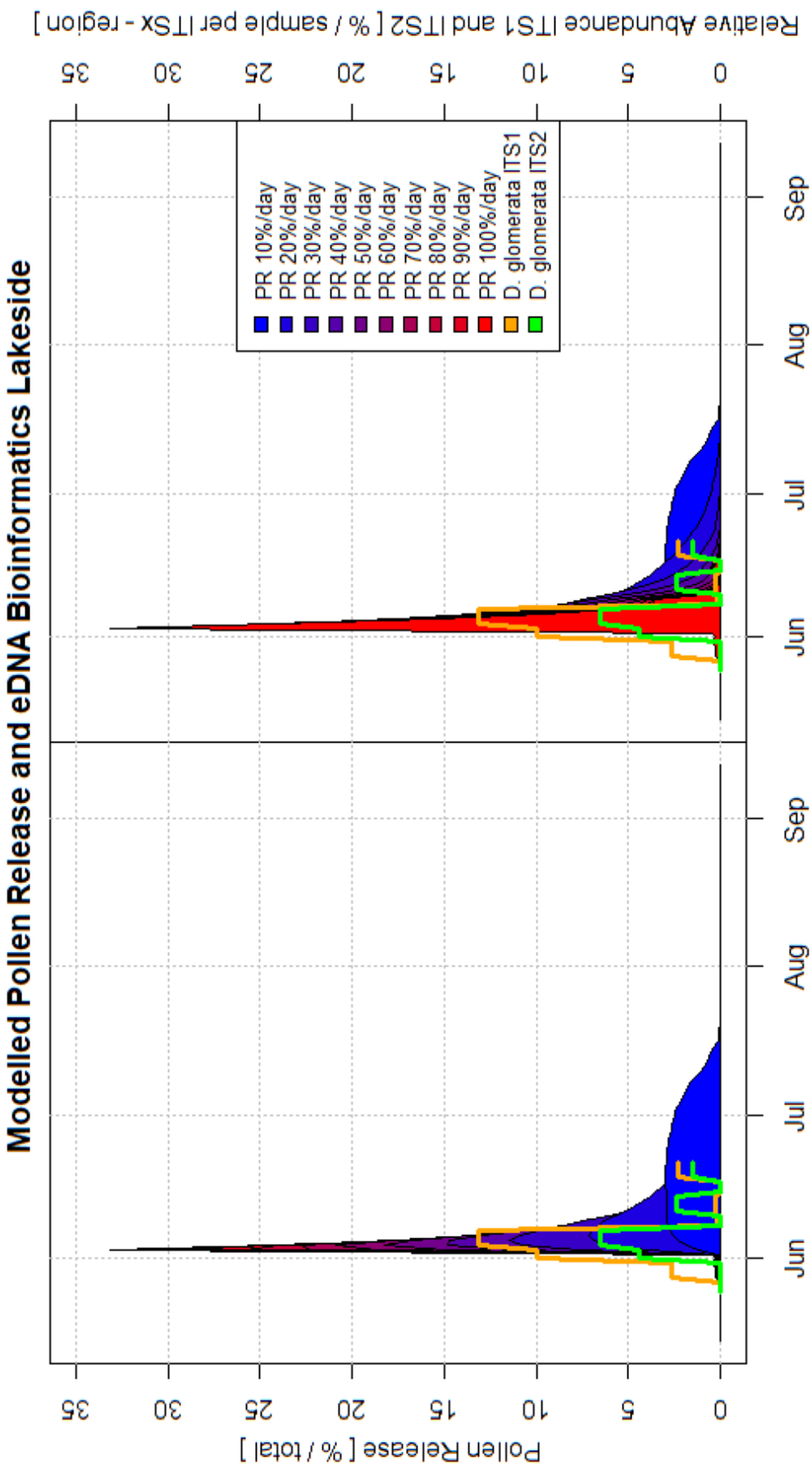

Figure 50. Modelled pollen release of *Dactylis glomerata* pollen for the Lakeside population in 2018. The graph also includes relative abundance of *Dactylis glomerata* pollen isolated from eDNA samples from the location. Ten pollen release scenarios are displayed, from 10% to 100% pollen release per day. The graphs are the same but with reverse order, to showcase all features of each curve.

6.2.5. Meteorology and abundance of *D. glomerata*, measured via eDNA Analysis

The combined locations and combined ITS-regions show Spearman correlations between -0.286 and 0.637 with the meteorological variables (**Table 13.**). Solar radiation shows highly significant positive correlation with the combined ITS-regions (rho = 0.637, $p < 0.001$). Temperature shows highly significant positive correlation with the combined ITS-regions (rho = 0.504, $p < 0.01$). The relative humidity, precipitation and wind speed show non-significant negative correlations with the combined ITS-regions (rho = -0.175 - -0.286, p = NS).

Table 13

Correlations between meteorological variables and the relative proportion of Dactylis glomerata pollen based on the ITS1 and ITS2 region bioinformatics of collected eDNA in St Johns and Lakeside 2018.

Variable	Type	Pooled Samples	ITS1 Data Points	ITS2 Data Points	Days	Spearman Rank Correlation			
						S	rho	P - value	Significance
Solar Radiation	Mean	16	16	12	28	1328.1	0.637	< 0.001	***
Temperature	Mean	16	16	12	28	1814	0.504	< 0.01	**
Relative Humidity	Mean	16	16	12	28	4294.7	-0.175	0.3722	NS
Precipitation	Sum	16	16	12	28	4623.7	-0.265	0.1723	NS
Wind Speed	Mean	16	16	12	28	4697.5	-0.286	0.1407	NS

6.3. Discussion

This novel research has shown for the first time that the flowering progression of a grass population corresponds directly to the pollen that is observed in the air. This has been shown using a direct model of pollen release and confirmed using eDNA that can only have come from this species. Pollen release is the only known process to cause pollen to appear in the atmosphere but the connection between the two has never previously been shown for a grass species. The method utilized can be replicated to show the same connection in other grass species, and will be essential in modelling how other highly allergenic grass species contribute pollen to the atmosphere. Without this information it will be impossible to determine where the grass pollen is coming from and how much is being contributed to the atmosphere.

6.3.1. Stochastic Population Modelling

The use of a transitional list comprised of twenty different stochastic matrices (each repeated six times) can model large flowering grass populations of randomly sampled tillers accurately, with correlations of 0.86 – 0.89, in comparison to observed flowering populations. The modelling of demographic processes in grasses using matrix models is well established (e.g. Fréville and Silvertown, 2005; Guàrdia et al., 2000; Hansen, 2007; O'Connor, 1993; Oliva et al., 2005), with specifically Markov Chain stochastic matrix modelling approaches being less common but equally applicable (Nakaoka, 1996)(e.g. Canales et al., 1994; Silva et al., 1991). However, it has never previously been explored in the flowering process of grasses. The use of one seasonal transition matrix was not accurate enough to explain population demographic

behaviour in terms of flowering progression. This is likely due to the presence of certain transitions, such as senescence, which is a time-sensitive transition which cannot occur during the early stages of the population development (Leopold, 1961). Temporality in the modelled population development is also reflected in the low levels of intermediate stages of flowering (p1, p2 and p3), which normally composes a large portion of the flowering population in the early stages of development. The temporal division of the seasonal population matrix (e.g. Transition List #4) allows transition matrices where the intermediate stages of flowering are dominant, albeit for a short period. This division can accurately reflect the temporally-distinct developmental pattern of grasses found in previous grass phenological studies (Cebrino et al., 2016; León-Ruiz et al., 2011) as well as the observed populations within the scope of this thesis (Chapter 5).

6.3.2. Grass Flowering and Pollen Release

Modelled grass pollen release rates of 70% of current pollen levels can accurately predict the atmospheric levels of *Dactylis glomerata* pollen released from entire flowering populations. This pattern is consistent between the two populations. Further increases or drops in pollen release rates (60 or 80 %) will result in decreases in accuracy compared to atmospheric pollen levels. The same applies to further differences (50 or 90 %). This illustrates that populations of tillers likely release pollen in a normally distributed rate, with around 70 % of current pollen amounts being the most common release rate. No other previous study has connected species-specific atmospheric pollen with detailed species-specific flowering dynamics. Previous studies have connected the overarching grass pollen seasonality with a wide range of flowering grasses to identify species likely causative of atmospheric grass pollen patterns (e.g. Ghitarrini et al., 2017; Rojo et al., 2017; Romero-Morte et al., 2018). Consequently, all above-mentioned studies concluded that *Dactylis glomerata* is likely to be a major contributor of the highest pollen peak during the grass pollen season. This conclusion has been based on many different correlative factors, such as pollen production, plant abundance, phenological development, life-history traits, and aerobiological modelling. One Spanish study showcased that the proportion of pollen shedding in *Dactylis glomerata* flowers coincides with the major seasonal peak in grass pollen concentrations, with the same pattern appearing consistently over three years (Tormo et al., 2011). Likewise, a previous study published in 2019 from the UK showcased using molecular eDNA approaches that *Dactylis glomerata* pollen quickly peaked in early June and then recedes down to background levels (Brennan et al., 2019). This is consistent with the findings of this study and likely caused by the quick potential for pollen release after anthesis has occurred (Heide, 1994; Khanduri, 2011). Anthesis and pollen release in grasses are predominantly

governed by local weather conditions (Emecz, 1962; Frenguelli, 1998), with solar radiation, air temperature and relative humidity being the most important factors (Liem, 1980; Liem and Groot, 1973). The correlations found between *Dactylis glomerata* eDNA and weather conditions confirms the positive importance of solar radiation and air temperature in the pollen release mechanism. It is uncertain if relative humidity would have been shown to be important too if the resolution of the eDNA sampling were higher, or alternatively there were longer time-series. This is a likely scenario due to the physiological importance of relative humidity in the context of anther desiccation (Keijzer, 1987a; Keijzer et al., 1987) and subsequently pollen release (Bhattacharya and Datta, 1992). Viner et al. (2010) showed that pollen release in maize can be predicted using solar radiation, air temperature, vapor pressure deficit (VPD) and the amount of remaining pollen within the anthers. They highlighted by using hourly-resolution models that pollen release happens almost instantaneously after anthesis, which confirms one of the pollen release model assumptions of no delay in anther dehiscence. Instantaneous pollen release mechanisms have also been found in other grasses (e.g. *Leymus chinensis* (Huang et al., 2004)). Other factors are also likely to play a role in the anther dehiscence, such as plant hormones (Wilson et al., 2011), which affect physiological changes to the pollen and anther (Keijzer, 1987b), but these transient factors are outside of the scope of this study.

6.3.3. Implications for Grass Pollen Allergy

The general connection between grass pollen seasons and grass pollen allergy is well established (Cebrino et al., 2017; D'Amato et al., 2007; García-Mozo, 2017), with the lynchpin likely being grass flowering phenology (Frenguelli et al., 2010). The results have showcased the direct connection between grass flowering and atmospheric grass pollen on a species-level in *Dactylis glomerata*. Allergens from *Dactylis glomerata* pollen have been isolated and described in detail in many different studies (e.g. Calam et al., 1983; Cauneau-Pigot and Peltre, 1991; Suphioglu and Mansur, 2000; Topping et al., 1978) with human allergies to these allergens being prominent issues (Aleksić et al., 2014; Toth et al., 1998; Van Ree et al., 1998; Yokouchi et al., 2002). The direct connection between species-specific grass flowering phenology and allergy has previously been investigated by Kmenta et al. (2016, 2017), in which they suggest highly significant positive effects between *Dactylis glomerata* flowering, non-specific atmospheric pollen concentrations and allergy symptom scores from grass pollen allergy sufferers. The connection showcased in this study confirms the findings of Kmenta *et al* (2016, 2017) and approaches the goals of genera-specific pollen research as specified in Menzels paper *The Allergen Riddle* (Menzel, 2019). Previous studies has suggested that the future of allergy prevention and aerobiological modelling is to combine classic aerobiological

methods with new biotechnological approaches (Devis et al., 2017; Ghitarrini et al., 2018; Leontidou et al., 2018; Longhi et al., 2009), which has been at the core of this study. However, a recent study estimated that the species-specific atmospheric abundance of *Dactylis glomerata* pollen did not have a significant effect on either asthma-related hospital emissions or the prescription rates of nasal allergy drugs and antihistamines (Rowney et al., 2021). The same study does state however that the finer details of these results were unlikely to have been captured due to the broad-scale sampling methodology. These findings and methodologies are predicted to be applicable to all types of grass species and populations to reveal direct connections between flowering and atmospheric grass pollen levels. This is likely to have fundamental applications in the modelling and forecasting of species-specific grass allergens.

6.4. Conclusion

The variation present in the demographic and stochastic distributions from observed populations could be accurately isolated using Markov Chain approaches. Markov Chain transition lists were used to create modelled general populations with high correlative similarity to the observed populations, with the same distribution of transition matrices being optimal for the populations at both main locations. All pollen release scenarios modelled from the fourth matrix transition list showed initial slow pollen release in May with seasonal peak in pollen release in the early June followed by a quick decline. The relative amount of *Dactylis glomerata* pollen isolated from the ITS1 and ITS2 regions showed that 70% pollen release rate of current pollen levels had the highest correlation. Further changes to the pollen release rate (70 to 60 to 50 %) or (70 to 80 to 90 %) showed decreases in accuracy in relation to the species-specific ITS-regions. This suggested that 70% were the most common pollen release rate but that the rate likely fluctuated. This is the first study to connect species-specific flowering to species-specific atmospheric grass pollen levels via pollen release modelling. The results and methodologies utilized in this study are likely to have fundamental applications to future research in understanding the connection between plant phenology, pollen release and atmospheric pollen concentrations. Understanding this connection is at the core of modelling and forecasting species-specific grass allergens in outdoor environments.

7. Local Scale Pollen Emission and Flowering Phenology in *Festuca rubra*

7.1. Introduction

Variations in micro-scale (< 2 km) atmospheric pollen have been understudied due to the complexity of accounting for all potential variables and factors involved. It is possible to account for and quantify some of this variation using a source-sink methodology on a species-specific level. The use of multiple pollen sampling stations along with confirmable sources, transportation pathways, confirmable sinks and meteorological factors influencing the system can comprehensibly identify the macro-scale workings of the atmospheric pollen release and dispersion process on a local scale. The sections below presents the local-scale grass pollen dynamics investigated in Lakeside 2019. Specifically, the general grass pollen dynamics are compared with a source-sink methodology focused on a local population of flowering *Festuca rubra* and the presence of species-specific grass pollen within each sampling location (processed using DNA metabarcoding of eDNA). Discussions surrounding local grass pollen distributions, the system-approach to and dynamics in grass pollen emission and meteorological factors likely causative of these patterns rounds off the chapter.

7.2. Results

7.2.1. Result Summary – Chapter 7

This chapter sought to explore variation in micro-scale local grass pollen concentrations and if this variation could be modelled using meteorology and wind conditions. It additionally sought out to explore if grass pollen emission processes in species-specific flowering grasses could be connected with collected eDNA to further investigate micro-scale variation. It was found that grass pollen concentrations show very high correlation over short distances (< 300m) but that differences could still be observed. Four meteorological variables were shown to have significant effects on local grass pollen concentrations: southerly wind-speeds, temperature, and solar radiation, with humidity having effects on two of the three sampled locations. A population of flowering *Festuca rubra* located within one of the sampling locations were shown to be able to disperse only small proportions of grass pollen to the other samplers located 300m away, while contributing major amounts of pollen to the within-located sampler.

7.2.2. Local Grass Pollen Variation

The bi-hourly grass pollen dynamics of the three different pollen sampling stations in Lakeside in 2019 (**Figure 51.**) can be viewed in Figure 52. A minor pre-peak of the season was observed in the Field sampler on the 23rd of May while being absent in the other samplers. The first major peak of the season was observed in the evening of the 1st of June in all three samplers. Minor

grass pollen peaks were observed between the 6th and 10th of June. The second major peak of the season was observed in the evening of the 15th of June in all three samplers. By including this second major peak and future observations within the overlapping season a total of 80% of all grass pollen within the overlap could be observed to have been collected within this period (results not shown). Only 20% of the grass pollen of the season were therefore collected before the second major peak. Several minor peaks were observed between the 16th of June and the evening of the 24th of June, when the third major peak of the season was observed. After this, three major peaks were observed on three consecutive days, 27th to the 29th of June. Three more major peaks were observed on three consecutive days, 3rd to 5th of July, with minor peaks preceding them. In total nine major peaks were observed in the bi-hourly grass pollen concentrations between the 15th of May and the 6th of July. The third of the first consecutive peaks (29th of June) were the highest grass pollen peak of the overlapping season while the second of the second consecutive peaks (4th of July) were the second highest grass pollen peak. The average differences between the three samplers showcase the dynamics in the bi-hourly grass pollen concentrations (**Figures 53 – 55.**). The daily grass pollen dynamics (**Supplementary Figure S52.**) and the average differences in the bi-hourly grass pollen in the previous 24h (**Supplementary Figures S53 – S55.**) can be found in the supplementary material. High correlations were found between all bi-hourly and daily grass pollen datasets between the three pollen samplers (**Table 14.**). The Pearson's product-moment correlation for the bi-hourly grass pollen datasets ranged from 0.864 to 0.914 ($p < 0.001$ x3). The Pearson's product-moment correlation for the daily grass pollen dataset ranged from 0.978 to 0.984 ($p < 0.001$ x3). Diurnal pollen concentrations profiles (**Supplementary Figure S56.**) can be found in the supplementary material. Grass pollen concentrations for all three locations were the lowest between 04:00 and 06:00 and the highest between 16:00 and 20:00.

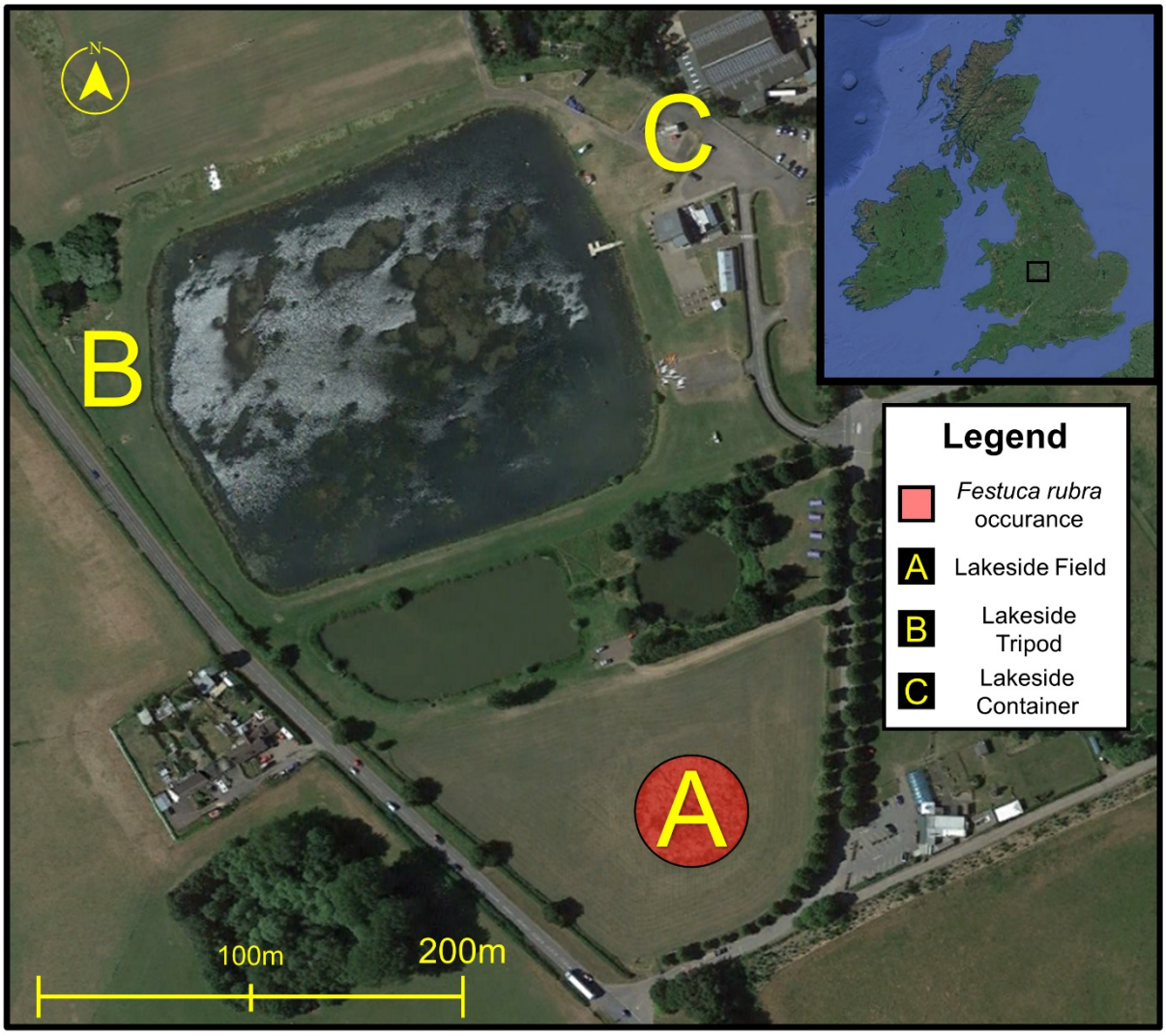

Figure 51. Local Lakeside map. The map illustrates the location of the three Lakeside grass pollen sampling locations (Field, TriPod, and Container) along with the occurrence of *Festuca rubra* in the Lakeside Field location.

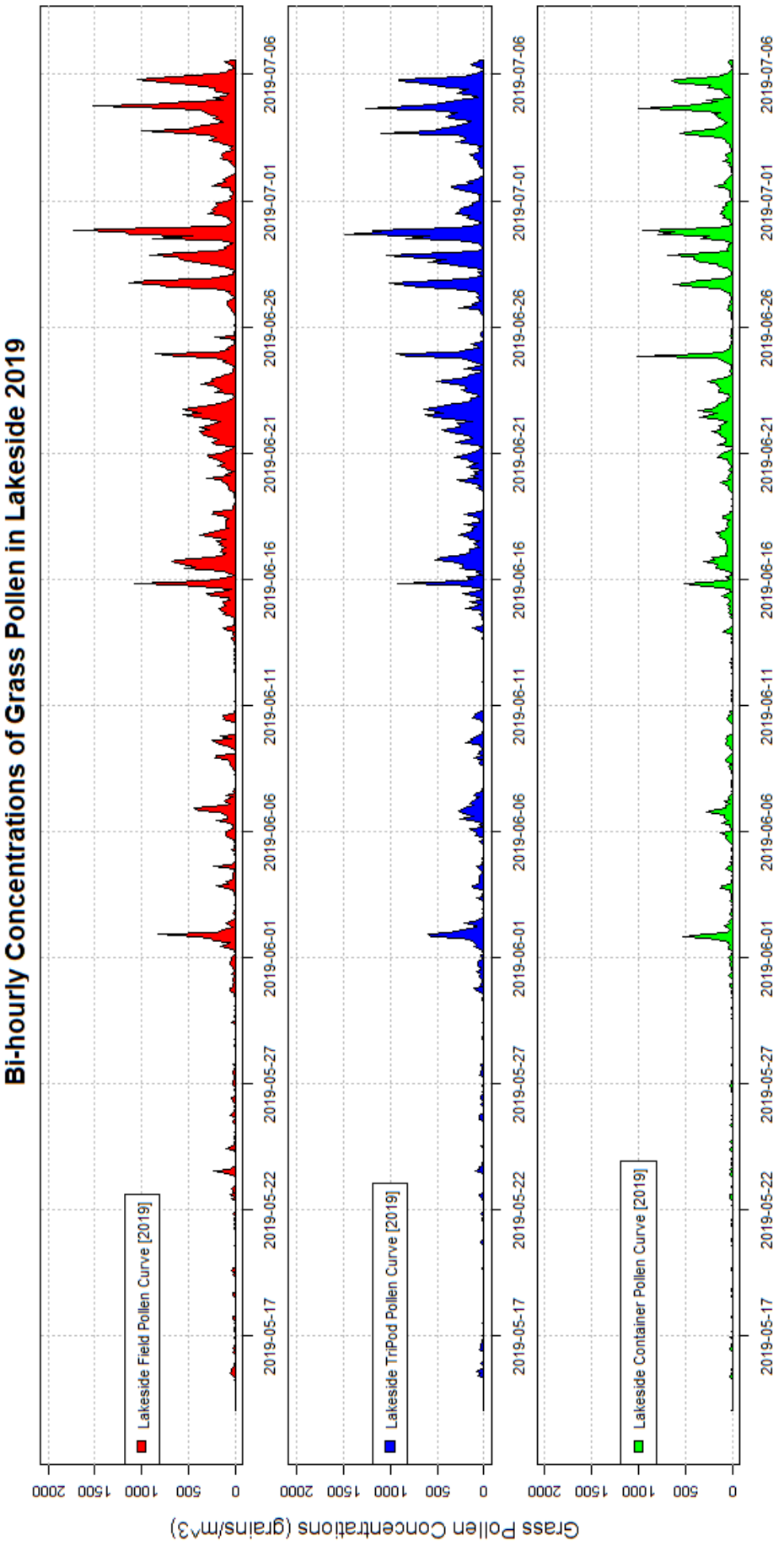

Figure 52. Bi-hourly concentrations of grass pollen from the three locations in Lakeside (Field, TriPod, and Container) during 2019 in Worcester. All datapoints are included between the 15th of May to the 6th of July 2019.

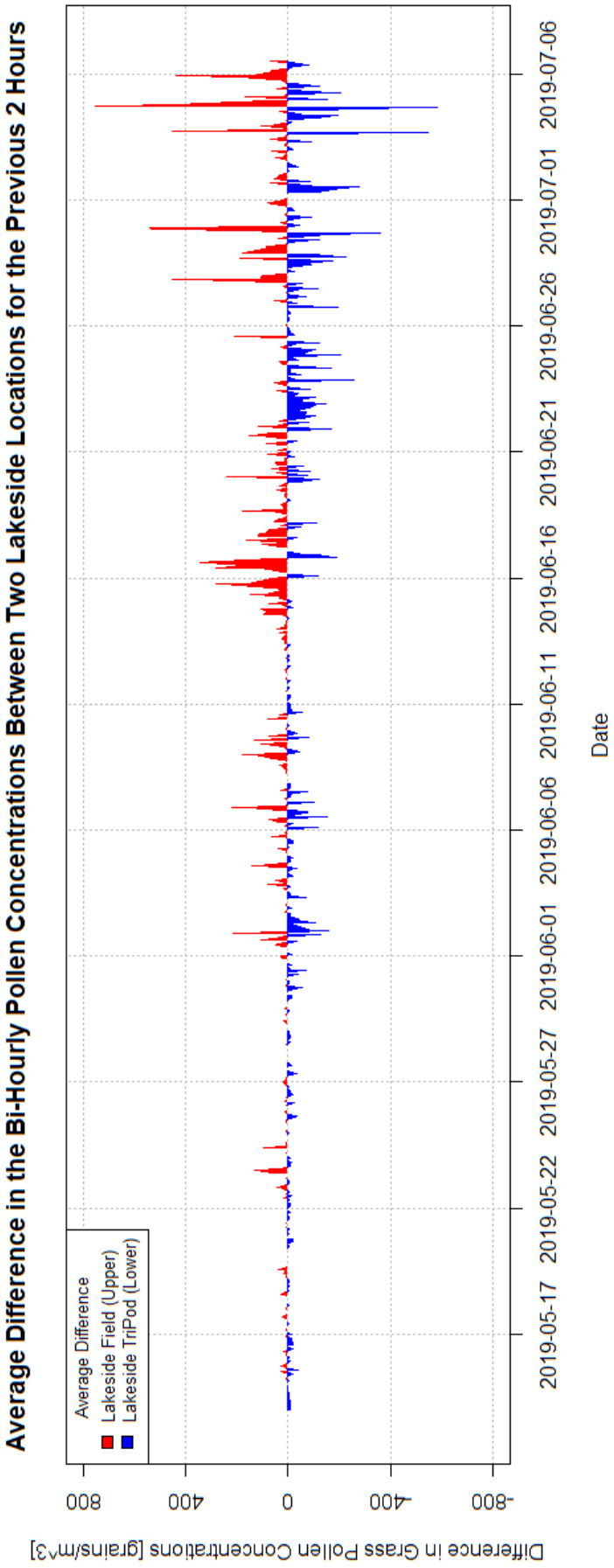

Figure 53. Difference in bi-hourly grass pollen concentrations from the past two hours between Lakeside Field and Lakeside TriPod during included season of 2019.

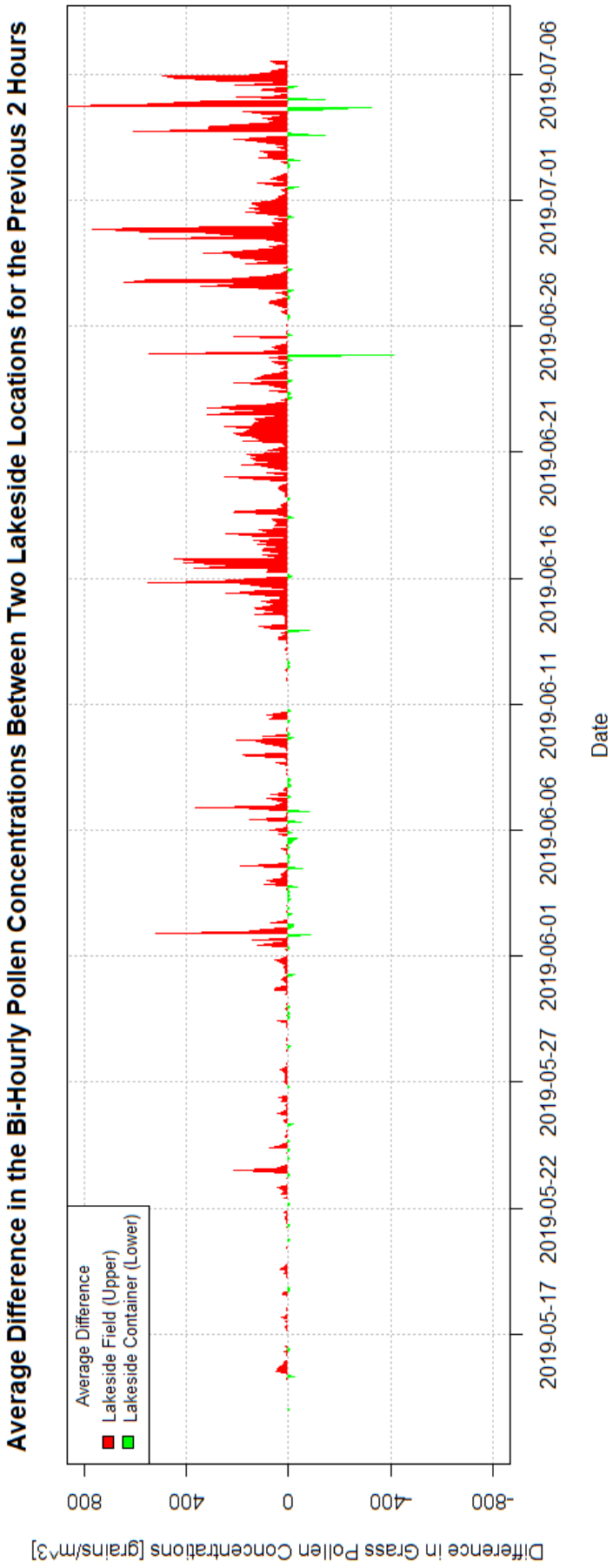

Figure 54. Difference in bi-hourly grass pollen concentrations from the past two hours between Lakeside Field and Lakeside Container during included season of 2019.

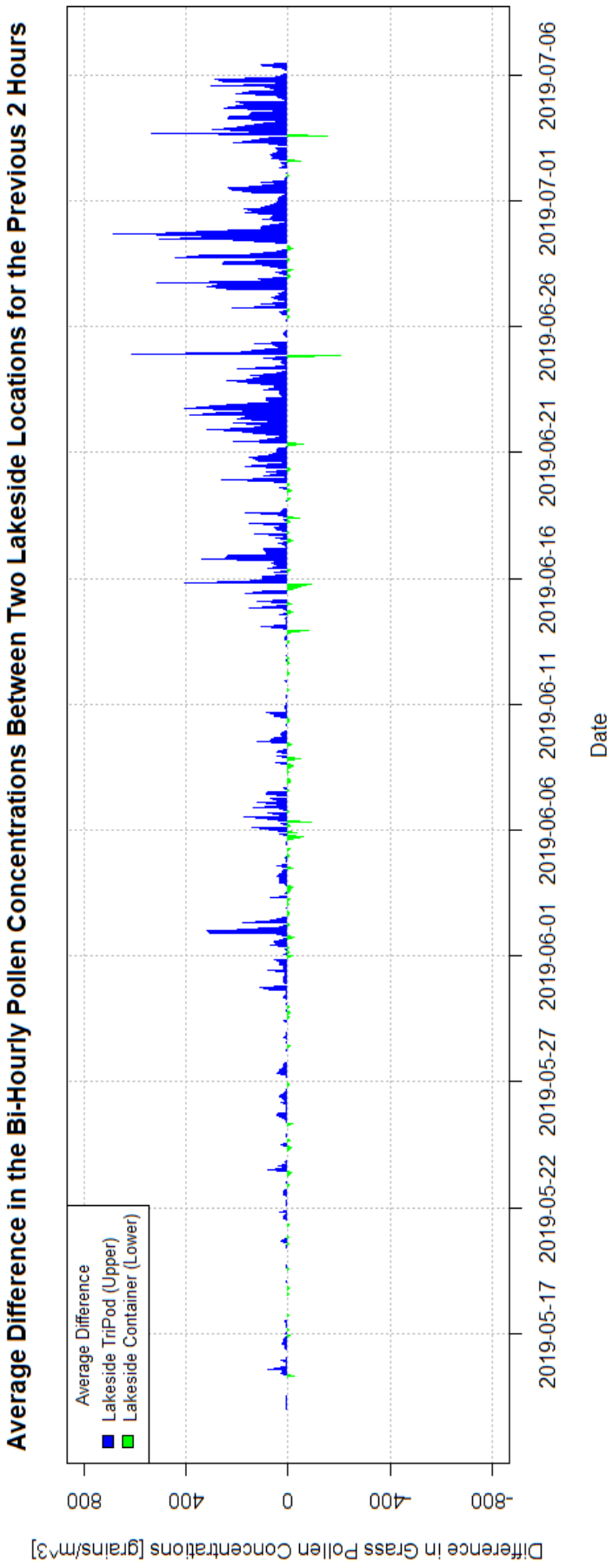

Figure 55. Difference in bi-hourly grass pollen concentrations from the past two hours between Lakeside TriPod and Lakeside Container during included season of 2019.

Table 14

Correlations in the pollen concentrations between the locations in Lakeside during the period May 15th to July 6th 2019. **Abbreviations: LS** - Lakeside.

Pollen Interval	Location 1	Location 2	Pearsons Product-Moment Correlation				
Concentration			t	df	cor	P - Value	Significance
Bi-Hourly	LS Field	LS TriPod	49.784	632	0.893	< 0.001	***
Bi-Hourly	LS Field	LS Container	43.06	632	0.864	< 0.001	***
Bi-Hourly	LS TriPod	LS Container	56.666	632	0.914	< 0.001	***
Daily	LS Field	LS TriPod	34.491	50	0.980	< 0.001	***
Daily	LS Field	LS Container	32.94	50	0.978	< 0.001	***
Daily	LS TriPod	LS Container	39.534	50	0.984	< 0.001	***

7.2.3. Local Meteorological Conditions

All included meteorological conditions and variables representing Lakeside were collected within the Lakeside Field circle from the Campbell meteorological mast. Temperature and precipitation of the 2019 Lakeside season can be found in Chapter 4. Wind direction, solar radiation and relative humidity showed a varied pattern throughout the season (**Figure 56.**). The wind direction originated from southernly directions (90 – 270 degrees) 48% of the time. The solar radiation was over 500 kJm^{-2} 32% of the time while being over 1000 kJm^{-2} 14% of the time. Additionally, solar radiation reached over 1500 kJm^{-2} 2% of the time. The relative humidity ranged between 42 – 98 % while being over 80 % relative humidity 44 % of the time. The three-directional wind speed recorded using the 3D anemometer varied in all three directions (**Figure 57.**). The X-axis (North or South) varied between 52% from the North (max 6.36 m/s) and 48% from the South (max 4.60 m/s). The Y-axis (West or East) varied between 34% from the West (max 3.74 m/s) and 66% from the East (max 5.59 m/s). The Z-axis (Up or Down) varied between 8% from Up/above (max 0.05 m/s) and 92% from Down/below (max 0.16 m/s). The minimum TKE was generally below 0.004 m^2s^{-2}, with 20 peaks above this level (**Figure 58.**). Three major minimum TKE peaks can be observed on the 8th, between the 10th – 11th and the 30th of June. The mean TKE was generally below 0.15 m^2s^{-2}, with 20 peaks above this level (**Figure 59.**). One major mean TKE peak can be observed between the 10th - 11th of June. The maximum TKE was generally below 3 m^2s^{-2}, with 15 peaks above this level (**Figure 60.**). One major maximum TKE peak can be observed between the 10th – 11th of June.

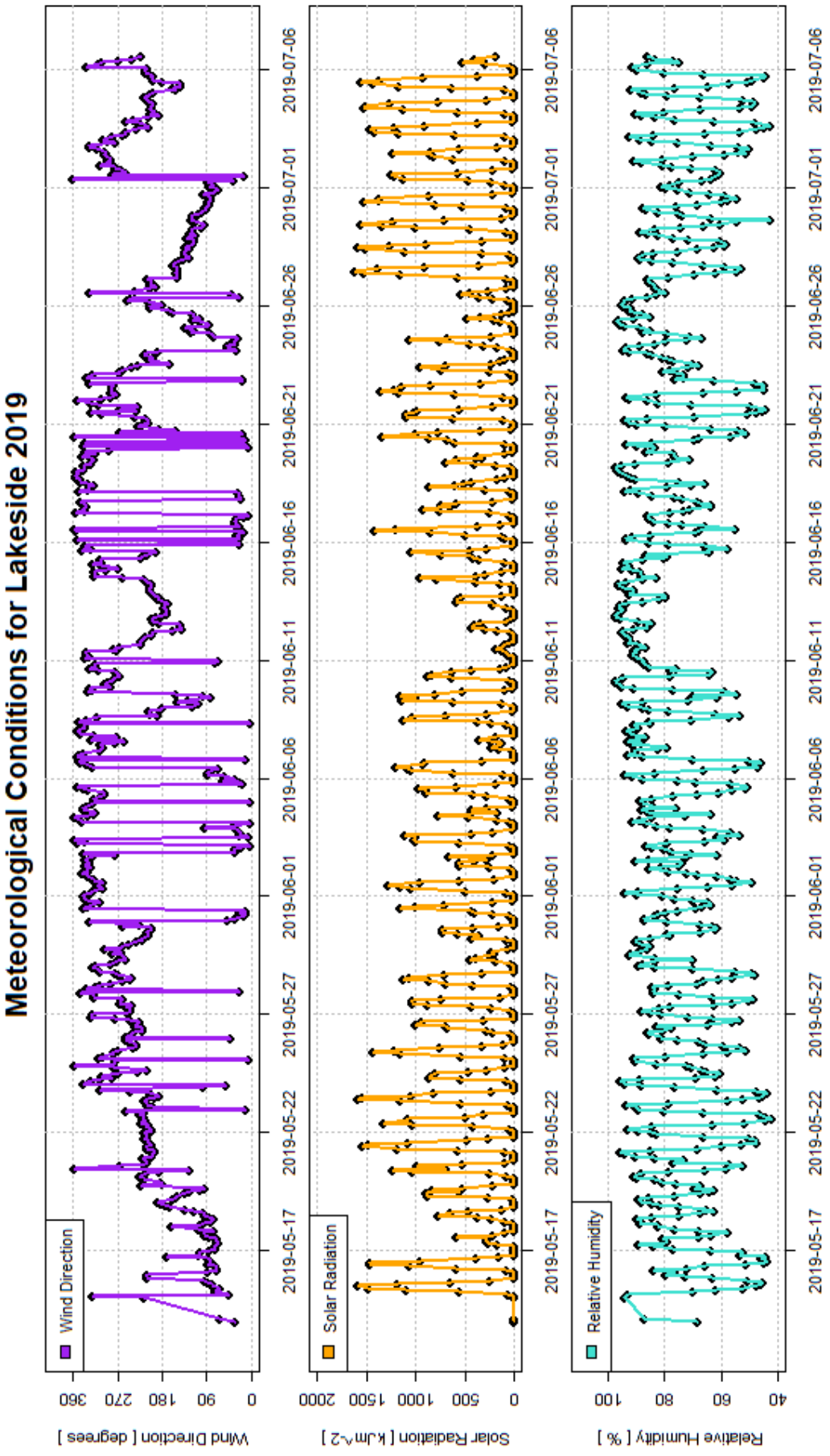

Figure 56. Variations in the meteorological variables Wind direction, Solar radiation, and Relative humidity during the included season of 2019 in Lakeside.

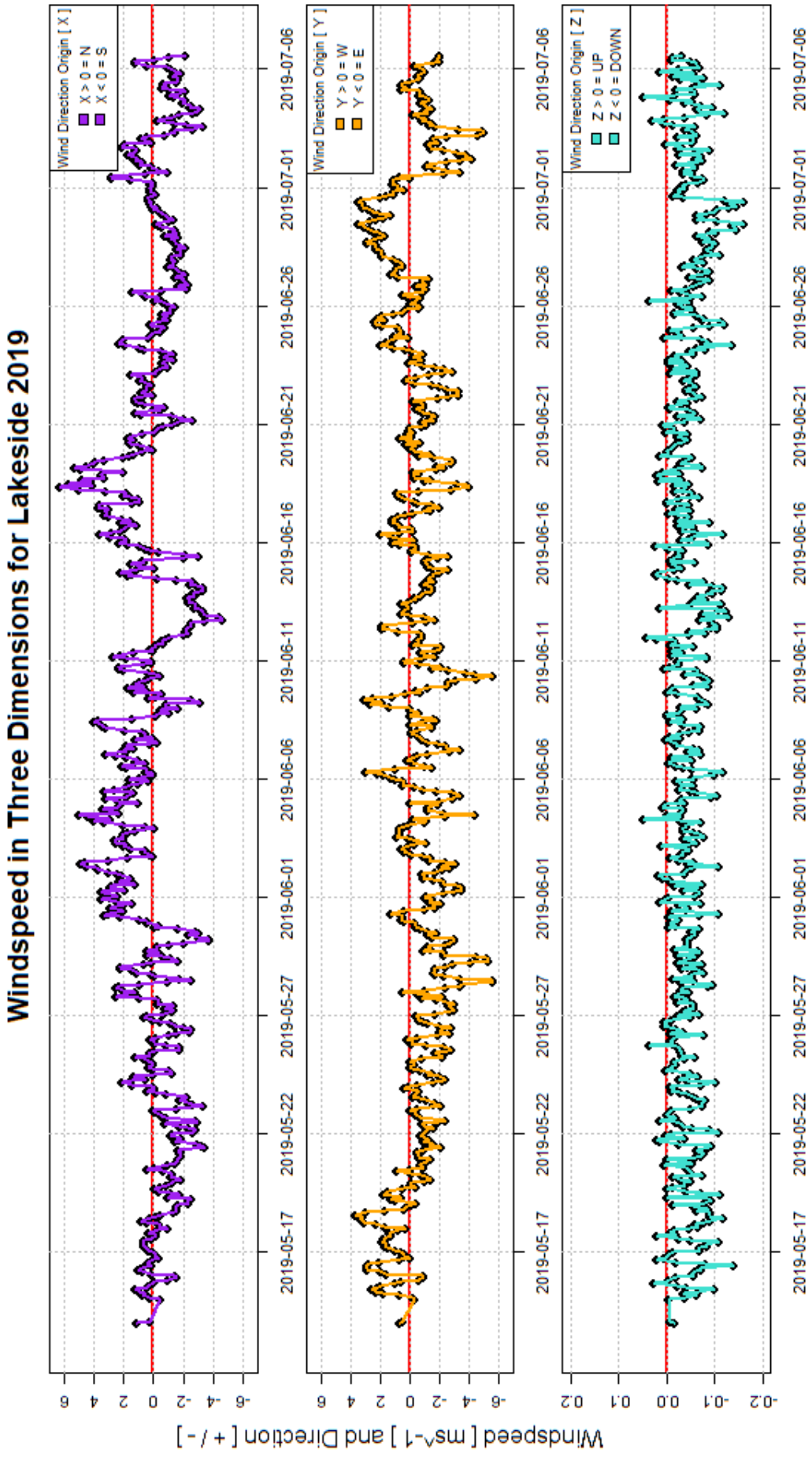

Figure 57. Variation in the wind speed variables X (North-South), Y (West-East) and Z (Up-Down) during the included season of 2019 in Lakeside.

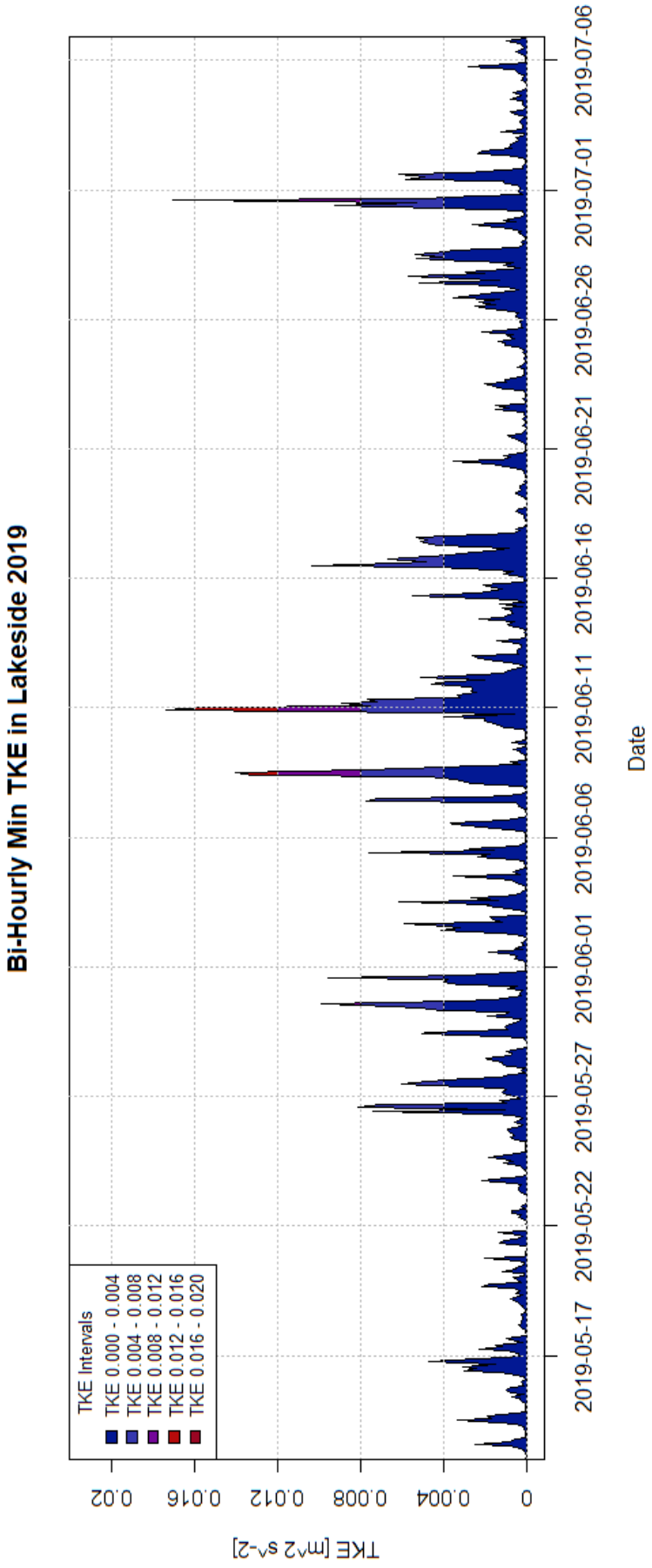

Figure 58. Variation in the minimum TKE during the included season of 2019 in Lakeside.

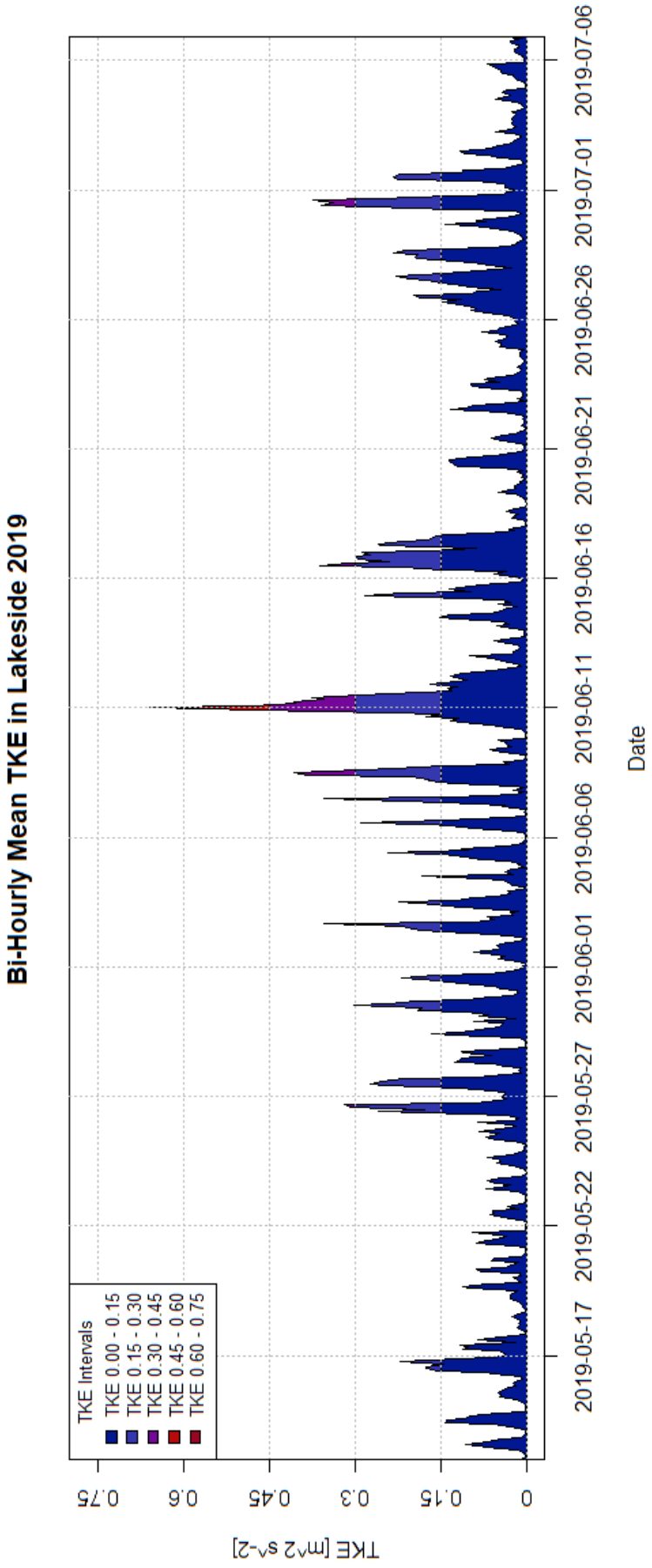

Figure 59. Variation in the mean TKE during the included season of 2019 in Lakeside.

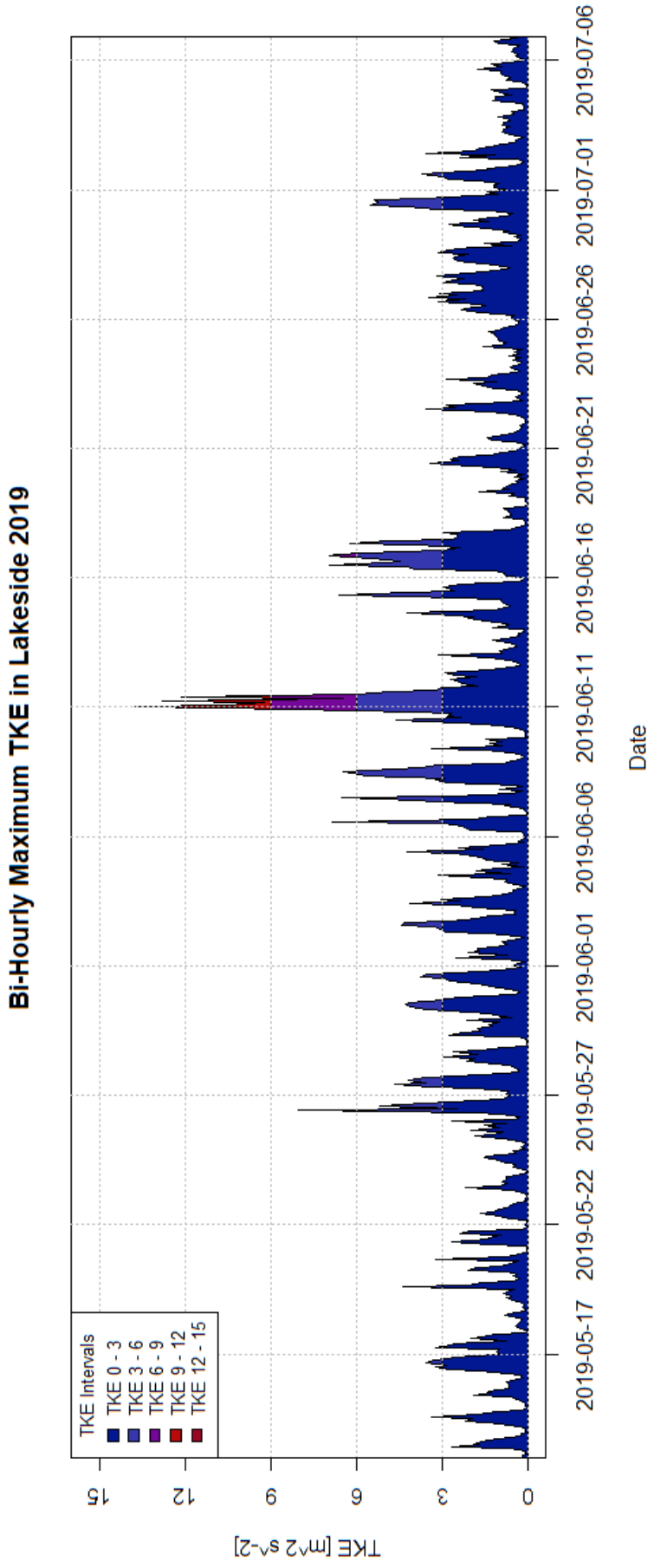

Figure 60. Variation in the maximum TKE during the included season of 2019 in Lakeside.

7.2.4. Local Grass Pollen Modelling

This section presents the results of the generalized linear modelling (GLM) approach. The response variable in this model is location-specific bi-hourly grass pollen concentrations. The predictor variables in this model are minimum, mean, and maximum TKE, windspeed in three directions (X, Y and Z), wind direction, solar radiation, temperature, relative humidity, and precipitation. Three models were created, one for each location, with the difference between these models being the location-specific bi-hourly grass pollen concentration dataset. The predictor variables remained the same for all three models due to the representability of the Campbell weather logger within the localized area. The total bi-hourly grass pollen concentration datasets (**Figure 52.**) have been filtered to account for bi-hourly pollen concentrations above 61.2 grains/m^3 (or 10 grains per bi-hourly microscopy transect). This created varying inclusion based on the location-specific dataset (**Figure 61.**). The model results are primarily expressed as estimates, t – values and p – values for each variable in the generalized linear regression. Diurnal pollen concentrations profiles of the filtered data (**Supplementary Figure S57.**) can be found in the supplementary material.

7.2.4.1. Lakeside Field GLM Results

The inclusion criteria included 240 bi-hourly grass pollen concentration datapoints for the Lakeside Field location (38% of total). The model statistics showed that the variables have differential effect on the bi-hourly grass pollen concentrations (**Table 15a.**). All three TKE variables had no significant effect on the bi-hourly grass pollen concentrations ($p = 0.927$ (NS), $p = 0.484$ (NS) & $p = 0.561$ (NS) respectively). Wind speed in the X-axis had a strong negative highly significant effect on the bi-hourly grass pollen concentrations ($p < 0.001$ (***)). However, the other two wind speed axes (Y-axis and Z-axis) had no significant effect ($p = 0.292$ (NS) & $p = 0.285$ (NS) respectively). Wind direction has no significant effect on the bi-hourly grass pollen concentrations ($p = 0.633$ (NS)). Solar radiation had a weak negative highly significant effect on the bi-hourly grass pollen concentrations ($p < 0.001$ (***)). Temperature had a strong positive highly significant effect on the bi-hourly grass pollen concentrations ($p < 0.001$ (***)). Relative humidity had a negative significant effect ($p < 0.05$ (*)) while precipitation had no significant effect on the bi-hourly grass pollen concentrations ($p = 0.745$ (NS)).

7.2.4.2. Lakeside TriPod GLM Results

The inclusion criteria included 251 bi-hourly grass pollen concentration datapoints for the Lakeside TriPod location (40% of total). The model statistics showed that the variables have differential effect on the bi-hourly grass pollen concentrations (**Table 15b.**). All three TKE variables had no significant effect on the bi-hourly grass pollen concentrations ($p = 0.682$ (NS), $p = 0.173$ (NS) & $p = 0.120$ (NS) respectively). Wind speed in the X-axis had a strong negative highly significant effect on the bi-hourly grass pollen concentrations ($p < 0.001$ (***)). However, the other two wind speed axes (Y-axis and Z-axis) had no significant effect ($p = 0.191$ (NS) & $p = 0.993$ (NS) respectively). Wind direction has no significant effect on the bi-hourly grass pollen concentrations ($p = 0.321$ (NS)). Solar radiation had a weak negative highly significant effect on the bi-hourly grass pollen concentrations ($p < 0.001$ (***)). Temperature had a strong positive highly significant effect on the bi-hourly grass pollen concentrations ($p < 0.001$ (***)). Relative humidity and precipitation had no significant effects on the bi-hourly grass pollen concentrations ($p = 0.102$ (NS) & $p = 0.430$ (NS) respectively).

7.2.4.3. Lakeside Container GLM Results

The inclusion criteria included 158 bi-hourly grass pollen concentration datapoints for the Lakeside Container location (25% of total). The model statistics showed that the variables have differential effect on the bi-hourly grass pollen concentrations (**Table 15c.**). All three TKE variables had no significant effect on the bi-hourly grass pollen concentrations ($p = 0.960$ (NS), $p = 0.357$ (NS) & $p = 0.255$ (NS) respectively). Wind speed in the X-axis had a strong negative highly significant effect on the bi-hourly grass pollen concentrations ($p < 0.01$ (**)). However, the other two wind speed axes (Y-axis and Z-axis) had no significant effect ($p = 0.661$ (NS) & $p = 0.427$ (NS) respectively). Wind direction has no significant effect on the bi-hourly grass pollen concentrations ($p = 0.274$ (NS)). Solar radiation had a weak negative highly significant effect on the bi-hourly grass pollen concentrations ($p < 0.001$ (***)). Temperature had a strong positive highly significant effect on the bi-hourly grass pollen concentrations ($p < 0.001$ (***)). Relative humidity had a negative significant effect ($p < 0.05$ (*)) while precipitation had no significant effect on the bi-hourly grass pollen concentrations ($p = 0.365$ (NS)).

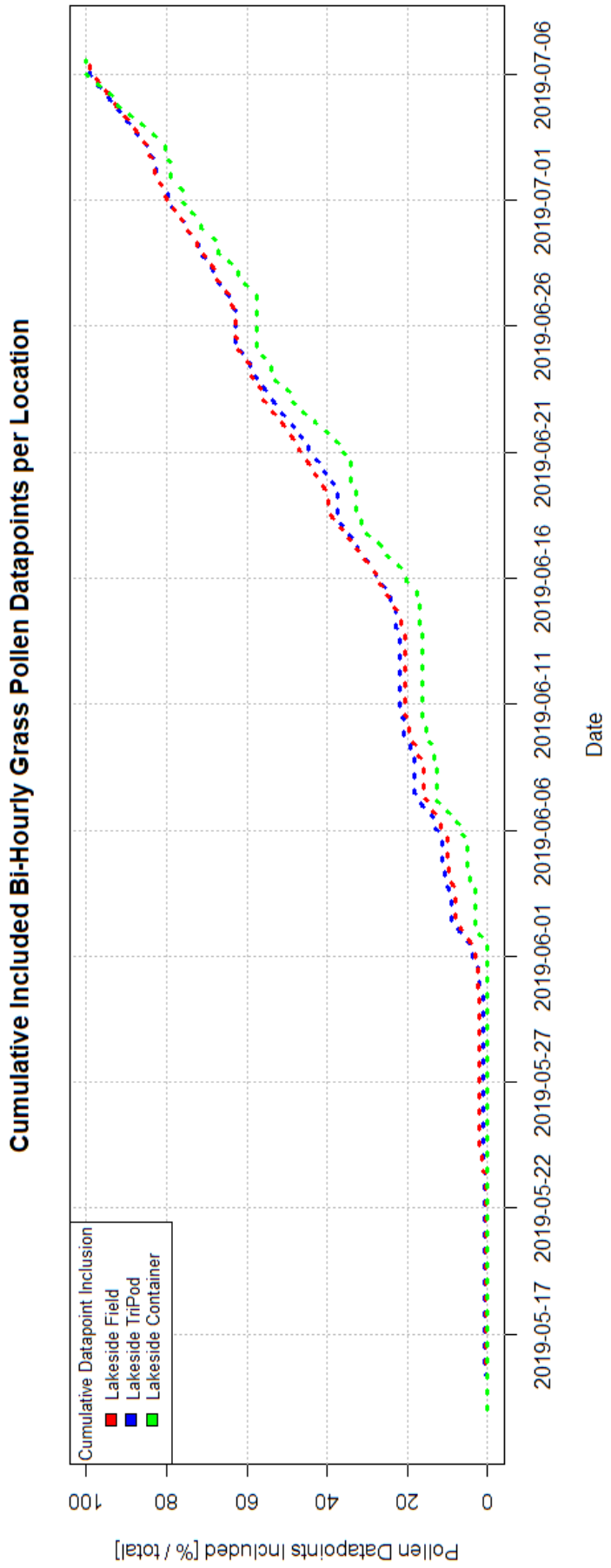

Figure 61. Cumulative inclusion of bi-hourly grass pollen concentration datapoints from the three locations in Lakeside (Field, TriPod, and Container) utilized in the Generalized Linear Model (GLM). Inclusion criteria is bi-hourly grass pollen concentration over 61.2 grains/m^3.

Table 15a

Model statistics and significance levels for the Generalized Linear Model (GLM) in regards to the Bi-hourly Grass Pollen concentrations for the sampler Lakeside Field. Only Grass Pollen concentrations over 61.2 grains/m^3 (10 grains per bi-hourly slide transect) are included in the analysis. **Abbreviations: TKE** - Turbulent Kinetic Energy, **O** - Wind Speed Origin, **N/A** - Not Applicable. **Data points included:** 240.

Sampler	Variables	Unit	Model Statistics				
			Estimate	Std. Error	t - value	P - value	Significance
Lakeside Field							
	Intecept	*N/A*	63.602	179.330	0.355	0.723	NS
	TKE Min	$m^2 s^{-2}$	1397.195	15170.070	0.092	0.927	NS
	TKE Mean	$m^2 s^{-2}$	435.434	620.860	0.701	0.484	NS
	TKE Max	$m^2 s^{-2}$	-14.421	24.771	-0.582	0.561	NS
North (+) / South (-)	Wind Speed (X,O) Mean	ms^{-1}	-27.918	7.979	-3.499	< 0.001	***
West (+) / East (-)	Wind Speed (Y,O) Mean	ms^{-1}	12.552	11.885	1.056	0.292	NS
Up (+) / Down (-)	Wind Speed (Z,O) Mean	ms^{-1}	508.808	475.061	1.071	0.285	NS
	Wind Direction Mean	*degress (0 - 359)*	0.084	0.176	0.478	0.633	NS
	Solar Radiation Mean	kJm^{-2}	-0.242	0.042	-5.739	< 0.001	***
	Temperature Mean	*°C*	34.108	4.909	6.948	< 0.001	***
	Relative Humdity Mean	*%*	-3.425	1.620	-2.115	< 0.05	*
	Precipitation Sum	*mm*	6.327	19.442	0.325	0.745	NS

Table 15b

Model statistics and significance levels for the Generalized Linear Model (GLM) in regards to the Bi-hourly Grass Pollen concentrations for the sampler Lakeside TriPod. Only Grass Pollen concentrations over 61.2 grains/m^3 (10 grains per bi-hourly slide transect) are included in the analysis. **Abbreviations: TKE** - Turbulent Kinetic Energy, **O** - Wind Speed Origin, **N/A** - Not Applicable. **Data points included:** 251.

Sampler	Variables	Unit	Model Statistics				
			Estimate	Std. Error	t - value	P - value	Significance
Lakeside TriPod							
	Intecept	*N/A*	-56.516	169.808	-0.333	0.740	NS
	TKE Min	$m^2 s^{-2}$	-5708.030	13922.851	-0.410	0.682	NS
	TKE Mean	$m^2 s^{-2}$	805.604	590.019	1.365	0.173	NS
	TKE Max	$m^2 s^{-2}$	-38.409	24.584	-1.562	0.120	NS
North (+) / South (-)	Wind Speed (X,O) Mean	ms^{-1}	-27.533	7.674	-3.588	< 0.001	***
West (+) / East (-)	Wind Speed (Y,O) Mean	ms^{-1}	14.617	11.134	1.313	0.191	NS
Up (+) / Down (-)	Wind Speed (Z,O) Mean	ms^{-1}	3.692	435.855	0.008	0.993	NS
	Wind Direction Mean	*degress (0 - 359)*	0.157	0.158	0.994	0.321	NS
	Solar Radiation Mean	kJm^{-2}	-0.193	0.040	-4.875	< 0.001	***
	Temperature Mean	*°C*	34.856	4.439	7.852	< 0.001	***
	Relative Humdity Mean	*%*	-2.541	1.548	-1.641	0.102	NS
	Precipitation Sum	*mm*	-12.293	15.556	-0.790	0.430	NS

Table 15c

Model statistics and significance levels for the Generalized Linear Model (GLM) in regards to the Bi-hourly Grass Pollen concentrations for the sampler Lakeside Container. Only Grass Pollen concentrations over 61.2 grains/m^3 (10 grains per bi-hourly slide transect) are included in the analysis. **Abbreviations: TKE** - Turbulent Kinetic Energy, **O** - Wind Speed Origin, **N/A** - Not Applicable. **Data points included:** 158.

Sampler	Variables	Unit	Model Statistics				
			Estimate	Std. Error	t - value	P - value	Significance
Lakeside Container							
	Intecept	*N/A*	18.253	155.529	0.117	0.907	NS
	TKE Min	$m^2 s^{-2}$	577.614	11480.589	0.050	0.960	NS
	TKE Mean	$m^2 s^{-2}$	461.165	499.194	0.924	0.357	NS
	TKE Max	$m^2 s^{-2}$	-23.424	20.518	-1.142	0.255	NS
North (+) / South (-)	Wind Speed (X,O) Mean	ms^{-1}	-25.420	7.773	-3.270	< 0.01	**
West (+) / East (-)	Wind Speed (Y,O) Mean	ms^{-1}	4.431	10.090	0.439	0.661	NS
Up (+) / Down (-)	Wind Speed (Z,O) Mean	ms^{-1}	-346.158	434.519	-0.797	0.427	NS
	Wind Direction Mean	*degress (0 - 359)*	0.161	0.147	1.097	0.274	NS
	Solar Radiation Mean	kJm^{-2}	-0.197	0.037	-5.360	< 0.001	***
	Temperature Mean	*°C*	25.812	4.089	6.312	< 0.001	***
	Relative Humdity Mean	*%*	-3.190	1.422	-2.244	< 0.05	*
	Precipitation Sum	*mm*	88.601	97.411	0.910	0.365	NS

7.2.5. Confirmable Source and Sink Dynamics

This section presents the results of the confirmable *Festuca rubra* pollen origin (source) from within the Lakeside Field circle and deposited species-specific eDNA (sink) in each of the pollen samplers within the three locations. No other specimens of *Festuca rubra* were found within the surroundings of Lakeside outside of the Lakeside Field circle. The density of *Festuca rubra* tillers within the circle ranged from 27 – 283 tillers/m^2 with an average of 143 tillers/m^2 (based on 10 1x1 m^2 sampling plots randomly scattered in the circle). The circle had a radius of 25m and an area of 1963.5 m^2.

7.2.5.1. Flowering Phenology in *Festuca rubra*

Phenological observations were conducted every third day starting on the 25th of May and ending on the 12th of July (**Figure 62.**). The first flowering of *Festuca rubra* within the circle started the 31st of May. The period between the 31st of May and the 15th of June was dominated by non-flowering tillers, with at most 10% of tillers showing any sign of flowering activity. On the 18th of June 20% of the tillers were observed in flowering, with two tillers being in full flowering (p4). Between the 18th and the 30th of June, the main flowering of *Festuca rubra* was observed, with up to 40% of the tillers in full flowering (p4) and an additional 24% in lower flowering phases (p1, p2 and p3). By the 30th of June no flowering tillers were observed from the random sampling strategy. During four subsequent visits no new tillers were observed to show any sign of flowering activity.

7.2.5.2. eDNA Bioinformatics Confirmation for *Festuca* Pollen

The eDNA bioinformatics results were compiled from equal parts of daily eDNA samples collected from each location from within the period of 24th of May to the 4th of July into three seasonal eDNA samples, one for each location. The results were then analysed through both ITS1 and ITS2 genomic regions using DNA metabarcoding. Two distinct *Festuca* species-profiles could be isolated: *Festuca rubra* and *Festuca sp.*. The relative abundance contribution of *Festuca* ITS1 eDNA included both species profiles (**Figure 63.**). Lakeside Container had 0.88 % *Festuca rubra* and 0 % *Festuca sp.*, Lakeside TriPod had 0.85 % *Festuca rubra* and 0.51 % *Festuca sp.* and Lakeside Field had 39.87% *Festuca rubra* and 8.21 % *Festuca sp.*. The relative abundance contribution of *Festuca* ITS2 eDNA included both species profiles (**Figure 64.**). Lakeside Container had 0.0 % *Festuca rubra* and 0.19 % *Festuca sp.*, Lakeside TriPod had 0.0 % *Festuca rubra* and 0.53 % *Festuca sp.* and Lakeside Field had 1.85% *Festuca rubra* and 0.88 % *Festuca sp.*.

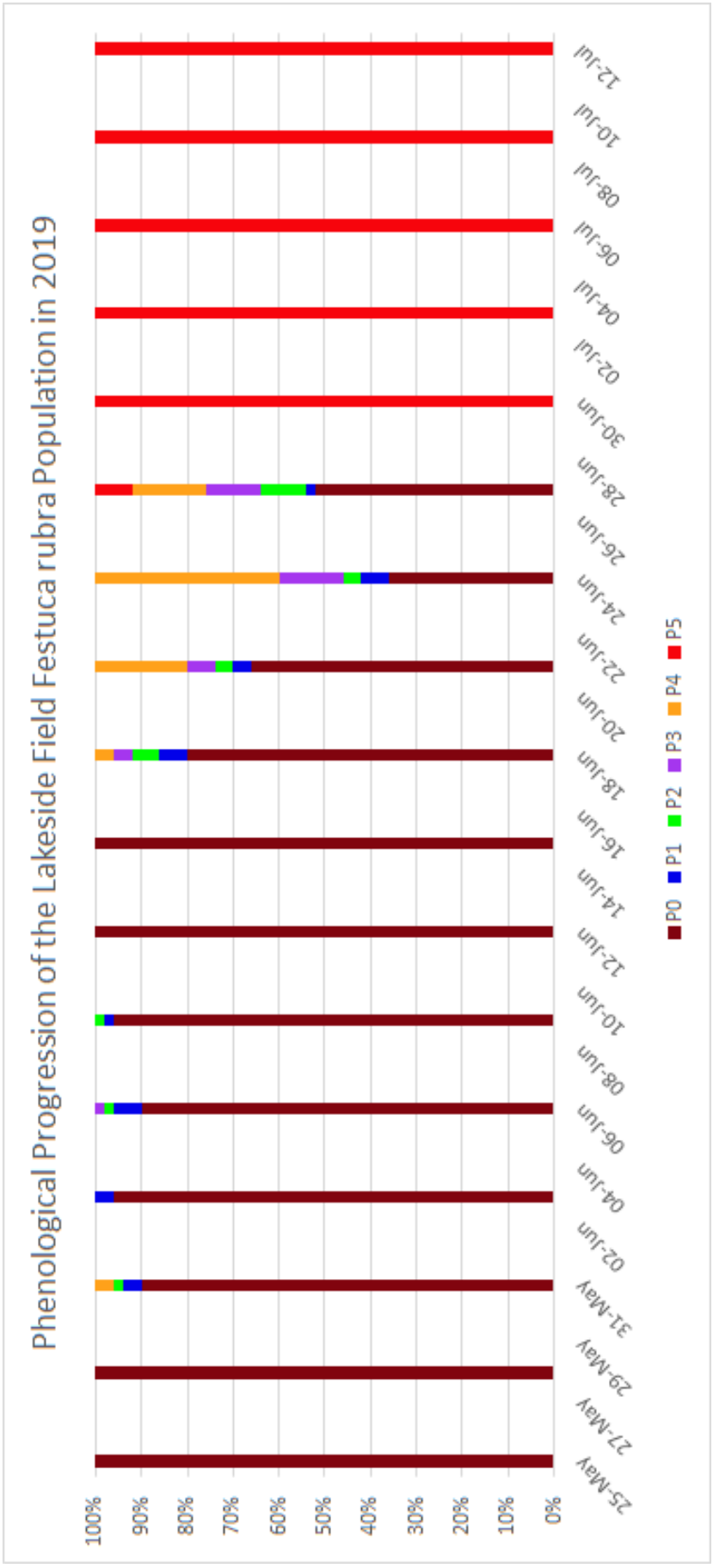

Figure 62. Phenological progression for the *Festuca rubra* population located in the Lakeside Field location circle.

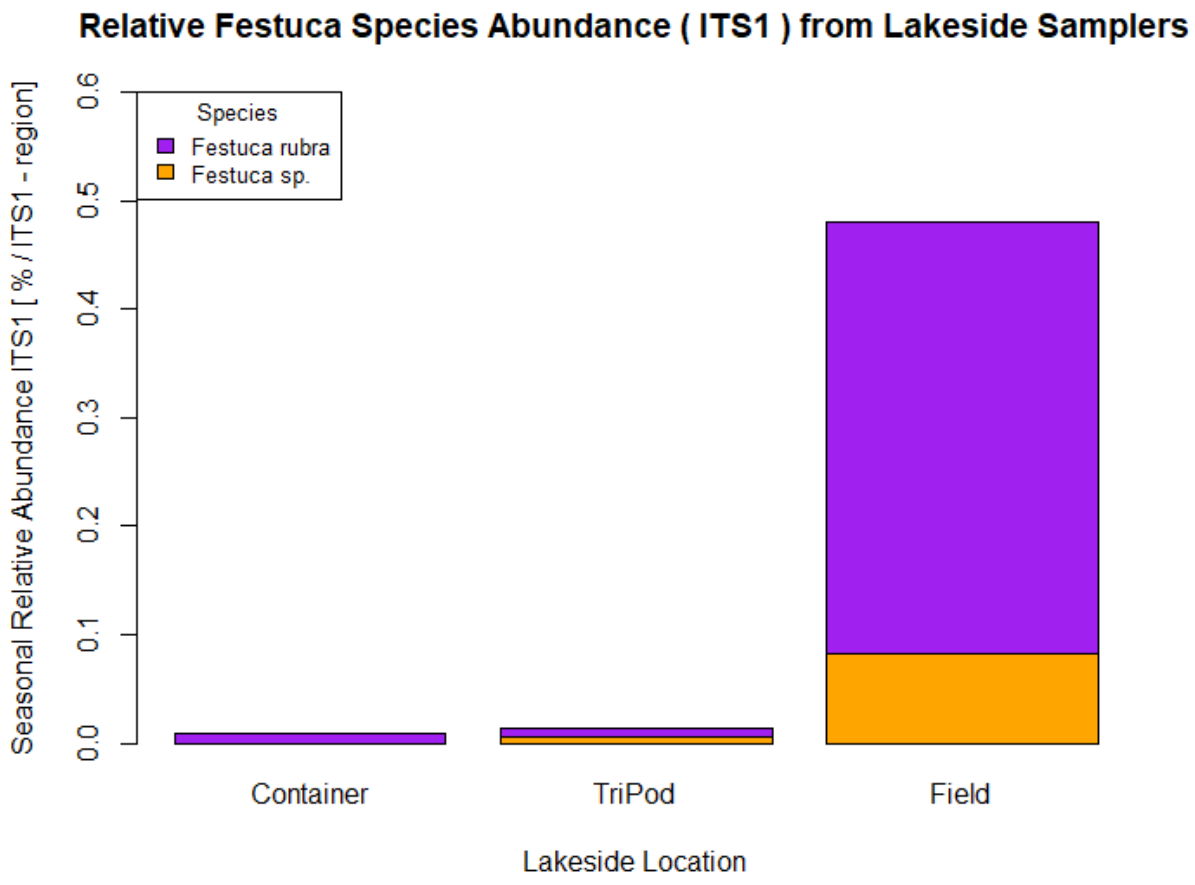

Figure 63. Relative abundance of *Festuca* species isolated from the ITS1-region and sampled from all three locations in Lakeside (Field, TriPod, and Container).

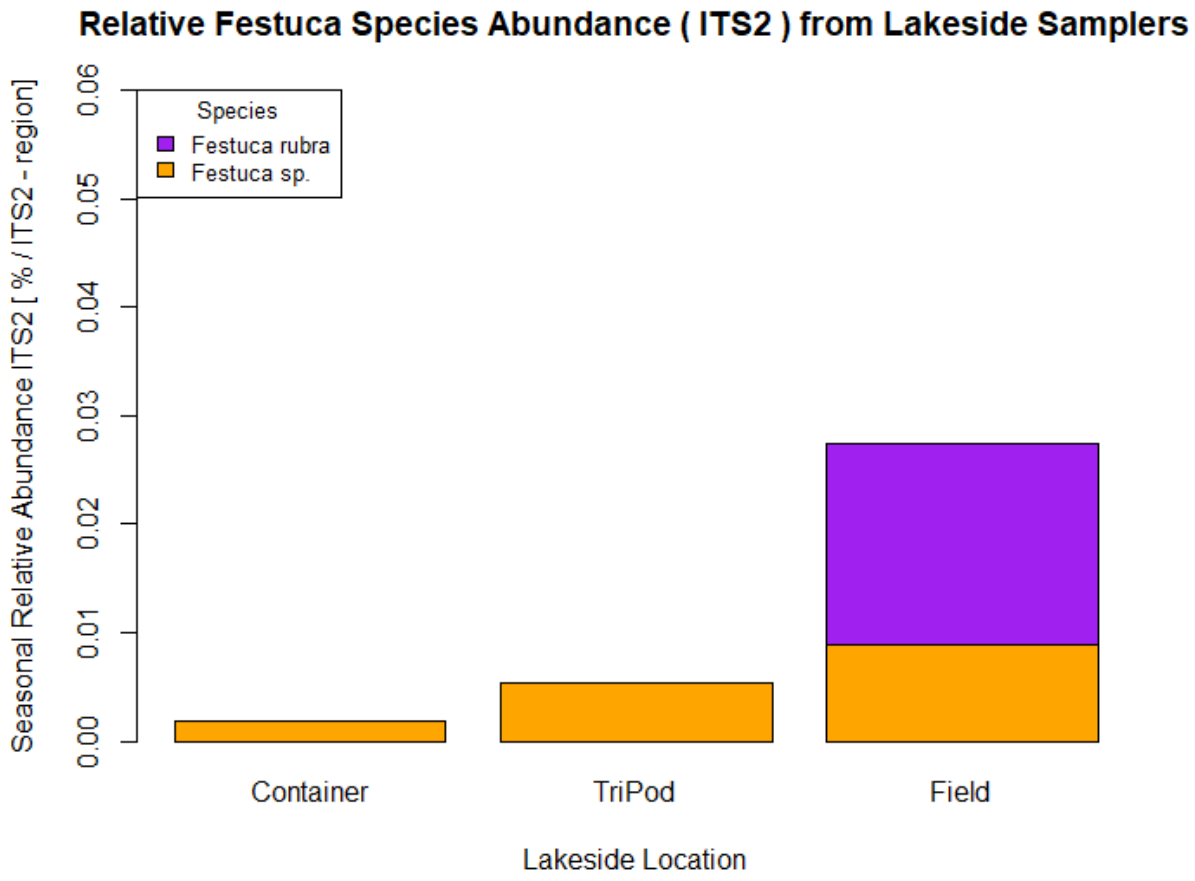

Figure 64. Relative abundance of *Festuca* species isolated from the ITS2-region and sampled from all three locations in Lakeside (Field, TriPod, and Container).

7.3. Discussion

This original research has shown that atmospheric grass pollen concentrations vary on a micro scale, within 300m, this has previously never been shown on such a localized scale. The blocking effect of surrounding vegetation is a possible cause of this effect. The dispersal distance of grasses are also causing this effect, with the only population of *Festuca rubra* contributing small proportions of pollen to locations 300m away. This provides conclusive evidence for the first time that flowering populations of grasses are likely to deposit most of their pollen within their immediate surroundings. These results provides essential data that can be used to model the pollen dispersal distance of other grass species likely to behave in a similar manner.

7.3.1. Local Grass Pollen Distributions

The three bi-hourly grass pollen timeseries highlight that there is a strong overlap in both frequency and amplitude for the entire season. The differential is more similar for the Lakeside Field and Tripod locations, but the correlation is higher for the Lakeside Field and Container locations. However, the average difference for the Lakeside Container location and the other two locations highlight that there are substantial differences in the grass pollen concentrations with a micro-scale rural area. Many previous studies have been conducted to explore the local variation of grass pollen concentrations within local areas (mostly cities) using multiple pollen monitoring stations and equipment (e.g. Arobba et al., 2000; Emberlin and Norris-Hill, 1991; Fernández-Rodríguez et al., 2014; Fornaciari et al., 1996; Katz and Batterman, 2020; Peel et al., 2014; Puc and Puc, 2004; Ríos et al., 2016; Simoleit et al., 2017; Skjøth et al., 2013; Werchan et al., 2017). All of these studies were conducted on a micro-alpha to meso-gamma scale (1 - 20 km) (Orlanski, 1975) with high correlations between monitoring sites but nonetheless big differences in the overall pattern and grass pollen concentrations. With this in mind, at least two recent studies have suggested that more than one pollen monitoring station is needed to account for the differential in grass pollen concentrations on a localized-scale (Katz and Batterman, 2020; Werchan et al., 2017). The results confirms that grass pollen concentrations vary on a local level. However, the study is conducted on a micro-beta scale (< 1 km). This is the first study to have investigated variations in grass pollen concentrations on such a local scale. The results also suggests that grass pollen trends homogenize as scale decreases, as previously demonstrated by Maya Manzano et al. (2017). Common suggested factors from the above-mentioned studies for the spatial discrepancy within cities are heterogenous distributions of source areas, differential effects to weather conditions and other features caused by the urban landscape, such as differential pollen transportation pathways and the urban heat island effect. However, none of these factors are applicable here due to the near identical response to meteorological variables and the same grass pollen source areas. One of the possible explanations for the discrepancies on a local level are dispersion eddies and transportation blockades caused by surrounding topography and/or vegetation, as previously suggested to be a leading cause of local differences in pollen levels (Auer et al., 2016; Boudreault et al., 2017; Emberlin and Norris-Hill, 1991; Viner et al., 2017). This has also been suggested to be the cause of the street-roof pollen differential in cities (Hugg et al., 2020; Peel et al., 2014). However, this is uncertain without an in-depth investigation. Another possible explanation for the discrepancy is the dispersal distance from the pollen sources themselves.

7.3.2. Grass Pollen Dispersal Dynamics

The main flowering of *Festuca rubra* within the circle of the Lakeside Field location were from June 18th to June 30th. It is likely that most of the *Festuca rubra* collected in the three samplers were released during this timeframe. This is the same timeframe as the majority of the grass pollen collected in all three samplers. However, the relative proportion of *Festuca rubra* pollen found in the Lakeside Field location was many times higher than within the other two locations, which means that only a small fraction of the *Festuca rubra* pollen was able to travel more than 300m within a flat landscape. The *Festuca rubra* pollen in the Lakeside Field sampler corresponded to almost 40% of the relative contribution to the grass pollen seasonal load (up until that point on July 4th), which means that the grass vegetation surrounding the sampler (within 25m, height 2.5m) will contribute significantly to the catch of the pollen sampler. This measure does not include the other grasses present in the circle to a major degree (*Lolium perenne*) and to a lesser degree (*Poa trivialis* and *Poa annua*). The *Festuca sp.* pollen could be *Festuca rubra* pollen that has been misclassified, but could also be another species that we have missed and that the bioinformatics did not recognize. Previous studies have suggested that the pollen frequency of *Festuca* species show a sharp decline from around 100 meters from the source area (Jones and Newell, 1946; Nurminiemi et al., 1998; Rognli et al., 2000). However, under the right conditions grass pollen can travel further (> 1 km) from a specific donor population to a specific recipient population (Giddings, 2000). This corresponds with the result findings, in which only small fractions of *Festuca rubra* pollen were found 300m from the source site. Parameters involved in the general pollen dispersal distance include plant height, settling velocity, wind speed, turbulence and morphological adaptations for dispersal (Okubo and Levin, 1989; Sjögren et al., 2015). However, for grasses the plant height, settling velocity and morphological adaptations for dispersal are generally the same (special case for cereal pollen, see e.g. Jarosz et al. (2003) for Maize pollen), leaving wind speed and turbulence as the two main factors. Flowering time and pollen trap positioning has been shown to not be adequate for describing grass pollen dispersal distance (Giddings et al., 1997a); neither was the addition of wind direction and turbulence (Giddings et al., 1997b). This agrees with the study results, in which turbulence and wind direction in the Lakeside Field does not influence grass pollen dispersal. However, this might be due to the turbulence measures being measured at 10m, while previous studies have connected the turbulence just above a ragweed canopy (2.5m) with source emission processes (Šikoparija et al., 2018). Meanwhile, windspeed from the south had a highly significant positive effect, suggesting that more of the grass pollen within all three samplers corresponded with stronger southernly winds. This also suggests how *Festuca rubra* pollen was able to disperse to the other two samplers during these high windspeeds from the south, due to

them being located north of the Lakeside Field in addition to the timing corresponding to the main flowering season. The effects of windspeed in previous studies have been mixed, with some studies suggesting that increase in windspeed does not affect grass pollen dispersal above a basic level (Viner et al., 2010) or atmospheric transport in grass pollen (Damialis et al., 2005) in any significant way. Other studies suggest that increase in wind speed does have a positive effect on grass pollen dispersal (van Hout et al., 2008) and on grass pollen concentrations (Emberlin and Norris-Hill, 1996; İnceoğlu et al., 1994; Puc and Puc, 2004). Additionally, wind speed is frequently included in the modelling of grass pollen atmospheric transport (e.g. Cresswell et al., 2010; Khwarahm et al., 2014; Voukantsis et al., 2010), which highlights its implicit importance for grass pollen movement within the landscape. The investigation into *Lolium perenne* from the circle was not included in the result and analysis due to uncertain species classification during the bioinformatics process, yielding exotic species that could not have been present and classifications to genus levels. This type of taxonomical uncertainty can happen due to natural species variation and incomplete taxonomical reference databases (Somervuo et al., 2017). Future research is needed to improve the ITS1- and ITS2-specific taxonomical databases used in the bioinformatics process to improve species classification for the genus *Lolium*.

7.3.3. Meteorological influence on Local Grass Pollen Concentrations

The same meteorological variables were important in the modelling of bi-hourly grass pollen concentrations for the datasets of all three local pollen samplers. Temperature had a strong positive effect; solar radiation had a weak negative effect and relative humidity had a negative effect (on two out of three datasets). The effects of these variables on the bi-hourly grass pollen concentrations can be fully understood through the temporal variation seen in these variables in relation to the diurnal patterns in pollen concentrations. The strong positive effect of temperature corresponds to the temporal variation pattern seen in the variable, with late-afternoon having higher temperatures, along with the higher temperatures seen during the latter part of the included season. Likewise, the weak negative effect of solar radiation corresponds to the lower solar intensity seen during the late-afternoon and evenings when pollen concentrations peak. The increase in solar radiation and temperature during the morning to mid-day brings decrease in relative humidity, with diurnal lows being during the peak of the pollen concentrations, likely causing anther desiccation and pollen release. This triad of meteorological variables are commonly connected together to investigate diurnal grass pollen trends (e.g. Peel et al., 2014; Toth et al., 2011; van Hout et al., 2008; Viner et al., 2010), with mixed results regarding the effects on grass pollen release. Previous studies have demonstrated

that *Festuca* species, and especially *Festuca rubra*, commonly release pollen during the late-afternoons to evenings (Hyde and Williams, 1945; Jones and Newell, 1946; Liem and Groot, 1973). This has previously been linked with low humidity, but not with temperature or solar radiation (Liem and Groot, 1973). The study results indicate that low humidity, but also temperature and solar radiation, plays a key role in the grass pollen emission of *Festuca rubra* due to the relative high abundance of pollen. One study has suggested that the *Festuca rubra* pollen is liberated from the anther during the morning due to the rise in temperature (Beddows, 1931). However, the results should be interpreted with caution, due to differential responses in flowering, and potential growth-requirements, having been reported between *Festuca rubra* subspecies and varieties (Cope and Gray, 2009; Heide, 1990; Hyde and Williams, 1945; Stace et al., 1992). Additionally, the uniformity of the effects of the meteorological variables on all sampling sites suggests that the variables affect the grass pollen emission of other grasses (outside of the *Festuca rubra* complex) in the Lakeside vicinity. This conclusion is reached based on the presence of other grass pollen in the Lakeside TriPod and Container grass pollen data-series, which also responds to the same meteorological effects.

7.4. Conclusion

Trends in the bi-hourly grass pollen concentrations in the micro-scale location Lakeside showed large overlap between pollen samplers. However, substantial differences could be identified between the samplers. One possible cause for these spatial discrepancies on such as localized scale could be the blocking of the vegetation and topography, which in turn could divert the aerial grass pollen and cause the observed concentration variations. The dispersal distance of local grass populations were also likely to impact these spatial discrepancies, with *Festuca rubra* pollen being demonstrated to only deposit small fractions 300m away from the source area. Local vegetation was determined to have a large effect on the pollen samplers, with at least 40% of the relative pollen load being identified to have originated from within 25m. Southernly windspeeds were important for the grass pollen in all three pollen samplers, suggesting that these winds and windspeeds brought much of the grass pollen to each samplers, in addition to the *Festuca rubra* pollen from the Lakeside Field. Temperature, solar radiation, and relative humidity were determined to be important in modelling grass pollen emission, specifically from *Festuca rubra* but also generally from other nearby grasses. The findings demonstrate that local vegetation and local wind conditions have large effects on the bi-hourly grass pollen time series in a micro-scale rural area. This holds true even if the overarching grass pollen trends within an area show high temporal and spatial similarity.

8. Summary and Final Conclusions

This chapter contains summarizing statements and information regarding each chapter. Additionally, conclusions regarding the totality of the knowledge gaps that these methods, results, and discussions have helped to fill will round off the chapter.

8.1. Summary

In Chapter 1 (Background) it was established that the connection between allergic rhinitis and pollen was discovered about 150 years ago by Charles Harrison Blackley. Overarching information regarding the dynamic relationship between grass pollen and the human immune-system was provided, with key focus on that not all grass pollen and grass allergens are the same. Grass pollen monitoring was presented as a tool to inform the research community, medical professionals, and the public alike for the patterns present in atmospheric grass pollen trends. Many factors have been identified as causative and transformative in regards to grass pollen trends, with the five overarching factors being meteorological, biological, physical, spatial, and temporal. There is great overlap between factors due to their impact on plant growth patterns, pollen emission patterns and pollen deposition patterns. The origin of grass pollen, grass phenology, was explored, with key focus on the flowering phenology, the definitive cause of all atmospheric grass pollen. Molecular approaches were explored as a viable way of identifying species-specific pollen, information otherwise inaccessible through microscopy techniques alone.

In Chapter 2 (Rationale) it was established that several overlapping fields of general knowledge gaps could be identified from the background. The project focus was presented as being the connection between grass pollen dynamics and flowering phenology. Eleven key studies were summarized to showcase the knowns and unknowns of the focus area, with overarching methodologies surrounding the community structure of contributory grass species. Furthermore, from these studies four specific knowledge gaps could be isolated, each addressing a specific gap that will need to be resolved in order to understand the overall connection between grass pollen dynamics and flowering phenology. These gaps were the use a taxonomically-limited grass pollen morphology, a lack of reasoning and mechanism for the connection, the use of a multitude of species with associated residual variation and the assumption that grass species function monolithically. Lastly, aims of the project along with objectives that could aid in the closing of these knowledge gaps were presented.

In Chapter 3 (Methods) it was established that many types of methodological approaches could be utilized to explore dynamics relating to the atmospheric grass pollen trends. The main one

was pollen monitoring methods, with associated pollen sampling technology and pollen counting strategies. The locations utilized for pollen sampling was also presented. Methodologies relating to phenological observations of flowering grasses were presented, with key focus on strategies of identifying the flowering processes within entire grass populations. Details regarding each specific population and species approaches were also provided along with information pertaining to the managed field circle created in Lakeside. Atmospheric modelling of grass pollen using regional transport modelling through HYSPLIT and grass source maps were presented along with detailed procedural approaches of how to create these using ArcGIS. Molecular approaches using eDNA and molecular methods were also explored, these were collected using Multivial Cyclone samplers, processed using DNA extraction methods and quantified using DNA metabarcoding techniques and bioinformatics. Markov Chain modelling approaches was used to identify demographic and stochastic elements in flowering grass populations, along with to model pollen release scenarios. Collection and processing of meteorological information was also presented. At last, a wide range of statistical methods and approaches were detailed to provide stable and reliable conclusions regarding the observed and modelled data.

In Chapter 4 (Atmospheric Modelling) it was established that pollen monitoring revealed temporal differences in bi-hourly grass pollen trends during the course of four years (2016 – 2019) between urban (St Johns) and rural (Lakeside) areas located six km apart. The regional differences were present both in the STL decomposition data and SPIn data, even though highly significant correlations were present. Atmospheric transport of the bi-hourly grass pollen concentrations for the years 2018 and 2019 were modelled using HYSPLIT to identify how the pollen were likely transported to the two locations. Additionally, likely grass pollen source areas were identified using the CEH Land Cover Plus ®: Crop dataset and connected to the modelling results to identify where the grass pollen likely originated. Temperature and precipitation were compared between the locations, with highly significant positive correlations in both variables, along with a significantly higher temperature in the urban area compared to the rural area. GLMER models were developed to model which variables that could predict the grass pollen concentrations for both locations, with three types of temporal variation being accounted for by the model. Local grass areas were important to predict the Lakeside grass pollen concentrations while regional grass areas were important to predict the St Johns concentrations. The models had R^2 values of 49.9 – 50.3 %. Both models were able to predict 74-79% of the bi-hourly grass pollen concentrations to within 30 grains/m^3, with only 7 – 10% having a predicted differential value over 90 grains/m^3.

In Chapter 5 (*Dactylis* Flowering) it was established that the phenological progression of flowering *Dactylis glomerata* populations overlapped both in time and in space. The developmental rate within the populations of each year showed strong similarity, with the date of general progression being only a few days apart at the most. Additional emphasis was put on the comparison between the average progression and phase-specific progression of each population. Here, key phenological events, such as beginning of flowering, full flowering and beginning of senescence remained consistent between populations. The main information gained from this is the absolute abundance of anthers possible of releasing pollen within each population and how this absolute abundance changed over the season based on the maturity of the population. Additionally, peak flowering was identified as the day with the maximum number of tillers in full flowering, which corresponds to the theoretically maximum pollen release potential. The main difference between the years was the senescence rate, likely attributed to differences in local meteorological conditions responsible for the drying process. Stochastic variation in the flowering progression was investigated using Markov Chain approaches. Tiller-specific transitions were investigated in the main populations, with some transitions being inherently more likely than others, which was identified through high correlations in the transition matrices. Tillers were more likely to stay in their occupied phases in 2017 while the opposite was true in 2018, where tillers were more likely to transition to full flowering.

In Chapter 6 (Pollen Release Modelling) it was established that lists of Markov Chain transitional matrices could be used to accurately model the observed *Dactylis glomerata* populations. Different combinations of transitional matrices were utilized to compare the most accurate combination. Twenty dynamic transitional matrices were able to model all six phases within the observed populations throughout the flowering development with a Kendall Rank correlation of 0.861 to 0.891. Ten pollen release scenarios were then modelled based on the aforementioned modelled flowering population, with a tiller-specific daily pollen release between 10 and 100%. The pollen release scenarios showed peak pollen release (between 2.5% and 32.6% of seasonal totals) for both populations between June 3rd and June 6th. Species-specific *Dactylis glomerata* pollen isolated from eDNA and processed through DNA metabarcoding was then compared with the pollen release estimates to find the most accurate release scenario. For St Johns alone 60 – 70 % pollen release per day had the highest significant correlation while for Lakeside alone 80 – 100 % pollen release per day had the highest significant correlation. The combination of both locations revealed that 70% pollen release per day had the highest significant correlation, with decreasing significant correlations on both

sides (80 – 90 – 100% and 60 – 50 – 40%). This showcased that flowering populations of *Dactylis glomerata* likely release pollen in a normally distributed rate, with 70% of current pollen being the most common release rate.

In Chapter 7 (*Festuca* Pollen Dispersion) it was established that three micro-beta scale (< 1 km) pollen monitoring stations show high correlations but nonetheless large differentials in bi-hourly grass pollen concentrations. The differential is possibly attributed to local dispersion eddies and transportation blockages caused by surrounding vegetation and topography. Another likely reason for the spatial discrepancy is the dispersal distance of local grass pollen sources. An isolated *Festuca rubra* population were demonstrated to contribute 46 times more pollen to the within-located Lakeside Field pollen sampler than to the other two pollen samplers, located within 300m away. The *Festuca rubra* pollen in these two samplers corresponded to less than 1% of the total amount. Meanwhile, 40% of the relative pollen contribution in the Field pollen sampler were from *Festuca rubra*, originating from within 25m. This number does not include other grasses found in the Lakeside Field circle, such as *Lolium perenne* or *Poa trivialis*. Wind direction and turbulence did not influence the grass pollen concentrations in any of the three pollen samplers. However, southerly windspeeds were highly significant, which explains how some of the *Festuca rubra* pollen was able to disperse to the other samplers located to the north. High temperatures, lower solar radiation and low humidity were also associated with high bi-hourly grass pollen collected in all three pollen samplers (except for humidity, only two out of three samplers).

8.2. Final Conclusions

The overall aims laid out in the beginning in this PhD project of investigating the mechanistic connection between atmospheric grass pollen and flowering grasses have revealed new understanding and many key pieces of information essential in closing several of the current gaps in knowledge present in the aerobiological discipline. New modelling approaches, both statistical, mechanistic, and molecular in nature have been fused with the sparse but nonetheless very relevant literature from the early-half of the last century to form a new set of approaches to investigate processes that until now have been largely unknown. This has only been possible due to the heavy emphasis on a cohesive multidisciplinary research ethos, in which botany, ecology, environmental science, atmospheric science and lab-based molecular biology has come together to fully encompass the problem-solving aspect of the unknown processes. The importance of local and regional grass pollen source areas have been explored with the focus on a defined differential in the response in rural and urban areas. Detailed demographic and stochastic elements in flowering *Dactylis glomerata* populations have been identified and showcased with a focus on the individual tillers contribution to a cohesive regional phenological progression rate. The stochastic modelling of *Dactylis glomerata* populations using Markov Chain approaches in combinations with DNA metabarcoding highlighted that pollen release can be modelled and confirmed by combining both phenology, modelling and molecular approaches. Finally, the use of a system-wide source-sink methodology was be used to investigate grass pollen emission differentials in a micro-scale rural area. These key findings will likely build new foundations for further research into the combinatory topics of grass pollen release, grass pollen dispersal and their respective connection to grass flowering phenology. If there would be any such thing as a main message, it would be this: Every new idea explored, every new piece of evidence discovered and every new connection made brings us closer to solving the conundrum that haunted Blackley and that still haunts us today one hundred-fifty years later.

9. Future Work

The new insights into the connection between the trends in atmospheric grass pollen and the flowering progression of grass species has contributed to closing several of the current gaps in knowledge present in the aerobiological discipline. These gaps have mainly been closed in relation to grass pollen release, grass pollen dispersal and detailed flowering phenology. However, this also contributed to the realization that further questions needs answering if general understanding and underlying causes of these processes are to be revealed. A main aspect to these questions is the understudied nature of pollen release and pollen dispersal within the field of aerobiology. Increased understanding about these processes will be essential in connecting what is observed in the landscape and what is observed in the atmosphere, without this understanding it can only be educated guesses and suggestions. Three main areas can be identified as being important for further progress in understanding:

I) The connection between flowering phenology and pollen release.

II) The connection between pollen release and pollen dispersal.

III) The connection between pollen dispersal and pollen transportation.

The main process of interest in the connection between flowering phenology and pollen release is the maturation of the freshly extruded anther, with special focus on how and what is causing the maturation process. If the maturation process can be characterized and accompanied factors responsible for this maturation and the subsequent pollen release from the anther, then this process can be mathematically modelled to predict grass pollen release within one anther. By combining this modelled process with population phenology it should be possible to model this process and behaviour for entire populations with certainty based on responsible factors. The upscaling of modelling should allow for many populations and even entire regions to be modelled with some measure of quantifiable certainty. If this can be adapted to many species then the total grass pollen release in entire regions can be quantified using measures of species occurrence, density measurements and detailed meteorological factors.

The main process of interest in the connection between pollen release and pollen dispersal is the distance-distribution of grass pollen from source areas, which factors that affects this distribution and how the distribution ranges between species. This has partially been accomplished for a select few species, which means that the methodologies should be able to be adapted to account for a wide-range of species and conditions. New advances in genomic and molecular research and the utilization of automatic pollen monitoring systems would allow for such studies to be conducted with increased ease. If the complete range of factors

responsible for the distance-distribution can be identified, then the process could be mathematically modelled using source-sink methodologies as confirmable data. Factors in need of further investigation in the dispersal process is windspeeds, turbulence, and how nearby features such as vegetation, buildings and topography affect the distance-distribution. Confirmable influences of settling velocity, release height and plant density will also likely be important for the understanding of the process.

The main process of interest in the connection between pollen dispersal and pollen transportation is mathematical applications of grass pollen dispersal in relation to landscape topography and atmospheric transportation factors. These applications could allow for local-scale grass pollen forecasts created using dispersal models that include high-resolution grass pollen source maps and detailed atmospheric transportation factors. Such applications would be able to benefit medical professionals and end-users alike to combat the grass pollen season. Even if such applications are currently unlikely due to the process-intensive aspect of creating personal local-scale grass pollen forecasts it is a prestigious end-goal. Instead, future research should investigate how the topography influence the movement of pollen through the landscape, with special focus on how rural and sub-urban grass pollen source areas affect urban centres. This would significantly contribute to the quantification of how atmospheric grass pollen is being transported from source to sink. Long-distance transport of grass pollen is also an area of key interest, primarily due to the out-of-season importance of grass pollen for the allergic priming-response. The creation of detailed dispersal models that can account for factors responsible for long-distance transport can be used to develop warning systems, similar to weather warning systems for cyclones/hurricanes or earthquake early warning systems.

References

Aalberse, R.C., 2000. Structural biology of allergens. J. Allergy Clin. Immunol. 106, 228–238. https://doi.org/10.1067/mai.2000.108434

Aboulaich, N., Bouziane, H., Kadiri, M., Del Mar Trigo, M., Riadi, H., Kazzaz, M., Merzouki, A., 2009. Pollen production in anemophilous species of the Poaceae family in Tetouan (NW Morocco). Aerobiologia (Bologna). 25, 27–38. https://doi.org/10.1007/s10453-008-9106-2

Abreu, I., Ribeiro, N., Ribeiro, H., Oliveira, M., Cruz, A., 2008. Airborne Poaceae pollen in Porto (Portugal) and allergenic profiles of several grass pollen types. Aerobiologia (Bologna). 24, 133–140. https://doi.org/10.1007/s10453-008-9093-3

Adams-Groom, B., Skjøth, C.A., Baker, M., Welch, T.E., 2017. Modelled and observed surface soil pollen deposition distance curves for isolated trees of Carpinus betulus, Cedrus atlantica, Juglans nigra and Platanus acerifolia. Aerobiologia (Bologna). 33, 407–416. https://doi.org/10.1007/s10453-017-9479-1

Adams-Groom, B., Skjøth, C.A., Selby, K., Pashley, C., Satchwell, J., Head, K., Ramsay, G., 2020. Regional calendars and seasonal statistics for the United Kingdom's main pollen allergens. Allergy Eur. J. Allergy Clin. Immunol. 75, 1492-1494. https://doi.org/10.1111/all.14168

Adier, P.B., Salguero-Gómez, R., Compagnoni, A., Hsu, J.S., Ray-Mukherjee, J., Mbeau-Ache, C., Franco, M., 2014. Functional traits explain variation in plant lifehistory strategies. Proc. Natl. Acad. Sci. U. S. A. 111, 740–745. https://doi.org/10.1073/pnas.1315179111

Aebersold, R., Mann, M., 2003. Mass spectrometry-based proteomics. Nature 422, 198–207. https://doi.org/10.1038/nature01511

Aguayo, J., Fourrier-Jeandel, C., Husson, C., Ioos, R., 2018. Assessment of Passive Traps Combined with High-Throughput Sequencing To Study Airborne Fungal Communities. Am. J. Microbiol. 84, 1–17. https://doi.org/10.1128/AEM.02637-17

Akdis, C.A., Agache, I., 2014. EAACI Global Atlas of Allergy. European Academy of Allergy and Clinical Immunology, Zürich.

Alan, Ş., Şahin, A.A., Sarışahin, T., Şahin, S., Kaplan, A., Pınar, N.M., 2018. The effect of geographical and climatic properties on grass pollen and Phl p 5 allergen release. Int. J. Biometeorol. 62, 1325–1337. https://doi.org/10.1007/s00484-018-1536-0

Alba-Sánchez, F., Sabariego-Ruiz, S., Díaz de la Guardia, C., Nieto-Lugilde, D., De Linares, C., 2010. Aerobiological behaviour of six anemophilous taxa in semi-arid environments of southern Europe (Almería, SE Spain). J. Arid Environ. 74, 1381–1391. https://doi.org/10.1016/j.jaridenv.2010.06.005

Aleksić, I., Vučković, O., Smiljanić, K., Jankulović, M.G., Krsmanović, V., Burazer, L., 2014. The importance of cross-reactivity in grass pollen allergy. Arch. Biol. Sci. 66, 1149–1155. https://doi.org/10.2298/ABS1403149A

Alexander, L. V., Zhang, X., Peterson, T.C., Caesar, J., Gleason, B., Klein Tank, A.M.G., Haylock, M., Collins, D., Trewin, B., Rahimzadeh, F., Tagipour, A., Rupa Kumar, K., Revadekar, J., Griffiths, G., Vincent, L., Stephenson, D.B., Burn, J., Aguilar, E., Brunet, M., Taylor, M., New, M., Zhai, P., Rusticucci, M., Vazquez-Aguirre, J.L., 2006. Global observed changes in daily climate extremes of temperature and precipitation. J. Geophys. Res. Atmos. 111, 1–22. https://doi.org/10.1029/2005JD006290

Andersson, K., Lidholm, J., 2003. Characteristics and immunobiology of grass pollen allergens. Int. Arch. Allergy Immunol. 130, 87–107. https://doi.org/10.1159/000069013

Andrade, C., Corte-Real, J., 2017. Assessment of the spatial distribution of continental-oceanic climate indices in the Iberian Peninsula. Int. J. Climatol. 37, 36–45. https://doi.org/10.1002/joc.4685

Anslow, R.C., Green, J.O., 1967. The seasonal growth of pasture grasses. J. Agric. Sci. 68, 109–122. https://doi.org/10.1017/S0021859600017925

Apangu, G.P., Frisk, C.A., Adams-Groom, B., Satchwell, J., Pashley, C.H., Skjøth, C.A., 2020. Air mass trajectories and land cover map reveal cereals and oilseed rape as major local sources of Alternaria spores in the Midlands, UK. Atmos. Pollut. Res. 11, 1668–1679. https://doi.org/10.1016/j.apr.2020.06.026

Arobba, D., Guido, M.A., Minale, P., Montanari, C., Placereani, S., Pracilio, S., Troise, C., Voltolini, S., Negrini, A.C., 2000. Airborne pollen in Genoa (NW-Italy): A comparison between two pollen-sampling stations. Aerobiologia (Bologna). 16, 233–243. https://doi.org/10.1023/A:1007674620285

Atzema, A.J., 1992. A model for the drying of grass with realtime weather data. J. Agric. Eng. Res. 53, 231–247. https://doi.org/10.1016/0021-8634(92)80085-7

Aud-In, S., Somkid, K., Songnuan, W., 2019. Group-1 grass pollen allergens with near-identical sequences identified in species of subtropical grasses commonly found in southeast Asia. Med. 55. https://doi.org/10.3390/medicina55050193

Auer, C., Meyer, T., Sagun, V., 2016. Reducing Pollen Dispersal using Forest Windbreaks. Plant Sci. Artic. 28.

Avolio, E., Pasqualoni, L., Federico, S., Fornaciari, M., Bonofiglio, T., Orlandi, F., Bellecci, C., Romano, B., 2008. Correlation between large-scale atmospheric fields and the olive pollen season in Central Italy. Int. J. Biometeorol. 52, 787–796. https://doi.org/10.1007/s00484-008-0172-5

Bąba, W., 2004. The species composition and dynamics in well-preserved and restored calcareous xerothermic grasslands (South Poland). Biol. - Sect. Bot. 59, 447–456.

Banchi, E., Ametrano, C.G., Greco, S., Stanković, D., Muggia, L., Pallavicini, A., 2020. PLANiTS: a curated sequence reference dataset for plant ITS DNA metabarcoding. Database (Oxford). 2020, 1–9. https://doi.org/10.1093/database/baz155

Barton, K., 2020. MuMIN: Multi-Model Inference.

Bartošová, L., Hájková, L., Kožnarová, V., Možný, M., Trnka, M., Žalud, Z., 2015. Are there any changes in the beginning of flowering of important allergens in the Czech Republic?, in: Urban, O., Šprtová, M., Klem, K. (Eds.), Global Change: A Complex Challenge. Global Change Research Centre, The Czech Academy of Sciences, v.v.i., Brno.

Bastl, M., Bastl, K., Dirr, L., Zechmeister, T., Berger, U., 2020. Late exposure to grass pollen in September: the case of Phragmites in Burgenland. Grana 59, 25–32. https://doi.org/10.1080/00173134.2019.1696886

Bates, D., Maechler, M., Bolker, B., Walker, S., 2015. Fitting Linear Mixed-Effects Models Using lme4. J. Stat. Softw. 67, 1-48. https://doi.org/10.18637/jss.v067.i01

Beckman, N.G., Bullock, J.M., Salguero-Gómez, R., 2018. High dispersal ability is related to fast life-history strategies. J. Ecol. 106, 1349–1362. https://doi.org/10.1111/1365-2745.12989

Beddows, A.R., 1931. Seed Setting and Flowering in Various Grasses. Bull. Welsh Plant Breed. Stn. Ser. H 12, 5-99.

Beggs, P.J., Katelaris, C.H., Medek, D., Johnston, F.H., Burton, P.K., Campbell, B., Jaggard, A.K., Vicendese, D., Bowman, D.M.J.S., Godwin, I., Huete, A.R., Erbas, B., Green, B.J., Newnham, R.M., Newbigin, E., Haberle, S.G., Davies, J.M., 2015. Differences in grass pollen allergen exposure across Australia. Aust. N. Z. J. Public Health 39, 51–55. https://doi.org/10.1111/1753-6405.12325

Bell, K., de Vere, N., Keller, A., Richardson, R.T., Gous, A., Burgess, K.S., Brosi, B., 2016. Pollen DNA barcoding: current applications and future prospects. Genome 12, 1–43. https://doi.org/10.1152/ajplung.00521.2007

Bertin, R.I., 2015. Climate Change and Flowering Phenology in Worcester County, Massachusetts. Int. J. Plant Sci. 176, 107–119. https://doi.org/10.1086/679619

Besancenot, J.P., Sindt, C., Thibaudon, M., 2019. Pollen and climate change. Birch and grasses in metropolitan France. Rev. Fr. Allergol. 59, 563–575. https://doi.org/10.1016/j.reval.2019.09.006

Bhattacharya, K., Datta, B.K., 1992. Anthesis and pollen release of some plants of West Bengal, India. Grana 31, 67–71. https://doi.org/10.1080/00173139209427828

Bik, H.M., Porazinska, D.L., Creer, S., Caporaso, J.G., Knight, R., Thomas, W.K., 2012. Sequencing our way towards understanding global eukaryotic biodiversity. Trends Ecol. Evol. 27, 233–243. https://doi.org/10.1016/j.tree.2011.11.010

Bilińska, D., Kryza, M., Werner, M., Malkiewicz, M., 2019. The variability of pollen concentrations at two stations in the city of Wrocław in Poland. Aerobiologia (Bologna). 1. https://doi.org/10.1007/s10453-019-09567-1

Blair, J., Nippert, J., Briggs, J., 2014. Grassland Ecology, 8th ed, The Plant Sciences, Ecology and the Environment. Springer Science & Business Media, New York. https://doi.org/10.1007/978-1-4614-7501-9

Bohmann, K., Evans, A., Gilbert, M.T.P., Carvalho, G.R., Creer, S., Knapp, M., Yu, D.W., de Bruyn, M., 2014. Environmental DNA for wildlife biology and biodiversity monitoring. Trends Ecol. Evol. 29, 358–367. https://doi.org/10.1016/j.tree.2014.04.003

Borrell, J.S., 2012. Rapid assessment protocol for pollen settling velocity: Implications for habitat fragmentation. Biosci. Horizons 5, 1–9. https://doi.org/10.1093/biohorizons/hzs002

Bouchenak-Khelladi, Y., Verboom, G.A., Savolainen, V., Hodkinson, T.R., 2010. Biogeography of the grasses

(Poaceae): A phylogenetic approach to reveal evolutionary history in geographical space and geological time. Bot. J. Linn. Soc. 162, 543–557. https://doi.org/10.1111/j.1095-8339.2010.01041.x

Boudreault, L.É., Dupont, S., Bechmann, A., Dellwik, E., 2017. How Forest Inhomogeneities Affect the Edge Flow. Boundary-Layer Meteorol. 162, 375–400. https://doi.org/10.1007/s10546-016-0202-5

Bousquet, J., Van Cauwenberge, P., Khaltaev, N., 2001. Allergic rhinitis and its impact on asthma. J. Allergy Clin. Immunol. 108. https://doi.org/10.1067/mai.2001.118891

Brennan, G.L., Potter, C., de Vere, N., Griffith, G.W., Skjøth, C.A., Osborne, N.J., Wheeler, B.W., McInnes, R.N., Clewlow, Y., Barber, A., Hanlon, H.M., Hegarty, M., Jones, L., Kurganskiy, A., Rowney, F.M., Armitage, C., Adams-Groom, B., Ford, C.R., Petch, G.M., Elliot, A., Frisk, C.A., Neilson, R., Potter, S., Rafiq, A.M., Roy, D.B., Selby, K., Steinberg, N., Creer, S., 2019. Temperate airborne grass pollen defined by spatio-temporal shifts in community composition. Nat. Ecol. Evol. 3, 750–754. https://doi.org/10.1038/s41559-019-0849-7

Breslow, N.E., Clayton, D.G., 1993. Approximate Inference in Generalized Linear Mixed Models. J. Am. Stat. Assoc. 88, 9. https://doi.org/10.2307/2290687

Breusch, T.S., 1978. Testing for Autocorrelation in Dynamic Linear Models*. Aust. Econ. Pap. 17, 334–355. https://doi.org/10.1111/j.1467-8454.1978.tb00635.x

Breusch, T.S., Pagan, A.R., 1979. A Simple Test for Heteroscedasticity and Random Coefficient Variation. Econometrica 47, 1287–1294. https://doi.org/10.2307/1911963

Brock, J.L., Hume, D.E., Fletcher, R.H., 1996. Seasonal variation in the morphology of perennial ryegrass (Lolium perenne) and cocksfoot (Dactylis glomerata) plants and populations in pastures under intensive sheep grazing. J. Agric. Sci. 126, 37–51. https://doi.org/10.1017/S0021859600088791

Broué, P., Nicholls, G.H., 1973. Flowering in Dactylis Glomerata. II. Interaction of Temperature and Photoperiod. Aust. J. Agric. Res. 24, 685–692. https://doi.org/10.1071/AR9730685

Brown, J.N., Ash, A., MacLeod, N., McIntosh, P., 2019. Diagnosing the weather and climate features that influence pasture growth in Northern Australia. Clim. Risk Manag. 24, 1–12. https://doi.org/10.1016/j.crm.2019.01.003

Burbach, G.J., Heinzerling, L.M., Edenharter, G., Bachert, C., Bindslev-Jensen, C., Bonini, S., Bousquet, J., Bousquet-Rouanet, L., Bousquet, P.J., Bresciani, M., Bruno, A., Canonica, G.W., Darsow, U., Demoly, P., Durham, S., Fokkens, W.J., Giavi, S., Gjomarkaj, M., Gramiccioni, C., Haahtela, T., Kowalski, M.L., Magyar, P., Muraközi, G., Orosz, M., Papadopoulos, N.G., Röhnelt, C., Stingl, G., Todo-Bom, A., Von Mutius, E., Wiesner, A., Wöhrl, S., Zuberbier, T., 2009. GA2LEN skin test study II: Clinical relevance of inhalant allergen sensitizations in Europe. Allergy Eur. J. Allergy Clin. Immunol. 64, 1507–1515. https://doi.org/10.1111/j.1398-9995.2009.02089.x

Bustin, S., Huggett, J., 2017. qPCR primer design revisited. Biomol. Detect. Quantif. 14, 19–28. https://doi.org/10.1016/j.bdq.2017.11.001

Bustin, S.A., Benes, V., Nolan, T., Pfaffl, M.W., 2005. Quantitative real-time RT-PCR - A perspective. J. Mol.

Endocrinol. 34, 597–601. https://doi.org/10.1677/jme.1.01755

Buters, J.T.M., Antunes, C., Galveias, A., Bergmann, K.C., Thibaudon, M., Galán, C., Schmidt-Weber, C., Oteros, J., 2018. Pollen and spore monitoring in the world. Clin. Transl. Allergy 8, 1–5. https://doi.org/10.1186/s13601-018-0197-8

Buters, J.T.M., Kasche, A., Weichenmeier, I., Schober, W., Klaus, S., Traidl-Hoffmann, C., Menzel, A., Huss-Marp, J., Krämer, U., Behrendt, H., 2008. Year-to-year variation in release of Bet v 1 allergen from birch pollen: Evidence for geographical differences between west and south Germany. Int. Arch. Allergy Immunol. 145, 122–130. https://doi.org/10.1159/000108137

Buters, J.T.M., Thibaudon, M., Smith, M., Kennedy, R., Rantio-Lehtimäki, A., Albertini, R., Reese, G., Weber, B., Galan, C., Brandao, R., Antunes, C.M., Jäger, S., Berger, U., Celenk, S., Grewling, Ł., Jackowiak, B., Sauliene, I., Weichenmeier, I., Pusch, G., Sarioglu, H., Ueffing, M., Behrendt, H., Prank, M., Sofiev, M., Cecchi, L., 2012. Release of Bet v 1 from birch pollen from 5 European countries. Results from the HIALINE study. Atmos. Environ. 55, 496–505. https://doi.org/10.1016/j.atmosenv.2012.01.054

Calam, D.H., Davidson, J., Ford, A.W., 1983. Investigations of the allergens of cocksfoot grass (dactylis glomerata) pollen. J. Chromatogr. 266, 293–300. https://doi.org/10.1016/S0021-9673(01)90903-3

Calder, D.M., 1964a. Stage Development and Flowering in Dactylis glomerata L. Ann. Bot. 28, 187–206. https://doi.org/10.1093/aob/28.2.187

Calder, D.M., 1964b. Flowering Behaviour of Populations of Dactylis Glomerata Under Field Conditions in Britain. J. Appl. Ecol. 1, 307–320. https://doi.org/10.2307/2401315

Calder, D.M., 1963. Environmental control of flowering in Dactylis glomerata L. Nature 197, 882–883. https://doi.org/10.1038/197882a0

Calderon-Ezquerro, M.C., Guerrero-Guerra, C., Galán, C., Serrano-Silva, N., Guidos-Fogelbach, G., Jiménez-Martínez, M.C., Larenas-Linnemann, D., López Espinosa, E.D., Ayala-Balboa, J., 2018. Pollen in the atmosphere of Mexico City and its impact on the health of the pediatric population. Atmos. Environ. 186, 198–208. https://doi.org/10.1016/j.atmosenv.2018.05.006

Callahan, B.J., MrMurdie, P.J., Rosen, M.J., Han, A.W., Johnson, A.J.A., Holmes, S.P., 2016. DADA2: High resolution sample inference from Illumina amplicon data. Nat. Methods 13, 581–583. https://doi.org/10.1038/nmeth.3869

Canales, J., Trevisan, M.C., Silva, J.F., Caswell, H., 1994. A Demographic Study of an Annual Grass (Andropogen brevifolius Schwarz) in Burnt and Unburnt Savanna. Acta Oecologia 15, 261–273.

Cariñanos, P., Casares-Porcel, M., Quesada-Rubio, J.M., 2014. Estimating the allergenic potential of urban green spaces: A case-study in Granada, Spain. Landsc. Urban Plan. 123, 134–144. https://doi.org/10.1016/j.landurbplan.2013.12.009

Cariñanos, P., Emberlin, J., Galán, C., Dominguez-Vilches, E., 2000. Comparison of two pollen counting methods of slides from a hirst type volumetric trap. Aerobiologia (Bologna). 16, 339–346. https://doi.org/10.1023/A:1026577406912

Cariñanos, P., Galán, C., Alcazar, P., Dominguez, E., 1999. Diurnal variation of biological and non-biological particles in the atmosphere of Cordoba, Spain. Aerobiologia (Bologna). 15, 177–182. https://doi.org/10.1023/A:1007590023585

Cauneau-Pigot, A., Peltre, G., 1991. Pollen allergens from different dactylis glomerata varieties harvested between 1986 and 1988. Grana 30, 528–531. https://doi.org/10.1080/00173139109432022

Cavan, G., 2004. Worcestershire Climate Change Impact Study.

Cebrino, J., Galán, C., Domínguez-Vilches, E., 2016. Aerobiological and phenological study of the main Poaceae species in Córdoba City (Spain) and the surrounding hills. Aerobiologia (Bologna). 32, 595–606. https://doi.org/10.1007/s10453-016-9434-6

Cebrino, J., García-Castaño, J.L., Domínguez-Vilches, E., Galán, C., 2018. Spatio-temporal flowering patterns in Mediterranean Poaceae. A community study in SW Spain. Int. J. Biometeorol. 62, 513–523. https://doi.org/10.1007/s00484-017-1461-7

Cebrino, J., Portero de la Cruz, S., Barasona, M.J., Alcázar, P., Moreno, C., Domínguez-Vilches, E., Galán, C., 2017. Airborne pollen in Córdoba City (Spain) and its implications for pollen allergy. Aerobiologia (Bologna). 33, 281–291. https://doi.org/10.1007/s10453-016-9469-8

Chabre, H., Gouyon, B., Huet, A., Boran-Bodo, V., Nony, E., Hrabina, M., Fenaille, F., Lautrette, A., Bonvalet, M., Maillère, B., Bordas-Le Floch, V., Van Overtvelt, L., Jain, K., Ezan, E., Batard, T., Moingeon, P., 2010. Molecular variability of group 1 and 5 grass pollen allergens between Pooideae species: Implications for immunotherapy. Clin. Exp. Allergy 40, 505–519. https://doi.org/10.1111/j.1365-2222.2009.03380.x

Chamecki, M., Meneveau, C., Parlange, M.B., 2009. Large eddy simulation of pollen transport in the atmospheric boundary layer. J. Aerosol Sci. 40, 241–255. https://doi.org/10.1016/j.jaerosci.2008.11.004

Charles-Edwards, D.A., Charles-Edwards, J., Cooper, J.P., 1971. The influence of temperature on photosynthesis and transpiration in ten temperate grass varieties grown in four different environments. J. Exp. Bot. 22, 650–662. https://doi.org/10.1093/jxb/22.3.650

Ciani, F., Marchi, G., Dell'Olmo, L., Foggi, B., Mariotti Lippi, M., 2020. Contribution of land cover and wind to the airborne pollen recorded in a South European urban area. Aerobiologia (Bologna). 0123456789. https://doi.org/10.1007/s10453-020-09634-y

Clark, R.M., Thompson, R., 2011. Estimation and comparison of flowering curves. Plant Ecol. Divers. 4, 189–200. https://doi.org/10.1080/17550874.2011.580382

Clayton, W.D., Vorontsova, M.S., Harman, K.T., Williamson, H., 2002. World Grass Species: Synonymy [WWW Document]. Kew GrassBase. URL http://www.kew.org/data/grasses-syn.html (accessed 7.1.20).

Cleugh, H.A., 1998. Effects of windbreaks on airflow, microclimates and crop yields. Agrofor. Syst. 41, 55–84. https://doi.org/10.1023/A:1006019805109

Cleveland, R.B., Cleveland, W.S., McRae, J.E., Terpenning, I., 1990. STL: A Seasonal-Trend Decomposition Procedure based on Loess. J. Off. Stat. 6, 3–73.

Cleveland, W.S., 1979. Robust locally weighted regression and smoothing scatterplots. J. Am. Stat. Assoc. 74, 829–836. https://doi.org/10.1080/01621459.1979.10481038

Comtois, P., Alcazar, P., Néron, D., 1999. Pollen counts statistics and its relevance to precision. Aerobiologia (Bologna). 15, 19–28. https://doi.org/10.1023/A:1007501017470

Cooper, J.P., Calder, D.M., 1964. The Inductive Requirements for Flowering of some Temperate Grasses. Grass Forage Sci. 19, 6-14. https://doi.org/10.1111/j.1365-2494.1964.tb01133.x

Cope, T., Gray, A., 2009. Grasses of the British Isles, BSBI Handb. ed. Botanical Society of the British Isles, London.

Cornelius, C., Petermeier, H., Estrella, N., Menzel, A., 2014. Erratum to: A comparison of methods to estimate seasonal phenological development from BBCH scale recording. Int. J. Biometeorol. 58, 1707. https://doi.org/10.1007/s00484-014-0858-9.

Cornelius, C., Petermeier, H., Estrella, N., Menzel, A., 2011. A comparison of methods to estimate seasonal phenological development from BBCH scale recording. Int. J. Biometeorol. 55, 867–877. https://doi.org/10.1007/s00484-011-0421-x

Creer, S., Deiner, K., Frey, S., Porazinska, D., Taberlet, P., Thomas, W.K., Potter, C., Bik, H.M., 2016. The ecologist's field guide to sequence-based identification of biodiversity. Methods Ecol. Evol. 7, 1008–1018. https://doi.org/10.1111/2041-210X.12574

Creer, S., Fonseca, V.G., Porazinska, D.L., Giblin-Davis, R.M., Sung, W., Power, D.M., Packer, M., Carvalho, G.R., Blaxter, M.L., Lambshead, P.J.D., Thomas, W.K., 2010. Ultrasequencing of the meiofaunal biosphere: Practice, pitfalls and promises. Mol. Ecol. 19, 4–20. https://doi.org/10.1111/j.1365-294X.2009.04473.x

Cresswell, J.E., Krick, J., Patrick, M.A., Lahoubi, M., 2010. The aerodynamics and efficiency of wind pollination in grasses. Funct. Ecol. 24, 706–713. https://doi.org/10.1111/j.1365-2435.2010.01704.x

Crilley, L.R., Shaw, M., Pound, R., Kramer, L.J., Price, R., Young, S., Lewis, A.C., Pope, F.D., 2018. Evaluation of a low-cost optical particle counter (Alphasense OPC-N2) for ambient air monitoring. Atmos. Meas. Tech. 11, 709–720. https://doi.org/10.5194/amt-11-709-2018

Crouzy, B., Stella, M., Konzelmann, T., Calpini, B., Clot, B., 2016. All-optical automatic pollen identification: Towards an operational system. Atmos. Environ. 140, 202–212. https://doi.org/10.1016/j.atmosenv.2016.05.062

Crystal-Peters, J., Crown, W.H., Goetzel, R.Z., Schutt, D.C., 2000. The Cost of Productivity Losses Associated with Allergenic Rhinitis. Am. J. Manag. Care 6, 373–378.

D'Amato, G., Cecchi, L., Bonini, S., Nunes, C., Annesi-Maesano, I., Behrendt, H., Liccardi, G., Popov, T., Van Cauwenberge, P., 2007. Allergenic pollen and pollen allergy in Europe. Allergy Eur. J. Allergy Clin. Immunol. 62, 976–990. https://doi.org/10.1111/j.1398-9995.2007.01393.x

D'Amato, G., Cecchi, L., D'Amato, M., Liccardi, G., 2010. Urban Air Pollution and Climate Change as Environmental Risk Factors of Respiratory Allergy: An Update. J Investig Allergol Clin Immunol 20, 95–

102. https://doi.org/http://dx.doi.org/10.1016/j.anai.2016.08.015

D'Amato, G., Spieksma, F.T.M., Liccardi, G., Jager, S., Russo, M., Kontou-Fili, K., Nikkels, H., Wuthrich, B., Bonini, S., 1998. Pollen-related allergy in Europe. Allergy 53, 567–578. https://doi.org/10.1111/J.1398-9995.1998.Tb03932.X

D'Amato, G., Vitale, C., Molino, A., Stanziola, A., Sanduzzi, A., Vatrella, A., Mormile, M., Lanza, M., Calabrese, G., Antonicelli, L., D'Amato, M., 2016. Asthma-related deaths. Multidiscip. Respir. Med. 11, 1–5. https://doi.org/10.1186/s40248-016-0073-0

Dahl, Å., 2018. Pollen Lipids Can Play a Role in Allergic Airway Inflammation. Front. Immunol. 9, 2816. https://doi.org/10.3389/fimmu.2018.02816

Dale, M.R.T., Fortin, M.J., 2002. Spatial autocorrelation and statistical tests in ecology. Ecoscience 9, 162–167. https://doi.org/10.1080/11956860.2002.11682702

Damialis, A., Gioulekas, D., Lazopoulou, C., Balafoutis, C., Vokou, D., 2005. Transport of airborne pollen into the city of Thessaloniki: The effects of wind direction, speed and persistence. Int. J. Biometeorol. 49, 139–145. https://doi.org/10.1007/s00484-004-0229-z

Damialis, A., Konstantinou, G.N., 2011. Cereal pollen sensitisation in pollen allergic patients: To treat or not to treat? Eur. Ann. Allergy Clin. Immunol. 43, 36–44.

Danby, R.K., Hik, D.S., 2007. Variability, contingency and rapid change in recent subarctic alpine tree line dynamics. J. Ecol. 95, 352–363. https://doi.org/10.1111/j.1365-2745.2006.01200.x

Danielson, B.J., 1991. Communities in a landscape: the influence of habitat heterogeneity on the interactions between species. Am. Nat. 138, 1105–1120. https://doi.org/10.1086/285272

Darquenne, C., 2012. Aerosol deposition in health and disease. J. Aerosol Med. Pulm. Drug Deliv. 25, 140–147. https://doi.org/10.1089/jamp.2011.0916

Davies, J.M., 2014. Grass pollen allergens globally: The contribution of subtropical grasses to burden of allergic respiratory diseases. Clin. Exp. Allergy. https://doi.org/10.1111/cea.12317

De Bruin, H.A.R., Stricker, J.N.M., 2000. Evaporation of grass under non-restricted soil moisture conditions. Hydrol. Sci. J. 45, 391–406. https://doi.org/10.1080/02626660009492337

De Linares, C., Delgado, R., Aira, M.J., Alcázar, P., Alonso-Pérez, S., Boi, M., Cariñanos, P., Cuevas, E., Díaz de la Guardia, C., Elvira-Rendueles, B., Fernández-González, D., Galán, C., Gutiérrez-Bustillo, A.M., Pérez-Badia, R., Rodríguez-Rajo, F.J., Ruíz-Valenzuela, L., Tormo-Molina, R., del Mar Trigo, M., Valencia-Barrera, R.M., Valle, A., Belmonte, J., 2017. Changes in the Mediterranean pine forest: pollination patterns and annual trends of airborne pollen. Aerobiologia (Bologna). 33, 375–391. https://doi.org/10.1007/s10453-017-9476-4

de Vere, N., Rich, T.C.G., Ford, C.R., Trinder, S.A., Long, C., Moore, C.W., Satterthwaite, D., Davies, H., Allainguillaume, J., Ronca, S., Tatarinova, T., Garbett, H., Walker, K., Wilkinson, M.J., 2012. DNA barcoding the native flowering plants and conifers of wales. PLoS One 7, 1–12. https://doi.org/10.1371/journal.pone.0037945

de Weger, L.A., Pashley, C.H., Šikoparija, B., Skjøth, C.A., Kasprzyk, I., Grewling, Ł., Thibaudon, M., Magyar, D., Smith, M., 2016. The long distance transport of airborne Ambrosia pollen to the UK and the Netherlands from Central and south Europe. Int. J. Biometeorol. 60, 1829–1839. https://doi.org/10.1007/s00484-016-1170-7

Derner, J.D., Briske, D.D., Polley, H.W., 2012. Tiller organization within the tussock grass schizachyrium scoparium: A field assessment of competition-cooperation tradeoffs. Botany 90, 669–677. https://doi.org/10.1139/B2012-025

Devadas, R., Huete, A.R., Vicendese, D., Erbas, B., Beggs, P.J., Medek, D., Haberle, S.G., Newnham, R.M., Johnston, F.H., Jaggard, A.K., Campbell, B., Burton, P.K., Katelaris, C.H., Newbigin, E., Thibaudon, M., Davies, J.M., 2018. Dynamic ecological observations from satellites inform aerobiology of allergenic grass pollen. Sci. Total Environ. 633, 441–451. https://doi.org/10.1016/j.scitotenv.2018.03.191

Devis, D.L., Davies, J.M., Zhang, D., 2017. Molecular features of grass allergens and development of biotechnological approaches for allergy prevention. Biotechnol. Adv. 35, 545–556. https://doi.org/10.1016/j.biotechadv.2017.05.005

Diniz, W.J.S., Canduri, F., 2017. Bioinformatics: An overview and its applications. Genet. Mol. Res. 16. https://doi.org/10.4238/gmr16019645

Dohan, K., 2017. Ocean surface currents from satellite data. J. Geophys. Res. Ocean. 122, 2647–2651. https://doi.org/10.1002/2017JC012961.Received

Donald, C.M., 1968. The breeding of crop ideotypes. Euphytica 17, 385–403. https://doi.org/10.1007/BF00056241

Donohoe, A., Dawson, E., McMurdie, L., Battisti, D.S., Rhines, A., 2020. Seasonal Asymmetries in the Lag between Insolation and Surface Temperature. J. Clim. 33, 3921–3945. https://doi.org/10.1175/jcli-d-19-0329.1

Dormontt, E.E., van Dijk, K.J., Bell, K.L., Biffin, E., Breed, M.F., Byrne, M., Caddy-Retalic, S., Encinas-Viso, F., Nevill, P.G., Shapcott, A., Young, J.M., Waycott, M., Lowe, A.J., 2018. Advancing DNA barcoding and metabarcoding applications for plants requires systematic analysis of herbarium collections-an Australian perspective. Front. Ecol. Evol. 6, 1–12. https://doi.org/10.3389/fevo.2018.00134

Draxler, R., Stunder, B., Rolph, G., Stein, A., Taylor, A., 2016. HYSPLIT4 User's Guide. Natl. Ocean. Atmos. Adm. Tech. Memo.

Draxler, R.R., Hess, G.D., 1998. An Overview of the HYSPLIT_4 Modelling System for Trajectories, Dispersion, and Deposition. Aust. Meteorol. Mag. 47, 295–308.

Driessen, M.N.B.M., Quanjer Ph., H., 1991. Pollen deposition in intrathoracic airways. Eur. Respir. J. 4, 359–363.

Drummond, M.A., Stier, M.P., Auch, R.F., Taylor, J.L., Griffith, G.E., Riegle, J.L., Hester, D.J., Soulard, C.E., McBeth, J.L., 2015. Assessing Landscape Change and Processes of Recurrence, Replacement, and Recovery in the Southeastern Coastal Plains, USA. Environ. Manage. 56, 1252–1271.

https://doi.org/10.1007/s00267-015-0574-1

Dupont, S., Brunet, Y., Jarosz, N., 2006. Eulerian modelling of pollen dispersal over heterogeneous vegetation canopies. Agric. For. Meteorol. 141, 82–104. https://doi.org/10.1016/j.agrformet.2006.09.004

Durham, O.C., 1943. The volumetric incidence of atmospheric allergens: I. Specific Gravity of Pollen Grains. J. Allergy 14, 455–461. https://doi.org/https://doi.org/10.1016/S0021-8707(43)90495-2

Eagles, C.F., 1972. Competition for Light and Nutrients Between Natural Populations of Dactylis glomerata. J. Appl. Ecol. 9, 141–151. https://doi.org/10.2307/2402052

Eagles, C.F., 1971. Effect of photoperiod on vegetative growth in two natural populations of *Dactylis glomerata* L. Ann. Bot. 35, 75–86.

Eagles, C.F., 1967. The effect of temperature on vegetative growth in climatic races of Dactylis glomerata in controlled environments. Ann. Bot. 31, 31–39.

Eagles, C.F., Williams, D.H., 1971. Competition between natural populations of Dactylis glomerata. J. Agric. Sci. 77, 187–193. https://doi.org/10.1017/S0021859600024291

Easterling, D.R., Meehl, G.A., Parmesan, C., Changnon, S.A., Karl, T.R., Mearns, L.O., 2000. Climate Extremes: Observations, Modeling, and Impacts. SCIENCE 289, 2068–2074. https://doi.org/10.1126/science.289.5487.2068

Edwards, E.J., Still, C.J., 2008. Climate, phylogeny and the ecological distribution of C4 grasses. Ecol. Lett. 11, 266–276. https://doi.org/10.1111/j.1461-0248.2007.01144.x

Emberlin, J., Jaeger, S., Dominguez-Vilches, E., Soldevilla, C.G., Hodal, L., Mandrioli, P., Lehtimäki, A.R., Savage, M., Spieksma, F.T., Bartlett, C., 2000. Temporal and geographical variations in grass pollen seasons in areas of western Europe: An analysis of season dates at sites of the European pollen information system. Aerobiologia (Bologna). 16, 373–379. https://doi.org/10.1023/A:1026521331503

Emberlin, J., Jones, S., Bailey, J., Caulton, E., Corden, J., Dubbels, S., Evans, J., McDonagh, N., Millington, W., Mullins, J., Russel, R., Spencer, T., 1994. Variation in the start of the grass pollen season at selected sites in the United Kingdom 1987-1992. Grana 33, 94–99. https://doi.org/10.1080/00173139409427839

Emberlin, J., Mullins, J., Corden, J., Jones, S., Millington, W., Brooke, M., Savage, M., 1999. Regional variations in grass pollen seasons in the UK, long-term trends and forecast models. Clin. Exp. Allergy 29, 347–356. https://doi.org/10.1046/j.1365-2222.1999.00369.x

Emberlin, J., Norris-Hill, J., 1996. The Influence of Wind Speed on the Ambient Concentrations of Pollen from Gramineae, Platanus, and Beulta in the Air of London, England, in: Muilenberg, M., Burge, H. (Eds.), Aerobiology. Lewis Publishers, Boca Raton, Florida, pp. 1-172.

Emberlin, J., Norris-Hill, J., 1991. Spatial variation of pollen deposition in North London. Grana 30, 190–195. https://doi.org/10.1080/00173139109427798

Emberlin, J., Savage, M., Jones, S., 1993. Annual variations in grass pollen seasons in London 1961-1990: Trends and forecast models. Clin. Exp. Allergy 23, 911–918. https://doi.org/10.1111/j.1365-

2222.1993.tb00275.x

Emberlin, J., Smith, M., Close, R., Adams-Groom, B., 2007. Changes in the pollen seasons of the early flowering trees Alnus spp. and Corylus spp. in Worcester, United Kingdom, 1996-2005. Int. J. Biometeorol. 51, 181–191. https://doi.org/10.1007/s00484-006-0059-2

Emecz, T.I., 1962. The Effect of Meteorological Conditions on Anthesis in Agricultural Grasses. Ann. Bot. 26, 159–172.

Estrella, N., Menzel, A., Krämer, U., Behrendt, H., 2006. Integration of flowering dates in phenology and pollen counts in aerobiology: Analysis of their spatial and temporal coherence in Germany (1992-1999). Int. J. Biometeorol. 51, 49–59. https://doi.org/10.1007/s00484-006-0038-7

Ezike, D.N., Nnamani, C. V., Ogundipe, O.T., Adekanmbi, O.H., 2016. Airborne pollen and fungal spores in Garki, Abuja (North-Central Nigeria). Aerobiologia (Bologna). 32, 697–707. https://doi.org/10.1007/s10453-016-9443-5

Fahlbusch, B., Muller, W.D., Diener, C., Jager, L., 1993. Detection of crossreactive determinants in grass pollen extracts using monoclonal antibodies against group IV and group V allergens. Clin. Exp. Allergy 23, 51–60. https://doi.org/10.1111/j.1365-2222.1993.tb02484.x

Fazekas, A.J., Burgess, K.S., Kesanakurti, P.R., Graham, S.W., Newmaster, S.G., Husband, B.C., Percy, D.M., Hajibabaei, M., Barrett, S.C.H., 2008. Multiple multilocus DNA barcodes from the plastid genome discriminate plant species equally well. PLoS One 3. https://doi.org/10.1371/journal.pone.0002802

Fenaille, F., Nony, E., Chabre, H., Lautrette, A., Couret, M.N., Batard, T., Moingeon, P., Ezan, E., 2009. Mass spectrometric investigation of molecular variability of grass pollen group 1 allergens. J. Proteome Res. 8, 4014–4027. https://doi.org/10.1021/pr900359p

Fenner, M., 1998. The phenology of growth and reproduction in plants. Perspect. Plant Ecol. Evol. Syst. 1, 78–91. https://doi.org/10.1078/1433-8319-00053

Fernández-Rodríguez, S., Adams-Groom, B., Palacios, I.S., Caeiro, E., Brandao, R., Ferro, R., Garijo, Á.G., Smith, M., Molina, R.T., 2015. Comparison of Poaceae pollen counts recorded at sites in Portugal, Spain and the UK. Aerobiologia (Bologna). 31. https://doi.org/10.1007/s10453-014-9338-2

Fernández-Rodríguez, S., Tormo-Molina, R., Maya-Manzano, J.M., Silva-Palacios, I., Gonzalo-Garijo, Á., 2014. A comparative study on the effects of altitude on daily and hourly airborne pollen counts. Aerobiologia (Bologna). 30, 257–268. https://doi.org/10.1007/s10453-014-9325-7

Ferreira, D., Marshall, J., O'Gorman, P.A., Seager, S., 2014. Climate at high-obliquity. Icarus 243, 236–248. https://doi.org/10.1016/j.icarus.2014.09.015

Firon, N., Nepi, M., Pacini, E., 2012. Water status and associated processes mark critical stages in pollen development and functioning. Ann. Bot. 109, 1201–1213. https://doi.org/10.1093/aob/mcs070

Fletcher, D., MacKenzie, D., Villouta, E., 2005. Modelling skewed data with many zeros: A simple approach combining ordinary and logistic regression. Environ. Ecol. Stat. 12, 45–54. https://doi.org/10.1007/s10651-005-6817-1

Foody, G.M., 2020. Explaining the unsuitability of the kappa coefficient in the assessment and comparison of the accuracy of thematic maps obtained by image classification. Remote Sens. Environ. 239, 111630. https://doi.org/10.1016/j.rse.2019.111630

Ford, M.A., Thorne, G.N., 1974. Effects of Atmospheric Humidity on Plant Growth. Ann. Bot. 38, 441–452.

Fornaciari, M., Bricchi, E., Frenguelli, G., Romano, B., 1996. The results of 2-year pollen monitoring of an urban network in Perugia, Central Italy. Aerobiologia (Bologna). 12, 219–227. https://doi.org/10.1007/BF02446278

Forrest, J., Miller-Rushing, A.J., 2010. Toward a synthetic understanding of the role of phenology in ecology and evolution. Philos. Trans. R. Soc. B Biol. Sci. 365, 3101–3112. https://doi.org/10.1098/rstb.2010.0145

Förster, L., Grant, J., Michel, T., Ng, C., Barth, S., 2018. Growth under cold conditions in a wide perennial ryegrass panel is under tight physiological control. PeerJ 2018, 1–13. https://doi.org/10.7717/peerj.5520

Fox, G.A., 1998. Failure time analysis: emergence, flowering, survivorship, and other waiting times, in: Scheiner, S. (Ed.), Design and Analysis of Ecological Experiments. Chapman and Hall, New York, pp. 253–289. https://doi.org/10.1201/9781003059813

Fox, G.A., Kendall, B.E., 2002. Demographic stochasticity and the variance reduction effect. Ecology 83, 1928–1934. https://doi.org/10.2307/3071775

Frenguelli, G., 1998. The contribution of aerobiology to agriculture. Aerobiologia (Bologna). 14, 95–100. https://doi.org/10.1007/BF02694192

Frenguelli, G., Passalacqua, G., Bonini, S., Fiocchi, A., Incorvaia, C., Marcucci, F., Tedeschini, E., Canonica, G.W., Frati, F., 2010. Bridging allergologic and botanical knowledge in seasonal allergy: A role for phenology. Ann. Allergy, Asthma Immunol. 105, 223–227. https://doi.org/10.1016/j.anai.2010.06.016

Fréville, H., Silvertown, J., 2005. Analysis of interspecific competition in perennial plants using Life Table Response Experiments. Plant Ecol. 176, 69–78. https://doi.org/10.1007/s11258-004-0017-1

Friedman, J., Harder, L.D., 2004. Inflorescence architecture and wind pollination in six grass species. Funct. Ecol. 18, 851–860. https://doi.org/10.1111/j.0269-8463.2004.00921.x

Friedman, J., Rubin, M.J., 2015. All in good time: Understanding annual and perennial strategies in plants. Am. J. Bot. 102, 497–499. https://doi.org/10.3732/ajb.1500062

Fröhlich-Nowoisky, J., Kampf, C.J., Weber, B., Huffman, J.A., Pöhlker, C., Andreae, M.O., Lang-Yona, N., Burrows, S.M., Gunthe, S.S., Elbert, W., Su, H., Hoor, P., Thines, E., Hoffmann, T., Després, V.R., Pöschl, U., 2016. Bioaerosols in the Earth system: Climate, health, and ecosystem interactions. Atmos. Res. 182, 346–376. https://doi.org/10.1016/j.atmosres.2016.07.018

Gadgil, S., 2003. The Indian Monsoon and Its Variability. Annu. Rev. Earth Planet. Sci. 31, 429–467. https://doi.org/10.1146/annurev.earth.31.100901.141251

Galán, C., Ariatti, A., Bonini, M., Clot, B., Crouzy, B., Dahl, A., Fernandez-González, D., Frenguelli, G., Gehrig, R., Isard, S., Levetin, E., Li, D.W., Mandrioli, P., Rogers, C.A., Thibaudon, M., Sauliene, I.,

Skjoth, C., Smith, M., Sofiev, M., 2017. Recommended terminology for aerobiological studies. Aerobiologia (Bologna). 33, 293–295. https://doi.org/10.1007/s10453-017-9496-0

Galán, C., Domínguez-Vilches, E., 1997. The capture media in aerobiological sampling. Aerobiologia (Bologna). 13, 155–160. https://doi.org/10.1007/BF02694502

Galán, C., Emberlin, J., Domínguez, E., Bryant, R.H., Villamandos, F., 1995. A comparative analysis of daily variations in the gramineae pollen counts at Córdoba, Spain and London, UK. Grana 34, 189–198. https://doi.org/10.1080/00173139509429042

Galán, C., Smith, M., Thibaudon, M., Frenguelli, G., Oteros, J., Gehrig, R., Berger, U., Clot, B., Brandao, R., 2014. Pollen monitoring: minimum requirements and reproducibility of analysis. Aerobiologia (Bologna). 30, 385–395. https://doi.org/10.1007/s10453-014-9335-5

Galimberti, A., De Mattia, F., Bruni, I., Scaccabarozzi, D., Sandionigi, A., Barbuto, M., Casiraghi, M., Labra, M., 2014. A DNA barcoding approach to characterize pollen collected by honeybees. PLoS One 9. https://doi.org/10.1371/journal.pone.0109363

García-Mozo, H., 2017. Poaceae pollen as the leading aeroallergen worldwide: A review. Allergy Eur. J. Allergy Clin. Immunol. https://doi.org/10.1111/all.13210

García-Mozo, H., Galán, C., Alcázar, P., De La Guardia, C.D., Nieto-Lugilde, D., Recio, M., Hidalgo, P., Gónzalez-Minero, F., Ruiz, L., Domínguez-Vilches, E., 2010a. Trends in grass pollen season in southern Spain. Aerobiologia (Bologna). 26, 157–169. https://doi.org/10.1007/s10453-009-9153-3

García-Mozo, H., Galán, C., Belmonte, J., Bermejo, D., Candau, P., Díaz de la Guardia, C., Elvira, B., Gutiérrez, M., Jato, V., Silva, I., Trigo, M.M., Valencia, R., Chuine, I., 2009. Predicting the start and peak dates of the Poaceae pollen season in Spain using process-based models. Agric. For. Meteorol. 149, 256–262. https://doi.org/10.1016/j.agrformet.2008.08.013

García-Mozo, H., Mestre, A., Galán, C., 2010b. Phenological trends in southern Spain: A response to climate change. Agric. For. Meteorol. 150, 575–580. https://doi.org/10.1016/j.agrformet.2010.01.023

Garcia, A., Lindner, R., 1998. Dactylis glomerata genetic resources: Allozyme frequencies and performance of two subspecies on an acid sandy loam with summer drought. Euphytica 102, 255–264. https://doi.org/10.1023/A:1018377513189

García de León, D., García-Mozo, H., Galán, C., Alcázar, P., Lima, M., González-Andújar, J.L., 2015. Disentangling the effects of feedback structure and climate on Poaceae annual airborne pollen fluctuations and the possible consequences of climate change. Sci. Total Environ. 530–531, 103–109. https://doi.org/10.1016/j.scitotenv.2015.05.104

Garibyan, L., Avashia, N., 2013. Polymerase chain reaction. J. Invest. Dermatol. 133, 1–4. https://doi.org/10.1038/jid.2013.1

Garnier, E., 1992. Growth Analysis of Congeneric Annual and Perennial Grass Species. J. Ecol. 80, 665–675.

Ghitarrini, S., Galán, C., Frenguelli, G., Tedeschini, E., 2017a. Phenological analysis of grasses (Poaceae) as a support for the dissection of their pollen season in Perugia (Central Italy). Aerobiologia (Bologna). 33,

339–349. https://doi.org/10.1007/s10453-017-9473-7

Ghitarrini, S., Pierboni, E., Rondini, C., Tedeschini, E., Tovo, G.R., Frenguelli, G., Albertini, E., 2018. New biomolecular tools for aerobiological monitoring: Identification of major allergenic Poaceae species through fast real-time PCR. Ecol. Evol. 8, 3996–4010. https://doi.org/10.1002/ece3.3891

Ghitarrini, S., Tedeschini, E., Timorato, V., Frenguelli, G., 2017b. Climate change: consequences on the pollination of grasses in Perugia (Central Italy). A 33-year-long study. Int. J. Biometeorol. 61, 149–158. https://doi.org/10.1007/s00484-016-1198-8

Giddings, G.D., 2000. Modelling the spread of pollen from Lolium perenne. The implications for the release of wind-pollinated transgenics. Theor. Appl. Genet. 100, 971–974. https://doi.org/10.1007/s001220051378

Giddings, G.D., Sackville Hamilton, N.R., Hayward, M.D., 1997a. The Release of Genetically Modified Grasses. Part 1: Pollen Dispersal to Traps in Lolium perenne. Theor. Appl. Genet. 94, 1000–1006. https://doi.org/10.1007/s001220050507

Giddings, G.D., Sackville Hamilton, N.R., Hayward, M.D., 1997b. The Release of Genetially Modified Grasses. Part 2: The Influence of Wind Direction on Pollen Dispersal. Theor. Appl. Genet. 94, 1007–1014. https://doi.org/10.1007/s001220050508

Gioulekas, D., Balafoutis, C., Damialis, A., Papakosta, D., Gioulekas, G., Patakas, D., 2004. Fifteen years' record of airborne allergenic pollen and meteorological parameters in Thessaloniki, Greece. Int. J. Biometeorol. 48, 128–136. https://doi.org/10.1007/s00484-003-0190-2

Godfrey, L.. G.., 1978. Testing Against General Autoregressive and Moving Average Error Models when the Regressors Include Lagged Dependent Variables. Econometrica 46, 1293–1301.

Google Earth Pro, 7.3.2.5776, 2019. Google Earth Pro. Worcestershire, 52°2N, -2°2W, Elev. 30 km.

Grebenstein, B., Röser, M., Sauer, W., Hemleben, V., 1998. Molecular phylogenetic relationships in Aveneae (Poaceae) species and other grasses as inferred from ITS1 and ITS2 rDNA sequences. Plant Syst. Evol. 213, 233–250. https://doi.org/10.1007/BF00985203

Grégori, M., Benkhelifa, K., Pautz, F., Schmitt, J.P., Bonnefoy, M., Gardeur, E., Seznec, G., Pallares, C., Boulangé, M., Kanny, G., 2019. The lessons provided by phenological monitoring. Rev. Fr. Allergol. 59, 514–523. https://doi.org/10.1016/j.reval.2018.10.010

Gregory, P.H., 1961. The microbiology of the Atmosphere, Plant Science Monographs. Leonard Hill [Books] Limited, Interscience Publishers, Inc., New York.

Greiner, A.N., Hellings, P.W., Rotiroti, G., Scadding, G.K., 2011. Allergic rhinitis. Lancet 378, 2112–2122. https://doi.org/10.1016/S0140-6736(11)60130-X

Grinn-Gofroń, A., Sadyś, M., Kaczmarek, J., Bednarz, A., Pawłowska, S., Jedryczka, M., 2016. Back-trajectory modelling and DNA-based species-specific detection methods allow tracking of fungal spore transport in air masses. Sci. Total Environ. 571, 658–669. https://doi.org/10.1016/j.scitotenv.2016.07.034

Grinstead, C.M., Snell, J.L., 1997. Markov chains, in: Introduction to Probability. American Mathematical

Society, Providence, Rhode Island, pp. 405–470.

Guàrdia, R., Raventós, J., Caswell, H., 2000. Spatial growth and population dynamics of a perennial tussock grass (Achnatherum calamagrostis) in a badland area. J. Ecol. 88, 950–963. https://doi.org/10.1046/j.1365-2745.2000.00504.x

Guéguen, F., Stille, P., Dietze, V., Gieré, R., 2012. Chemical and isotopic properties and origin of coarse airborne particles collected by passive samplers in industrial, urban, and rural environments. Atmos. Environ. 62, 631–645. https://doi.org/10.1016/j.atmosenv.2012.08.044

Guisan, A., Zimmermann, N.E., 2000. Predictive habitat distribution models in ecology. Ecol. Modell. 135, 147–186. https://doi.org/10.1016/S0304-3800(00)00354-9

Hansen, J., Sato, M., Ruedy, R., Lo, K., Lea, D.W., Medina-Elizade, M., 2006. Global temperature change. Proc. Natl. Acad. Sci. U. S. A. 103, 14288–14293. https://doi.org/10.1073/pnas.0606291103

Hansen, M.J., 2007. Evaluating management strategies and recovery of an invasive grass (Agropyron cristatum) using matrix population models. Biol. Conserv. 140, 91–99. https://doi.org/10.1016/j.biocon.2007.07.028

Hardegree, S.P., Van Vactor, S.S., 2000. Germination and emergence of primed grass seeds under field and simulated-field temperature regimes. Ann. Bot. 85, 379–390. https://doi.org/10.1006/anbo.1999.1076

Harrington, J., Oliver, J.E., 2000. Understanding and portraying the global atmospheric circulation. J. Geog. 99, 23–31. https://doi.org/10.1080/00221340008978950

Hatzler, L., Panetta, V., Lau, S., Wagner, P., Bergmann, R.L., Illi, S., Bergmann, K.E., Keil, T., Hofmaier, S., Rohrbach, A., Bauer, C.P., Hoffman, U., Forster, J., Zepp, F., Schuster, A., Wahn, U., Matricardi, P.M., 2012. Molecular spreading and predictive value of preclinical IgE response to Phleum pratense in children with hay fever. J. Allergy Clin. Immunol. 130, 894-901.e5. https://doi.org/10.1016/j.jaci.2012.05.053

Havstad, L.T., Aamlid, T.S., Heide, O.M., Junttila, O., 2004. Transfer of flower induction stimuli to non-exposed tillers in a selection of temperate grasses. Acta Agric. Scand. Sect. B Soil Plant Sci. 54, 23–30. https://doi.org/10.1080/09064710310019711

Hawkins, J., De Vere, N., Griffith, A., Ford, C.R., Allainguillaume, J., Hegarty, M.J., Baillie, L., Adams-Groom, B., 2015. Using DNA metabarcoding to identify the floral composition of honey: A new tool for investigating honey bee foraging preferences. PLoS One 10, 1–20. https://doi.org/10.1371/journal.pone.0134735

Hayhoe, H.N., Jackson, L.P., 1974. Weather Effects on Hay Drying Rates. Can. J. Plant Sci. 54, 479–484. https://doi.org/10.4141/cjps74-081

Heide, O.M., 1994. Control of Flowering and Reproduction in Temperate Grasses. New Phytol. 128, 347–362. https://doi.org/10.1111/j.1469-8137.1994.tb04019.x

Heide, O.M., 1990. Primary and secondary induction requirements for flowering of Festuca rubra. Physiol. Plant. 79, 51–56. https://doi.org/10.1111/j.1399-3054.1990.tb05865.x

Heide, O.M., 1987. Photoperiodic control of flowering in Dactylis glomerata, a true short-long-day plant.

Physiol. Plant. 70, 523–529. https://doi.org/10.1111/j.1399-3054.1987.tb02853.x

Heinzerling, L., Mari, A., Bergmann, K.-C., Bresciani, M., Burbach, G., Darsow, U., Durham, S., Fokkens, W., Gjomarkaj, M., Haahtela, T., Bom, A.T., Wöhrl, S., Maibach, H., Lockey, R., 2013. The skin prick test – European standards. Clin. Transl. Allergy 3, 3. https://doi.org/10.1186/2045-7022-3-3

Heinzerling, L.M., Burbach, G.J., Edenharter, G., Bachert, C., Bindslev-Jensen, C., Bonini, S., Bousquet, J., Bousquet-Rouanet, L., Bousquet, P.J., Bresciani, M., Bruno, A., Burney, P., Canonica, G.W., Darsow, U., Demoly, P., Durham, S., Fokkens, W.J., Giavi, S., Gjomarkaj, M., Gramiccioni, C., Haahtela, T., Kowalski, M.L., Magyar, P., Muraközi, G., Orosz, M., Papadopoulos, N.G., Röhnelt, C., Stingl, G., Todo-Bom, A., Von Mutius, E., Wiesner, A., Wöhrl, S., Zuberbier, T., 2009. GA2LEN skin test study I: GALEN harmonization of skin prick testing: Novel sensitization patterns for inhalant allergens in Europe. Allergy Eur. J. Allergy Clin. Immunol. 64, 1498–1506. https://doi.org/10.1111/j.1398-9995.2009.02093.x

Henningson, E.W., Ahlberg, M.S., 1994. Evaluation of Microbiological Aerosol Samplers: A Review. J. Aerosol Sci. 25, 1459–1492. https://doi.org/10.1016/0021-8502(94)90219-4

Hernández-Ceballos, M.A., Skjøth, C.A., García-Mozo, H., Bolívar, J.P., Galán, C., 2014. Improvement in the accuracy of back trajectories using WRF to identify pollen sources in southern Iberian Peninsula. Int. J. Biometeorol. 58, 2031–2043. https://doi.org/10.1007/s00484-014-0804-x

Hill, J.D., 1976. Predicting the Natural Drying of Hay. Agric. Meteorol. 17, 195–204. https://doi.org/10.1016/0002-1571(76)90055-8

Hirst, J.M., 1952. An automatic volumetric pollen trap. Ann. Appl. Biol. 36, 257–265.

Hirzel, A.H., Le Lay, G., 2008. Habitat suitability modelling and niche theory. J. Appl. Ecol. 45, 1372–1381. https://doi.org/10.1111/j.1365-2664.2008.01524.x

Holdaway, R.J., Wiser, S.K., Williams, P.A., 2012. Status Assessment of New Zealand's Naturally Uncommon Ecosystems. Conserv. Biol. 26, 619–629. https://doi.org/10.1111/j.1523-1739.2012.01868.x

Holgate, S.T., Polosa, R., 2008. Treatment strategies for allergy and asthma. Nat. Rev. Immunol. 8, 218–230. https://doi.org/10.1038/nri2262

Hollósy, F., 2002. Effects of ultraviolet radiation on plant cells. Micron 33, 179–197. https://doi.org/10.1016/S0968-4328(01)00011-7

Hong, S.Y., Park, J.H., Cho, S.H., Yang, M.S., Park, C.M., 2011. Phenological growth stages of Brachypodium distachyon: Codification and description. Weed Res. 51, 612–620. https://doi.org/10.1111/j.1365-3180.2011.00877.x

Hornung, B.V.H., Zwittink, R.D., Kuijper, E.J., 2019. Issues and current standards of controls in microbiome research. FEMS Microbiol. Ecol. 95, 1–7. https://doi.org/10.1093/femsec/fiz045

Howarth, P.H., Holgate, S.T., 1984. Comparative trial of two non-sedative H1 antihistamines, terfenadine and astemizole, for hay fever. Thorax 39, 668–672. https://doi.org/10.1136/thx.39.9.668

Hruška, K., 2003. Assessment of urban allergophytes using an allergen index. Aerobiologia (Bologna). 19, 107–

111. https://doi.org/10.1023/A:1024450601697

Hruška, K., 2000. Phytoecological research in the urban environment in Italy. Acta Bot. Croat. 59, 135–143.

Hsiao, C., Chatterton, N.J., Asay, K.H., Jensen, K.B., 1995. Molecular phylogeny of the Pooideae (Poaceae) based on nuclear rDNA (ITS) sequences. Theor. Appl. Genet. 90, 389–398. https://doi.org/10.1007/BF00221981

Huang, Z., Zhu, J., Mu, X., Lin, J., 2004. Pollen dispersion, pollen viability and pistil receptivity in Leymus chinensis. Ann. Bot. 93, 295–301. https://doi.org/10.1093/aob/mch044

Hugg, T.T., Tuokila, M., Korkonen, S., Weckström, J., Jaakkola, M.S., Jaakkola, J.J.K., 2020. The effect of sampling height on grass pollen concentrations in different urban environments in the Helsinki Metropolitan Area, Finland. PLoS One 15, 1–12. https://doi.org/10.1371/journal.pone.0239726

Hurtado-Uria, C., Hennessy, D., Shalloo, L., O'Connor, D., Delaby, L., 2013. Relationships between meteorological data and grass growth over time in the south of Ireland. Irish Geogr. 46, 175–201. https://doi.org/10.1080/00750778.2013.865364

Hyde, H.A., 1973. Atmospheric pollen grains and spores in relation to allergy. II. Clin. Exp. Allergy 3, 109–126. https://doi.org/10.1111/j.1365-2222.1973.tb01315.x

Hyde, H.A., 1972. Atmospheric pollen and spores in relation to allergy. I. Clin. Exp. Allergy 2, 153–179. https://doi.org/10.1111/j.1365-2222.1972.tb01280.x

Hyde, H.A., Williams, D.A., 1945. Studies in Atmospheric Pollen: II. Diurnal Variation in the Incidence of Grass Pollen. New Phytol. 44, 83–94. https://doi.org/10.1111/j.1469-8137.1945.tb05020.x

Ickovic, M.R., Boussioud-Corbieres, F., Sutra, J.P., Thibaudon, M., 1989. Hay fever symptoms compared to atmospheric pollen counts and floral phenology within Paris suburban area in 1987 and 1988. Aerobiologia (Bologna). 5, 30–36. https://doi.org/10.1007/BF02446485

İnceoğlu, Ö., Pinar, N.M., Şakiyan, N., Sorkun, K., 1994. Airborne pollen concentration in Ankara, Turkey 1990-1993. Grana 33, 158–161. https://doi.org/10.1080/00173139409428993

Indahl, U.G., Næs, T., Liland, K.H., 2018. A similarity index for comparing coupled matrices. J. Chemom. 32, 1–18. https://doi.org/10.1002/cem.3049

Izquierdo, R., Belmonte, J., Avila, A., Alarcón, M., Cuevas, E., Alonso-Pérez, S., 2011. Source areas and long-range transport of pollen from continental land to Tenerife (Canary Islands). Int. J. Biometeorol. 55, 67–85. https://doi.org/10.1007/s00484-010-0309-1

Jackson, M.T., 1966. Effects of Microclimate on Spring Flowering Phenology. Ecology 47, 407–315. https://doi.org/10.2307/1932980

Jan, F., Schüler, L., Behling, H., 2015. Trends of pollen grain size variation in C3 and C4 Poaceae species using pollen morphology for future assessment of grassland ecosystem dynamics. Grana 54, 129–145. https://doi.org/10.1080/00173134.2014.966754

Jantunen, J., Saarinen, K., Valtonen, A., Saarnio, S., 2007. Flowering and seed production success along roads

with different mowing regimes. Appl. Veg. Sci. 10, 285–292. https://doi.org/10.1111/j.1654-109X.2007.tb00528.x

Jantunen, J., Saarinen, K., Valtonen, A., Saarnio, S., 2006. Grassland Vegetation along road differing in size and traffic density. Ann. Bot Fenn. 43, 107–117.

Jarosz, N., Loubet, B., Durand, B., Mccartney, A., Foueillassar, X., Huber, L., 2003. Field measurements of airborne concentrations and deposition rates of maize pollen. Agric. For. Meteorol. 119, 37–51. https://doi.org/10.1016/S0168-1923(03)00118-7

Jentsch, A., Kreyling, J., Boettcher-Treschkow, J., Beierkuhnlein, C., 2009. Beyond gradual warming: Extreme weather events alter flower phenology of European grassland and heath species. Glob. Chang. Biol. 15, 837–849. https://doi.org/10.1111/j.1365-2486.2008.01690.x

Jewiss, O.R., 1972. Tillering in Grasses—Its Significance and Control. Grass Forage Sci. 27, 65–82. https://doi.org/10.1111/j.1365-2494.1972.tb00689.x

Jochner, S., Ziello, C., Böck, A., Estrella, N., Buters, J., Weichenmeier, I., Behrendt, H., Menzel, A., 2012. Spatio-temporal investigation of flowering dates and pollen counts in the topographically complex Zugspitze area on the German-Austrian border. Aerobiologia (Bologna). 28, 541–556. https://doi.org/10.1007/s10453-012-9255-1

Johansson, S.G.O., Bieber, T., Dahl, R., Friedmann, P.S., Lanier, B.Q., Lockey, R.F., Motala, C., Ortega Martell, J.A., Platts-Mills, T.A.E., Ring, J., Thien, F., Van Cauwenberge, P., Williams, H.C., 2004. Revised nomenclature for allergy for global use: Report of the Nomenclature Review Committee of the World Allergy Organization, October 2003. J. Allergy Clin. Immunol. 113, 832–836. https://doi.org/10.1016/j.jaci.2003.12.591

Johansson, S.G.O., Hourihane, J.O.B., Bousquet, J., Bruijnzeel-Koomen, C., Dreborg, S., Haahtela, T., Kowalski, M.L., Mygind, N., Ring, J., Van Cauwenberge, P., Van Hage-Hamsten, M., Wüthrich, B., 2001. A revised nomenclature for allergy. An EAACI position statement from the EAACI nomenclature task force. Allergy Eur. J. Allergy Clin. Immunol. 56, 813–824. https://doi.org/10.1034/j.1398-9995.2001.t01-1-00001.x

Johnson, G.T., Hunter, L.J., 1999. Some insights into typical urban canyon airflows. Atmos. Environ. 33, 3991–3999. https://doi.org/10.1016/S1352-2310(99)00164-8

Johnson, P.G., White, D.B., 1998. Inheritance of flowering pattern among four annual bluegrass (Poa annua L.) genotypes. Crop Sci. 38, 163–168. https://doi.org/10.2135/cropsci1998.0011183X003800010027x

Joly, C., Barillé, L., Barreau, M., Mancheron, A., Visset, L., 2007. Grain and annulus diameter as criteria for distinguishing pollen grains of cereals from wild grasses. Rev. Palaeobot. Palynol. 146, 221–233. https://doi.org/10.1016/j.revpalbo.2007.04.003

Jones, A.M., Harrison, R.M., 2004. The effects of meteorological factors on atmospheric bioaerosol concentrations - A review. Sci. Total Environ. https://doi.org/10.1016/j.scitotenv.2003.11.021

Jones, M.D., Newell, L.C., 1946. Pollination Cycles and Pollen Dispersal in Relation to Grass Improvement.

Univ. Nebraska, Coll. Agric. Res. Bull. 148.

Jung, I.Y., Choi, K.R., 2013. Relationship between airborne pollen concentrations and meteorological parameters in Ulsan, Korea. J. Ecol. Environ. 36, 65–71. https://doi.org/10.5141/ecoenv.2013.008

Jung, S., Estrella, N., Pfaffl, M.W., Hartmann, S., Ewald, F., Menzel, A., 2021. Impact of elevated air temperature and drought on pollen characteristics of major agricultural grass species. PLoS One 16, 1–19. https://doi.org/10.1371/journal.pone.0248759

Jutel, M., Jaeger, L., Suck, R., Meyer, H., Fiebig, H., Cromwell, O., 2005. Allergen-specific immunotherapy with recombinant grass pollen allergens. J. Allergy Clin. Immunol. 116, 608–613. https://doi.org/10.1016/j.jaci.2005.06.004

Käpylä, M., Penttinen, A., 1981. An evaluation of the microscopical counting methods of the tape in hirst-burkard pollen and spore trap of the tape in Hirst-Burkard pollen and spore trap. Grana 3134, 131–141. https://doi.org/10.1080/00173138109427653

Karatzas, K., Tsiamis, A., Charalampopoulos, A., Damialis, A., Vokou, D., 2019. Pollen season identification for three pollen taxa in Thessaloniki, Greece: a 30-year retrospective analysis. Aerobiologia (Bologna). 35, 659–669. https://doi.org/10.1007/s10453-019-09605-y

Kasprzyk, I., 2006. Comparative study of seasonal and intradiurnal variation of airborne herbaceous pollen in urban and rural areas. Aerobiologia (Bologna). 22, 185–195. https://doi.org/10.1007/s10453-006-9031-1

Katelaris, C.H., Burke, T. V., Byth, K., 2004. Spatial variability in the pollen count in Sydney, Australia: Can one sampling site accurately reflect the pollen count for a region? Ann. Allergy, Asthma Immunol. 93, 131–136. https://doi.org/10.1016/S1081-1206(10)61464-0

Katz, D.S.W., Batterman, S.A., 2020. Urban-scale variation in pollen concentrations: a single station is insufficient to characterize daily exposure. Aerobiologia (Bologna). 36, 417–431. https://doi.org/10.1007/s10453-020-09641-z

Keijzer, C.J., 1987a. The Processes of Anther Dehiscence and Pollen Dispersal: I. The Opening Mechanism of Longitudinally Dehiscing Anthers. New Phytol. 105, 487–498. https://doi.org/10.1111/j.1469-8137.1987.tb00887.x

Keijzer, C.J., 1987b. The Process of Anther Dehiscence and Pollen Dispersal: II. The Formation and the Transer Mechanism of Pollenkitt, Cell-Wall Development of the Loulus Tissues and A Function of Orbicules in Pollen Dispersal. New Phytol. 105, 499–507.

Keijzer, C.J., Hoek, I.H.S., Willemse, M.T.M., 1987. The Process of Anther Dehiscence and Pollen Dispersal: III. The Dehydration of the Filament Tip and The Anther in Three Monocotyledonous Species. New Phytol. 106, 281–287. https://doi.org/10.1111/j.1469-8137.1987.tb00143.x

Keijzer, C.J., Leferink-Ten Klooster, H.B., Reinders, M.C., 1996. The Mechanics of the Grass Flower : Anther Dehiscence and Pollen Shedding in Maize. Ann. Bot. 78, 15–21. https://doi.org/10.1006/anbo.1996.0089

Kendall, B.E., Fox, G.A., 2002. Variation among individuals and reduced demographic stochasticity. Conserv. Biol. 16, 109–116. https://doi.org/10.1046/j.1523-1739.2002.00036.x

Kendall, M.G., 1938. A New Measure of Rank Correlation. Biometrika 30, 81. https://doi.org/10.2307/2332226

Khanchi, A., Birrell, S., Mitchell, R.B., 2018. Modelling the influence of crop density and weather conditions on field drying characteristics of switchgrass and maize stover using random forest. Biosyst. Eng. 169, 71–84. https://doi.org/10.1016/j.biosystemseng.2018.02.002

Khanduri, V.P., 2011. Variation in Anthesis and Pollen Production in Plants. Am. J. Agric. Environ. Sci. 11, 834–839.

Khwarahm, N., Dash, J., Atkinson, P.M., Newnham, R.M., Skjøth, C.A., Adams-Groom, B., Caulton, E., Head, K., 2014. Exploring the spatio-temporal relationship between two key aeroallergens and meteorological variables in the United Kingdom. Int. J. Biometeorol. 58, 529–545. https://doi.org/10.1007/s00484-013-0739-7

Khwarahm, N.R., Dash, J., Skjøth, C.A., Newnham, R.M., Adams-Groom, B., Head, K., Caulton, E., Atkinson, P.M., 2017. Mapping the birch and grass pollen seasons in the UK using satellite sensor time-series. Sci. Total Environ. 578, 586–600. https://doi.org/10.1016/j.scitotenv.2016.11.004

Kim, H.H., 1992. Urban heat island. Int. J. Remote Sens. 13, 2319-2336. https://doi.org/10.1080/01431169208904271

Kladnik, D., Geršič, M., Pipan, P., Buhan, M.V., 2019. Land-Use Changes in Slovenian Terraced Landscapes. Acta Geogr. Slov. 59, 119–141. https://doi.org/10.3986/AGS.6988

Kluska, K., Piotrowicz, K., Kasprzyk, I., 2020. The impact of rainfall on the diurnal patterns of atmospheric pollen concentrations. Agric. For. Meteorol. 291, 108042. https://doi.org/10.1016/j.agrformet.2020.108042

Kmenta, M., Bastl, K., Berger, U., Kramer, M.F., Heath, M.D., Pätsi, S., Pessi, A.M., Saarto, A., Werchan, B., Werchan, M., Zetter, R., Bergmann, K.C., 2017. The grass pollen season 2015: A proof of concept multi-approach study in three different European cities. World Allergy Organ. J. 10, 1-12. https://doi.org/10.1186/s40413-017-0163-2

Kmenta, M., Bastl, K., Kramer, M.F., Hewings, S.J., Mwange, J., Zetter, R., Berger, U., 2016. The grass pollen season 2014 in Vienna: A pilot study combining phenology, aerobiology and symptom data. Sci. Total Environ. 566–567, 1614–1620. https://doi.org/10.1016/j.scitotenv.2016.06.059

Kmenta, M., Zetter, R., Bastl, K., Kramer, M.F., Mwange, J., Hewings, S.J., Skinner, M., Berger, U., 2015. Grass pollen allergy season 2014 , a multidisciplinary case study in Vienna : Temporal variation in pollination of grass species, impact on pollen allergy sufferers and species-dependent allergenicity, in: Environmental Heteorogeneity and Asthma and Allergies. p. 130.

Koons, D.N., Iles, D.T., Schaub, M., Caswell, H., 2016. A life-history perspective on the demographic drivers of structured population dynamics in changing environments. Ecol. Lett. 19, 1023–1031. https://doi.org/10.1111/ele.12628

Kottek, M., Grieser, J., Beck, C., Rudolf, B., Rubel, F., 2006. World Map of the Köppen-Geiger Climate Classification. Meteorol. Zeitschrift 15, 259–263. https://doi.org/10.1127/0941-2948/2006/0130

Kožnarová, V., Sulovská, S., Richterová, D., Hájková, L., 2011. Evaluation of „ Poaceae “ allergens

phenological onset in dependence on weather conditions within the period 1991-2010. Bioclimate Source Limit Soc. Dev. Int. Sci. Conferece.

Kraaijeveld, K., de Weger, L.A., Ventayol García, M., Buermans, H., Frank, J., Hiemstra, P.S., den Dunnen, J.T., 2015. Efficient and sensitive identification and quantification of airborne pollen using next-generation DNA sequencing. Mol. Ecol. Resour. 15, 8–16. https://doi.org/10.1111/1755-0998.12288

Kreissl, B., Höschele, K., Staiger, H., Schultz, E., 1991. Meteorological Influence on Particle Dry Deposition. J. Aerosol Sci. 22, 573–576. https://doi.org/10.1016/S0021-8502(05)80166-1

Kurganskiy, A., Creer, S., Vere, N. De, Griffith, G.W., Osborne, N.J., Wheeler, B.W., Mcinnes, R.N., Clewlow, Y., Barber, A., Brennan, G.L., Hanlon, H.M., Hegarty, M., Potter, C., Rowney, F., Adams-groom, B., Petch, G.M., Pashley, C.H., Satchwell, J., Weger, L.A. De, Rasmussen, K., Oliver, G., Sindt, C., Bruffaerts, N., Allen, J., Bartle, J., Bevan, J., Frisk, C.A., Nielson, R., Potter, S., Selby, K., Tait, J., Zaragoza-Castells, J., Skjøth, C.A., 2021. Predicting the severity of the grass pollen season and the effect of climate change in Northwest Europe. Sci. Adv. 7, 1–12. https://doi.org/10.1126/sciadv.abd7658

Kuznetsova, A., Brockhoff, P.B., Christensen, R.H.B., 2017. lmerTest Package: Test in Linear Mixed Effects Models. J. Stat. Softw. 82, 1-26. https://doi.org/10.18637/jss.v082.i13

Lacey, J., Allitt, U., 1995. Airborne Pollens and Spores : A Guide to Trapping and Counting. BAF (British Aerobiology Federation), Harpenden.

Lamb, C.E., Ratner, P.H., Johnson, C.E., Ambegaonkar, A.J., Joshi, A. V., Day, D., Sampson, N., Eng, B., 2006. Economic impact of workplace productivity losses due to allergic rhinitis compared with select medical conditions in the United States from an employer perspective. Curr. Med. Res. Opin. 22, 1203–1210. https://doi.org/10.1185/030079906X112552

Last, L., Widmer, F., Fjellstad, W., Stoyanova, S., Kölliker, R., 2013. Genetic diversity of natural orchardgrass (Dactylis glomerata L.) populations in three regions in Europe. BMC Genet. 14. https://doi.org/10.1186/1471-2156-14-102

Latałowa, M., Uruska, A., Pędziszewska, A., Góra, M., Dawidowska, A., 2005. Diurnal patterns of airborne pollen concentration of the selected tree and herb taxa in Gdańsk (northern Poland). Grana 44, 192–201. https://doi.org/10.1080/00173130500219692

León-Ruiz, E., Alcázar, P., Domínguez-Vilches, E., Galán, C., 2011. Study of Poaceae phenology in a Mediterranean climate. Which species contribute most to airborne pollen counts? Aerobiologia (Bologna). 27, 37–50. https://doi.org/10.1007/s10453-010-9174-y

León-Ruiz, E.J., García-Mozo, H., Domínguez-Vilches, E., Galán, C., 2012. The Use of Geostatistics in the Study of Floral Phenology of Vulpia geniculata (L.) Link. Sci. World J. 2012, 1–19. https://doi.org/10.1100/2012/624247

Leontidou, K., Vernesi, C., De Groeve, J., Cristofolini, F., Vokou, D., Cristofori, A., 2018. DNA metabarcoding of airborne pollen: new protocols for improved taxonomic identification of environmental samples. Aerobiologia (Bologna). 34, 63–74. https://doi.org/10.1007/s10453-017-9497-z

Leopold, A.C., 1961. Senescence in Plant Development. SCIENCE 134, 1727–1732. https://doi.org/10.1126/science.134.3492.1727

Levetin, E., 2013. Use of the Burkard Spore Trap [WWW Document]. Univ. Tulsa. URL http://aaaai.confex.com/aaaai/2013/recordingredirect.cgi/oid/Handout297/Burkard_Directions.pdf

Li, P., Peng, C., Wang, M., Luo, Y., Li, M., Zhang, K., Zhang, D., Zhu, Q., 2018. Dynamics of vegetation autumn phenology and its response to multiple environmental factors from 1982 to 2012 on Qinghai-Tibetan Plateau in China. Sci. Total Environ. 637–638, 855–864. https://doi.org/10.1016/j.scitotenv.2018.05.031

Liem, A.S.N., 1980. Effects of Light and Temperature on Anthesis of Holcus Lanatus, Festuca Rubra and Poa Annua. Grana 19, 21–29. https://doi.org/10.1080/00173138009424984

Liem, A.S.N., Groot, J., 1973. Anthesis and pollen dispersal of holcus lanatus L. and Festuca rubra L. in relation to climate factors. Rev. Palaeobot. Palynol. 15, 3–16. https://doi.org/10.1016/0034-6667(73)90012-2

Lin, J.J., Noll, K.E., Holsen, T.M., 1994. Dry deposition velocities as a function of particle size in the ambient atmosphere. Aerosol Sci. Technol. 20, 239–252. https://doi.org/10.1080/02786829408959680

Linder, H.P., Lehmann, C.E.R., Archibald, S., Osborne, C.P., Richardson, D.M., 2018. Global grass (Poaceae) success underpinned by traits facilitating colonization, persistence and habitat transformation. Biol. Rev. 93, 1125–1144. https://doi.org/10.1111/brv.12388

Lindner, R., Garcia, A., 1997. Geographic distribution and genetic resources of Dactylis in Galicia (northwest Spain). Genet. Resour. Crop Evol. 44, 499–507. https://doi.org/10.1023/A:1008690831828

Lo, F., Bitz, C.M., Battisti, D.S., Hess, J.J., 2019. Pollen calendars and maps of allergenic pollen in North America. Aerobiologia (Bologna). 35, 613–633. https://doi.org/10.1007/s10453-019-09601-2

Longhi, S., Cristofori, A., Gatto, P., Cristofolini, F., Grando, M.S., Gottardini, E., 2009. Biomolecular identification of allergenic pollen: A new perspective for aerobiological monitoring? Ann. Allergy, Asthma Immunol. 103, 508–514. https://doi.org/10.1016/S1081-1206(10)60268-2

Majeed, H.T., Periago, C., Alarcón, M., Belmonte, J., 2018. Airborne pollen parameters and their relationship with meteorological variables in NE Iberian Peninsula. Aerobiologia (Bologna). 34, 375–388. https://doi.org/10.1007/s10453-018-9520-z

Makra, L., Matyasovszky, I., Páldy, A., Deák, Á.J., 2012. The influence of extreme high and low temperatures and precipitation totals on pollen seasons of Ambrosia, Poaceae and Populus in Szeged, southern Hungary. Grana 51, 215–227. https://doi.org/10.1080/00173134.2012.661764

Maya-Manzano, J.M., FernÁndez-RodrÍguez, S., Silva-Palacios, I., Gonzalo-Garijo, Á., Tormo-Molina, R., 2018. Comparison between two adhesives (silicone and petroleum jelly) in Hirst pollen traps in a controlled environment. Grana 57, 137–143. https://doi.org/10.1080/00173134.2017.1319973

Maya-Manzano, J.M., Sadyś, M., Tormo-Molina, R., Fernández-Rodríguez, S., Oteros, J., Silva-Palacios, I., Gonzalo-Garijo, A., 2017. Relationships between airborne pollen grains, wind direction and land cover using GIS and circular statistics. Sci. Total Environ. 584, 603–613.

https://doi.org/10.1016/j.scitotenv.2017.01.085

Maya Manzano, J.M., Fernández Rodríguez, S., Vaquero Del Pino, C., Gonzalo Garijo, Á., Silva Palacios, I., Tormo Molina, R., Moreno Corchero, A., Cosmes Martín, P.M., Blanco Pérez, R.M., Domínguez Noche, C., Fernández Moya, L., Alfonso Sanz, J.V., Vaquero Pérez, P., Pérez Marín, M.L., Rapp, A., Rojo, J., Pérez-Badia, R., 2017. Variations in airborne pollen in central and south-western Spain in relation to the distribution of potential sources. Grana 56, 228–239. https://doi.org/10.1080/00173134.2016.1208680

Mayer, C.D., Lorent, J., Horgan, G.W., 2011. Exploratory analysis of multiple omics datasets using the adjusted RV coefficient. Stat. Appl. Genet. Mol. Biol. 10, 1-27. https://doi.org/10.2202/1544-6115.1540

McCulloch, C.E., 2001. Generalized linear models. Stat. 21st Century 135, 387–396. https://doi.org/10.4135/9781446251119.n40

McDonald, J.E., 1962. Collection and Washout of Airborne Pollens and Spores by Raindrops. SCIENCE 135, 435–437. https://doi.org/10.1126/science.135.3502.435

McInnes, R.N., Hemming, D., Burgess, P., Lyndsay, D., Osborne, N.J., Skjøth, C.A., Thomas, S., Vardoulakis, S., 2017. Mapping allergenic pollen vegetation in UK to study environmental exposure and human health. Sci. Total Environ. 599–600, 483–499. https://doi.org/10.1016/j.scitotenv.2017.04.136

McMurdie, P.J., Holmes, S., 2013. Phyloseq: An R Package for Reproducible Interactive Analysis and Graphics of Microbiome Census Data. PLoS One 8. https://doi.org/10.1371/journal.pone.0061217

Meier, U., 2018. Growth stages of mono- and dicotyledonous plants. BBCH Monograph. Julius Kühn-Institute (JKI), Quedlinburg, Germany. https://doi.org/10.5073/20180906-074619

Meier, U., Bleiholder, H., Buhr, L., Feller, C., Hack, H., Heß, M., Lancashire, P., Schnock, U., Stauß, R., Van den Boom, T., Weber, E., Zwerger, P., 2009. The BBCH system to coding the phenological growth stages of plants-history and publications. J. für Kult. 61, 41–52. https://doi.org/10.5073/JfK.2009.02.01

Menzel, A., 2019. The allergen riddle. Nat. Ecol. Evol. 3, 716–717. https://doi.org/10.1038/s41559-019-0873-7

Meyn, S.P., Tweedie, R.L., 1993. Markov Chains and Stochastic Stability, 1st ed. Springer-Verlag London, London.

Mikolaskova, K., 2009. Continental and oceanic precipitation régime in Europe. Cent. Eur. J. Geosci. 1, 176–182. https://doi.org/10.2478/v10085-009-0013-8

Miller-Rushing, A.J., Inouye, D.W., Primack, R.B., 2008. How well do first flowering dates measure plant responses to climate change? The effects of population size and sampling frequency. J. Ecol. 96, 1289–1296. https://doi.org/10.1111/j.1365-2745.2008.01436.x

Mohapatra, S.S., Lockey, R.F., Shirley, S., 2005. Immunobiology of grass pollen allergens. Curr. Allergy Asthma Rep. 5, 381–387. https://doi.org/10.1007/s11882-005-0011-2

Montgomery, K., 2006. Variation in Temperature With Altitude and Latitude. J. Geog. 105, 133–135. https://doi.org/10.1080/00221340608978675

Montserrat Gutierrez-Bustillo, A., Ferencova, Z., Nunez, A., Alcami, A., Campoy, P., Guantes, R., Moreno,

D.A., 2016. Morphological analysis and DNA sequencing of atmospheric pollen in Madrid region: preliminary study. Rev. Salud Ambient. 16, 71–77.

Morgado, L.N., Gonçalves-Esteves, V., Resendes, R., Ventura, M.A.M., 2015. Pollen morphology of Poaceae (Poales) in the Azores, Portugal. Grana 54, 282–293. https://doi.org/10.1080/00173134.2015.1096301

Morrow Brown, H., Jackson, F.A., 1978a. Aerobiological studies based in Derby: I. A simplified automatic volumetric spore trap. Clin. Exp. Allergy 8, 589–597. https://doi.org/10.1111/j.1365-2222.1978.tb01513.x

Morrow Brown, H., Jackson, F.A., 1978b. Aerobiological studies based in Derby: III. A comparison of simultaneous pollen and spore counts from the east coast, Midlands and west coast of England and Wales. Clin. Exp. Allergy 8, 611–619. https://doi.org/10.1111/j.1365-2222.1978.tb01515.x

Morrow Brown, H., Jackson, F.A., 1978c. Aerobiological studies based in Derby: II. Simultaneous pollen and spore sampling at eight sites within a 60 km radius. Clin. Exp. Allergy 8, 599–609. https://doi.org/10.1111/j.1365-2222.1978.tb01514.x

Mucina, L., 2019. Biome: evolution of a crucial ecological and biogeographical concept. New Phytol. 222, 97–114. https://doi.org/10.1111/nph.15609

Mueller, L., Schindler, U., Mirschel, W., Shepherd, G.T., Ball, B.C., Helming, K., Rogasik, J., Eulenstein, F., Wiggering, H., 2010. Assessing the productivity function of soils. A review. Agron. Sustain. Dev. 30, 601–614. https://doi.org/10.1051/agro/2009057

Munshi, A.H., 2000. Flowering calendar of grasses in Srinagar, Kashmir Himalaya (India). Aerobiologia (Bologna). 16, 449–452. https://doi.org/10.1023/A:1026597816660

Myszkowska, D., 2014. Poaceae pollen in the air depending on the thermal conditions. Int. J. Biometeorol. 58, 975–986. https://doi.org/10.1007/s00484-013-0682-7

Nakagawa, S., Johnson, P.C.D., Schielzeth, H., 2017. The coefficient of determination R2 and intra-class correlation coefficient from generalized linear mixed-effects models revisited and expanded. J. R. Soc. Interface 14. https://doi.org/10.1098/rsif.2017.0213

Nakaoka, M., 1996. Dynamics of Age- and Size-Structured Populations in Fluctuating Environments: Applications of Stochastic Matrix Models to Natural Populations. Res. Popul. Ecol. (Kyoto). 38, 141–152. https://doi.org/10.1007/BF02515722

Nathan, R., Perry, G., Cronin, J.T., Strand, A.E., Cain, M.L., 2003. Methods for estimating long-distance dispersal. OIKOS 103, 261–273. https://doi.org/10.1034/j.1600-0706.2003.12146.x

Nony, E., Timbrell, V., Hrabina, M., Boutron, M., Solley, G., Moingeon, P., Davies, J.M., 2015. Specific IgE recognition of pollen allergens from subtropic grasses in patients from the subtropics. Ann. Allergy, Asthma Immunol. 114, 214-220.e2. https://doi.org/10.1016/j.anai.2014.12.005

Nord, E.A., Lynch, J.P., 2009. Plant phenology: A critical controller of soil resource acquisition. J. Exp. Bot. 60, 1927–1937. https://doi.org/10.1093/jxb/erp018

Norris-Hill, J., 1999. The diurnal variation of poaceae pollen concentrations in a rural area. Grana 38, 301–305.

https://doi.org/10.1080/001731300750044528

Norris-Hill, J., 1997. The influence of ambient temperature on the abundance of Poaceae pollen. Aerobiologia (Bologna). 13, 91–97. https://doi.org/10.1007/BF02694424

Norris-Hill, J., 1995. The modelling of daily poaceae pollen concentrations. Grana 34, 182–188. https://doi.org/10.1080/00173139509429041

Norris-Hill, J., Emberlin, J., 1993. The incidence of increased pollen concentrations during rainfall in the air of London. Aerobiologia (Bologna). 9, 27–32. https://doi.org/10.1007/BF02311367

Norris-Hill, J., Emberlin, J., 1991. Diurnal variation of pollen concentration in the air of north-central London. Grana 30, 229–234. https://doi.org/10.1080/00173139109427803

Núñez, A., de Paz, G.A., Rastrojo, A., García, A.M., Alcamí, A., Montserrat Gutiérrez-Bustillo, A., Moreno, D.A., 2016. Monitoring of airborne biological particles in outdoor atmosphere. Part 2: Metagenomics applied to urban environments. Int. Microbiol. 19, 69–80. https://doi.org/10.2436/20.1501.01.265

Nurminiemi, M., Tufto, J., Nilsson, N.O., Rognli, O.A., 1998. Spatial models of pollen dispersal in the forage grass meadow fescue. Evol. Ecol. 12, 487–502. https://doi.org/10.1023/A:1006529023036

O'Connor, T.G., 1993. The Influence of Rainfall and Grazing on the Demography of Some African Savanna Grasses: A Matrix Modelling Approach. J. Appl. Ecol. 30, 119. https://doi.org/10.2307/2404276

Okubo, A., Levin, S.A., 1989. A Theoretical Framework for Data Analysis of Wind Dispersal of Seeds and Pollen. Ecology 70, 329–338. https://doi.org/10.2307/1937537

Oliva, G., Collantes, M., Humano, G., 2005. Demography of grazed tussock grass populations in Patagonia. Rangel. Ecol. Manag. 58, 466–473. https://doi.org/10.2111/1551-5028(2005)58[466:DOGTGP]2.0.CO;2

Op De Beeck, M., Lievens, B., Busschaert, P., Declerck, S., Vangronsveld, J., Colpaert, J. V., 2014. Comparison and validation of some ITS primer pairs useful for fungal metabarcoding studies. PLoS One 9. https://doi.org/10.1371/journal.pone.0097629

Orlanski, I., 1975. A Rational Subdivision of Scales for Atmospheric Processes. Bull. Am. Meteorol. Soc. 56, 527–530.

Ortiz-Rodríguez, D.O., Guisan, A., Holderegger, R., van Strien, M.J., 2019. Predicting species occurrences with habitat network models. Ecol. Evol. 9, 10457–10471. https://doi.org/10.1002/ece3.5567

Osborne, N.J., Alcock, I., Wheeler, B.W., Hajat, S., Sarran, C., Clewlow, Y., McInnes, R.N., Hemming, D., White, M., Vardoulakis, S., Fleming, L.E., 2017. Pollen exposure and hospitalization due to asthma exacerbations: daily time series in a European city. Int. J. Biometeorol. 61, 1837–1848. https://doi.org/10.1007/s00484-017-1369-2

Oteros, J., Bergmann, K.C., Menzel, A., Damialis, A., Traidl-Hoffmann, C., Schmidt-Weber, C.B., Buters, J., 2019a. Spatial interpolation of current airborne pollen concentrations where no monitoring exists. Atmos. Environ. 199, 435–442. https://doi.org/10.1016/j.atmosenv.2018.11.045

Oteros, J., Buters, J., Laven, G., Röseler, S., Wachter, R., Schmidt-Weber, C., Hofmann, F., 2017. Errors in

determining the flow rate of Hirst-type pollen traps. Aerobiologia (Bologna). 33, 201–210. https://doi.org/10.1007/s10453-016-9467-x

Oteros, J., Galán, C., Alcazar, P., Dominguez-Vilches, E., 2013. Quality control in bio-monitoring networks, Spanish Aerobiology Network. Sci. Total Environ. 443, 559–565. https://doi.org/10.1016/j.scitotenv.2012.11.040

Oteros, J., García-Mozo, H., Alcázar, P., Belmonte, J., Bermejo, D., Boi, M., Cariñanos, P., Díaz de la Guardia, C., Fernández-González, D., González-Minero, F., Gutiérrez-Bustillo, A.M., Moreno-Grau, S., Pérez-Badía, R., Rodríguez-Rajo, F.J., Ruíz-Valenzuela, L., Suárex-Pérez, J., Trigo, M.M., Domínguez-Vilches, E., Galán, C., 2015. A new method for determining the sources of airborne particles. J. Environ. Manage. 155, 212–218. https://doi.org/10.1016/j.jenvman.2015.03.037

Oteros, Jose., García-Mozo, H., Botey, R., Mestre, A., Galán, C., 2015. Variations in cereal crop phenology in Spain over the last twenty-six years (1986–2012). Clim. Change 130, 545–558. https://doi.org/10.1007/s10584-015-1363-9

Oteros, J., Sofiev, M., Smith, M., Clot, B., Damialis, A., Prank, M., Werchan, M., Wachter, R., Weber, A., Kutzora, S., Heinze, S., Herr, C.E.W., Menzel, A., Bergmann, K.C., Traidl-Hoffmann, C., Schmidt-Weber, C.B., Buters, J.T.M., 2019b. Building an automatic pollen monitoring network (ePIN): Selection of optimal sites by clustering pollen stations. Sci. Total Environ. 688, 1263–1274. https://doi.org/10.1016/j.scitotenv.2019.06.131

Papaik, M.J., Canham, C.D., 2006. Species resistance and community response to wind disturbance regimes in northern temperate forests. J. Ecol. 94, 1011–1026. https://doi.org/10.1111/j.1365-2745.2006.01153.x

Parducci, L., Alsos, I.G., Unneberg, P., Pedersen, M.W., Han, L., Lammers, Y., Salonen, J.S., Väliranta, M.M., Slotte, T., Wohlfarth, B., 2019. Shotgun environmental DNA, pollen, and macrofossil analysis of lateglacial lake sediments from southern Sweden. Front. Ecol. Evol. 7. https://doi.org/10.3389/fevo.2019.00189

Park, I.W., 2014. Impacts of differing community composition on flowering phenology throughout warm temperate, cool temperate and xeric environments. Glob. Ecol. Biogeogr. 23, 789–801. https://doi.org/10.1111/geb.12163

Park, I.W., Schwartz, M.D., 2015. Long-term herbarium records reveal temperature-dependent changes in flowering phenology in the southeastern USA. Int. J. Biometeorol. 59, 347–355. https://doi.org/10.1007/s00484-014-0846-0

Pashley, C.H., Fairs, A., Edwards, R.E., Bailey, J.P., Corden, J.M., Wardlaw, A.J., 2009. Reproducibility between counts of airborne allergenic pollen from two cities in the East Midlands, UK. Aerobiologia (Bologna). 25, 249–263. https://doi.org/10.1007/s10453-009-9130-x

Pau, S., Edwards, E.J., Still, C.J., 2013. Improving our understanding of environmental controls on the distribution of C3 and C4 grasses. Glob. Chang. Biol. 19, 184–196. https://doi.org/10.1111/gcb.12037

Peel, M.C., Finlayson, B.L., McMahon, T.A., 2007. Updated world map of the Köppen-Geiger climate classification. Hydrol. Earth Syst. Sci. 11, 1633–1644. https://doi.org/10.5194/hess-11-1633-2007

Peel, R.G., Hertel, O., Smith, M., Kennedy, R., 2013. Personal exposure to grass pollen: Relating inhaled dose to background concentration. Ann. Allergy, Asthma Immunol. 111, 548–554. https://doi.org/10.1016/j.anai.2013.09.002

Peel, R.G., Kennedy, R., Smith, M., Hertel, O., 2014a. Do urban canyons influence street level grass pollen concentrations? Int. J. Biometeorol. 58, 1317–1325. https://doi.org/10.1007/s00484-013-0728-x

Peel, R.G., Ørby, P. V, Skjøth, C.A., Kennedy, R., Schlünssen, V., Smith, M., Sommer, J., Hertel, O., 2014b. Seasonal variation in diurnal atmospheric grass pollen concentration profiles. Biogeosciences 11, 821–832. https://doi.org/10.5194/bg-11-821-2014

Peng, Y., Zhang, X., Deng, Y., Ma, X., 2008. Evaluation of genetic diversity in wild orchardgrass (Dactylis glomerata L.) based on AFLP markers. Hereditas 145, 174–181. https://doi.org/10.1111/j.0018-0661.2008.02038.x

Penk, M.R., Perrin, P.M., Kelly, R., O'Neill, F., Waldren, S., 2020. Plant diversity and community composition in temperate northeast Atlantic salt marshes are linked to nutrient concentrations. Appl. Veg. Sci. 23, 3–13. https://doi.org/10.1111/avsc.12459

Pérez, C.F., Gassmann, M.I., Covi, M., 2009. An evaluation of the airborne pollen-precipitation relationship with the superposed epoch method. Aerobiologia (Bologna). 25, 313–320. https://doi.org/10.1007/s10453-009-9135-5

Pilette, C., Nouri-Aria, K.T., Jacobson, M.R., Wilcock, L.K., Detry, B., Walker, S.M., Francis, J.N., Durham, S.R., 2007. Grass Pollen Immunotherapy Induces an Allergen-Specific IgA2 Antibody Response Associated with Mucosal TGF-β Expression. J. Immunol. 178, 4658–4666. https://doi.org/10.4049/jimmunol.178.7.4658

Plaza, M.P., Alcázar, P., Hernández-Ceballos, M.A., Galán, C., 2016. Mismatch in aeroallergens and airborne grass pollen concentrations. Atmos. Environ. 144, 361–369. https://doi.org/10.1016/j.atmosenv.2016.09.008

Pomés, A., Davies, J.M., Gadermaier, G., Hilger, C., Holzhauser, T., Lidholm, J., Lopata, A.L., Mueller, G.A., Nandy, A., Radauer, C., Chan, S.K., Jappe, U., Kleine-Tebbe, J., Thomas, W.R., Chapman, M.D., van Hage, M., van Ree, R., Vieths, S., Raulf, M., Goodman, R.E., 2018. WHO/IUIS Allergen Nomenclature: Providing a common language. Mol. Immunol. 100, 3–13. https://doi.org/10.1016/j.molimm.2018.03.003

Poorter, H., Garnier, E., 1996. Plant growth analysis: an evaluation of experimental design and computational methods. J. Exp. Bot. 47, 1343–1351. https://doi.org/10.1093/jxb/47.9.1343

Prieto-Baena, J.C., Hidalgo, P.J., Domínguez, E., Galán, C., 2003. Pollen production in the Poaceae family. Grana 42, 153–160. https://doi.org/10.1080/00173130310011810

Puc, M., Puc, M.I., 2004. Allergenic Airborne Grass Pollen in Szczencin, Poland. Ann. Agric. Environ. Med. 11, 237–244.

Puppi, G., Zanotti, A.L., 2011. Comparison of phytophenological data: A proposal for converting between GFI and BBCH scales. Ital. J. Agrometeorol. 29.

Puth, M.T., Neuhäuser, M., Ruxton, G.D., 2015. Effective use of Spearman's and Kendall's correlation coefficients forassociation between two measured traits. Anim. Behav. 102, 77–84. https://doi.org/10.1016/j.anbehav.2015.01.010

Radauer, C., Nandy, A., Ferreira, F., Goodman, R.E., Larsen, J.N., Lidholm, J., Pomés, A., Raulf-Heimsoth, M., Rozynek, P., Thomas, W.R., Breiteneder, H., 2014. Update of the WHO/IUIS Allergen Nomenclature Database based on analysis of allergen sequences. Allergy Eur. J. Allergy Clin. Immunol. 69, 413–419. https://doi.org/10.1111/all.12348

Recio, M., Docampo, S., García-Sánchez, J., Trigo, M.M., Melgar, M., Cabezudo, B., 2010. Influence of temperature, rainfall and wind trends on grass pollination in Malaga (western Mediterranean coast). Agric. For. Meteorol. 150, 931–940. https://doi.org/10.1016/j.agrformet.2010.02.012

Ribeiro, H., Cunha, M., Abreu, I., 2003. Airborne pollen concentration in the region of Braga, Portugal, and its relationship with meteorological parameters. Aerobiologia (Bologna). 19, 21–27. https://doi.org/10.1023/A:1022620431167

Ríos, B., Torres-Jardón, R., Ramírez-Arriaga, E., Martínez-Bernal, A., Rosas, I., 2016. Diurnal variations of airborne pollen concentration and the effect of ambient temperature in three sites of Mexico City. Int. J. Biometeorol. 60, 771–787. https://doi.org/10.1007/s00484-015-1061-3

Robert, P., Escoufier, Y., 1976. A Unifying Tool for Linear Multivariate Statistical Methods: The RV-Coefficient. Appl. Stat. 25, 257–265. https://doi.org/10.2307/2347233

Rodionov, A. V., Gnutikov, A.A., Kotsinyan, A.R., Kotseruba, V. V., Nosov, N.N., Punina, E.O., Rayko, M.P., Tyupa, N.B., Kim, E.S., 2017. ITS1–5.8S rDNA–ITS2 sequence in 35S rRNA genes as marker for reconstruction of phylogeny of grasses (Poaceae family). Biol. Bull. Rev. 7, 85–102. https://doi.org/10.1134/s2079086417020062

Rodríguez-Rajo, F.J., Fdez-Sevilla, D., Stach, A., Jato, V., 2010. Assessment between pollen seasons in areas with different urbanization level related to local vegetation sources and differences in allergen exposure. Aerobiologia (Bologna). 26, 1–14. https://doi.org/10.1007/s10453-009-9138-2

Rognli, O.A., Nilsson, N.O., Nurminiemi, M., 2000. Effects of distance and pollen competition on gene flow in the wind-pollinated grass Festuca pratensis Huds. Heredity (Edinb). 85, 550–560. https://doi.org/10.1046/j.1365-2540.2000.00789.x

Rojo, J., Oteros, J., Pérez-Badia, R., Cervigón, P., Ferencova, Z., Gutiérrez-Bustillo, A.M., Bergmann, K.C., Oliver, G., Thibaudon, M., Albertini, R., Rodríguez-De la Cruz, D., Sánchez-Reyes, E., Sánchez-Sánchez, J., Pessi, A.M., Reiniharju, J., Saarto, A., Calderón, M.C., Guerrero, C., Berra, D., Bonini, M., Chiodini, E., Fernández-González, D., García, J., Trigo, M.M., Myszkowska, D., Fernández-Rodríguez, S., Tormo-Molina, R., Damialis, A., Kolek, F., Traidl-Hoffmann, C., Severova, E., Caeiro, E., Ribeiro, H., Magyar, D., Makra, L., Udvardy, O., Alcázar, P., Galán, C., Borycka, K., Kasprzyk, I., Newbigin, E., Adams-Groom, B., Apangu, G.P., Frisk, C.A., Skjøth, C.A., Radišić, P., Šikoparija, B., Celenk, S., Schmidt-Weber, C.B., Buters, J., 2019. Near-ground effect of height on pollen exposure. Environ. Res. 174, 160–169. https://doi.org/10.1016/j.envres.2019.04.027

Rojo, J., Rivero, R., Romero-Morte, J., Fernández-González, F., Pérez-Badia, R., 2017. Modeling pollen time series using seasonal-trend decomposition procedure based on LOESS smoothing. Int. J. Biometeorol. 61, 335–348. https://doi.org/10.1007/s00484-016-1215-y

Rollett, A., Taylor, M., Chambers, B., Litterick, A., 2015. Guidance on Suitable Organic Material Applications for Land Restoration and Improvement: Final Report.

Romero-Morte, J., Rojo, J., Pérez-Badia, R., 2020. Meteorological factors driving airborne grass pollen concentration in central Iberian Peninsula. Aerobiologia (Bologna). 36, 527–540. https://doi.org/10.1007/s10453-020-09647-7

Romero-Morte, J., Rojo, J., Rivero, R., Fernández-González, F., Pérez-Badia, R., 2018. Standardised index for measuring atmospheric grass-pollen emission. Sci. Total Environ. 612, 180–191. https://doi.org/10.1016/j.scitotenv.2017.08.139

Rossignol, N., Andueza, D., Carrère, P., Cruz, P., Duru, M., Fiorelli, J.L., Michaud, A., Plantureux, S., Pottier, E., Baumont, R., 2014. Assessing population maturity of three perennial grass species: Influence of phenology and tiller demography along latitudinal and altitudinal gradients. Grass Forage Sci. 69, 534–548. https://doi.org/10.1111/gfs.12067

Rousseau, D.D., Schevin, P., Duzer, D., Cambon, G., Ferrier, J., Jolly, D., Poulsen, U., 2006. New evidence of long distance pollen transport to southern Greenland in late spring. Rev. Palaeobot. Palynol. 141, 277–286. https://doi.org/10.1016/j.revpalbo.2006.05.001

Rousseau, D.D., Schevin, P., Ferrier, J., Jolly, D., Andreasen, T., Ascanius, S.E., Hendriksen, S.E., Poulsen, U., 2008. Long-distance pollen transport from North America to Greenland in spring. J. Geophys. Res. Biogeosciences 113, 1–10. https://doi.org/10.1029/2007JG000456

Rowney, F.M., Brennan, G.L., Skjøth, C.A., Griffith, G.W., McInnes, R.N., Clewlow, Y., Adams-Groom, B., Barber, A., De Vere, N., Economou, T., Hegarty, M., Hanlon, H.M., Jones, L., Kurganskiy, A., Petch, G.M., Potter, C., Rafiq, A.M., Warner, A., Consortium., T.P., Wheeler, B.W., Osborne, N.J., Creer, S., 2021. Environmental DNA reveals links between abundance and composition of airborne grass pollen and respiratory health. Curr. Biol. 31, 1–9. https://doi.org/10.1016/j.cub.2021.02.019

Rozema, J., Van De Staaij, J., Björn, L.O., Caldwell, M., 1997. UV-B as an environmental factor in plant life: Stress and regulation. Trends Ecol. Evol. 12, 22–28. https://doi.org/10.1016/S0169-5347(96)10062-8

Ruiz-Valenzuela, L., Aguilera, F., 2018. Trends in airborne pollen and pollen-season-related features of anemophilous species in Jaen (south Spain): A 23-year perspective. Atmos. Environ. 180, 234–243. https://doi.org/10.1016/j.atmosenv.2018.03.012

Sabariego, S., Pérez-Badia, R., Bouso, V., Gutiérrez, M., 2011. Poaceae pollen in the atmosphere of Aranjuez, Madrid and Toledo (central Spain). Aerobiologia (Bologna). 27, 221–228. https://doi.org/10.1007/s10453-010-9191-x

Saeys, Y., Inza, I., Larrañaga, P., 2007. A review of feature selection techniques in bioinformatics. Bioinformatics 23, 2507–2517. https://doi.org/10.1093/bioinformatics/btm344

Salisbury, E.J., 1939. Ecological aspects of meteorology. Q. J. R. Meteorol. Soc. 65, 337–358. https://doi.org/10.1002/qj.49706528111

Sánchez-Mesa, J.A., Galan, C., Martínez-Heras, J.A., Hervás-Martínez, C., 2002. The use of a neural network to forecast daily grass pollen concentration in a Mediterranean region: The southern part of the Iberian Peninsula. Clin. Exp. Allergy 32, 1606–1612. https://doi.org/10.1046/j.1365-2222.2002.01510.x

Šauliene, I., Šukiene, L., Daunys, G., Valiulis, G., Vaitkevičius, L., Matavulj, P., Brdar, S., Panic, M., Sikoparija, B., Clot, B., Crouzy, B., Sofiev, M., 2019. Automatic pollen recognition with the Rapid-E particle counter: The first-level procedure, experience and next steps. Atmos. Meas. Tech. 12, 3435–3452. https://doi.org/10.5194/amt-12-3435-2019

Šaulienė, I., Šukienė, L., Kainov, D., Greičiuvienė, J., 2016. The impact of pollen load on quality of life: a questionnaire-based study in Lithuania. Aerobiologia (Bologna). 32, 157–170. https://doi.org/10.1007/s10453-015-9387-1

Ščevková, J., Vašková, Z., Sepšiová, R., Dušička, J., Kováč, J., 2020. Relationship between Poaceae pollen and Phl p 5 allergen concentrations and the impact of weather variables and air pollutants on their levels in the atmosphere. Heliyon 6. https://doi.org/10.1016/j.heliyon.2020.e04421

Schenk, M.F., Gilissen, L.J., Smulders, R.J., America, T.H., 2010. Mass spectrometry and pollen allergies. Expert Rev. Proteomics 7, 627–630. https://doi.org/10.1586/epr.10.32

Schroeder, M.J., 1961. Down-Canyon Afternoon Winds. Bull. Am. Meteorol. Soc. 42, 527–542. https://doi.org/10.1175/1520-0477-42.8.527

Sedgwick, P., 2012. Pearson's correlation coefficient. BMJ 345, 1–2. https://doi.org/10.1136/bmj.e4483

Shapiro, S.S., Wilk, M.B., 1965. An Analysis of Variance Test for Normality (Complete Samples). Biometrika 52, 591–611. https://doi.org/10.2307/2333709

Shoko, C., Mutanga, O., Dube, T., 2016. Progress in the remote sensing of C3 and C4 grass species aboveground biomass over time and space. ISPRS J. Photogramm. Remote Sens. 120, 13–24. https://doi.org/10.1016/j.isprsjprs.2016.08.001

Šikoparija, B., Mimić, G., Panić, M., Marko, O., Radišić, P., Pejak-Šikoparija, T., Pauling, A., 2018. High temporal resolution of airborne Ambrosia pollen measurements above the source reveals emission characteristics. Atmos. Environ. 192, 13–23. https://doi.org/10.1016/j.atmosenv.2018.08.040

Siljamo, P., Sofiev, M., Ranta, H., Linkosalo, T., Kubin, E., Ahas, R., Genikhovich, E., Jatczak, K., Jato, V., Nekovář, J., Minin, A., Severova, E., Shalaboda, V., 2008. Representativeness of point-wise phenological Betula data collected in different parts of Europe. Glob. Ecol. Biogeogr. 17, 489–502. https://doi.org/10.1111/j.1466-8238.2008.00383.x

Silva, J.F., Raventos, J., Caswell, H., Trevisan, M.C., 1991. Population Responses to Fire in a Tropical Savanna Grass, Andropogon semiberbis: A Matrix Model Approach. J. Ecol. 79, 345. https://doi.org/10.2307/2260717

Simoleit, A., Gauger, U., Mücke, H.G., Werchan, M., Obstová, B., Zuberbier, T., Bergmann, K.C., 2016.

Intradiurnal patterns of allergenic airborne pollen near a city motorway in Berlin, Germany. Aerobiologia (Bologna). 32, 199–209. https://doi.org/10.1007/s10453-015-9390-6

Simoleit, A., Werchan, M., Werchan, B., Mücke, H.-G., Gauger, U., Zuberbier, T., Bergmann, K.-C., 2017. Birch, grass, and mugwort pollen concentrations and intradiurnal patterns at two different urban sites in Berlin, Germany. Allergo J. Int. 26, 155–164. https://doi.org/10.1007/s40629-017-0012-4

Sjögren, P., van der Knaap, W.O., van Leeuwen, J.F.N., 2015. Pollen dispersal properties of Poaceae and Cyperaceae: First estimates of their absolute pollen productivities. Rev. Palaeobot. Palynol. 216, 123–131. https://doi.org/10.1016/j.revpalbo.2015.02.004

Skjøth, C.A., Baker, P., Sadyś, M., Adams-Groom, B., 2015. Pollen from alder (Alnus sp.), birch (Betula sp.) and oak (Quercus sp.) in the UK originate from small woodlands. Urban Clim. 14, 414–428. https://doi.org/10.1016/j.uclim.2014.09.007

Skjøth, C.A., Ørby, P. V., Becker, T., Geels, C., Schlünssen, V., Sigsgaard, T., Bønløkke, J.H., Sommer, J., Søgaard, P., Hertel, O., 2013. Identifying urban sources as cause of elevated grass pollen concentrations using GIS and remote sensing. Biogeosciences 10, 541–554. https://doi.org/10.5194/bg-10-541-2013

Skjøth, C.A., Smith, M., Brandt, J., Emberlin, J., 2009. Are the birch trees in Southern England a source of Betula pollen for North London? Int. J. Biometeorol. 53, 75–86. https://doi.org/10.1007/s00484-008-0192-1

Skjøth, C.A., Sommer, J., Frederiksen, L., Gosewinkel Karlson, U., 2012. Crop harvest in Denmark and Central Europe contributes to the local load of airborne Alternaria spore concentrations in Copenhagen. Atmos. Chem. Phys. 12, 11107–11123. https://doi.org/10.5194/acp-12-11107-2012

Skjøth, C.A., Sommer, J., Stach, A., Smith, M., Brandt, J., 2007. The long-range transport of birch (Betula) pollen from Poland and Germany causes significant pre-season concentrations in Denmark. Clin. Exp. Allergy 37, 1204–1212. https://doi.org/10.1111/j.1365-2222.2007.02771.x

Skjøth, C.A., Sun, Y., Karrer, G., Sikoparija, B., Smith, M., Schaffner, U., Müller-Schärer, H., 2019. Predicting abundances of invasive ragweed across Europe using a “top-down” approach. Sci. Total Environ. 686, 212–222. https://doi.org/10.1016/j.scitotenv.2019.05.215

Smilde, A.K., Kiers, H.A.L., Bijlsma, S., Rubingh, C.M., Van Erk, M.J., 2009. Matrix correlations for high-dimensional data: The modified RV-coefficient. Bioinformatics 25, 401–405. https://doi.org/10.1093/bioinformatics/btn634

Smith, D.C., 1944. Pollination and seeds formation in grasses. J. Agric. Res. 68, 79–95.

Smith, M., Cecchi, L., Skjøth, C.A., Karrer, G., Šikoparija, B., 2013. Common ragweed: A threat to environmental health in Europe. Environ. Int. 61, 115–126. https://doi.org/10.1016/j.envint.2013.08.005

Smith, M., Emberlin, J., 2006. A 30-day-ahead forecast model for grass pollen in north London, United Kingdom. Int. J. Biometeorol. 50, 233–242. https://doi.org/10.1007/s00484-005-0010-y

Smith, M., Emberlin, J., Kress, A., 2005. Examining high magnitude grass pollen episodes at Worcester, United Kingdom, using back-trajectory analysis. Aerobiologia (Bologna). 21, 85–94.

https://doi.org/10.1007/s10453-005-4178-8

Smith, M., Emberlin, J., Stach, A., Rantio-Lehtimäki, A., Caulton, E., Thibaudon, M., Sindt, C., Jäger, S., Gehrig, R., Frenguelli, G., Jato, V., Rajo, F.J.R., Alcázar, P., Galán, C., 2009. Influence of the North Atlantic Oscillation on grass pollen counts in Europe. Aerobiologia (Bologna). 25, 321–332. https://doi.org/10.1007/s10453-009-9136-4

Smith, M., Jäger, S., Berger, U., Šikoparija, B., Hallsdottir, M., Sauliene, I., Bergmann, K.C., Pashley, C.H., De Weger, L., Majkowska-Wojciechowska, B., Rybníček, O., Thibaudon, M., Gehrig, R., Bonini, M., Yankova, R., Damialis, A., Vokou, D., Gutiérrez Bustillo, A.M., Hoffmann-Sommergruber, K., Van Ree, R., 2014. Geographic and temporal variations in pollen exposure across Europe. Allergy Eur. J. Allergy Clin. Immunol. 69, 913–923. https://doi.org/10.1111/all.12419

Smith, R.S., Shiel, R.S., Millward, D., Corkhill, P., 2000. The interactive effects of management on the productivity and plant community structure of an upland meadow: An 8-year field trial. J. Appl. Ecol. 37, 1029–1043. https://doi.org/10.1046/j.1365-2664.2000.00566.x

Solomon, W.R., 1984. Aerobiology of pollinosis. J. Allergy Clin. Immunol. 74, 449–461. https://doi.org/10.1016/0091-6749(84)90376-2

Somantri, L., Nandi, N., 2018. Land Use: One of Essential Geography Concept Based on Remote Sensing Technology. IOP Conf. Ser. Earth Environ. Sci. 145. https://doi.org/10.1088/1755-1315/145/1/012039

Somervuo, P., Yu, D.W., Xu, C.C.Y., Ji, Y., Hultman, J., Wirta, H., Ovaskainen, O., 2017. Quantifying uncertainty of taxonomic placement in DNA barcoding and metabarcoding. Methods Ecol. Evol. 8, 398–407. https://doi.org/10.1111/2041-210X.12721

Soreng, R.J., Peterson, P.M., Romaschenko, K., Davidse, G., Teisher, J.K., Clark, L.G., Barberá, P., Gillespie, L.J., Zuloaga, F.O., 2017. A worldwide phylogenetic classification of the Poaceae (Gramineae) II: An update and a comparison of two 2015 classifications. J. Syst. Evol. 55, 259–290. https://doi.org/10.1111/jse.12262

Spearman, C., 1904. The Proof and Measurement of Association Between Two Things. Am. J. Psychol. 15, 72–101.

Spedicato, G.A., 2017. Discrete Time Markov Chains with R. R J. 9, 84–104. https://doi.org/10.32614/RJ-2017-036

Stace, C. a., Al-Bermani, a.-K.K. a., Wilkinson, M.J., 1992. The distinction between the Festuca ovina L. and Festuca rubra L. aggregates in the British Isles. Watsonia 19, 107–112.

Stapledon, R.G., 1928. Cocksfoot Grass (Dactylis Glomerata L.): Ecotypes in Relation to the Biotic Factor. J. Ecol. 16, 71–104.

Stein, A.F., Draxler, R.R., Rolph, G.D., Stunder, B.J.B., Cohen, M.D., Ngan, F., 2015. Noaa's hysplit atmospheric transport and dispersion modeling system. Bull. Am. Meteorol. Soc. https://doi.org/10.1175/BAMS-D-14-00110.1

Stenken, J.A., Poschenrieder, A.J., 2015. Bioanalytical Chemistry of Cytokines-A Review. Anal. Chim. Acta

853, 95–115. https://doi.org/10.1016/j.aca.2014.10.009

Su, L., Yuan, Z., Fung, J.C.H., Lau, A.K.H., 2015. A comparison of HYSPLIT backward trajectories generated from two GDAS datasets. Sci. Total Environ. 506–507, 527–537. https://doi.org/10.1016/j.scitotenv.2014.11.072

Subba Reddi, C., Reddi, N.S., Atluri Janaki, B., 1988. Circadian patterns of pollen release in some species of poaceae. Rev. Palaeobot. Palynol. 54, 11–42. https://doi.org/10.1016/0034-6667(88)90003-6

Suphioglu, C., Mansur, A.H., 2000. What are the important allergens in grass pollen that are linked to human allergic disease? Clin. Exp. Allergy 30, 1335–1341. https://doi.org/10.1046/j.1365-2222.2000.00955.x

Takahashi, Y., Sasaki, K., Nakamura, S., Miki-Hirosige, H., Nitta, H., 1995. Aerodynamic size distribution of the particles emitted from the flowers of allergologically important plants. Grana 34, 45–49. https://doi.org/10.1080/00173139509429032

Talman, C.F., 1922. Meteorology: The Science of the Atmosphere, Vol. I. of. ed. P. F. Collier & Son Company, New York.

Taylor, S.H., Hulme, S.P., Rees, M., Ripley, B.S., Ian Woodward, F., Osborne, C.P., 2010. Ecophysiological traits in C3 and C4 grasses: A phylogenetically controlled screening experiment. New Phytol. 185, 780–791. https://doi.org/10.1111/j.1469-8137.2009.03102.x

Teng, M., Glaum, M.C., Ledford, D.K., 2016. Rapid Molecular Identification and Quantification of Allergenic Pollen By Real-Time PCR. J. Allergy Clin. Immunol. 137, AB119. https://doi.org/10.1016/j.jaci.2015.12.519

Teramura, A.H., Sullivan, J.H., 1994. Effects of UV-B radiation on photosynthesis and growth of terrestrial plants. Photosynth. Res. 39, 463–473. https://doi.org/10.1007/BF00014599

Theuerkauf, M., Dräger, N., Kienel, U., Kuparinen, A., Brauer, A., 2015. Effects of changes in land management practices on pollen productivity of open vegetation during the last century derived from varved lake sediments. Holocene 25, 733–744. https://doi.org/10.1177/0959683614567881

Tng, D.Y.P., Hopf, F., Haberle, S.G., Bowman, D.M.J.S., 2010. Seasonal pollen distribution in the atmosphere of Hobart, Tasmania: Preliminary observations and congruence with flowering phenology. Aust. J. Bot. 58, 440–452. https://doi.org/10.1071/BT10095

Toju, H., Tanabe, A.S., Yamamoto, S., Sato, H., 2012. High-coverage ITS primers for the DNA-based identification of ascomycetes and basidiomycetes in environmental samples. PLoS One 7. https://doi.org/10.1371/journal.pone.0040863

Tooke, F., Battey, N.H., 2010. Temperate flowering phenology. J. Exp. Bot. 61, 2853–2862. https://doi.org/10.1093/jxb/erq165

Topping, M.D., Brostoff, J., Brighton, W.D., Danks, J., Minnis, M., 1978. Allergenic activity of fractions of cocksfoot (Dactylis glomerata) pollen. Clin. Exp. Allergy 8, 33–38. https://doi.org/10.1111/j.1365-2222.1978.tb00445.x

Tormo-Molina, R., Maya-Manzano, J.M., Silva-Palacios, I., Fernández-Rodríguez, S., Gonzalo-Garijo, Á., 2015. Flower production and phenology in Dactylis glomerata. Aerobiologia (Bologna). 31, 469–479. https://doi.org/10.1007/s10453-015-9381-7

Tormo, R., Silva, I., Gonzalo, Á., Moreno, A., Pérez, R., Fernández, S., 2011. Phenological records as a complement to aerobiological data. Int. J. Biometeorol. 55, 51–65. https://doi.org/10.1007/s00484-010-0308-2

Toth, I., Peternel, R., Srnec, L., Vojniković, B., 2011. Diurnal variation in airborne pollen concentrations of the selected taxa in Zagreb, Croatia. Coll. Antropol. 35 Suppl 2, 43–50.

Toth, J., Schultze-Werninghaus, C., Marks, B., Temmel, A.F.P., Stübner, P., Jäger, S., Horak, F., 1998. Environmental priming influences allergenspecific nasal reactivity. Allergy Eur. J. Allergy Clin. Immunol. 53, 1172–1177. https://doi.org/10.1111/j.1398-9995.1998.tb03837.x

Tranquillini, W., 1963. The Physiology of Plants at Higher Altitudes. Annu. Rev. Plant Physiol. 15, 345–362.

Trejo-Calzada, R., O'Connell, M.A., 2005. Genetic diversity of drought-responsive genes in populations of the desert forage Dactylis glomerata. Plant Sci. 168, 1327–1335. https://doi.org/10.1016/j.plantsci.2005.01.010

Tripodi, S., Frediani, T., Lucarelli, S., MacR, F., Pingitore, G., Di Rienzo Businco, A., Dondi, A., Pansa, P., Ragusa, G., Asero, R., Faggian, D., Plebani, M., Matricardi, P.M., 2012. Molecular profiles of IgE to Phleum pratense in children with grass pollen allergy: Implications for specific immunotherapy. J. Allergy Clin. Immunol. 129. https://doi.org/10.1016/j.jaci.2011.10.045

Tseng, Y.T., Kawashima, S., Kobayashi, S., Takeuchi, S., Nakamura, K., 2020. Forecasting the seasonal pollen index by using a hidden Markov model combining meteorological and biological factors. Sci. Total Environ. 698, 1-10. https://doi.org/10.1016/j.scitotenv.2019.134246

Valencia-Barrera, R.M., Comtois, P., Fernaández-Gonzaález, D., 2001. Biogeography and bioclimatology in pollen forecasting. Grana 40, 223–229. https://doi.org/10.1080/001731301317223259

Van de Water, P., Keever, T., Main, C., Levetin, E., 2000. Forecasting Long-Distance Transport of Allergenic Mountain Cedar (Juniperus ashei) Pollen from Source Areas in Central Texas and South-Central Oklahoma. J. Allergy Clin. Immunol. 105, 685. https://doi.org/10.1016/S0091-6749(00)91113-8

Van De Water, P.K., Levetin, E., 2001. Contribution of upwind pollen sources to the characterization of Juniperus ashei phenology. Grana 40, 133–141. https://doi.org/10.1080/00173130152625879

van Hout, R., Chamecki, M., Brush, G., Katz, J., Parlange, M.B., 2008. The influence of local meteorological conditions on the circadian rhythm of corn (Zea mays L.) pollen emission. Agric. For. Meteorol. 148, 1078–1092. https://doi.org/10.1016/j.agrformet.2008.02.009

Van Ree, R., Van Leeuwen, W.A., Aalberse, R.C., 1998. How far can we simplify in vitro diagnostics for grass pollen allergy?: A study with 17 whole pollen extracts and purified natural and recombinant major allergens. J. Allergy Clin. Immunol. 102, 184–190. https://doi.org/10.1016/S0091-6749(98)70084-3

Veriankaitė, L., Siljamo, P., Sofiev, M., Šaulienė, I., Kukkonen, J., 2010. Modelling analysis of source regions of long-range transported birch pollen that influences allergenic seasons in Lithuania. Aerobiologia

(Bologna). 26, 47–62. https://doi.org/10.1007/s10453-009-9142-6

Viner, B.J., Arritt, R.W., 2012. Small-scale circulations caused by complex terrain affect pollen deposition. Crop Sci. 52, 904–913. https://doi.org/10.2135/cropsci2011.07.0354

Viner, B.J., Arritt, R.W., Westgate, M.E., 2017. Examination of climatological wind patterns and simulated pollen dispersion in a complex island environment. Int. J. Biometeorol. 61, 1481–1492. https://doi.org/10.1007/s00484-017-1325-1

Viner, B.J., Westgate, M.E., Arritt, R.W., 2010. A model to predict diurnal pollen shed in maize. Crop Sci. 50, 235–245. https://doi.org/10.2135/cropsci2008.11.0670

Visser, M.E., Caro, S.P., Oers, K. Van, Schaper, S. V., Helm, B., 2010. Phenology, seasonal timing and circannual rhythms: Towards a unified framework. Philos. Trans. R. Soc. B Biol. Sci. 365, 3113–3127. https://doi.org/10.1098/rstb.2010.0111

Voukantsis, D., Niska, H., Karatzas, K., Riga, M., Damialis, A., Vokou, D., 2010. Forecasting daily pollen concentrations using data-driven modeling methods in Thessaloniki, Greece. Atmos. Environ. 44, 5101–5111. https://doi.org/10.1016/j.atmosenv.2010.09.006

Wallace, D. V., Dykewicz, M.S., Bernstein, D.I., Blessing-Moore, J., Cox, L., Khan, D.A., Lang, D.M., Nicklas, R.A., Oppenheimer, J., Portnoy, J.M., Randolph, C.C., Schuller, D., Spector, S.L., Tilles, S.A., 2008. The diagnosis and management of rhinitis: An updated practice parameter. J. Allergy Clin. Immunol. 122, 1–84. https://doi.org/10.1016/j.jaci.2008.06.003

Wang, D., Wang, L., Liu, J., Zhu, H., Zhong, Z., 2018. Grassland ecology in China: Perspectives and challenges. Front. Agric. Sci. Eng. https://doi.org/10.15302/J-FASE-2018205

Wang, K., Sun, J., Cheng, G., Jiang, H., 2011. Effect of altitude and latitude on surface air temperature across the Qinghai-Tibet Plateau. J. Mt. Sci. 8, 808–816. https://doi.org/10.1007/s11629-011-1090-2

Wang, Q., Garrity, G.M., Tiedje, J.M., Cole, J.R., 2007. Naïve Bayesian classifier for rapid assignment of rRNA sequences into the new bacterial taxonomy. Appl. Environ. Microbiol. 73, 5261–5267. https://doi.org/10.1128/AEM.00062-07

Werchan, B., Werchan, M., Mücke, H.G., Gauger, U., Simoleit, A., Zuberbier, T., Bergmann, K.C., 2017. Spatial distribution of allergenic pollen through a large metropolitan area. Environ. Monit. Assess. 189, 1-19. https://doi.org/10.1007/s10661-017-5876-8

West, J.S., Kimber, R.B.E., 2015. Innovations in air sampling to detect plant pathogens. Ann. Appl. Biol. 166, 4–17. https://doi.org/10.1111/aab.12191

White, T. J., Bruns, T., Lee, S., Taylor, J.W., 1990. Amplification and direct sequencing of fungal ribosomal RNA genes for phylogenetics, in: Innis, M.A., Gelfand, D.H., Sninsky, J.J., White, Thomas J. (Eds.), PCR Protocols: A Guide to Methods and Applications. Academic Press, Inc., New York, pp. 315–322.

Wilcoxon, F., 1945. Individual Comparisons by Ranking Methods. Biometrics Bull. 1, 80–83. https://doi.org/10.2307/3001968

Wilson, D., Thomas, R.G., 1971. Flowering responses to daylength and temperature in Dactylis glomerata L. New Zeal. J. Bot. 9, 307–321. https://doi.org/10.1080/0028825X.1971.10429143

Wilson, Z.A., Song, J., Taylor, B., Yang, C., 2011. The final split: The regulation of anther dehiscence. J. Exp. Bot. 62, 1633–1649. https://doi.org/10.1093/jxb/err014

Wodehouse, R.P., 1935. Pollen Grains. Their Structure, identification and significance in Science and Medicine., First. ed. McGraw-Hill Book Company, Inc., New York.

Wu, Y.L., Russell, A.G., 1992. Controlled wind tunnel experiments for particle bounceoff and resuspension. Aerosol Sci. Technol. 17, 245–262. https://doi.org/10.1080/02786829208959574

Yang, R.H., Su, J.H., Shang, J.J., Wu, Y.Y., Li, Y., Bao, D.P., Yao, Y.J., 2018. Evaluation of the ribosomal DNA internal transcribed spacer (ITS), specifically ITS1 and ITS2, for the analysis of fungal diversity by deep sequencing. PLoS One 13, 1–17. https://doi.org/10.1371/journal.pone.0206428

Yilmaz, E., 2011. A systematic study on the monthly mean global solar radiation between latitudes 65S and 65N. Energy Sources, Part A Recover. Util. Environ. Eff. 33, 434–439. https://doi.org/10.1080/15567030903096923

Yokouchi, Y., Shibasaki, M., Noguchi, E., Nakayama, J., Ohtsuki, T., Kamioka, M., Yamakawa-Kobayashi, K., Ito, S., Takeda, K., Ichikawa, K., Nukaga, Y., Matsui, A., Hamaguchi, H., Arinami, T., 2002. A genome-wide linkage analysis of orchard grass-sensitive childhood seasonal allergic rhinitis in Japanese families. Genes Immun. 3, 9–13. https://doi.org/10.1038/sj.gene.6363815

Zanotti, A.L., Puppi, G., 2000. Phenological surveys of allergenic species in the neighbourhood of Bologna (Italy). Aerobiologia (Bologna). 16, 199–206. https://doi.org/10.1023/A:1007659611624

Zerboni, R., Arrigoni, P. V., Manfredi, M., Rizzotto, M., Paoletti, L., Ricceri, C., 1991. Geobotanical and phenological monitoring of allergenic pollen grains in the florence area. Grana 30, 357–363. https://doi.org/10.1080/00173139109431991

Zhang, J., Zhang, M., Li, Y., Fang, C., 2020. Comparison of wind characteristics at different heights of deep-cut canyon based on field measurement. Adv. Struct. Eng. 23, 219–233. https://doi.org/10.1177/1369433219868074

Zhang, R., Duhl, T., Salam, M.T., House, J.M., Flagan, R.C., Avol, E.L., Gilliland, F.D., Guenther, A., Chung, S.H., Lamb, B.K., VanReken, T.M., 2014. Development of a regional-scale pollen emission and transport modeling framework for investigating the impact of climate change on allergic airway disease. Biogeosciences 11, 1461–1478. https://doi.org/10.5194/bg-11-1461-2014

Zhang, Y., Bielory, L., Cai, T., Mi, Z., Georgopoulos, P., 2015. Predicting onset and duration of airborne allergenic pollen season in the United States. Atmos. Environ. 103, 297–306. https://doi.org/10.1016/j.atmosenv.2014.12.019

Zhao, X., Bushman, B.S., Zhang, X., Robbins, M.D., Larson, S.R., Robins, J.G., Thomas, A., 2017. Association of candidate genes with heading date in a diverse Dactylis glomerata population. Plant Sci. 265, 146–153. https://doi.org/10.1016/j.plantsci.2017.10.002

Supplementary Material

Supplementary Figure S1. Burkard Volumetric Spore Trap of Hirst Design, utilized for pollen monitoring.

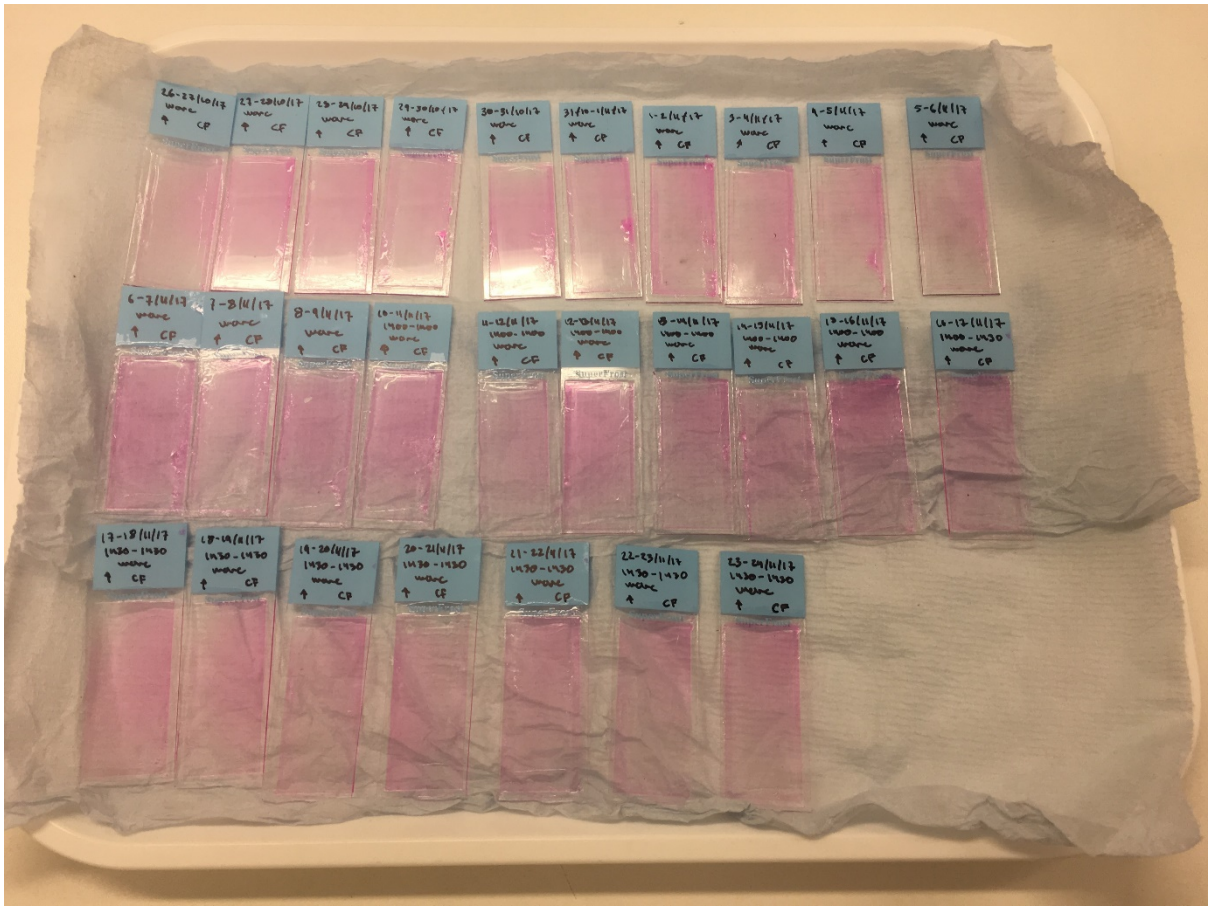

Supplementary Figure S2. Pollen microscopy slides created during the pollen monitoring process.

Supplementary Figure S3. Campbell Scientific meteorological logger station with associated sensors. Placement in photograph is in City Campus, University of Worcester.

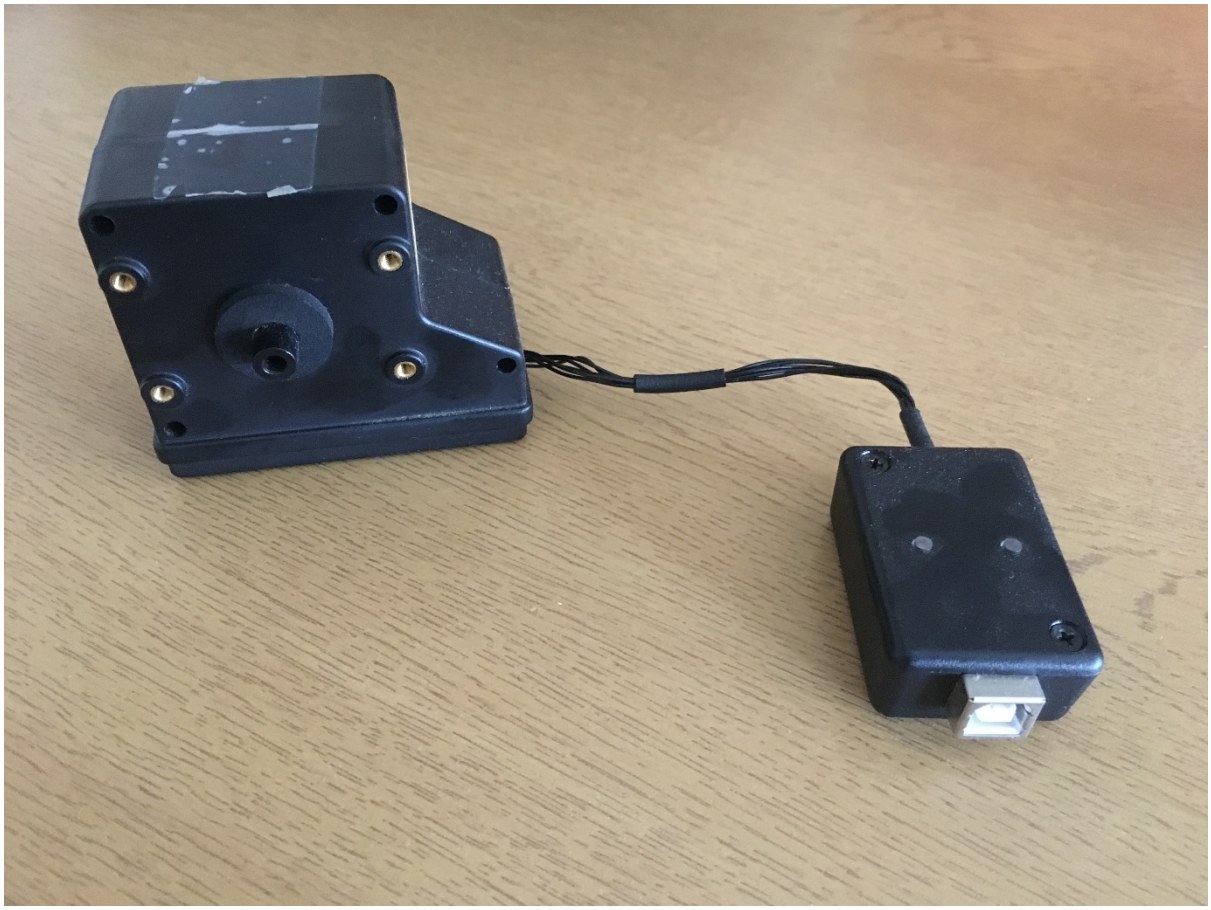

Supplementary Figure S4. AlphaSense Hi-Range particle counter with associated connector.

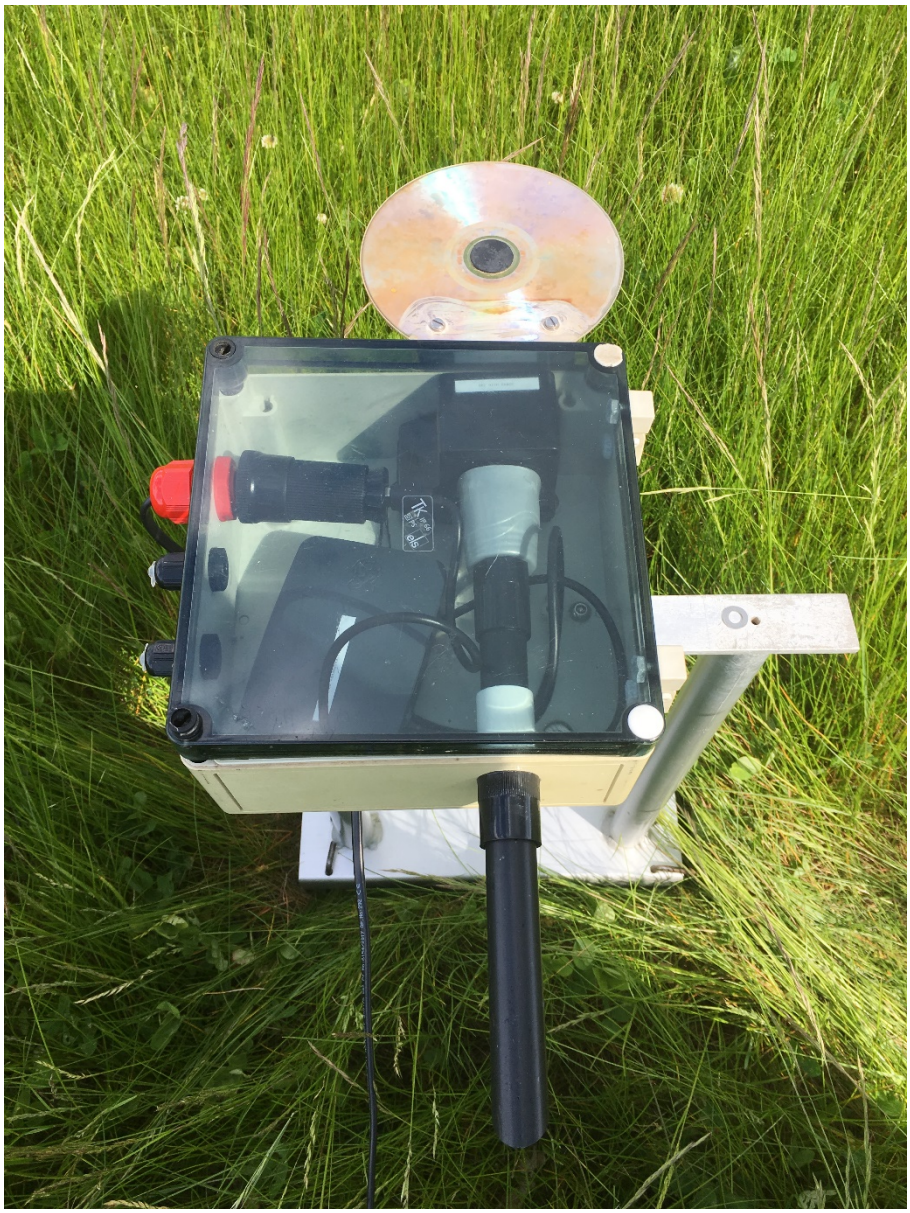

Supplementary Figure S5. One of the two particle counter set-ups used in the artificial circle/Field in Lakeside.

Supplementary Figure S6. The particle counter set-up used in placement 3/TriPod in Lakeside.

Supplementary Figure S7. *Dactylis glomerata* flowering location St Johns during the 2017 sampling campaign.

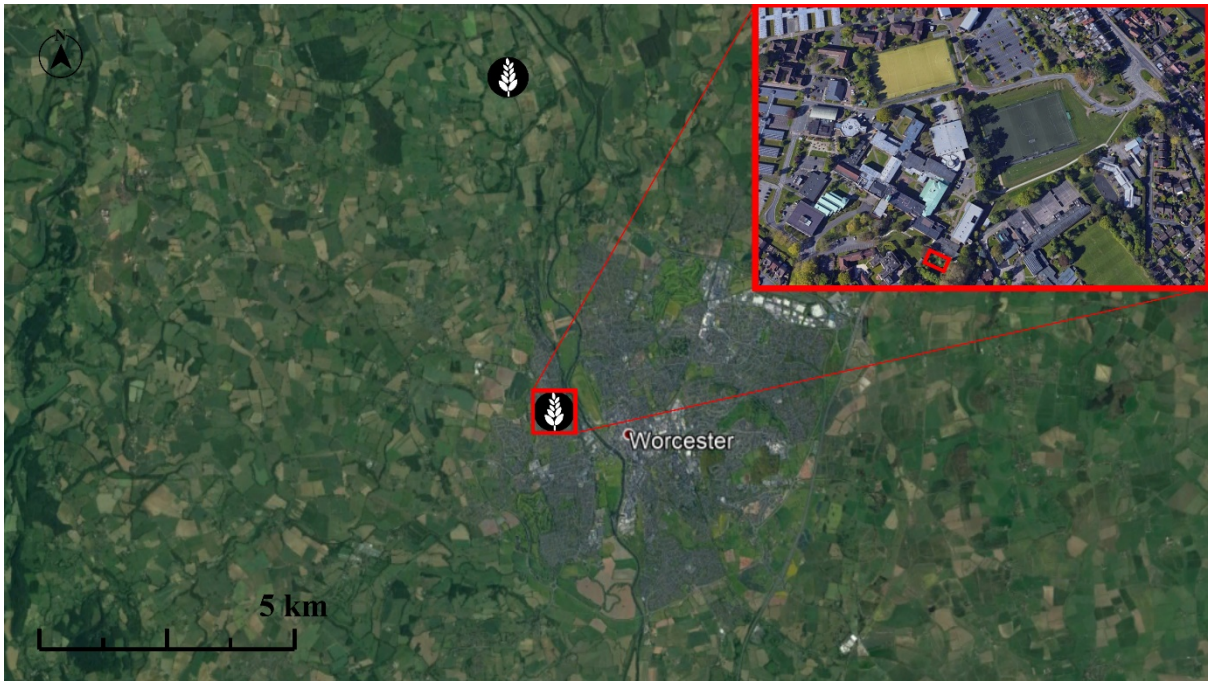

Supplementary Figure S8. One of the two main locations during the *Dactylis glomerata* 2018 sampling campaign, St Johns.

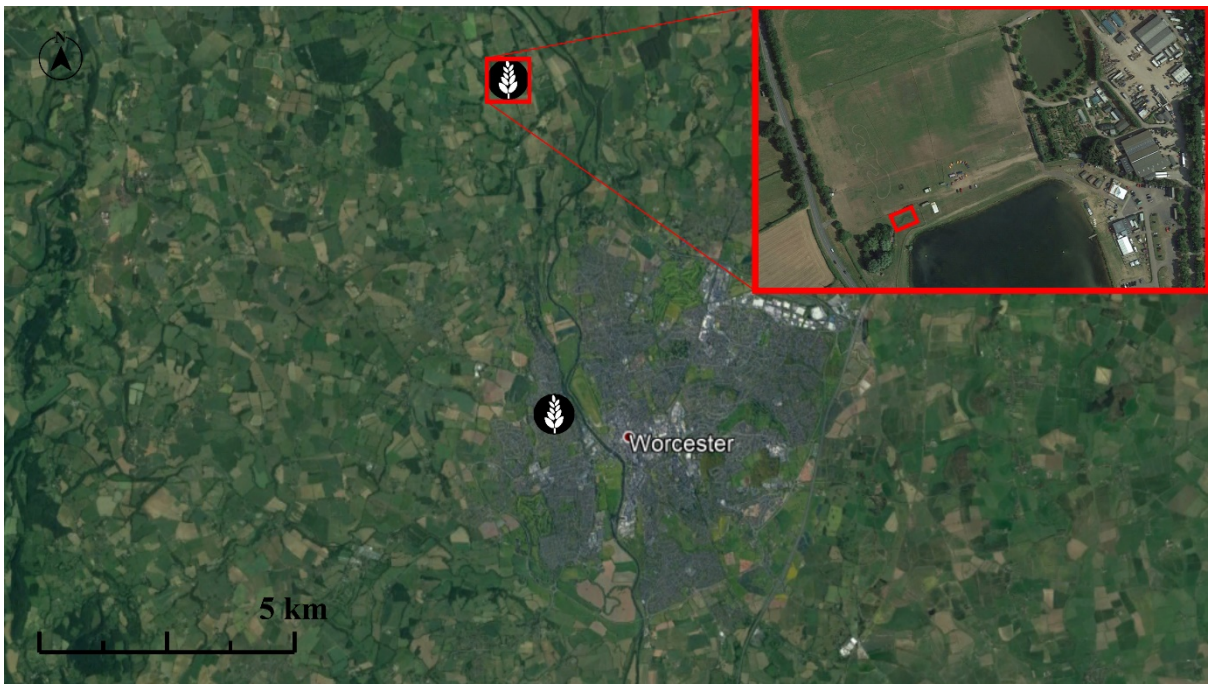

Supplementary Figure S9. One of the two main locations during the *Dactylis glomerata* 2018 sampling campaign, Lakeside.

Supplementary Figure S10. One of the six secondary locations during the *Dactylis glomerata* 2018 sampling campaign, Lower Lakeside.

Supplementary Figure S11. One of the six secondary locations during the *Dactylis glomerata* 2018 sampling campaign, Football Field.

Supplementary Figure S12. One of the six secondary locations during the *Dactylis glomerata* 2018 sampling campaign, Upper Bridge.

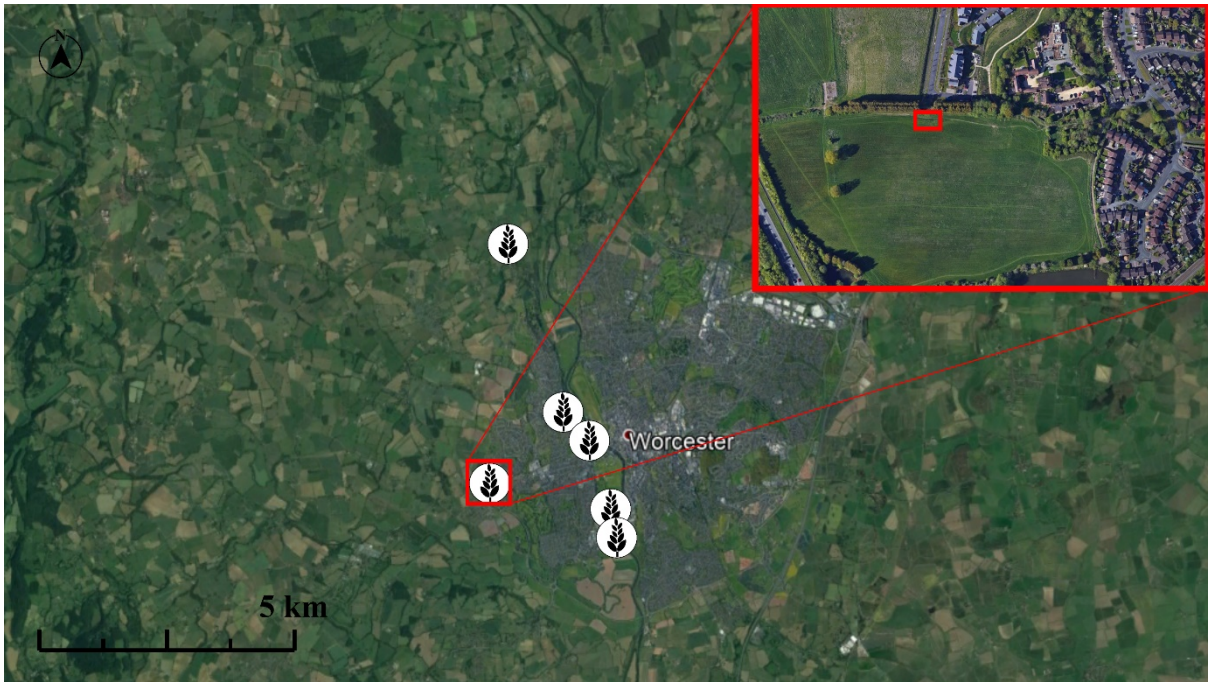

Supplementary Figure S13. One of the six secondary locations during the *Dactylis glomerata* 2018 sampling campaign, West Field.

Supplementary Figure S14. One of the six secondary locations during the *Dactylis glomerata* 2018 sampling campaign, Lower Field.

Supplementary Figure S15. One of the six secondary locations during the *Dactylis glomerata* 2018 sampling campaign, Lower Bridge.

Supplementary Figure S16. *Dactylis glomerata* flowering location St Johns during the 2018 sampling campaign.

Supplementary Figure S17. *Dactylis glomerata* flowering location Lakeside during the 2018 sampling campaign.

Supplementary Figure S18. *Dactylis glomerata* flowering location Lower Lakeside during the 2018 sampling campaign.

Supplementary Figure S19. *Dactylis glomerata* flowering location Football Field during the 2018 sampling campaign.

Supplementary Figure S20. *Dactylis glomerata* flowering location Upper Bridge during the 2018 sampling campaign.

Supplementary Figure S21. *Dactylis glomerata* flowering location West Field during the 2018 sampling campaign.

Supplementary Figure S22. *Dactylis glomerata* flowering location Lower Field during the 2018 sampling campaign.

Supplementary Figure S23. *Dactylis glomerata* flowering location Lower Bridge during the 2018 sampling campaign.

Supplementary Table S1.

Species list and associated information regarding the botanical inventories conducted in the Lakeside Circle artificial field study in 2018 and 2019.

Type	Species	Species	Abundance Cover 2018	Abundance Cover 2019	Pollination
Grass, Herb, Other	Latin	English [American, United Kingdom]	Miniscule, Minor, Major	Miniscule, Minor, Major	Anemophily, Entomophily
Grass	Agrostis capillaris	Common bent	N/A	Miniscule	Anemophily
Grass	Bromus hordeaceus	Soft brome, Bull grass	Miniscule	Miniscule	Anemophily
Grass	Dactylis glomerata	Cock's-foot, Orchard grass	Miniscule	N/A	Anemophily
Grass	Festuca rubra	Red festue, Creeping red fescue	Major	Major	Anemophily
Grass	Holcus lanatus	Yorkshire fog, Tufted grass, Meadow soft grass	Miniscule	Miniscule	Anemophily
Grass	Lolium perenne	Perennial ryegrass, English ryegrass	Major	Major	Anemophily
Grass	Phleum pratense	Timothy, Meadow cat's-tail	Minor	N/A	Anemophily
Grass	Poa annua	Annual meadow grass	Major	Minor	Anemophily
Grass	Poa trivialis	Rough bluegrass, Rough-stalked meadow-grass	Minor	Minor	Anemophily
Herb	Achillea millifolium	Yarrow, Common yarrow	Miniscule	Miniscule	Entomophily
Herb	Artemisia vulgaris	Common mugwort, Common Wormwood	Minor	Minor	Anemophily
Herb	Bellis perennis	Common daisy, Lawn daisy, English daisy	Minor	Miniscule	Entomophily
Herb	Capsella bursa-pastoris	Shepard's Purse	N/A	Miniscule	Entomophily
Herb	Cerastium fontanum	Common Mouse-Ear	N/A	Miniscule	Entomophily
Herb	Coronopus squamatus	Swine Cress	N/A	Miniscule	Entomophily

Supplementary Table S1 cont. 2/2.

Type	Species	Species	Abundance Cover 2018	Abundance Cover 2019	Pollination
Grass, Herb, Other	Latin	English [American, United Kingdom]	Miniscule, Minor, Major	Miniscule, Minor, Major	Anemophily, Entomophily
Herb	Crepis capillaris	Smooth hawksbeard	Minor	Minor	Entomophily
Herb	Geranium pusillum	Small-flowered Crane's-bill	N/A	Miniscule	Entomophily
Herb	Jacobaea vulgaris	Common ragwort	N/A	Miniscule	Entomophily
Herb	Lathyrus hirsutus	Hairy Vetchling	N/A	Minor	Entomophily
Herb	Malva sylvestris	Common mallow	Miniscule	Miniscule	Entomophily
Herb	Medicago lupulina	Black medick, Nonesuch, Hop clover	Major	N/A	Entomophily
Herb	Plantago lanceolata	Ribword Plantain	N/A	Minor	Anemophily
Herb	Rumex conglomeratus	Clustered dock, Sharp dock	Miniscule	Miniscule	Anemophily
Herb	Rumex obtusifolius	Bitter dock, Broad-leaved dock	Minor	Minor	Anemophily
Herb	Silene latifolia	White campion	Miniscule	Miniscule	Entomophily
Herb	Sonchus asper	Prickly sow-thistle, Rough sow-thistle	Minor	Minor	Entomophily
Herb	Taraxacum officinale	Common dandelion	Minor	Minor	Entomophily
Herb	Trifolium hybridum	Alsike clover	Minor	Minor	Entomophily
Herb	Trifolium repens	White clover	Major	Major	Entomophily
Herb	Veronica persica	Common Field Speedwell	N/A	Miniscule	Entomophily
Other	Calliergonella Moss	Calliergonella cuspidata	N/A	Miniscule	Anemophily

Supplementary Figure S24. Burkard MultiVial Cyclone active sampler, exterior, utilized for eDNA sampling.

Supplementary Figure S25. Burkard MultiVial Cyclone active sampler, interior, utilized for eDNA sampling.

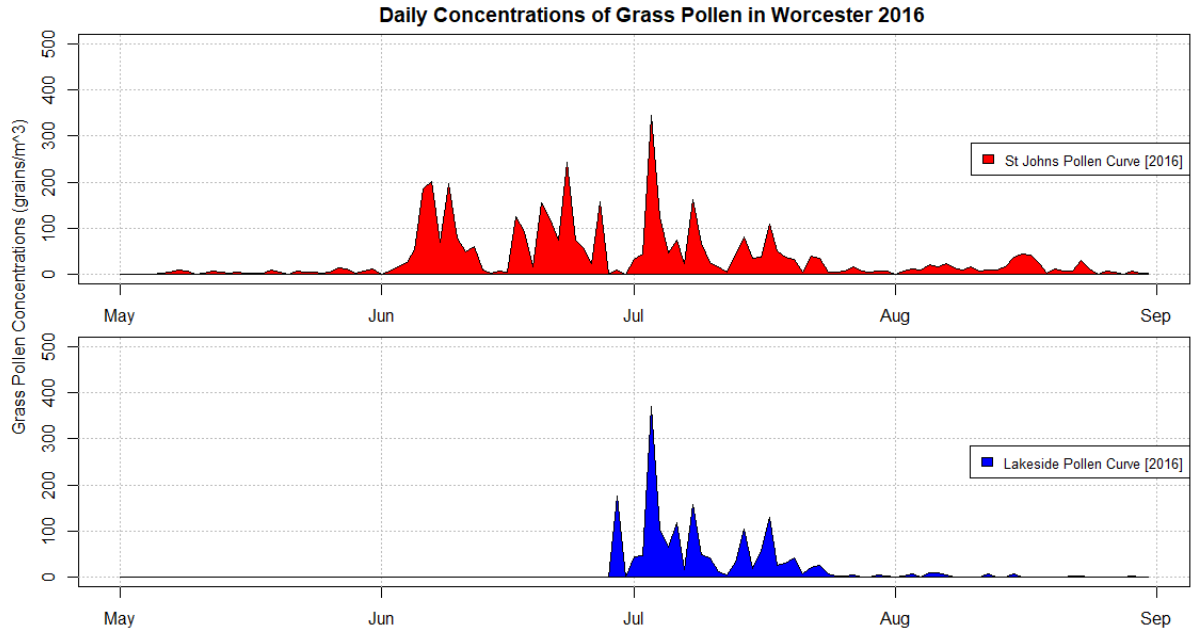

Supplementary Figure S26. Daily concentrations of grass pollen from two locations (St Johns and Lakeside) during the 2016 season in Worcester.

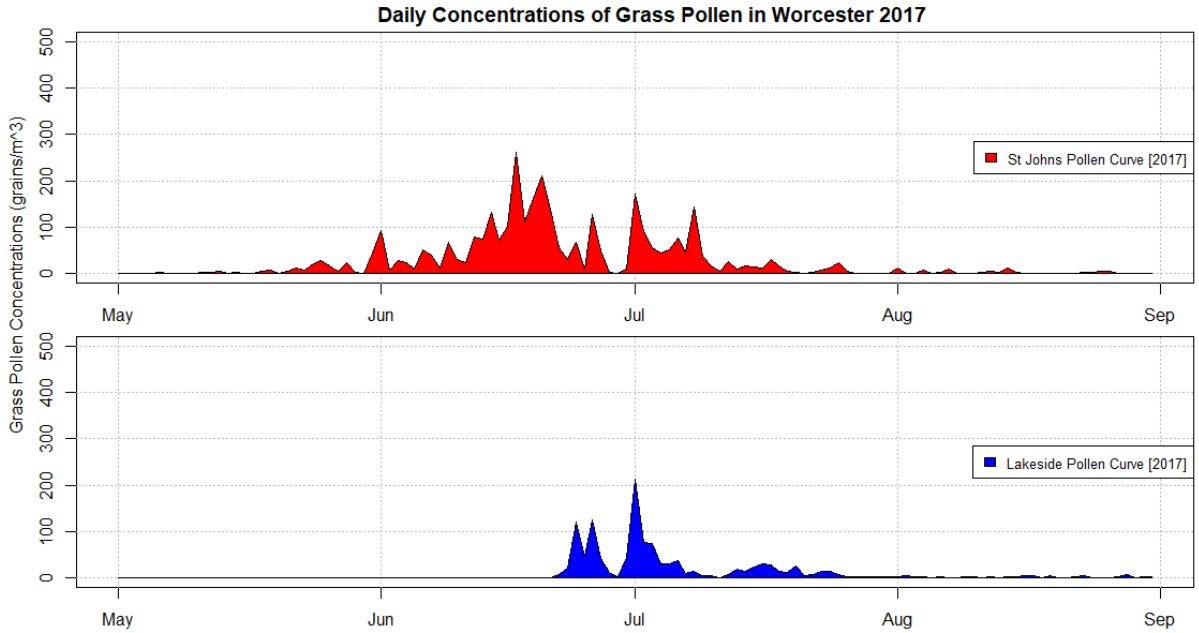

Supplementary Figure S27. Daily concentrations of grass pollen from two locations (St Johns and Lakeside) during the 2017 season in Worcester.

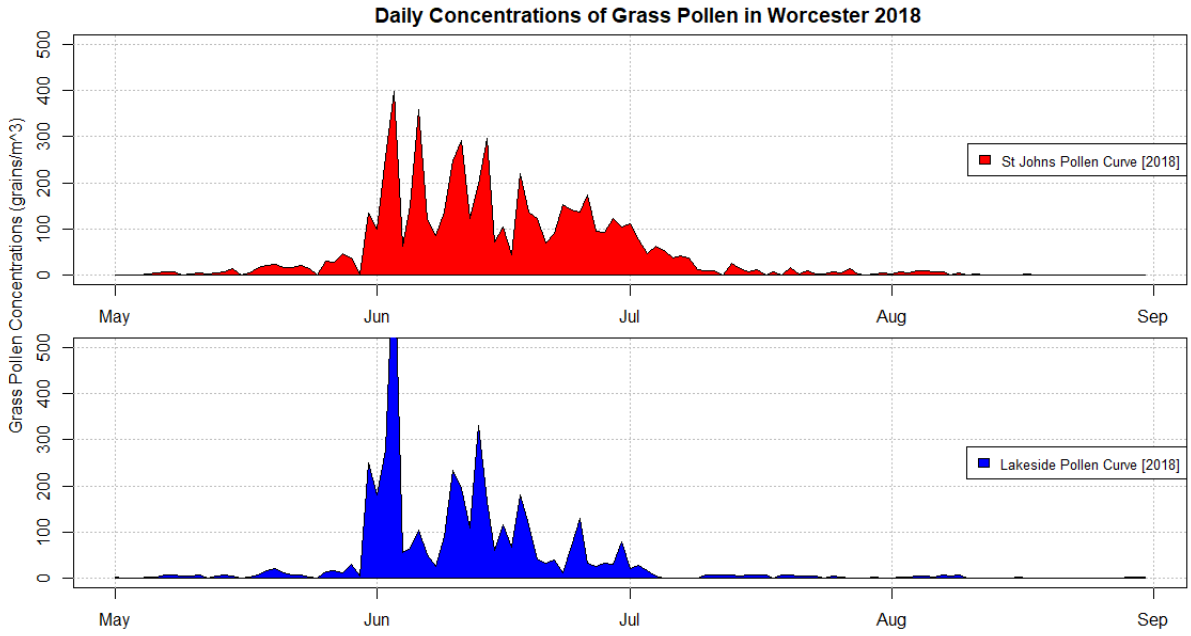

Supplementary Figure S28. Daily concentrations of grass pollen from two locations (St Johns and Lakeside) during the 2018 season in Worcester.

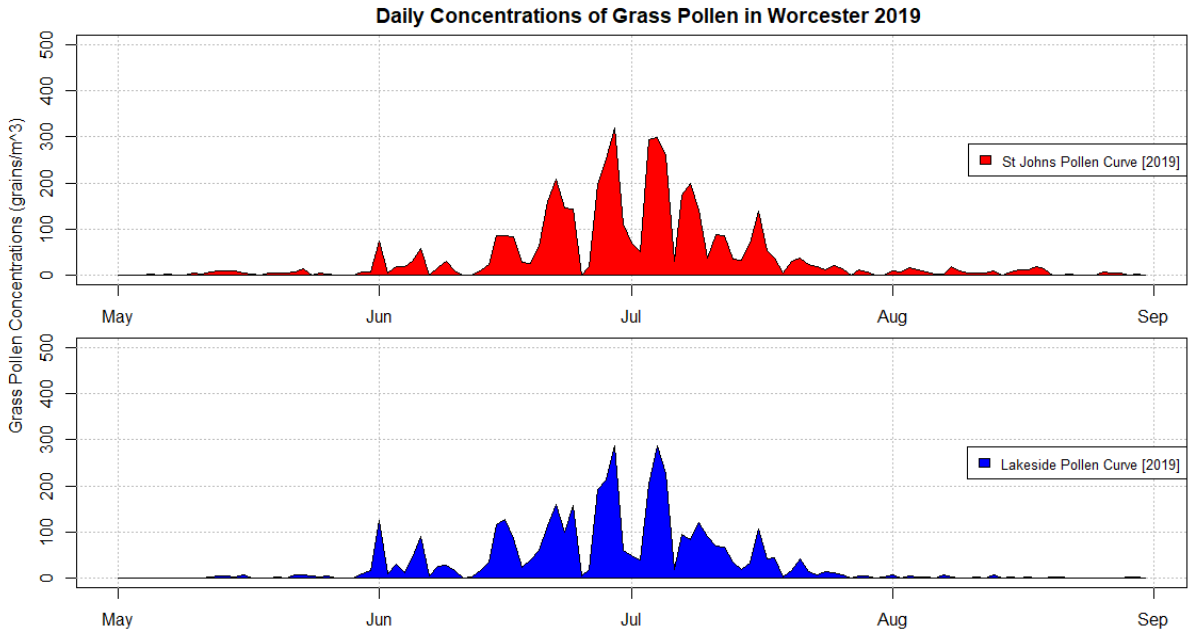

Supplementary Figure S29. Daily concentrations of grass pollen from two locations (St Johns and Lakeside) during the 2019 season in Worcester.

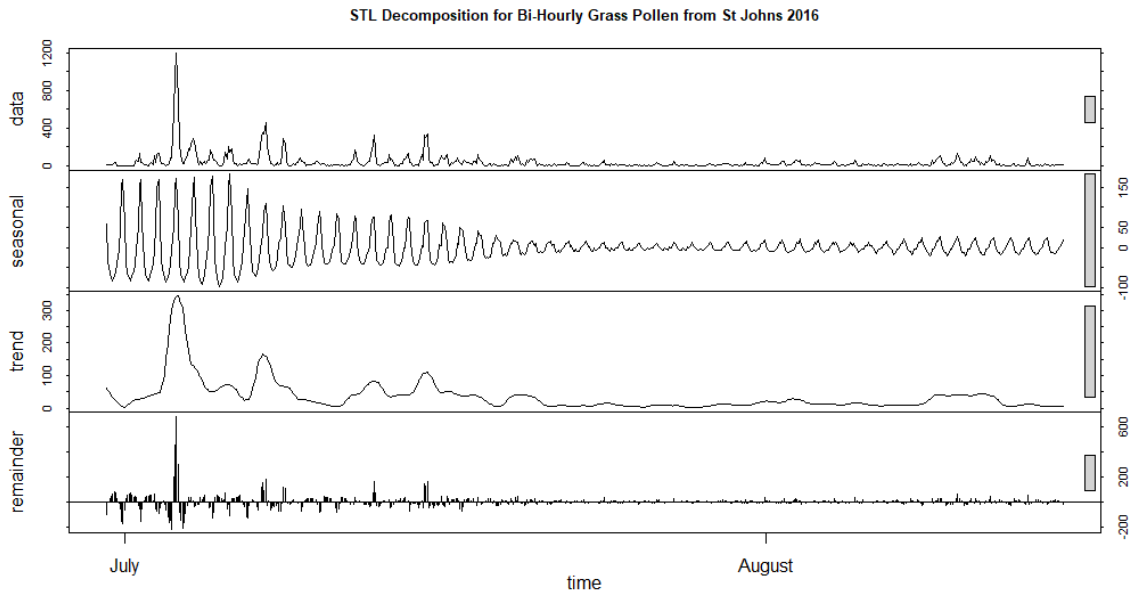

Supplementary Figure S30. STL Decomposition for the 95% overlapping period of bi-hourly grass pollen concentrations for St Johns during the 2016 season in Worcester.

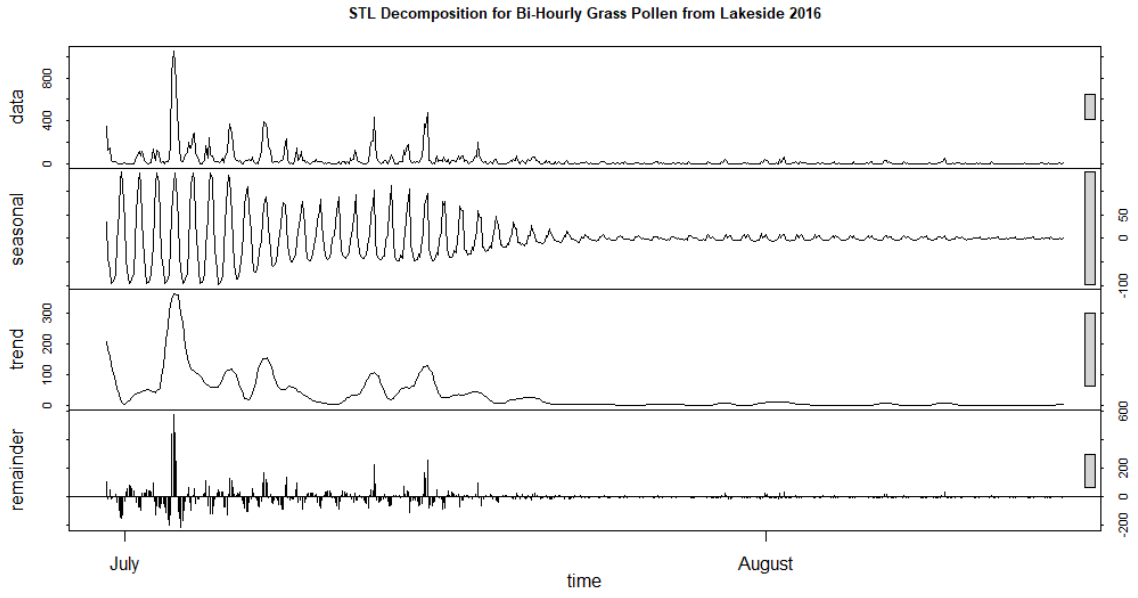

Supplementary Figure S31. STL Decomposition for the 95% overlapping period of bi-hourly grass pollen concentrations for Lakeside during the 2016 season in Worcester.

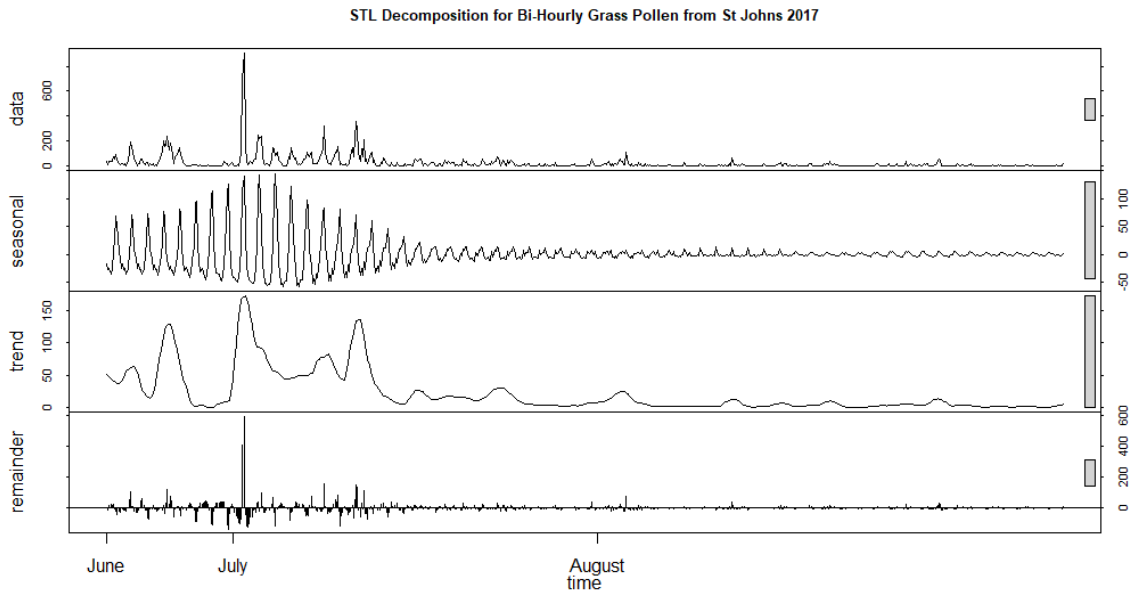

Supplementary Figure S32. STL Decomposition for the 95% overlapping period of bi-hourly grass pollen concentrations for St Johns during the 2017 season in Worcester.

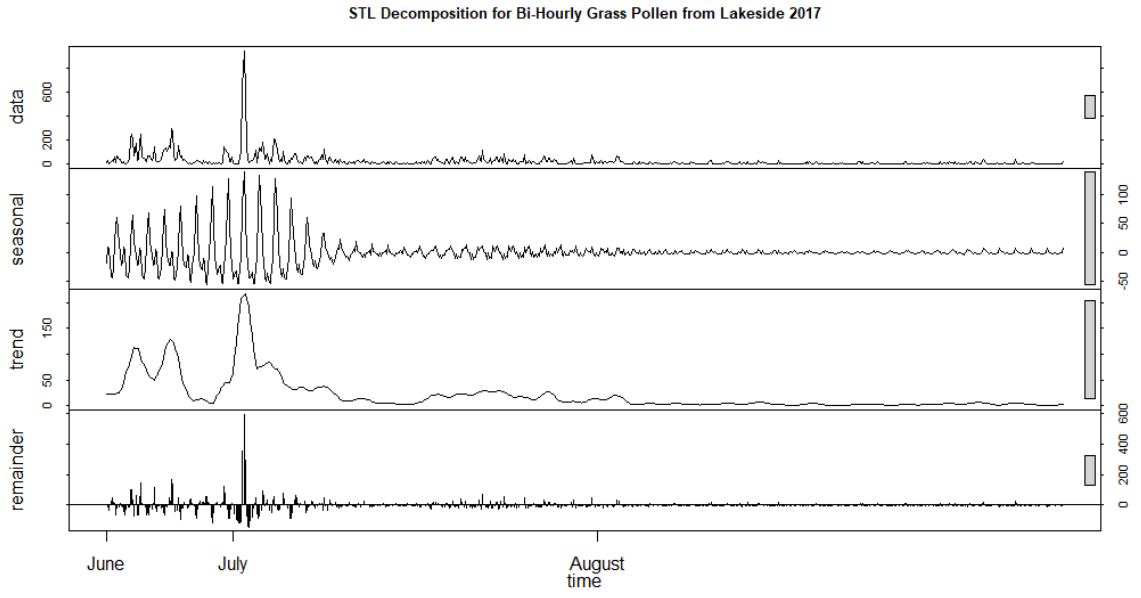

Supplementary Figure S33. STL Decomposition for the 95% overlapping period of bi-hourly grass pollen concentrations for Lakeside during the 2017 season in Worcester.

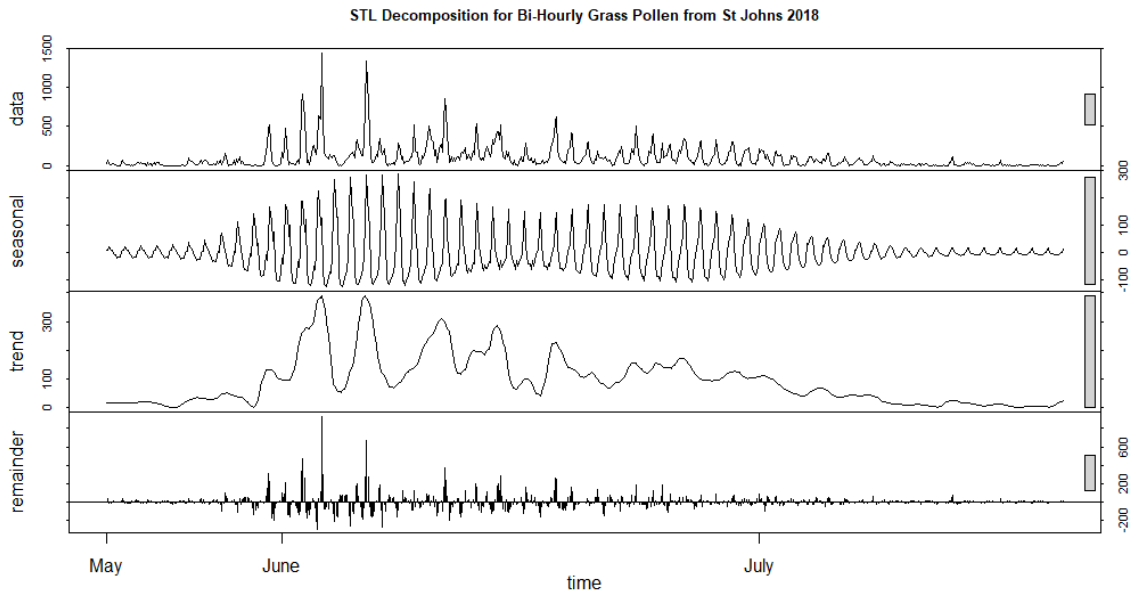

Supplementary Figure S34. STL Decomposition for the 95% overlapping period of bi-hourly grass pollen concentrations for St Johns during the 2018 season in Worcester.

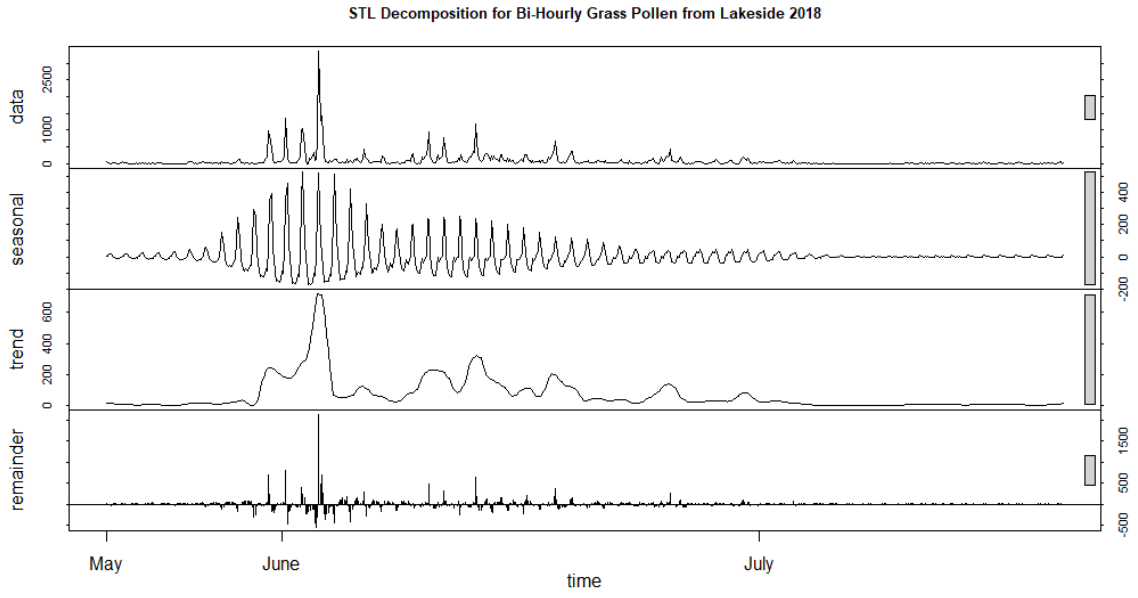

Supplementary Figure S35. STL Decomposition for the 95% overlapping period of bi-hourly grass pollen concentrations for Lakeside during the 2018 season in Worcester.

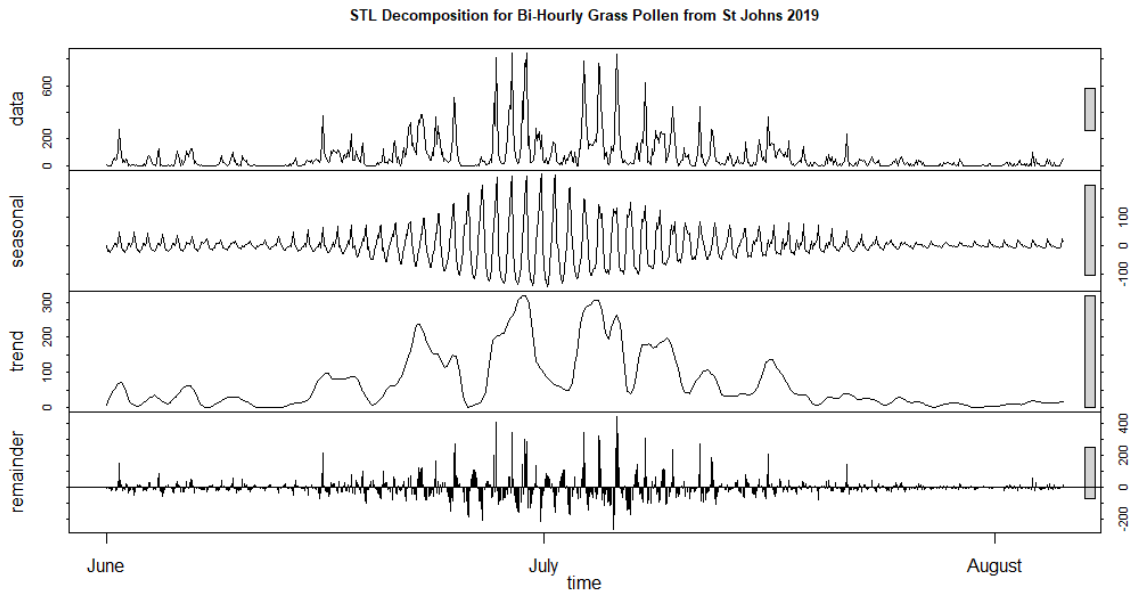

Supplementary Figure S36. STL Decomposition for the 95% overlapping period of bi-hourly grass pollen concentrations for St Johns during the 2019 season in Worcester.

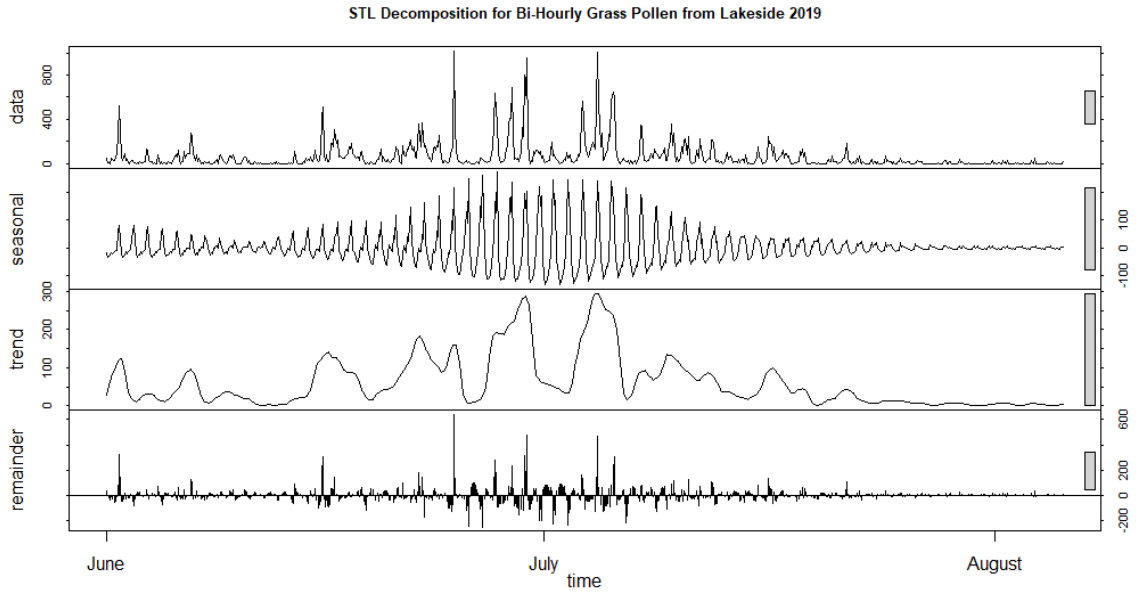

Supplementary Figure S37. STL Decomposition for the 95% overlapping period of bi-hourly grass pollen concentrations for Lakeside during the 2019 season in Worcester.

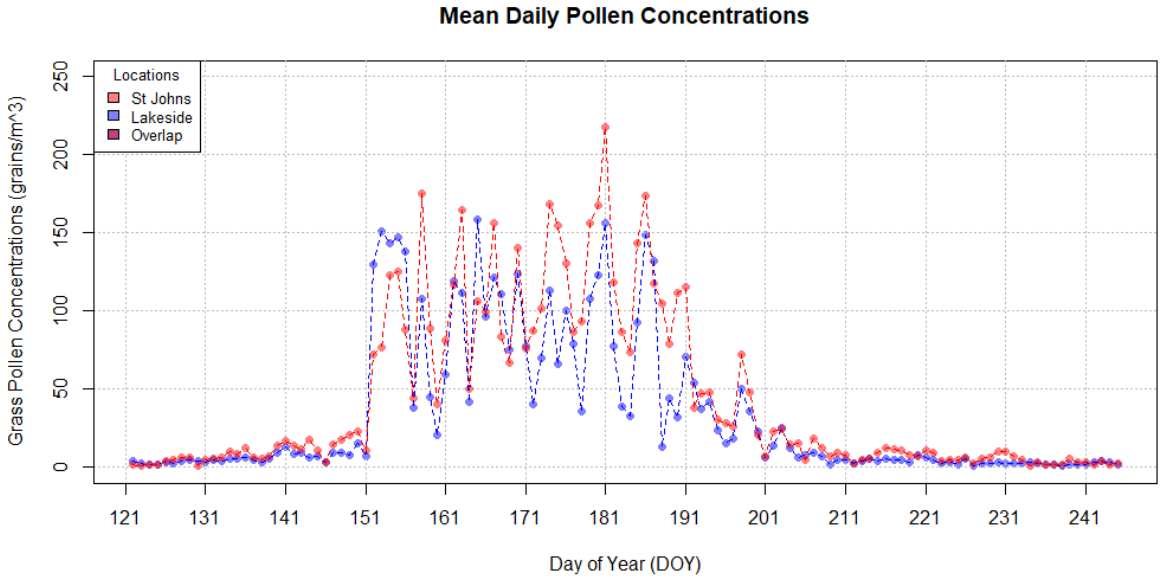

Supplementary Figure S38. Comparison of mean daily grass pollen concentrations for St Johns and Lakeside, averaged between all bi-hourly and years values.

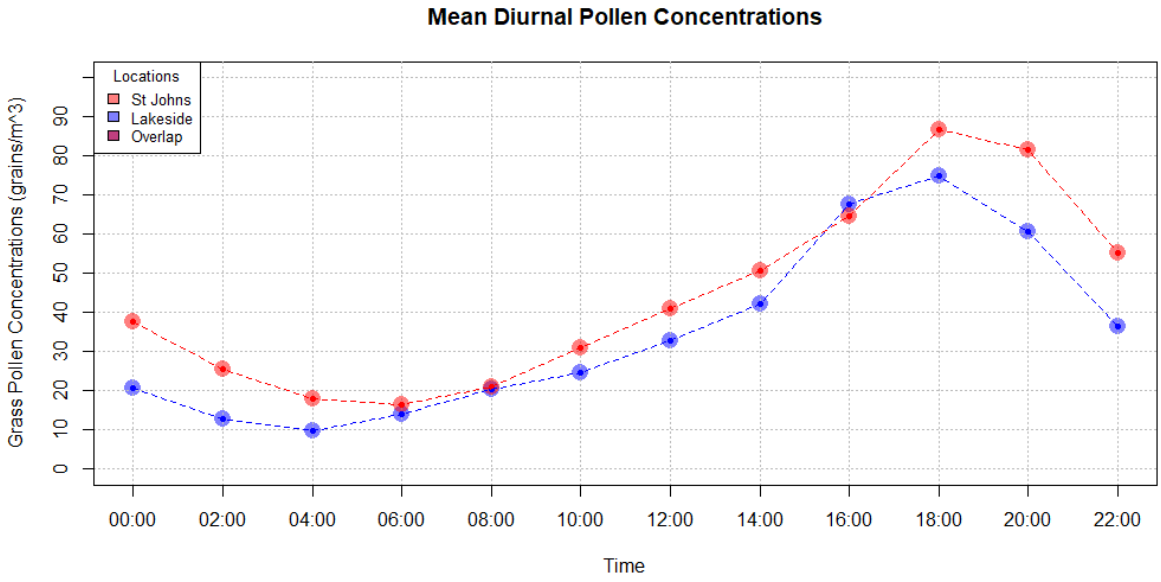

Supplementary Figure S39. Comparison of mean diurnal grass pollen concentrations for St Johns and Lakeside, averaged between all daily and yearly values.

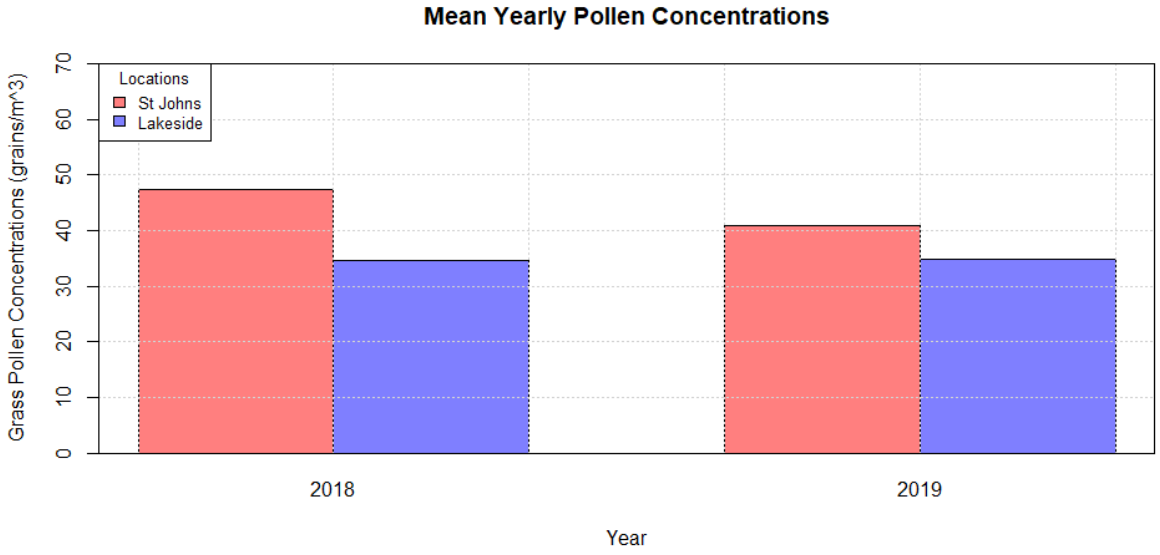

Supplementary Figure S40. Comparison of mean year grass pollen concentrations for St Johns and Lakeside, averaged between all bi-hourly and daily values.

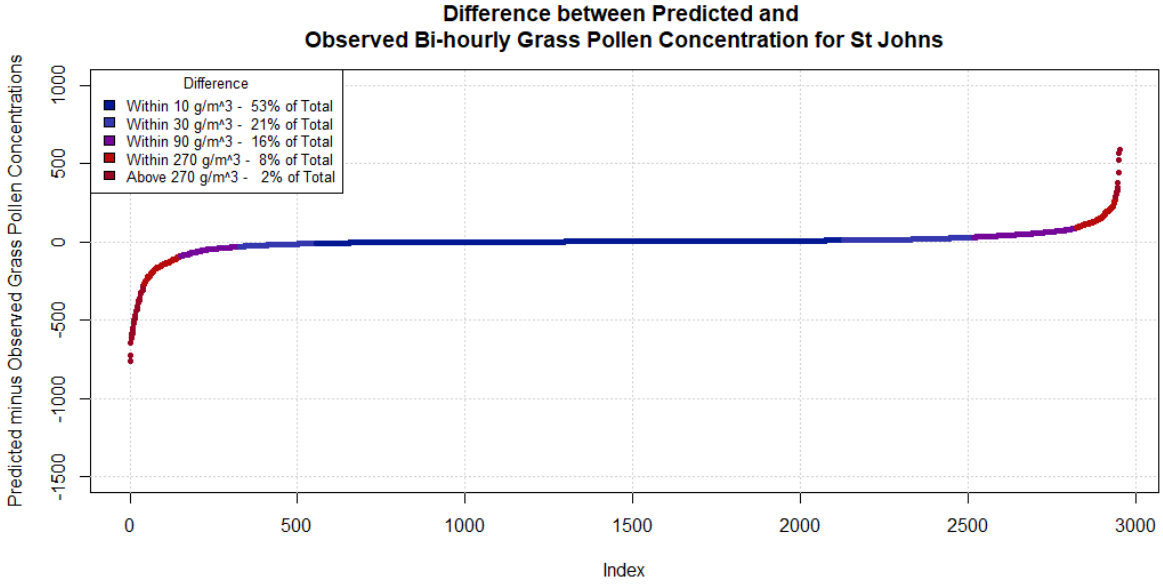

Supplementary Figure S41. Difference between predicted and observed bi-hourly grass pollen concentrations for St Johns, modelled using the generalized linear mixed-model. Extension of Figure 28.

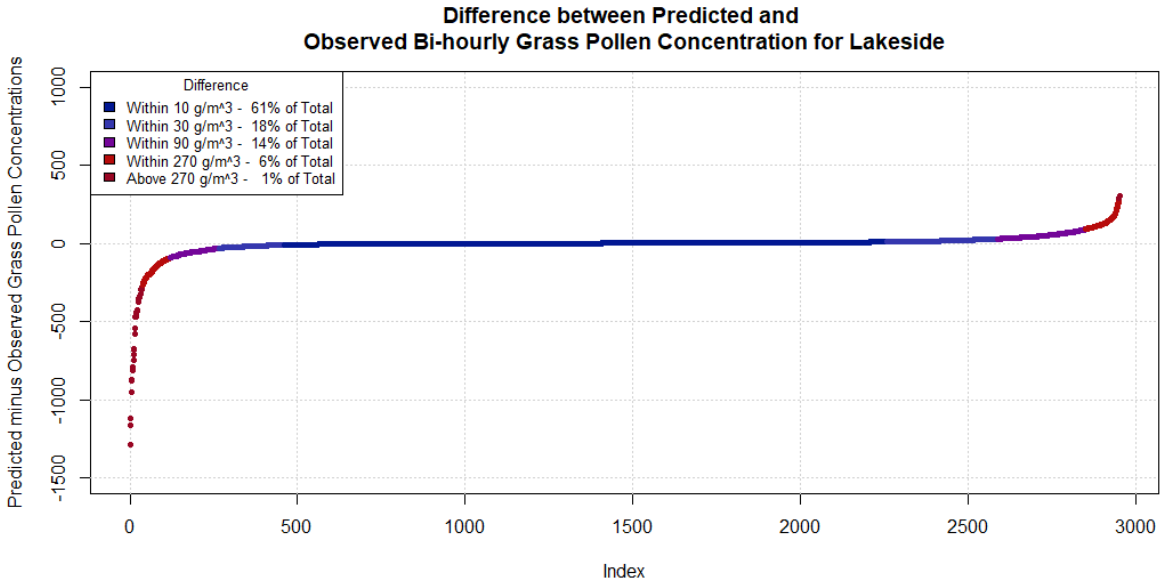

Supplementary Figure S42. Difference between predicted and observed bi-hourly grass pollen concentrations for Lakeside, modelled using the generalized linear mixed-model. Extension of Figure 29.

Supplementary Table S2

Breusch-Godfrey serial correlation statistics for different time lags on the remainder of the STL Decomposition in relation to the autocorrelation for the 95% seasonal Bi-hourly grass pollen concentration overlaps between St Johns and Lakeside for the years 2016-2019.

Order	LM-Statistic				P-Value			
	2016	2017	2018	2019	2016	2017	2018	2019
Order 1	134.88	32.24	126.99	97.74	< 0.001	< 0.001	< 0.001	< 0.001
Order 2	175.48	63.99	210.34	120.25	< 0.001	< 0.001	< 0.001	< 0.001
Order 3	214.31	70.06	215.84	142.61	< 0.001	< 0.001	< 0.001	< 0.001
Order 4	218.86	86.88	238.71	157.98	< 0.001	< 0.001	< 0.001	< 0.001
Order 5	228.65	93.80	252.21	173.75	< 0.001	< 0.001	< 0.001	< 0.001
Order 6	250.41	96.85	253.36	177.02	< 0.001	< 0.001	< 0.001	< 0.001
Order 7	252.86	102.42	253.89	181.33	< 0.001	< 0.001	< 0.001	< 0.001
Order 8	261.35	107.67	257.89	187.49	< 0.001	< 0.001	< 0.001	< 0.001
Order 9	267.05	112.56	257.94	201.08	< 0.001	< 0.001	< 0.001	< 0.001
Order 10	267.89	113.47	263.66	219.98	< 0.001	< 0.001	< 0.001	< 0.001
Order 11	278.94	118.97	283.06	262.01	< 0.001	< 0.001	< 0.001	< 0.001
Order 12	295.80	186.57	297.36	278.32	< 0.001	< 0.001	< 0.001	< 0.001
Order 13	296.25	186.69	298.05	278.34	< 0.001	< 0.001	< 0.001	< 0.001
Order 14	300.82	189.55	300.73	279.64	< 0.001	< 0.001	< 0.001	< 0.001
Order 15	307.18	191.49	304.95	285.08	< 0.001	< 0.001	< 0.001	< 0.001
Order 16	309.06	191.71	309.49	285.71	< 0.001	< 0.001	< 0.001	< 0.001
Order 17	310.25	193.05	312.70	287.91	< 0.001	< 0.001	< 0.001	< 0.001
Order 18	310.29	193.36	313.46	289.78	< 0.001	< 0.001	< 0.001	< 0.001
Order 19	310.43	195.12	313.46	290.53	< 0.001	< 0.001	< 0.001	< 0.001
Order 20	310.51	199.59	313.46	293.04	< 0.001	< 0.001	< 0.001	< 0.001
Order 21	310.51	199.60	314.14	293.05	< 0.001	< 0.001	< 0.001	< 0.001
Order 22	310.69	199.60	315.09	293.05	< 0.001	< 0.001	< 0.001	< 0.001
Order 23	311.17	199.89	316.96	293.48	< 0.001	< 0.001	< 0.001	< 0.001
Order 24	332.17	240.35	337.45	303.44	< 0.001	< 0.001	< 0.001	< 0.001
Order 25	332.91	240.52	340.49	304.09	< 0.001	< 0.001	< 0.001	< 0.001

Supplementary Table S2 cont. 2/4.

Order	LM-Statistic				P-Value			
	2016	2017	2018	2019	2016	2017	2018	2019
Order 26	337.18	249.18	343.96	309.80	< 0.001	< 0.001	< 0.001	< 0.001
Order 27	338.59	252.63	344.00	319.50	< 0.001	< 0.001	< 0.001	< 0.001
Order 28	343.00	252.70	351.87	322.03	< 0.001	< 0.001	< 0.001	< 0.001
Order 29	346.72	252.70	355.19	322.41	< 0.001	< 0.001	< 0.001	< 0.001
Order 30	349.37	252.90	355.67	323.52	< 0.001	< 0.001	< 0.001	< 0.001
Order 31	349.47	253.23	355.69	323.77	< 0.001	< 0.001	< 0.001	< 0.001
Order 32	349.49	253.30	355.89	325.55	< 0.001	< 0.001	< 0.001	< 0.001
Order 33	353.31	253.48	362.45	325.61	< 0.001	< 0.001	< 0.001	< 0.001
Order 34	354.91	255.99	364.76	328.70	< 0.001	< 0.001	< 0.001	< 0.001
Order 35	359.03	256.13	377.91	331.62	< 0.001	< 0.001	< 0.001	< 0.001
Order 36	367.96	282.31	390.73	350.80	< 0.001	< 0.001	< 0.001	< 0.001
Order 37	369.85	282.40	392.20	366.67	< 0.001	< 0.001	< 0.001	< 0.001
Order 38	375.41	287.66	394.24	367.04	< 0.001	< 0.001	< 0.001	< 0.001
Order 39	375.71	294.39	394.36	369.02	< 0.001	< 0.001	< 0.001	< 0.001
Order 40	383.82	294.48	401.80	369.37	< 0.001	< 0.001	< 0.001	< 0.001
Order 41	384.21	294.67	402.18	372.42	< 0.001	< 0.001	< 0.001	< 0.001
Order 42	384.23	296.01	402.98	372.51	< 0.001	< 0.001	< 0.001	< 0.001
Order 43	384.34	296.25	403.46	372.52	< 0.001	< 0.001	< 0.001	< 0.001
Order 44	385.82	296.30	403.46	373.35	< 0.001	< 0.001	< 0.001	< 0.001
Order 45	386.25	296.41	403.73	374.03	< 0.001	< 0.001	< 0.001	< 0.001
Order 46	386.61	296.80	403.75	374.04	< 0.001	< 0.001	< 0.001	< 0.001
Order 47	388.61	298.00	406.19	377.65	< 0.001	< 0.001	< 0.001	< 0.001
Order 48	392.61	308.60	416.10	399.89	< 0.001	< 0.001	< 0.001	< 0.001
Order 49	398.35	308.65	417.01	401.33	< 0.001	< 0.001	< 0.001	< 0.001
Order 50	399.74	310.11	417.01	401.38	< 0.001	< 0.001	< 0.001	< 0.001

Supplementary Table S2 cont 3/4.

Order	LM-Statistic				P-Value			
	2016	2017	2018	2019	2016	2017	2018	2019
Order 51	400.31	310.21	417.18	402.77	< 0.001	< 0.001	< 0.001	< 0.001
Order 52	401.42	310.65	418.66	407.27	< 0.001	< 0.001	< 0.001	< 0.001
Order 53	403.85	310.95	421.31	410.41	< 0.001	< 0.001	< 0.001	< 0.001
Order 54	406.14	311.21	422.97	410.45	< 0.001	< 0.001	< 0.001	< 0.001
Order 55	408.40	311.54	423.04	410.57	< 0.001	< 0.001	< 0.001	< 0.001
Order 56	408.48	311.58	424.80	411.57	< 0.001	< 0.001	< 0.001	< 0.001
Order 57	408.52	311.79	426.14	411.58	< 0.001	< 0.001	< 0.001	< 0.001
Order 58	408.52	315.73	426.41	412.46	< 0.001	< 0.001	< 0.001	< 0.001
Order 59	409.99	320.90	426.56	413.61	< 0.001	< 0.001	< 0.001	< 0.001
Order 60	410.56	325.47	436.67	424.06	< 0.001	< 0.001	< 0.001	< 0.001
Order 61	413.66	325.95	436.72	430.63	< 0.001	< 0.001	< 0.001	< 0.001
Order 62	413.84	330.88	441.07	434.46	< 0.001	< 0.001	< 0.001	< 0.001
Order 63	414.16	334.27	441.40	436.06	< 0.001	< 0.001	< 0.001	< 0.001
Order 64	414.24	334.55	443.51	436.54	< 0.001	< 0.001	< 0.001	< 0.001
Order 65	414.36	334.66	444.22	436.80	< 0.001	< 0.001	< 0.001	< 0.001
Order 66	414.61	334.75	444.26	437.05	< 0.001	< 0.001	< 0.001	< 0.001
Order 67	414.68	339.35	444.71	438.13	< 0.001	< 0.001	< 0.001	< 0.001
Order 68	415.98	343.05	444.71	438.22	< 0.001	< 0.001	< 0.001	< 0.001
Order 69	416.19	343.15	444.71	438.57	< 0.001	< 0.001	< 0.001	< 0.001
Order 70	416.33	343.57	445.86	439.27	< 0.001	< 0.001	< 0.001	< 0.001
Order 71	416.39	343.67	450.57	439.27	< 0.001	< 0.001	< 0.001	< 0.001
Order 72	416.50	344.96	458.51	447.72	< 0.001	< 0.001	< 0.001	< 0.001
Order 73	416.57	345.09	458.60	448.72	< 0.001	< 0.001	< 0.001	< 0.001
Order 74	417.53	346.29	462.74	452.06	< 0.001	< 0.001	< 0.001	< 0.001
Order 75	417.74	346.59	462.92	452.48	< 0.001	< 0.001	< 0.001	< 0.001

Supplementary Table S2 cont 4/4.

Order	LM-Statistic				P-Value			
	2016	2017	2018	2019	2016	2017	2018	2019
Order 76	418.04	347.96	463.69	453.68	< 0.001	< 0.001	< 0.001	< 0.001
Order 77	418.04	348.20	464.27	453.70	< 0.001	< 0.001	< 0.001	< 0.001
Order 78	418.59	349.20	464.49	454.32	< 0.001	< 0.001	< 0.001	< 0.001
Order 79	420.26	349.87	464.58	455.46	< 0.001	< 0.001	< 0.001	< 0.001
Order 80	422.50	351.31	464.59	455.46	< 0.001	< 0.001	< 0.001	< 0.001
Order 81	423.94	351.33	468.13	458.14	< 0.001	< 0.001	< 0.001	< 0.001
Order 82	425.31	351.62	470.71	459.33	< 0.001	< 0.001	< 0.001	< 0.001
Order 83	425.52	355.53	470.71	459.39	< 0.001	< 0.001	< 0.001	< 0.001
Order 84	425.71	369.05	470.75	464.57	< 0.001	< 0.001	< 0.001	< 0.001
Order 85	429.89	369.07	471.30	467.39	< 0.001	< 0.001	< 0.001	< 0.001
Order 86	430.05	369.83	471.83	467.84	< 0.001	< 0.001	< 0.001	< 0.001
Order 87	430.43	369.83	472.02	469.49	< 0.001	< 0.001	< 0.001	< 0.001
Order 88	430.97	370.76	472.09	470.77	< 0.001	< 0.001	< 0.001	< 0.001
Order 89	431.15	370.77	472.11	471.95	< 0.001	< 0.001	< 0.001	< 0.001
Order 90	432.94	371.07	472.17	472.12	< 0.001	< 0.001	< 0.001	< 0.001
Order 91	433.24	374.80	472.57	472.92	< 0.001	< 0.001	< 0.001	< 0.001
Order 92	434.46	374.80	472.64	472.94	< 0.001	< 0.001	< 0.001	< 0.001
Order 93	434.57	374.95	472.81	473.03	< 0.001	< 0.001	< 0.001	< 0.001
Order 94	434.98	375.26	473.74	473.84	< 0.001	< 0.001	< 0.001	< 0.001
Order 95	435.00	375.62	474.30	474.69	< 0.001	< 0.001	< 0.001	< 0.001
Order 96	435.05	377.38	477.35	479.83	< 0.001	< 0.001	< 0.001	< 0.001
Order 97	436.11	379.24	477.44	479.90	< 0.001	< 0.001	< 0.001	< 0.001
Order 98	436.37	379.34	478.06	481.13	< 0.001	< 0.001	< 0.001	< 0.001
Order 99	436.44	379.47	478.27	482.21	< 0.001	< 0.001	< 0.001	< 0.001
Order 100	436.47	381.42	478.59	484.35	< 0.001	< 0.001	< 0.001	< 0.001

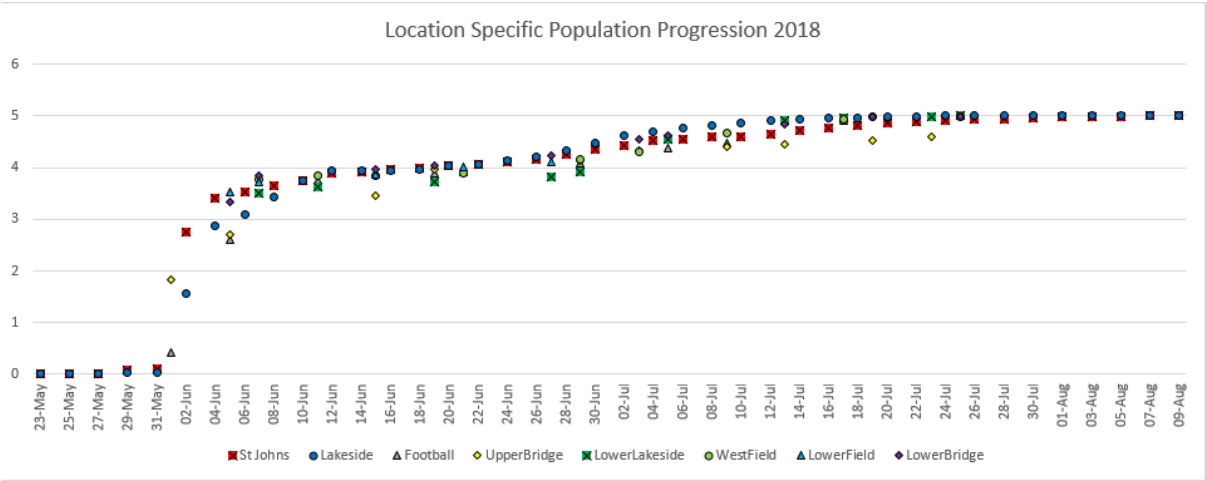

Supplementary Figure S43. This figure contains the average phenological progression of each of the eight *Dactylis glomerata* populations in 2018. This figure is an extension of Figure 40.

Supplementary Table S3

Transitional matrices for all main populations.

St Johns 2017		From					
		P0	P1	P2	P3	P4	P5
To	P0	0.000	0.000	0.000	0.000	0.000	0.000
	P1	0.407	0.692	0.000	0.000	0.000	0.000
	P2	0.164	0.038	0.573	0.000	0.000	0.000
	P3	0.151	0.041	0.157	0.508	0.000	0.000
	P4	0.278	0.215	0.264	0.486	0.946	0.000
	P5	0.000	0.014	0.006	0.006	0.054	1.000

St Johns 2018		From					
		P0	P1	P2	P3	P4	P5
To	P0	0.000	0.000	0.000	0.000	0.000	0.000
	P1	0.104	0.167	0.000	0.000	0.000	0.000
	P2	0.052	0.045	0.234	0.000	0.000	0.000
	P3	0.055	0.015	0.033	0.243	0.000	0.000
	P4	0.789	0.758	0.733	0.727	0.940	0.000
	P5	0.000	0.015	0.000	0.030	0.060	1.000

Lakeside 2018		From					
		P0	P1	P2	P3	P4	P5
To	P0	0.000	0.000	0.000	0.000	0.000	0.000
	P1	0.139	0.225	0.000	0.000	0.000	0.000
	P2	0.093	0.020	0.243	0.000	0.000	0.000
	P3	0.130	0.029	0.000	0.263	0.000	0.000
	P4	0.638	0.726	0.757	0.737	0.926	0.000
	P5	0.000	0.000	0.000	0.000	0.074	1.000

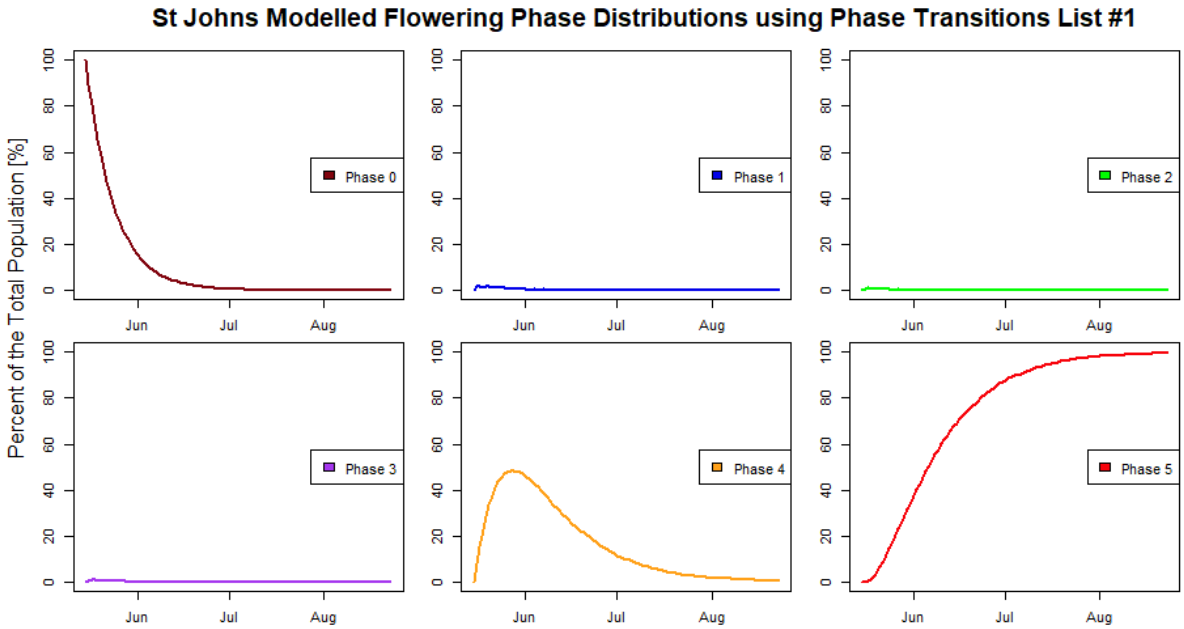

Supplementary Figure S44. Phase distribution of *Dactylis glomerata* tillers within the modelled population created using the phase transition list #1 isolated from the observed St Johns population in 2018. See **Table 8** and **Table 9** for more details.

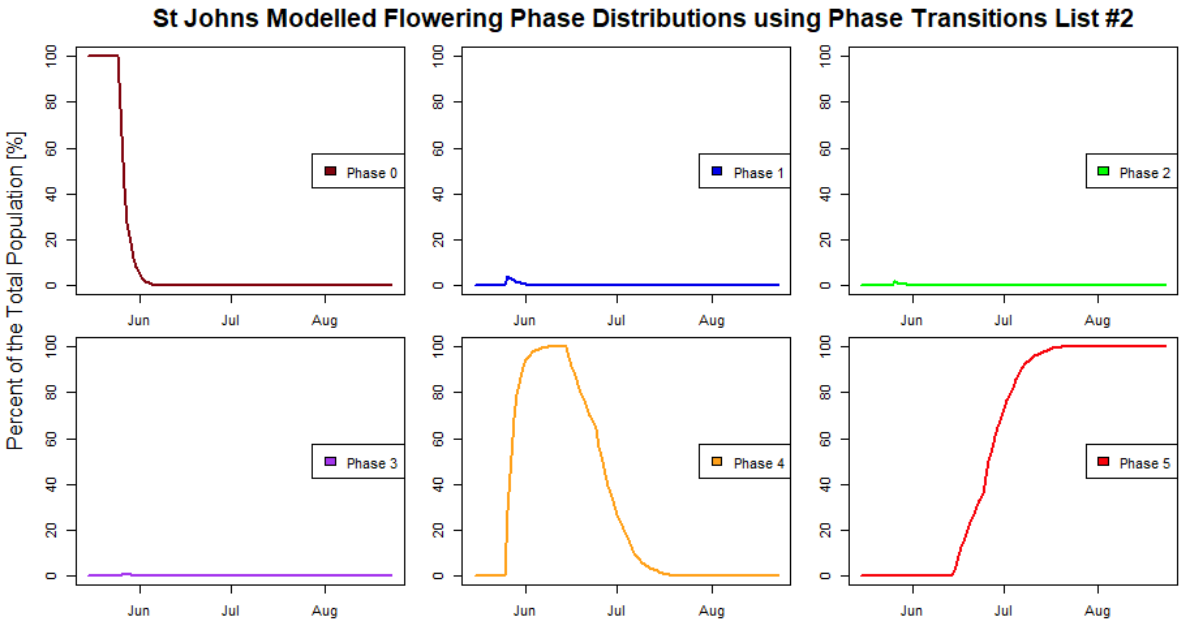

Supplementary Figure S45. Phase distribution of *Dactylis glomerata* tillers within the modelled population created using the phase transition list #2 isolated from the observed St Johns population in 2018. See **Table 8** and **Table 9** for more details.

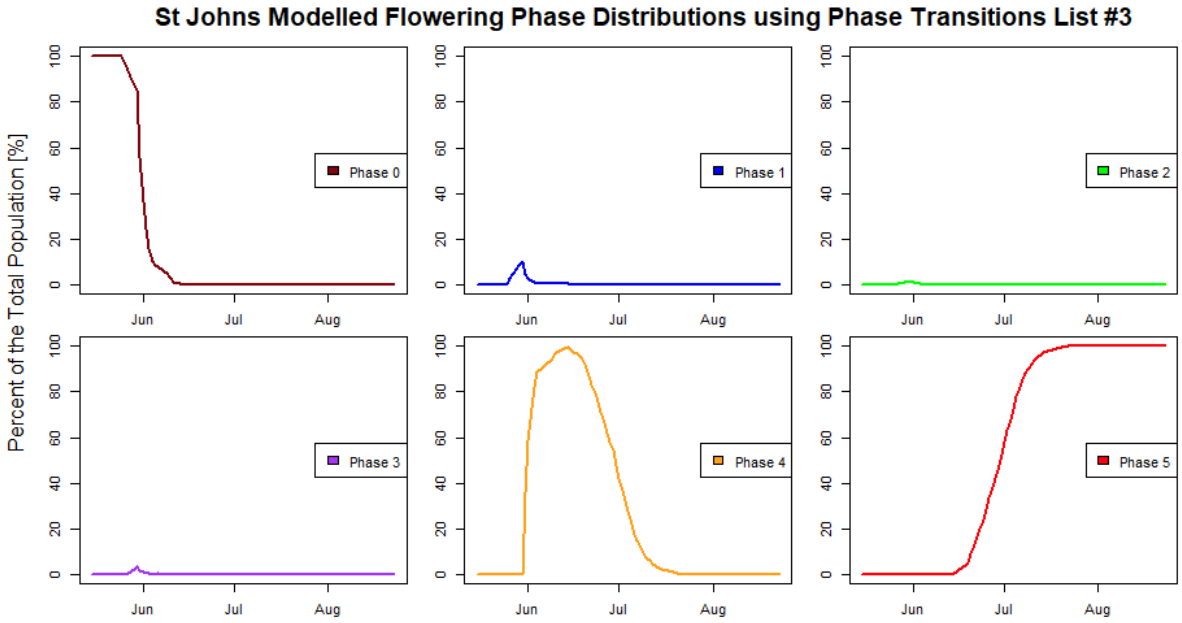

Supplementary Figure S46. Phase distribution of *Dactylis glomerata* tillers within the modelled population created using the phase transition list #3 isolated from the observed St Johns population in 2018. See **Table 8** and **Table 9** for more details.

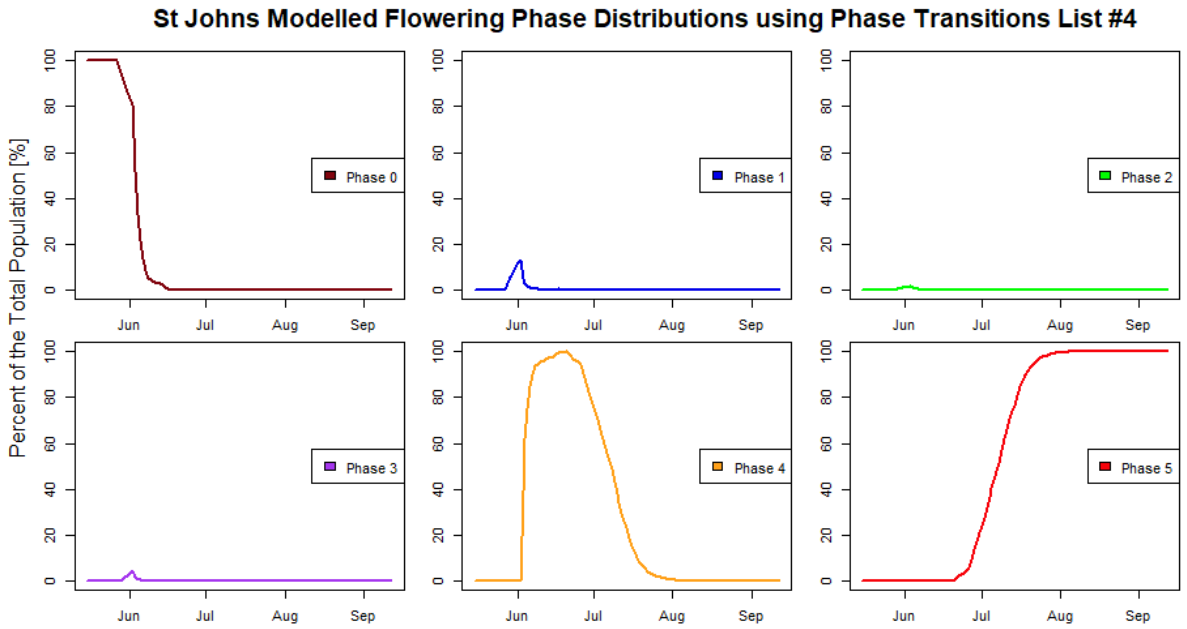

Supplementary Figure S47. Phase distribution of *Dactylis glomerata* tillers within the modelled population created using the phase transition list #4 isolated from the observed St Johns population in 2018. See **Table 8** and **Table 9** for more details.

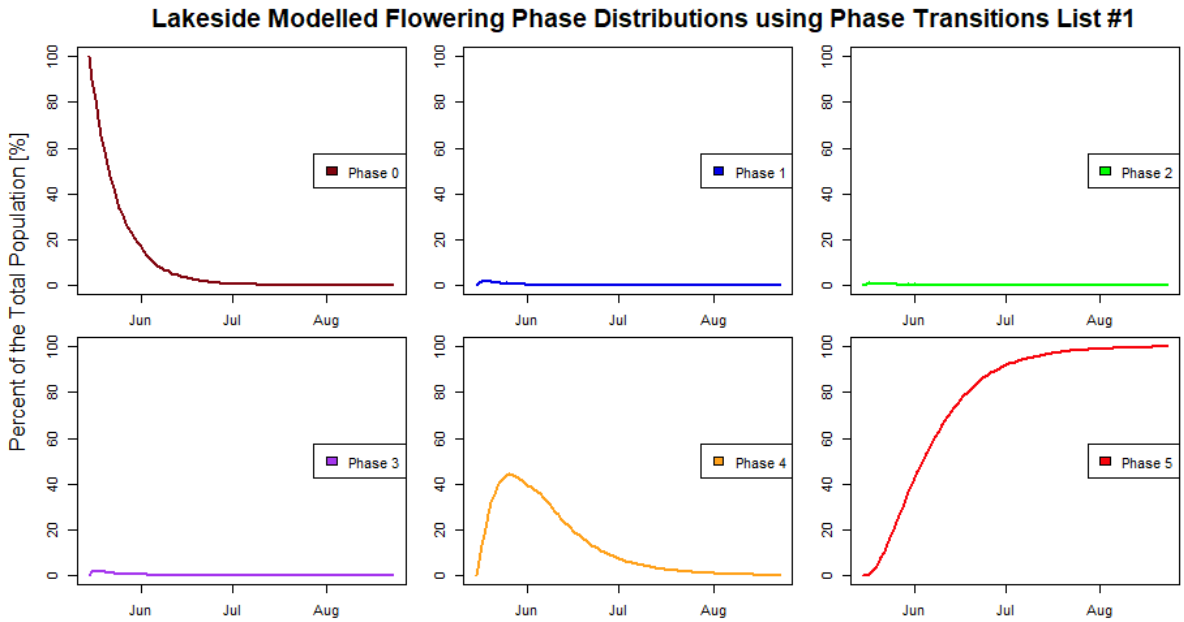

Supplementary Figure S48. Phase distribution of *Dactylis glomerata* tillers within the modelled population created using the phase transition list #1 isolated from the observed Lakeside population in 2018. See **Table 8** and **Table 9** for more details.

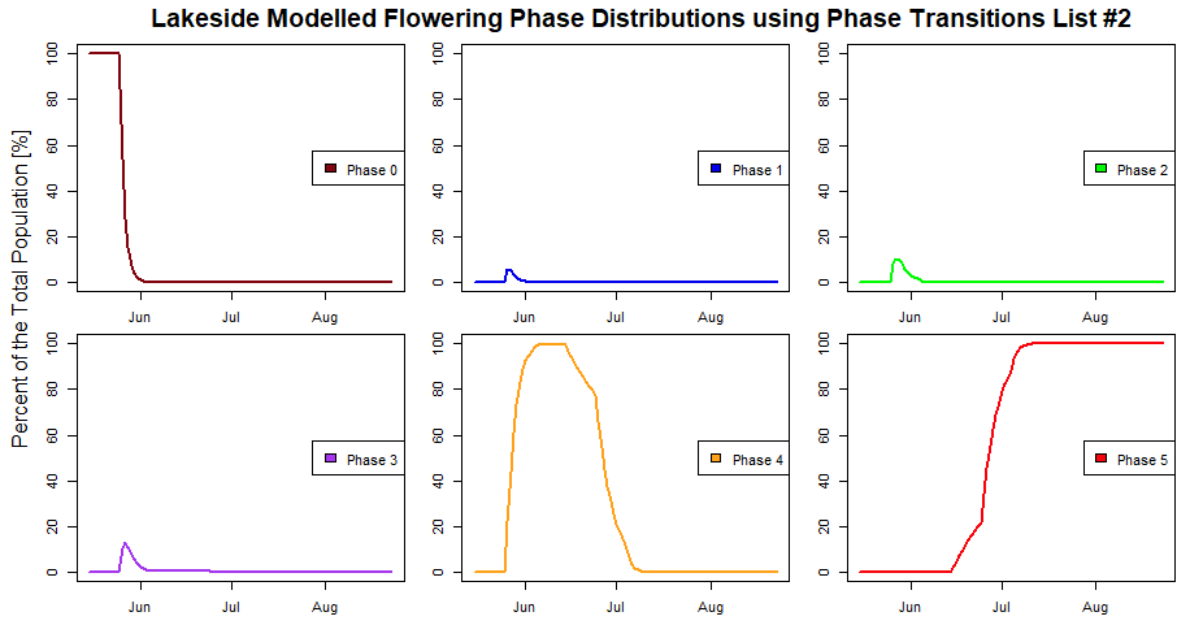

Supplementary Figure S49. Phase distribution of *Dactylis glomerata* tillers within the modelled population created using the phase transition list #2 isolated from the observed Lakeside population in 2018. See **Table 8** and **Table 9** for more details.

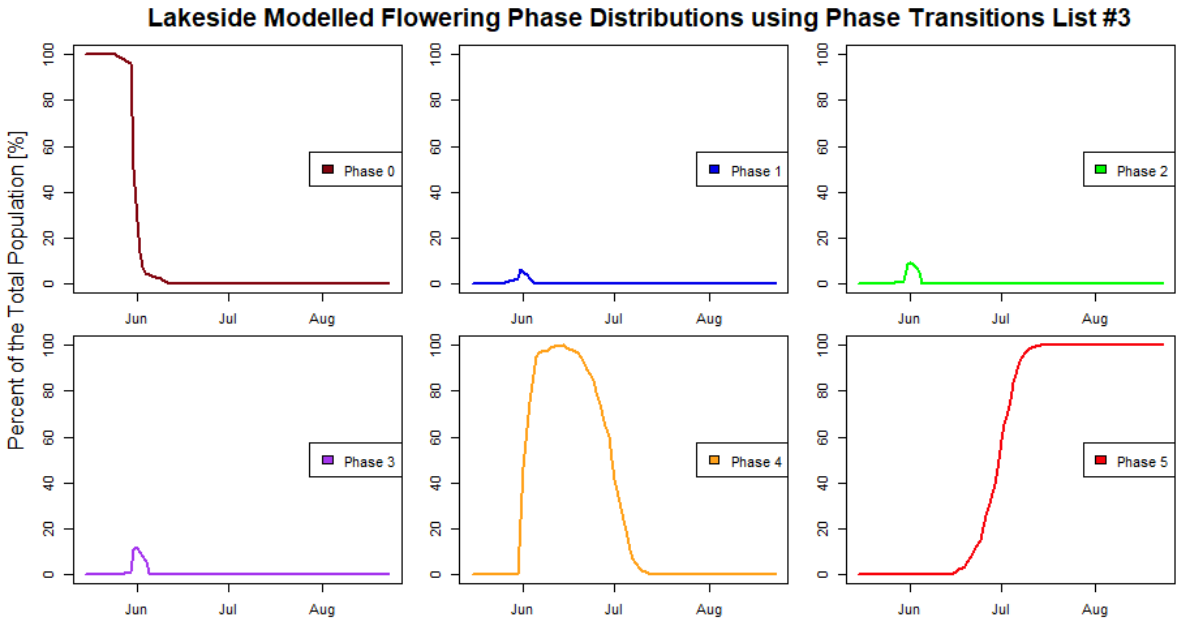

Supplementary Figure S50. Phase distribution of *Dactylis glomerata* tillers within the modelled population created using the phase transition list #3 isolated from the observed Lakeside population in 2018. See **Table 8** and **Table 9** for more details.

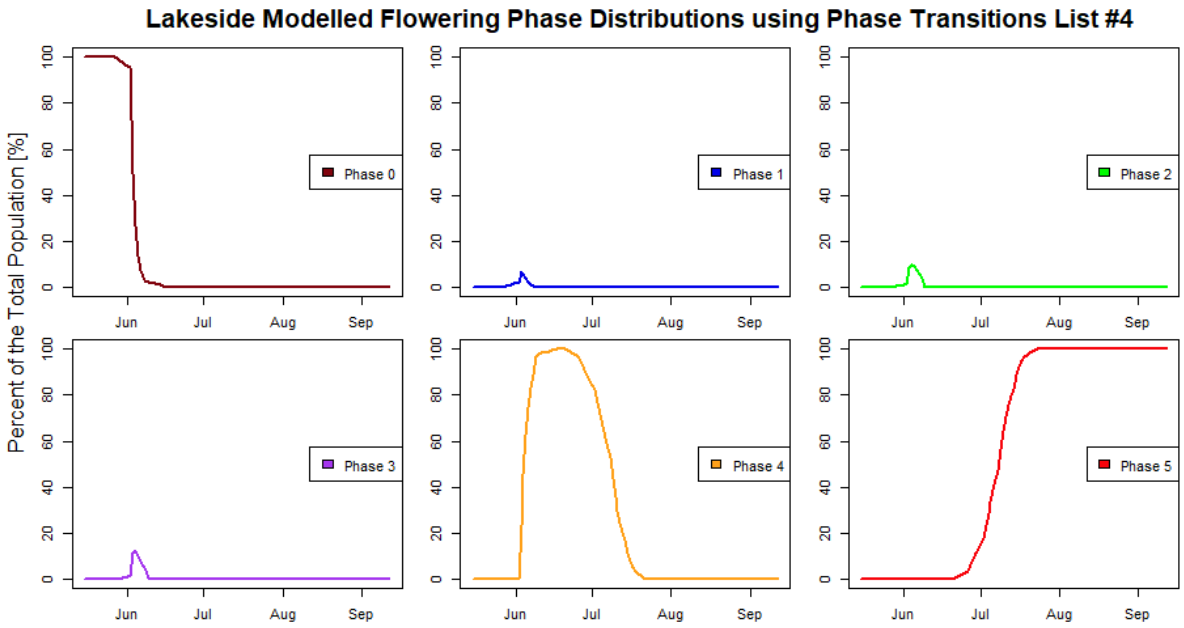

Supplementary Figure S51. Phase distribution of *Dactylis glomerata* tillers within the modelled population created using the phase transition list #4 isolated from the observed Lakeside population in 2018. See **Table 8** and **Table 9** for more details.

Supplementary Table 4a

Correlations between the temporal phase distributions in each modelled *Dactylis glomerata* population and the observed St Johns population in 2018.

Phase Transitions	**Phases**	**Kendall Rank Correlation**			
List Combination	Single	z	tau	P - value	Significance
List #1 *(unique for St Johns)*	Phase 0	7.814	0.887	< 0.001	***
	Phase 1	3.7734	0.479	< 0.001	***
	Phase 2	3.3275	0.438	< 0.001	***
	Phase 3	3.0812	0.404	< 0.01	**
	Phase 4	3.278	0.349	< 0.01	**
	Phase 5	8.6895	0.943	< 0.001	***
List #2 *(unique for St Johns)*	Phase 0	6.3521	0.814	< 0.001	***
	Phase 1	4.8493	0.665	< 0.001	***
	Phase 2	4.2441	0.599	< 0.001	***
	Phase 3	3.3485	0.475	< 0.001	***
	Phase 4	6.66	0.733	< 0.001	***
	Phase 5	8.488	0.974	< 0.001	***
List #3 *(unique for St Johns)*	Phase 0	7.7347	0.951	< 0.001	***
	Phase 1	5.1016	0.696	< 0.001	***
	Phase 2	6.1205	0.838	< 0.001	***
	Phase 3	5.4464	0.745	< 0.001	***
	Phase 4	8.2339	0.906	< 0.001	***
	Phase 5	8.6094	0.982	< 0.001	***
List #4 *(unique for St Johns)*	Phase 0	8.1015	0.991	< 0.001	***
	Phase 1	6.4717	0.871	< 0.001	***
	Phase 2	6.085	0.826	< 0.001	***
	Phase 3	5.4925	0.757	< 0.001	***
	Phase 4	8.213	0.893	< 0.001	***
	Phase 5	8.3613	0.960	< 0.001	***

Supplementary Table 4b

Correlations between the temporal phase distributions in each modelled *Dactylis glomerata* population and the observed Lakeside population in 2018.

Phase Transitions	Phases	Kendall Rank Correlation			
List Combination	Single	z	tau	P - value	Significance
List #1 *(unique for Lakeside)*	Phase 0	7.693	0.878	< 0.001	***
	Phase 1	2.5043	0.324	< 0.05	*
	Phase 2	2.9046	0.380	< 0.01	**
	Phase 3	3.176	0.412	< 0.01	**
	Phase 4	3.2641	0.359	< 0.01	**
	Phase 5	8.3587	0.922	< 0.001	***
List #2 *(unique for Lakeside)*	Phase 0	5.8691	0.767	< 0.001	***
	Phase 1	3.3301	0.477	< 0.001	***
	Phase 2	3.7584	0.542	< 0.001	***
	Phase 3	4.9253	0.694	< 0.001	***
	Phase 4	6.2815	0.734	< 0.001	***
	Phase 5	8.0821	0.964	< 0.001	***
List #3 *(unique for Lakeside)*	Phase 0	6.5768	0.843	< 0.001	***
	Phase 1	3.6218	0.518	< 0.001	***
	Phase 2	5.295	0.756	< 0.001	***
	Phase 3	5.2867	0.735	< 0.001	***
	Phase 4	7.7254	0.900	< 0.001	***
	Phase 5	8.2736	0.978	< 0.001	***
List #4 *(unique for Lakeside)*	Phase 0	7.2161	0.912	< 0.001	***
	Phase 1	4.3784	0.623	< 0.001	***
	Phase 2	5.9298	0.850	< 0.001	***
	Phase 3	5.688	0.782	< 0.001	***
	Phase 4	7.7068	0.893	< 0.001	***
	Phase 5	8.0392	0.953	< 0.001	***

Supplementary Table S5a

Correlations between modelled pollen release estimates in the modelled Dactylis glomerata populations and the relative proportion of Dactylis glomerata pollen based on the ITS1 region bioinformatics of collected eDNA in St Johns 2018.

Pollen Release	Pooled Samples	ITS1 Data Points	ITS2 Data Points	Days	Spearman Rank Correlation			
					S	rho	P - value	Significance
100%/day	8	8	0	28	22.518	0.732	< 0.05	*
90%/day	8	8	0	28	22.518	0.732	< 0.05	*
80%/day	8	8	0	28	22.518	0.732	< 0.05	*
70%/day	8	8	0	28	16.37	0.805	< 0.05	*
60%/day	8	8	0	28	16.37	0.805	< 0.05	*
50%/day	8	8	0	28	18.42	0.781	< 0.05	*
40%/day	8	8	0	28	14.321	0.830	< 0.05	*
30%/day	8	8	0	28	20.469	0.756	< 0.05	*
20%/day	8	8	0	28	40.963	0.512	0.1942	NS
10%/day	8	8	0	28	71.704	0.146	0.7294	NS

Supplementary Table S5b

Correlations between modelled pollen release estimates in the modelled Dactylis glomerata populations and the relative proportion of Dactylis glomerata pollen based on the ITS2 region bioinformatics of collected eDNA in St Johns 2018.

Pollen Release	Pooled Samples	ITS1 Data Points	ITS2 Data Points	Days	Spearman Rank Correlation			
					S	rho	P - value	Significance
100%/day	4	0	4	14	2	0.800	0.2	NS
90%/day	4	0	4	14	2	0.800	0.2	NS
80%/day	4	0	4	14	2	0.800	0.2	NS
70%/day	4	0	4	14	2	0.800	0.2	NS
60%/day	4	0	4	14	2	0.800	0.2	NS
50%/day	4	0	4	14	2	0.800	0.2	NS
40%/day	4	0	4	14	2	0.800	0.2	NS
30%/day	4	0	4	14	2	0.800	0.2	NS
20%/day	4	0	4	14	4	0.600	0.4	NS
10%/day	4	0	4	14	14	-0.400	0.6	NS

Supplementary Table S5c

Correlations between modelled pollen release estimates in the modelled Dactylis glomerata populations and the relative proportion of Dactylis glomerata pollen based on the ITS1 region bioinformatics of collected eDNA in Lakeside 2018.

Pollen Release	Pooled Samples	ITS1 Data Points	ITS2 Data Points	Days	Spearman Rank Correlation			
					S	rho	P - value	Significance
100%/day	8	8	0	28	25.652	0.695	0.05588	.
90%/day	8	8	0	28	25.652	0.695	0.05588	.
80%/day	8	8	0	28	25.652	0.695	0.05588	.
70%/day	8	8	0	28	34.706	0.587	0.1262	NS
60%/day	8	8	0	28	42.754	0.491	0.2166	NS
50%/day	8	8	0	28	42.754	0.491	0.2166	NS
40%/day	8	8	0	28	50.802	0.395	0.3325	NS
30%/day	8	8	0	28	50.802	0.395	0.3325	NS
20%/day	8	8	0	28	65.892	0.216	0.6081	NS
10%/day	8	8	0	28	91.042	-0.084	0.8435	NS

Supplementary Table S5d

Correlations between modelled pollen release estimates in the modelled Dactylis glomerata populations and the relative proportion of Dactylis glomerata pollen based on the ITS2 region bioinformatics of collected eDNA in Lakeside 2018.

Pollen Release	Pooled Samples	ITS1 Data Points	ITS2 Data Points	Days	Spearman Rank Correlation			
					S	rho	P - value	Significance
100%/day	8	0	8	28	28.598	0.660	0.07518	.
90%/day	8	0	8	28	28.598	0.660	0.07518	.
80%/day	8	0	8	28	28.598	0.660	0.07518	.
70%/day	8	0	8	28	28.598	0.660	0.07518	.
60%/day	8	0	8	28	38.187	0.545	0.1621	NS
50%/day	8	0	8	28	38.187	0.545	0.1621	NS
40%/day	8	0	8	28	34.99	0.583	0.1289	NS
30%/day	8	0	8	28	34.99	0.583	0.1289	NS
20%/day	8	0	8	28	48.841	0.419	0.302	NS
10%/day	8	0	8	28	66.953	0.203	0.6298	NS

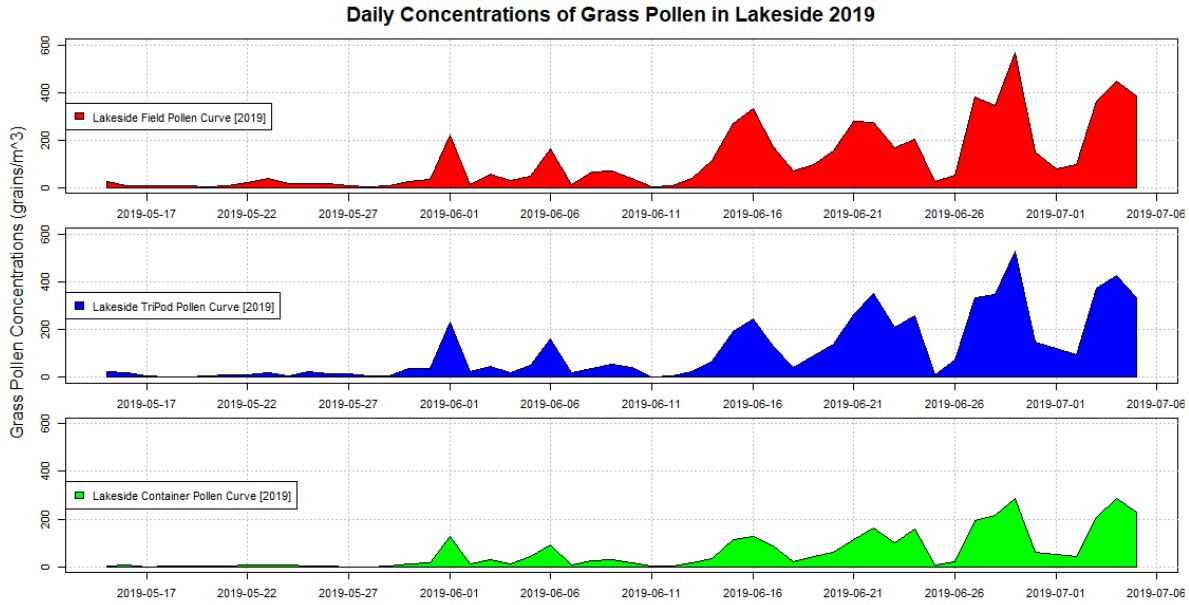

Supplementary Figure S52. Daily concentrations of grass pollen from the three locations in Lakeside (Field, TriPod, and Container) during 2019 in Worcester. All datapoints are included between the 15th of May to the 6th of July 2019.

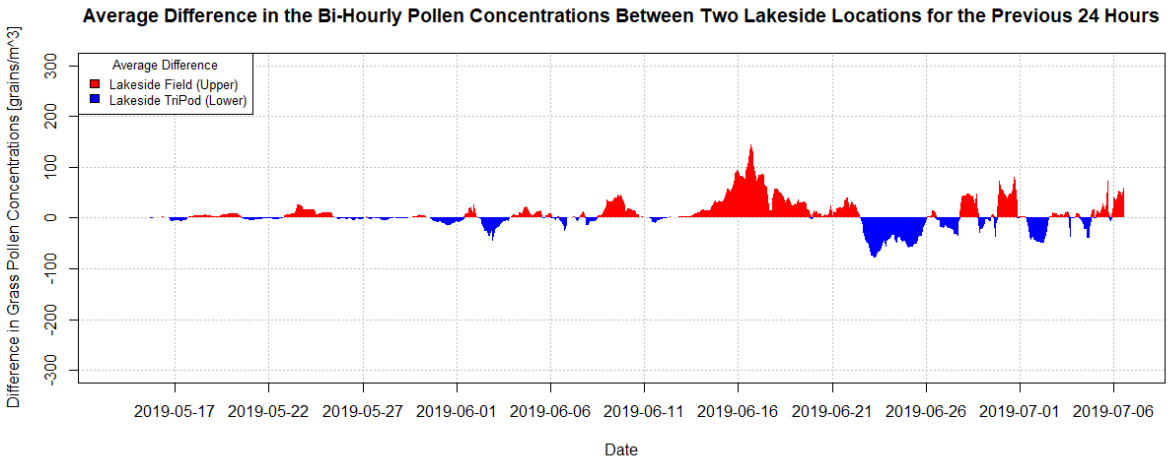

Supplementary Figure S53. Difference in bi-hourly grass pollen concentrations from the past twenty-four hours between Lakeside Field and Lakeside TriPod during included season of 2019.

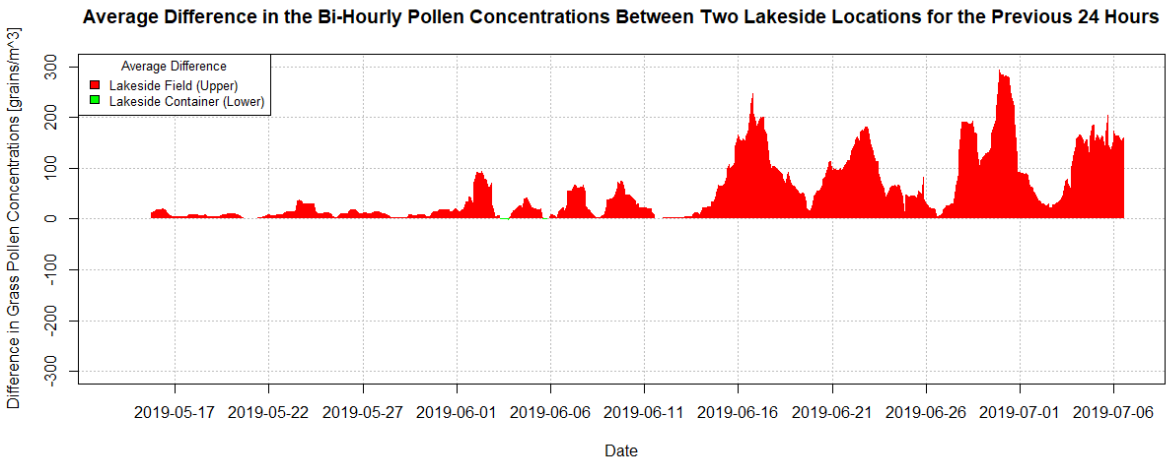

Supplementary Figure S54. Difference in bi-hourly grass pollen concentrations from the past twenty-four hours between Lakeside Field and Lakeside Container during included season of 2019.

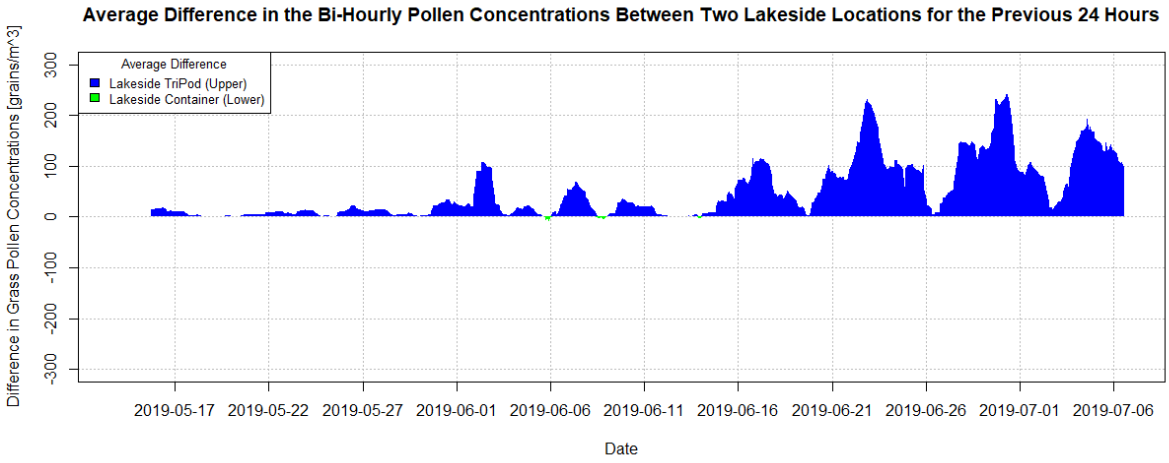

Supplementary Figure S55. Difference in bi-hourly grass pollen concentrations from the past twenty-four hours between Lakeside Container and Lakeside Field during included season of 2019.

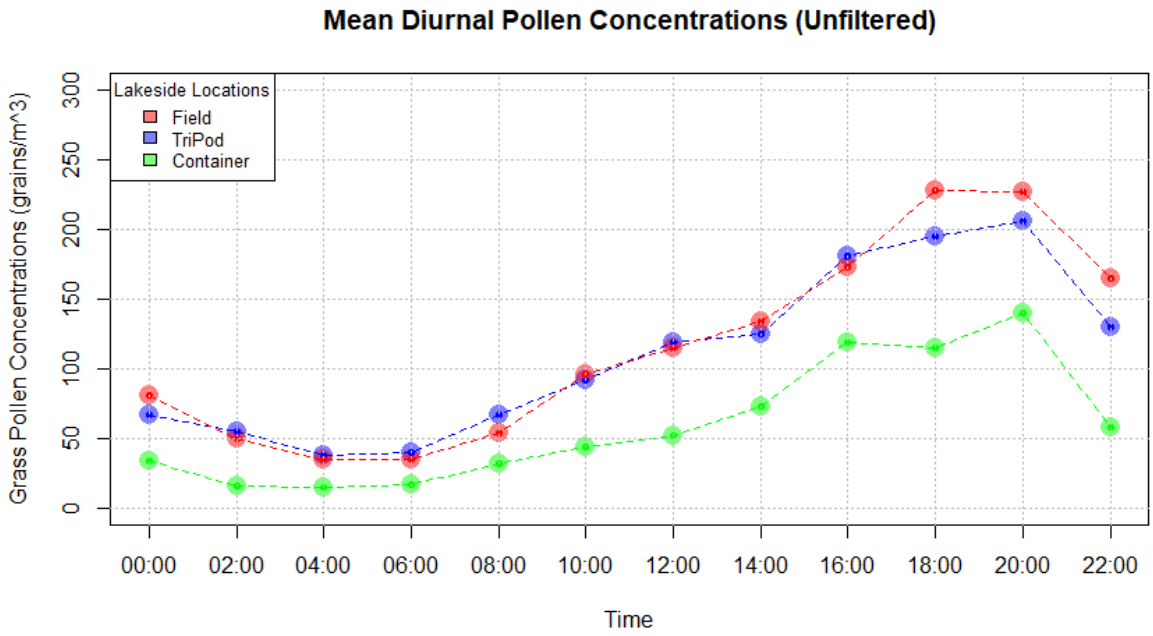

Supplementary Figure S56. Comparison of mean diurnal grass pollen concentrations for the three Lakeside locations: Field, TriPod, and Container. This data is the unfiltered data presented in Figure 52.

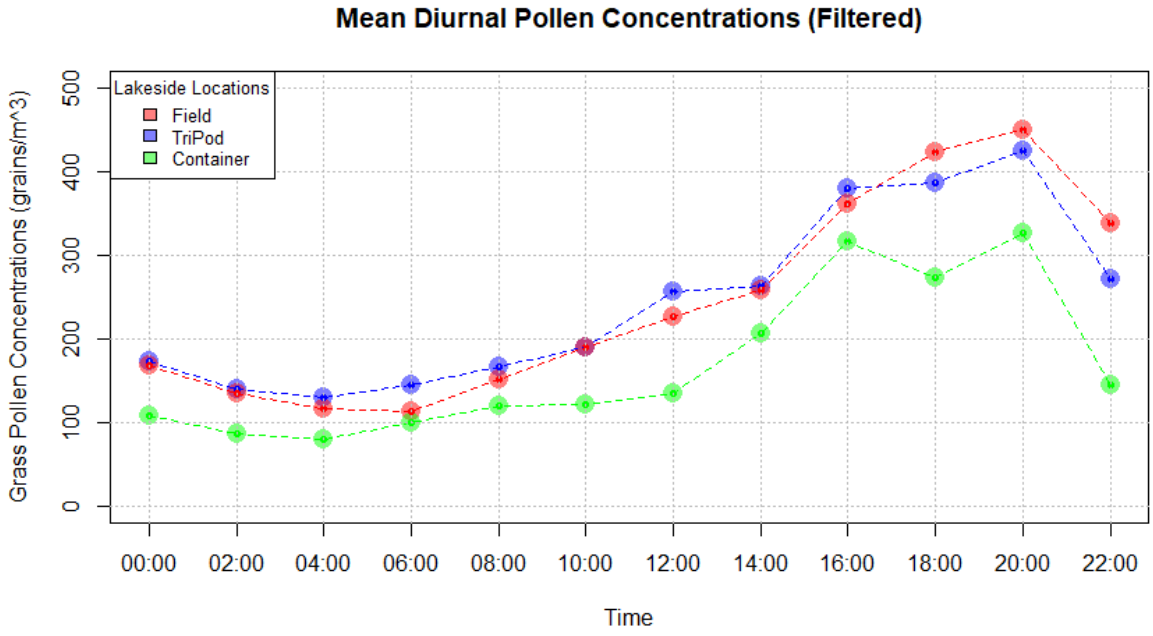

Supplementary Figure S57. Comparison of mean diurnal grass pollen concentrations for the three Lakeside locations: Field, TriPod, and Container. This data is the filtered data presented in Figure 61 and Tables 15a, 15b and 15c.

Aerobiologia
https://doi.org/10.1007/s10453-020-09685-1

ORIGINAL PAPER

Stochastic flowering phenology in *Dactylis glomerata* populations described by Markov chain modelling

Carl A. Frisk · Beverley Adams-Groom · Carsten A. Skjøth

Received: 17 August 2020 / Accepted: 17 December 2020

Abstract Understanding the relationship between flowering patterns and pollen dispersal is important in climate change modelling, pollen forecasting, forestry and agriculture. Enhanced understanding of this connection can be gained through detailed spatial and temporal flowering observations on a population level, combined with modelling simulating the dynamics. Species with large distribution ranges, long flowering seasons, high pollen production and naturally large populations can be used to illustrate these dynamics. Revealing and simulating species-specific demographic and stochastic elements in the flowering process will likely be important in determining when pollen release is likely to happen in flowering plants. Spatial and temporal dynamics of eight populations of *Dactylis glomerata* were collected over the course of two years to determine high-resolution demographic elements. Stochastic elements were accounted for using Markov chain approaches in order to evaluate tiller-specific contribution to overall population dynamics. Tiller-specific developmental dynamics were evaluated using three different RV matrix correlation coefficients. We found that the demographic patterns in population development were the same for all populations with key phenological events differing only by a few days over the course of the seasons. Many tillers transitioned very quickly from non-flowering to full flowering, a process that can be replicated with Markov chain modelling. Our novel approach demonstrates the identification and quantification of stochastic elements in the flowering process of *D. glomerata*, an element likely to be found in many flowering plants. The stochastic modelling approach can be used to develop detailed pollen release models for *Dactylis*, other grass species and probably other flowering plants.

Keywords Pollen · Population statistics · Anthesis · Grass · Poaceae · UK

1 Introduction

Grass ecology is of considerable importance to human society and culture, mainly through cereal cultivation, animal fodder and forestry but also through grass pollen allergy. Grass pollen is arguably the most important outdoor aeroallergen with the highest amount of sensitization (D'Amato et al. 2007; Heinzerling et al. 2009). Studies have shown that there is a strong relationship between airborne pollen

Supplementary Information The online version contains supplementary material available at (https://doi.org/10.1007/s10453-020-09685-1).

C. A. Frisk (✉) · B. Adams-Groom · C. A. Skjøth
National Pollen and Aerobiological Research Unit, School of Science and the Environment, University of Worcester, Worcester WR2 6AJ, UK
e-mail: c.frisk@worc.ac.uk

Published online: 03 February 2021

concentrations and the flowering phenology of grasses (Ghitarrini et al. 2017; Kmenta et al. 2016; Romero-Morte et al. 2020). The identification and modelling of demographic and stochastic processes in grass flowering should increase understanding of this relationship.

To fully understand the ecology of grasses, a population-based approach is often needed (Bolnick et al. 2003; Watkinson and Ormerod 2001). Spatial and temporal observations of flowering of multiple populations are often used to understand demographic elements in the study of grasses in agriculture (Rossignol et al. 2014; Smith 1944), ecology (Eagles 1972; Lindner and Garcia 1997) and aerobiology (Rojo et al. 2017; Romero-Morte et al. 2018). Combining this approach with a stochastic Markov chain modelling approach (Balzter 2000) and a model grass species may provide deeper multifaceted understanding with respect to underlying flowering processes. Markov chain approaches have previously been used to accurately model demographic and stochastic elements in grass populations (Nakaoka 1996) (e.g. Canales et al. 1994; Silva et al. 1991).

The species *Dactylis glomerata*, being (probably) the only species in its genus, has been investigated for more than a century regarding its growth and flowering processes (Wolfe 1925; Wolfe and Kipps 1925, 1926). This has been due to its widespread use as a common pasture grass (Eagles and Williams 1971; Mizianty 1986) and its cross-pollination capacity (Jones and Newell 1948). It occurs abundantly throughout its extensive biogeographic distribution, with a native range between the USA and Japan, and from northern Africa to northern Sweden (Clayton et al. 2002). The species can be divided into a few different sub-species based on genetic and morphological divergencies (Yan et al. 2016). However, *D. glomerata subsp. glomerata* is by far the most common sub-species, defining the standard of the species (Mizianty 1990). Cebrino et al. (2018) found that *D. glomerata* starts flowering around the same time in Spain, regardless of habitat. This holds true between years and locations (Cebrino et al. 2016). Observations in cultivated gardens have shown that earlier starting times promote longer flowering in individual flowers (Tormo-Molina et al. 2015), common in wild grass species and important for climate change scenarios (Cleland et al. 2006; Munson and Long 2017). The higher pollen production in *D. glomerata* compared to other grasses (Aboulaich et al. 2009; Prieto-Baena et al. 2003) heightens the relevance of these processes. All the above-mentioned considerations make *D. glomerata* a model species for phenological investigation. Information about the detailed flowering dynamics in populations will enable climatic and mechanistic modelling of *D. glomerata* and other grasses with similar behaviour, a key aspect for phenological modelling of grasses and their impact on the grass pollen seasonality (García-Mozo et al. 2009). The inclusion of stochastic elements in the phenological development will be able to account for intrinsic attributes of the flowering process, which has been suggested to have implications for pollen and seed dispersal patterns (Soons et al. 2004; Tufto et al. 1997), processes-based range modelling (Evans et al. 2016) and cellular differentiation modelling (Davila-Velderrain et al. 2016). Our objective in this study was to investigate demographic and stochastic elements in grass flowering phenology by using *Dactylis glomerata* as a model species. This was done by incorporating population dynamics through detailed spatial and temporal demographic observations and by using Markov chain modelling to explain the stochastic behaviour.

2 Materials and methods

2.1 Locations

Eight locations across the surroundings of Worcester, UK (**Fig. 1**), were monitored over two years (15 May to 31 August 2017 and 2018) to investigate *D. glomerata* population dynamics (**Table 1**). The population at each location were considered as biologically distinct unit since it was spatially isolated from other specimens of the same species within the immediate surroundings. The locations are distinguished between two main populations at St Johns and Lakeside campuses belonging to the University of Worcester and six other unique locations each containing one secondary population. The populations at both campus sites were chosen as main populations due to increased accessibility and lower chances of disturbance. All locations were selected based on three criteria: 1) should contain more than 150 tillers (grass flowering stems) of *D. glomerata* within a 10 m x 10 m area, 2) should not be a road verge and 3) should

Fig. 1 Map showing the eight locations utilized in the phenological observations of *Dactylis glomerata*. The black icons represent the two main locations, while the white icons represent the six secondary locations

be easily accessible. A large minimum population size would limit the variation contributed from each tiller and produce a smaller and more stable standard error for the overall population development (Fox and Kendall 2002). The microclimate contributed to road verges would produce uncertainty regarding the stability of population dynamics (Jantunen et al. 2007), coupled with aspects of disturbances such as

Table 1 Population type, number of individual tillers, coordinates and surrounding habitat for all locations visited during the flowering phenological observations in the populations of *Dactylis glomerata*

Location	Population Type	Tillers # 2017/2018	Latitude	Longitude	Habitats
St Johns	Main	317/355	52.196362 N	−2.241592 E	Park Landscapes, Uncut Grass Areas
Lakeside	Main	0/535	52.254039 N	−2.257216 E	Agricultural Fields, Uncut Grass Areas
Lower Lakeside	Secondary	0/210	52.226128 N	−2.255737 E	Agricultural Fields
Football Field	Secondary	0/160	52.197030 N	−2.240321 E	Park Landscapes, Uncut Grass Areas
Upper Bridge	Secondary	0/418	52.194382 N	−2.232060 E	Verges
West Field	Secondary	0/427	52.186106 N	−2.260664 E	Uncut Grass Areas
Lower Field	Secondary	0/322	52.180686 N	−2.225638 E	Uncut Grass Areas
Lower Bridge	Secondary	0/245	52.176371 N	−2.225622 E	Uncut Grass Areas, Verges

cutting or grazing (Brock et al. 1996). Easily accessible locations were due to simplicity and reproducibility of the study.

2.2 Grass flowering phenology

The flowering phenology was investigated using the 'Biologische Bundesanstalt, Bundessortenamt und Chemische Industrie' (BBCH) scale (Meier 2018). The scale, originally designed to monitor phenological changes in agricultural crops, functions by systematically observing a primary growth characteristic and a secondary growth characteristic, resulting in a two-number sequence. By observing changes to the sequence, detailed phenological change can be monitored (Cornelius et al. 2011, 2014; Meier et al. 2009). The primary growth characteristic focused on in the study is the flowering stage, which starts at tiller heading and ends in tiller senescence. The secondary growth characteristics are focused on the percentage of visible anthers. Each tiller is assigned one of six phases, representing an amount range of visible anthers (**Table 2**). The percent of visible anthers is the proxy of flowering progression due to the increased potential of pollen release, the ultimate evolutionary and ecological goal of Poaceae-specific flowering (Khanduri 2011). The tiller is assigned phase p0 until sign of first flowering and phase p5 when the last anther has detached. The reasoning behind last anther detachment is due to the slight theoretical possibility that pollen could still be emitted from desiccated anthers. Phases p1–p4 represent fractions of flowering anthers in steps of 25%. Examples of *Dactylis glomerata* tillers in each phase can be found in the supplementary material (**Figs. S1–S6**). By observing each tiller within a population, it is possible to measure the phenological progression of the population. Regular observations will allow for a detailed progression profile and reveal inter- (between population) and intra- (within population) demographic variation into flowering phenology through population dynamics of the species.

2.3 Observational strategy

Each population is defined as all tillers of the species within two to four 1.5 m × 1.5 m plots with less than 3 m between each plot within each location. The

Table 2 Phases and criteria used to identify the progression of flowering phenological observations in the populations of *Dactylis glomerata*

Phase	Abbreviation	Criteria	BBCH number
0	P0	Between plant emergence and start of flowering	60
1	P1	Between 1 and 25% of tillers' anthers are extruded	61
2	P2	Between 26 and 50% of tillers' anthers are extruded	63
3	P3	Between 51 and 75% of tillers' anthers are extruded	65
4	P4	Between 76 and 100% of tillers' anthers are extruded	68
5	P5	All tillers' anthers have detached	69

reasoning is to allow a population size large enough to capture statistically unlikely events in regard to population demographic stochasticity (Kendall and Fox 2002). Denser populations utilized the lower number of plots and sparser populations the higher number of plots. Phenological progression of all tillers in each population was observed from the first flowering tiller to the last tillers' senescence. The reasoning is to allow the full range of population dynamics within the main population locations, as adopted from previous grass population studies (e.g. Liddle et al. 1982). During 2017, the main population located in St Johns was visited once a day to investigate flowering progression. During 2018, each of the eight populations was visited. The main populations located in St Johns and Lakeside were visited every second day to investigate whether there was a difference in locations between years. All tillers at the main locations were marked with an ID tag; this allowed observations of tiller-specific progression through the season. The six secondary populations were each visited ten times over the 2018 seasons, resulting in a weekly observational frequency, widely used in grass phenology studies (e.g. García-Mozo et al. 2010; Jochner et al. 2012). Note that the population located at the location Lower Field was only visited five times, due to silage cutting, which removed all tillers. The observations of the six secondary populations stopped as the first main population reached full senescence. The distinctions between main and secondary populations are the continuity of visits, number of visits and the ID tagging of tillers. The use of frequent and continuous observations enhanced the resolution of the phenological progression within the main populations, with the St Johns 2017 population having twice the temporal resolution of the two 2018 populations.

2.4 Analytical framework

2.4.1 General flowering progression of all populations

The general flowering progression was investigated for each year and location by incorporating the average phase of all tillers at each available timestep. A mean phenological progression was then calculated per timestep and year based on all available populations. Due to the observational strategy employed, some dates were missing flowering values. A mean value was thus estimated using the two surrounding values. For 2017, the population at St Johns was used for this mean progression. For 2018, all eight populations were incorporated into the calculation and combined with a standard error.

2.4.2 Markov chain model

The Markov chain stochastic modelling approach was utilized to analyse tiller-specific dynamics within each of the two main populations (in a similar way as Tseng et al. (2020)) for the years 2017 and 2018. The stochastic model uses the records of the temporal phase change for each tiller, by summarizing the overall phase change of all tillers into a six-by-six transitional matrix. The R package *markovchain* (Spedicato 2017) was used to create the transitional matrices. Not all phase changes are possible due to the tiller not being able to revert in phase or go directly from non-flowering to end-flowering (within the daily/bi-daily observational approach). This matrix describes the likelihood for flowering progression (or phase change) for the full season for all tillers in each of the main populations (see approach in Meyn and Tweedie (1993)). These transitional matrices can be translated into Markov chain diagrams, which display the directional change between phases and the likelihood expressed between zero and one of transitioning for all possible transitions within each population (Grinstead and Snell 1997). Note that this analysis was not possible for the secondary locations, in the same manner, due to the limited number of visits, thereby not being able to observe tiller-specific progression.

2.4.3 Correlations

The general flowering progression for each year was tested for statistical normality using the Shapiro non-normality test (Shapiro and Wilk 1965). The nonparametric Spearman rho correlation was utilized to analyse the general flowering progression due to non-normality expressed by the data. The rank-order correlation produces a more reliable estimate in cases of violated parametric assumptions (Spearman 1904). Correlation was tested without significance testing due to the strong autocorrelations found in accumulated time series. The R package *MatrixCorrelation* (Indahl et al. 2018) was utilized to analyse the similarity

between the Markov chain transitional matrices for the three main locations. Three different types of related matrix correlation coefficients were compared: RV (Robert and Escoufier 1976), RV2 (Smilde et al. 2009) and adjusted RV (Mayer et al. 2011). Three coefficients were used to avoid potential bias using only one type of correlation. All statistical analyses were employed and analysed in the statistical software R (R Core Team, 2020; R: A language and environment for statistical computing. R Foundation for Statistical Computing, Vienna, Austria. Available online at https://www.R-project.org/).

3 Results

3.1 Main population dynamics

The main populations at St Johns had 317 and 355 tillers in 2017 and 2018, respectively, while Lakeside had 535 (**Table 1**). The flowering started in late May (May 27 ± 2 days) in both years at St Johns and Lakeside (**Fig. 2**). During the first few days (May 29 ± 2 days), 10–20% of the tillers in the population reached the flowering phases p1, p2 and p3; hence, each of these may have up to 75% of their anther extruded. Most of these, augmented by non-flowering, tillers reached the full flowering in p4 during the first few days of June (June 1 ± 1 day). At this point, about 40% of the population was in full flowering (p4) and two days later an additional 20% of the population reached full flowering (p4) (June 3 ± 1 days). Most tillers in lower flowering phases progressed into full flowering over the coming few days (June 6 ± 2 days). At this time, most tillers were either in full flowering (p4) or had not yet started (p0). This continued until the middle of June (June 12 ± 3 days) when the first tillers reached senescence (p5), showcased by the detachment of the last anther. Around the same time (June 12 ± 1 day), the populations reached peak flowering. Peak flowering is the event where the maximum number of tillers in the season occupies the phase full flowering (p4). The phenological progression of the populations continued as an increasing number of tillers reached senescence and where the last tillers took considerable time to reach phase p5, illustrated by the long tail in Fig. 2. This progression continued until the last tiller had reached senescence, which happened on July 17, August 9 and July 24 for each main population, respectively (**Fig. 2**).

3.2 Secondary population dynamics

The six secondary populations contained between 160 and 427 tillers (**Table 1**). The populations started flowering before the beginning of June (June 1–3–4 days) (**Fig. 3**). All of them had reached more than 60% full flowering (p4) in early June (June 7). By the middle of June (June 19), all populations had started senescence with at least some tillers in the senescence phase (p5). To check for spatial differentiation between the populations, phase ratios were compared. There was no discernible spatial differentiation found between the most western/eastern or northern/southern locations.

3.3 General flowering progression

The development of the 2017 population was mostly two days ahead of the 2018 population, with the full flowering phase being reached with only one day difference (**Fig. 4**). The main difference between the years was the amount of time needed to reach senescence: it was reached 20 days later in the 2018 population. In terms of development between the two years, the 2017 population was on average one-fifth of one phase earlier than the 2018 population. For example, if on day X the 2018 population was average phase 3.5, then the 2017 population was average phase 3.7. The standard error in the 2018 population ranged between 0.70 and 0.22 in the beginning of the season (June 1 to June 6), never reaching more than 0.15 for the rest of the season and reducing to almost zero towards the late season. See supplementary data (**Fig. S7**) for the contribution of each population to the general progression of 2018. A nonparametric correlation was used to compare the years due to both general populations expressing non-normality measured in the Shapiro test ($p < 0.001$ for both years). The Spearman rho correlation showed that there was a high correlation between the two years (Spearman $r_s = 0.98$).

3.4 Tiller-specific phase dynamics

The Markov chain diagrams (**Fig. 5a** and **Table S1** for the transitional matrices) show that the 2017 St Johns

Fig. 2 Flowering phenology development of *Dactylis glomerata* populations shown per phase for the three main populations and years

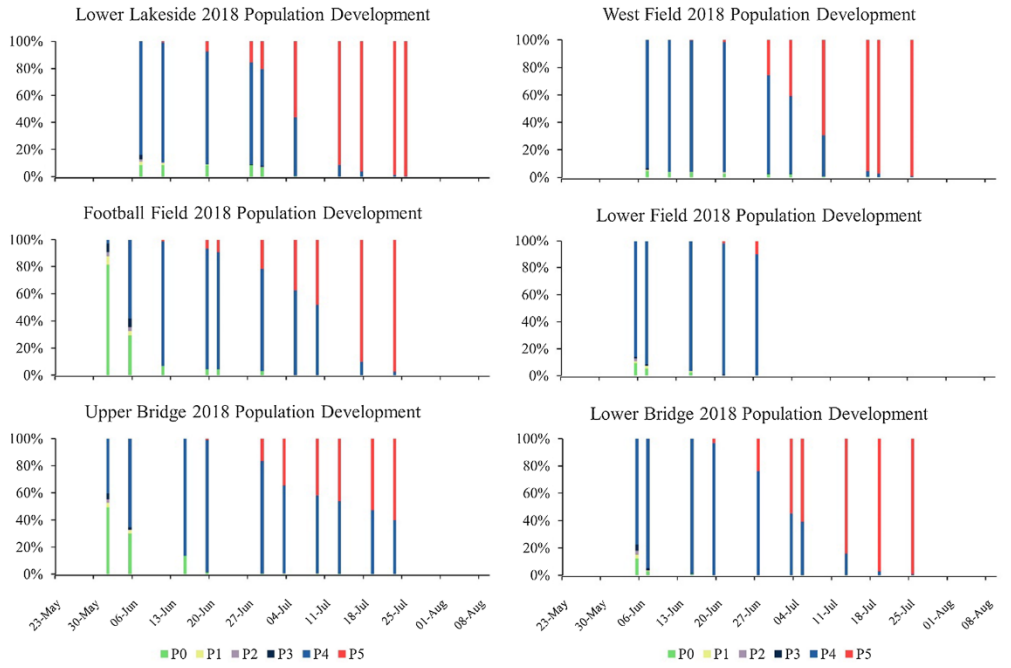

Fig. 3 Flowering phenology development of *Dactylis glomerata* populations shown per phase for the secondary populations in 2018

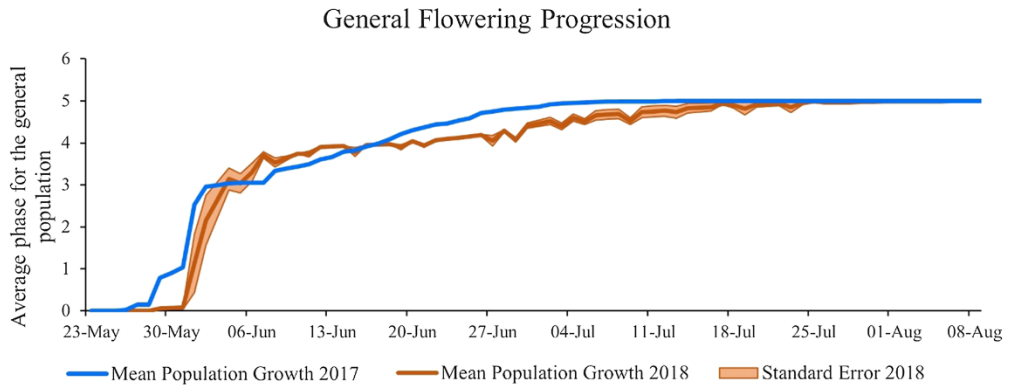

Fig. 4 General *Dactylis glomerata* flowering progression of all observed populations for both years

population flowers first transition either to low flowering (p1) or directly to full flowering (p4), with chances of 0.41 and 0.28, respectively. The second most likely transition for all lower flowering phases (p1, p2 and p3) was to full flowering (p4), with a 0.20 to 0.25 chance for p1 and p2 but almost a 0.50 chance for p3. Tillers in p4 had only a 0.05 chance of transitioning to senescence (p5). Also note that all possible transitions were present in this population, even the less prevalent ones such as p2 to p5, with only

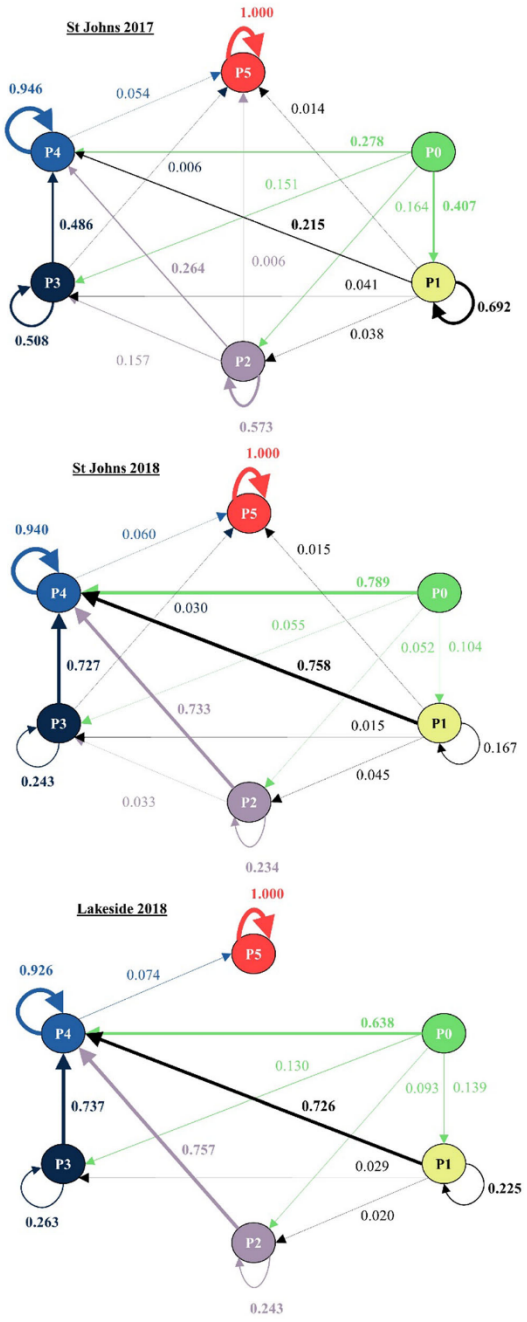

Fig. 5 Tiller-specific phase dynamics for the main populations and years. Arrows indicate the direction of the transition, with all arrows from each phase adding up to 1. The thickness of each arrow is directly associated with the strength of the transition

a 0.006 chance, where tillers never reached full flowering before they reached senescence. The 2018 St Johns population tillers had about a 0.73 to 0.79 chance of going into full flowering (p4) from each of the three phases p1, p2 and p3 (**Fig. 5b**). Most of the remaining chance was to stay in their respective phases. The exception was pre-flowering (p0), which had a 0.10 chance to transition into p1. Tillers in p1, p3 and p4 had chances of 0.02, 0.03 and 0.06 chance of transitioning into senescence (p5). One of the possible transitions was not observed. In the 2018 Lakeside population, tillers were most likely to transition into full flowering (p4), with chances ranging from 0.64 to 0.76 (**Fig. 5c**). The second most likely transition for the lower flowering phases was to stay in their respective phase, with chances of 0.225, 0.243 and 0.263 for p1, p2 and p3, respectively. The senescence rate for p4 into p5 was 0.074. Four of the possible transitions were not observed. The RV correlation coefficients for all the population comparisons ranged from 0.824 to 0.999 (**Table 3**). The RV coefficients ranged between 0.995 and 0.999, 0.824 and 0.932 and 0.847 and 0.950 for the spatial, temporal and spatiotemporal correlations, respectively.

4 Discussion

4.1 Demographic flowering progression

The phenological progressions of the *Dactylis glomerata* populations illustrate the same general pattern of development. The general flowering progression shows that populations in a larger area will display uniformity in average phenological progression between years. The phase distributions show small differences in day-to-day variation between all populations. Key phenological events were clearly distinguished, with start of flowering, peak flowering and start of senescence all overlapping, in both time and space. This supports previous findings by León-Ruiz et al. (2011) that *Dactylis* flowering development is synchronistic between populations over a larger region and between years. The only main difference between populations was the senescence rates, likely attributed to local conditions responsible for drying (Atzema 1992; Hayhoe and Jackson 1974). In this study, full flowering of the first 60% of the tillers was reached within roughly 14 days, while the remaining 40% took more than a month. This demonstrates that the flowering of a population follows a non-normal distribution. We also found that tillers that start flowering later are more likely to flower for a shorter time (results not shown), as previously demonstrated by Tormo-Molina et al. (2015). The synchronal phenological progression of all populations indicates that *Dactylis* pollen release is likely to happen simultaneously over a larger area. This is supported by findings from Italy (Ghitarrini et al. 2017), Spain (Cebrino et al. 2016) and Austria (Kmenta et al. 2017). If pollen release will be proportional to the percent of extruded anthers in each tiller, then higher flowering phases will likely release more pollen (Tormo et al. 2011) and that the largest amount of pollen will be released faster than the remaining 40%. This complements a previous study by Comtois (2000), suggesting that aerobiological studies should utilize gamma distributions instead of a normal distribution when conducting a hypothesis test. Furthermore, our results illustrate that average full flowering in a population follows an uneven distribution with a mixture of some non-flowering (p0) tillers, most in full flowering (p4) and some senescent (p5). This highlights a distinct difference between peak flowering and full flowering, with peak flowering of the season being the day of maximum numbers of tillers in full flowering. Therefore, peak flowering of populations will likely be more connected with pollen release, than the average full

Table 3 RV coefficients between the three main seasonal Markov chain population matrices calculated from the flowering phenological observations in *Dactylis glomerata*

Matrix 1	Matrix 2	Correlation tested	RV coefficient	RV2 coefficient	RVadj coefficient
St Johns 2018	Lakeside 2018	Spatial	0.999	0.995	0.999
St Johns 2017	St Johns 2018	Temporal	0.849	0.932	0.824
St Johns 2017	Lakeside 2018	Temporal and spatial	0.868	0.950	0.847

flowering. If pollen has the potential to disperse evenly during the flowering progression, then peak flowering will also explain maximum pollen release potential (Frenguelli et al. 2010; Romero-Morte et al. 2018). This study therefore suggests that the daily or bi-daily resolution of *Dactylis* phenology is needed to illustrate the narrow window of maximum pollen release potential that occurs during the peak flowering of *Dactylis glomerata* populations. This information can increase the certainty of species pollen release estimates, which can be of great importance in dispersion modelling, forecasting and the usage of regional pollen calendars (e.g. Adams-Groom et al. 2020; Lo et al. 2019).

4.2 Stochastic tiller dynamics

Our findings illustrate that each population is a heterogeneous distribution of tillers occupying varying phases throughout the flowering development. The population matrix correlations are high between populations, which suggests an inherently uniform developmental dynamics shared between populations. However, the correlations also indicate that the spatial correlation is stronger than the temporal and spatiotemporal correlations in the developmental stochasticity between populations. This suggests that differences are larger between years than between separate locations, probably due to regional phenomena that vary on a temporal basis.

Although no other studies have been performed on the phase-based developmental dynamics in *Dactylis* (or any other grasses for that matter), at least two connected studies (Calder 1964a, b) propose that stage-based development is the result of physiological processes caused by photoperiod and temperature. Three stages were proposed: juvenile stage (irresponsive to photoperiod and temperature), inductive stage (responsive to photoperiod and temperature) and post-inductive stage (responsive to long days). Calder (1964a) further states the continuation of studies into *Dactylis* stage-based differentiation is essential in determining the full extent of the flowering process. Later studies confirm the differentiated physiological response to photoperiod and temperature (Broué and Nicholls 1973; Heide 1987). The likelihood of tillers to stay in lower flowering phases (as seen in 2017) is consistent with a lack of external growth stimuli to progress to full flowering (Calder 1963; Heide 1994). On the other hand, tillers expressed high likelihoods of transitioning directly from pre-flowering (p0) to full flowering (p4) (as seen in 2018). This complements studies from Spain as it confirms *Dactylis* tillers' capacity to quickly reach full pollen release potential from one day to the next (Cebrino et al. 2016). Such rapid responses might be a contributing factor to the large daily variation in grass pollen concentrations that have previously been observed within the urban environment (Hjort et al. 2016; Simoleit et al. 2017; Werchan et al. 2017). The observed small variation in the stochastic element implies the presence of a consistent developmental progression within the species, likely to be seen in other species using the same approach. Although this study has not included a meteorological component, we suggest that small variations in meteorological factors such as solar radiation or temperature would likely explain the differential in tiller-specific flowering dynamics between 2017 and 2018. This has previously been shown using Markov chain approaches to be the case for yearly variation in Birch masting behaviour (Tseng et al. 2020). The novel aspect of including stochasticity in flowering dynamics demonstrates that grass populations have defined probabilistic developmental patterns that can be applied to populations over a larger region and potentially utilized to investigate pollen release scenarios. In contrast, the behaviour of small populations or individual plants can be difficult to predict due to the nature of probability.

4.3 Connection to grass pollen concentrations

The findings in this study increase knowledge on airborne grass pollen concentrations considerably and may have direct application in the development and improvement of numerical forecasting models for grass pollen using regional scale atmospheric transport models. In Europe, models have been developed for trees (e.g. Kurganskiy et al. 2020; Sofiev et al. 2015; Zhang et al. 2014; Zink et al. 2013) and ragweed (e.g. Prank et al. 2013; Zink et al. 2017), partly due to availability of large-scale source maps (Pauling et al. 2012; Skjøth et al. 2019) and their tendency to long distance transport (de Weger et al. 2016; Šikoparija et al. 2013; Siljamo et al. 2008; Skjøth et al. 2007). This makes regional-scale models particularly useful for simulating pollen concentrations for these species. For grasses, this may be different. Firstly, pollen

consists of a range of species all contributing to the overall pollen concentration (Ghitarrini et al. 2017). This can make current emission models developed for trees difficult to implement, depending on the local characteristics. In Australia, first attempts have been made with the CSIRO Chemical Transport Model, but with limited success (C-CTM) using mechanistic emission modelling (Emmerson et al. 2019). In the UK, the different grass species have been found to flower in a non-unified pattern throughout the country (Brennan et al. 2019), suggesting that flowering of individual species responds to local environmental variables. A recent study by Rowney et al. (2021) detecting *D. glomerata* and other grass species within the UK network found that 83% of the catch of *D. glomerata* in 2017 in Worcester was captured during the period 4–21 June. This corresponded to the period dominated by p4 and partly p5. In addition, on days before 4 June, when no or limited amounts of *D. glomerata* pollen were present in Worcester, the period was dominated by lower flowering phases (p1–p3). During this period, larger amounts of *D. glomerata* pollen were found at other sites in the UK (Rowney et al. 2021). This suggests that the first part of the flowering sequence (p1–p3) contributes only small amounts of pollen to the airborne pollen concentration. It is likely that other grass species will show a similar behaviour. It also suggests limited or no long-distance transport of grass pollen to Worcester of *D. glomerata* outside the local flowering period. This complements previous findings that grass pollen concentrations are much more localised phenomena compared to trees and ragweed with significant variations at the urban scale (e.g. Hugg et al. 2017; Skjøth et al. 2013). It has been suggested that such variations are caused by variations in emission patterns between different grass species (Peel et al. 2014) and localised emission sources (e.g. Skjøth et al. 2013). The Markov chain modelling approach can take this stochastic emission pattern into account, including potential rapid changes in emission potential. This concept is currently not implemented in state-of-the-art emission models designed for regional scale models (e.g. Zhang et al. 2014; Zink et al. 2013) and conceptually introduces a numerical approach to quantify the element of chance (or risk) of high pollen emission. This approach may be needed for fine-scale modelling of grass pollen concentrations at the urban scale.

5 Conclusion

This study demonstrates that the flowering progression of *Dactylis glomerata* populations follows a non-normal distribution, with a skewness towards the beginning of the season. The study shows that several populations are synchronal within an entire region and between years, with key phenological events only differing by a few days. Populations share similar phase distributions between timesteps, highlighting the uniformity of development dynamics throughout each season. Tiller-specific flowering development revealed that stochastic elements are critical in explaining inherent population demographic properties of the flowering process within grass species and that rapid development of the entire population can happen from day to day. The development may be important in forecasting. Markov chain modelling approaches utilized in the study can be further combined with local grass maps and meteorology to develop grass pollen emission models for use by numerical models.

Acknowledgements Thanks are due to Dr Geoffrey Petch for providing assistance during the fieldwork. This research was funded by the European Commission through a Marie Curie Career Integration Grant (Project ID CIG631745 and Acronym SUPREME to CAS) and by the University of Worcester.

Author contributions CAF was involved in conceptualization, methodology, validation, formal analysis, investigation, resources, data curation and writing—original draft. CAF, BAG and CAS were involved in writing—review and editing and visualization. CAS was involved in supervision, project administration and funding acquisition.

Funding This research was funded by the European Commission through a Marie Curie Career Integration Grant (Project ID CIG631745 and Acronym SUPREME to CAS) and by the University of Worcester.

Compliance with ethical standards

Conflicts of interests The authors declare that they have no conflict of interest.

References

Aboulaich, N., Bouziane, H., Kadiri, M., Del Mar Trigo, M., Riadi, H., Kazzaz, M., & Merzouki, A. (2009). Pollen production in anemophilous species of the Poaceae family in Tetouan (NW Morocco). *Aerobiologia, 25*(1), 27–38. https://doi.org/10.1007/s10453-008-9106-2.

Adams-Groom, B., Skjøth, C. A., Selby, K., Pashley, C., Satchwell, J., Head, K., & Ramsay, G. (2020). Regional calendars and seasonal statistics for the United Kingdom's main pollen allergens. *Allergy: European Journal of Allergy and Clinical Immunology, 75*(6), 1492–1494. https://doi.org/10.1111/all.14168.

Atzema, A. J. (1992). A model for the drying of grass with realtime weather data. *Journal of Agricultural Engineering Research, 53*(C), 231–247. https://doi.org/10.1016/0021-8634(92)80085-7.

Balzter, H. (2000). Markov chain models for vegetation dynamics. *Ecological Modelling, 126*(2–3), 139–154. https://doi.org/10.1016/S0304-3800(00)00262-3.

Bolnick, D. I., Svanbäck, R., Fordyce, J. A., Yang, L. H., Davis, J. M., Hulsey, C. D., & Forister, M. L. (2003). The ecology of individuals: Incidence and implications of individual specialization. *American Naturalist, 161*(1), 1–28. https://doi.org/10.1086/343878.

Brennan, G. L., Potter, C., de Vere, N., Griffith, G. W., Skjøth, C. A., Osborne, N. J., et al. (2019). Temperate airborne grass pollen defined by spatio-temporal shifts in community composition. *Nature Ecology and Evolution, 3*(5), 750–754. https://doi.org/10.1038/s41559-019-0849-7.

Brock, J. L., Hume, D. E., & Fletcher, R. H. (1996). Seasonal variation in the morphology of perennial ryegrass (*Lolium perenne*) and cocksfoot (*Dactylis glomerata*) plants and populations in pastures under intensive sheep grazing. *Journal of Agricultural Science, 126*(1), 37–51. https://doi.org/10.1017/S0021859600088791.

Broué, P., & Nicholls, G. H. (1973). Flowering in Dactylis Glomerata. II. Interaction of Temperature and Photoperiod. *Australian Journal of Agricultural Research, 24*(5), 685–692. https://doi.org/10.1071/AR9730685.

Calder, D. M. (1963). Environmental control of flowering in Dactylis glomerata L. *Nature, 197*(4870), 882–883. https://doi.org/10.1038/197882a0.

Calder, D. M. (1964a). Stage development and flowering in *Dactylis glomerata* L. *Annals of Botany, 28*(2), 187–206. https://doi.org/10.1093/aob/28.2.187.

Calder, D. M. (1964b). Flowering Behaviour of Populations of Dactylis Glomerata Under Field Conditions in Britain. *Journal of Applied Ecology, 1*(2), 307–320. https://doi.org/10.2307/2401315.

Canales, J., Trevisan, M. C., Silva, J. F., & Caswell, H. (1994). A demographic study of an annual grass (Andropogen brevifolius Schwarz) in burnt and unburnt Savanna. *Acta Oecologia, 15*(3), 261–273.

Cebrino, J., Galán, C., & Domínguez-Vilches, E. (2016). Aerobiological and phenological study of the main Poaceae species in Córdoba City (Spain) and the surrounding hills. *Aerobiologia, 32*(4), 595–606. https://doi.org/10.1007/s10453-016-9434-6.

Cebrino, J., García-Castaño, J. L., Domínguez-Vilches, E., & Galán, C. (2018). Spatio-temporal flowering patterns in Mediterranean Poaceae. A community study in SW Spain. *International Journal of Biometeorology, 62*(4), 513–523. https://doi.org/10.1007/s00484-017-1461-7.

Clayton, W. D., Vorontsova, M. S., Harman, K. T., & Williamson, H. (2002). World Grass Species: Synonymy. *Kew: GrassBase*. http://www.kew.org/data/grasses-syn.html. Accessed 1 July 2020

Cleland, E. E., Chiariello, N. R., Loarie, S. R., Mooney, H. A., & Field, C. B. (2006). Diverse responses of phenology to global changes in a grassland ecosystem. *Proceedings of the National Academy of Sciences, 103*(37), 13740–13744. https://doi.org/https://doi.org/10.1073/pnas.0600815103

Comtois, P. (2000). The gamma distribution as the true aerobiological probability density function (PDF). *Aerobiologia, 16*(2), 171–176. https://doi.org/10.1023/A:1007667531246.

Cornelius, C., Petermeier, H., Estrella, N., & Menzel, A. (2011). A comparison of methods to estimate seasonal phenological development from BBCH scale recording. *International Journal of Biometeorology, 55,* 867–877. https://doi.org/10.1007/s00484-011-0421-x.

Cornelius, C., Petermeier, H., Estrella, N., & Menzel, A. (2014). Erratum to: A comparison of methods to estimate seasonal phenological development from BBCH scale recording. *International Journal of Biometeorology, 58,* 1707. https://doi.org/10.1007/s00484-014-0858-9.

D'Amato, G., Cecchi, L., Bonini, S., Nunes, C., Annesi-Maesano, I., Behrendt, H., et al. (2007). Allergenic pollen and pollen allergy in Europe. *Allergy: European Journal of Allergy and Clinical Immunology, 62*(9), 976–990. https://doi.org/10.1111/j.1398-9995.2007.01393.x.

Davila-Velderrain, J., Martinez-Garcia, J. C., & Alvarez-Buylla, E. R. (2016). Dynamic network modelling to understand flowering transition and floral patterning. *Journal of Experimental Botany, 67*(9), 2565–2572. https://doi.org/10.1093/jxb/erw123.

de Weger, L. A., Pashley, C. H., Šikoparija, B., Skjøth, C. A., Kasprzyk, I., Grewling, Ł, et al. (2016). The long distance transport of airborne Ambrosia pollen to the UK and the Netherlands from Central and south Europe. *International Journal of Biometeorology, 60*(12), 1829–1839. https://doi.org/10.1007/s00484-016-1170-7.

Eagles, C. F. (1972). Competition for Light and Nutrients Between Natural Populations of Dactylis glomerata. *The Journal of Applied Ecology, 9*(1), 141–151. https://doi.org/10.2307/2402052.

Eagles, C. F., & Williams, D. H. (1971). Competition between natural populations of Dactylis glomerata. *The Journal of Agricultural Science, 77*(2), 187–193. https://doi.org/10.1017/S0021859600024291.

Emmerson, K. M., Silver, J. D., Newbigin, E., Lampugnani, E. R., Suphioglu, C., Wain, A., & Ebert, E. (2019). Development and evaluation of pollen source methodologies for the Victorian Grass Pollen Emissions Module VGPEM1.0. *Geoscientific Model Development, 12*(6), 2195–2214. https://doi.org/10.5194/gmd-12-2195-2019.

Evans, M. E. K., Merow, C., Record, S., McMahon, S. M., & Enquist, B. J. (2016). Towards Process-based Range Modeling of Many Species. *Trends in Ecology and Evolution, 31*(11), 860–871. https://doi.org/10.1016/j.tree.2016.08.005.

Fox, G. A., & Kendall, B. E. (2002). Demographic stochasticity and the variance reduction effect. *Ecology, 83*(7), 1928–1934. https://doi.org/10.2307/3071775.

Frenguelli, G., Passalacqua, G., Bonini, S., Fiocchi, A., Incorvaia, C., Marcucci, F., et al. (2010). Bridging allergologic and botanical knowledge in seasonal allergy: A role for phenology. *Annals of Allergy, Asthma and Immunology, 105*(3), 223–227. https://doi.org/10.1016/j.anai.2010.06.016.

García-Mozo, H., Galán, C., Belmonte, J., Bermejo, D., Candau, P., Díaz de la Guardia, C., et al. (2009). Predicting the start and peak dates of the Poaceae pollen season in Spain using process-based models. *Agricultural and Forest Meteorology, 149*(2), 256–262. https://doi.org/10.1016/j.agrformet.2008.08.013.

García-Mozo, H., Mestre, A., & Galán, C. (2010). Phenological trends in southern Spain: A response to climate change. *Agricultural and Forest Meteorology, 150*(4), 575–580. https://doi.org/10.1016/j.agrformet.2010.01.023.

Ghitarrini, S., Galán, C., Frenguelli, G., & Tedeschini, E. (2017). Phenological analysis of grasses (Poaceae) as a support for the dissection of their pollen season in Perugia (Central Italy). *Aerobiologia, 33*(3), 339–349. https://doi.org/10.1007/s10453-017-9473-7.

Grinstead, C. M., & Snell, J. L. (1997). Markov chains. In *Introduction to Probability* (Second Rev., pp. 405–470). Providence, Rhode Island: American Mathematical Society.

Hayhoe, H. N., & Jackson, L. P. (1974). Weather Effects on Hay Drying Rates. *Canadian Journal of Plant Science, 54*(3), 479–484. https://doi.org/10.4141/cjps74-081.

Heide, O. M. (1987). Photoperiodic control of flowering in Dactylis glomerata, a true short-long-day plant. *Physiologia Plantarum, 70*(3), 523–529. https://doi.org/10.1111/j.1399-3054.1987.tb02853.x.

Heide, O. M. (1994). Control of Flowering and Reproduction in Temperate Grasses. *New Phytologist, 128*(2), 347–362. https://doi.org/10.1111/j.1469-8137.1994.tb04019.x.

Heinzerling, L. M., Burbach, G. J., Edenharter, G., Bachert, C., Bindslev-Jensen, C., Bonini, S., et al. (2009). GA2LEN skin test study I: GALEN harmonization of skin prick testing: Novel sensitization patterns for inhalant allergens in Europe. *Allergy: European Journal of Allergy and Clinical Immunology, 64*(10), 1498–1506. https://doi.org/10.1111/j.1398-9995.2009.02093.x.

Hjort, J., Hugg, T. T., Antikainen, H., Rusanen, J., Sofiev, M., Kukkonen, J., et al. (2016). Fine-Scale exposure to allergenic pollen in the Urban environment: Evaluation of land use regression approach. *Environmental Health Perspectives, 124*(5), 619–626. https://doi.org/10.1289/ehp.1509761.

Hugg, T. T., Hjort, J., Antikainen, H., Rusanen, J., Tuokila, M., Korkonen, S., et al. (2017). Urbanity as a determinant of exposure to grass pollen in Helsinki Metropolitan area. *Finland. PLoS ONE, 12*(10), 1–17. https://doi.org/10.1371/journal.pone.0186348.

Indahl, U. G., Næs, T., & Liland, K. H. (2018). A similarity index for comparing coupled matrices. *Journal of Chemometrics, 32*(10), 1–18. https://doi.org/10.1002/cem.3049.

Jantunen, J., Saarinen, K., Valtonen, A., & Saarnio, S. (2007). Flowering and seed production success along roads with different mowing regimes. *Applied Vegetation Science, 10*(2), 285–292. https://doi.org/10.1111/j.1654-109X.2007.tb00528.x.

Jochner, S., Ziello, C., Böck, A., Estrella, N., Buters, J., Weichenmeier, I., et al. (2012). Spatio-temporal investigation of flowering dates and pollen counts in the topographically complex Zugspitze area on the German-Austrian border. *Aerobiologia, 28*(4), 541–556. https://doi.org/10.1007/s10453-012-9255-1.

Jones, M. D., & Newell, L. C. (1948). Size, Variability, and Identification of Grass Pollen. *Agronomy Journal, 40*(2), 136–143. https://doi.org/10.2134/agronj1948.00021962004000020004x.

Kendall, B. E., & Fox, G. A. (2002). Variation among individuals and reduced demographic stochasticity. *Conservation Biology, 16*(1), 109–116. https://doi.org/10.1046/j.1523-1739.2002.00036.x.

Khanduri, V. P. (2011). Variation in Anthesis and Pollen Production in Plants. *American-Eurasian J. Agric. & Environ. Sci., 11*(6), 834–839.

Kmenta, M., Bastl, K., Berger, U., Kramer, M. F., Heath, M. D., Pätsi, S., et al. (2017). The grass pollen season 2015: A proof of concept multi-approach study in three different European cities. *World Allergy Organization Journal, 10*(31), 1–12. https://doi.org/10.1186/s40413-017-0163-2.

Kmenta, M., Bastl, K., Kramer, M. F., Hewings, S. J., Mwange, J., Zetter, R., & Berger, U. (2016). The grass pollen season 2014 in Vienna: A pilot study combining phenology, aerobiology and symptom data. *Science of the Total Environment, 566–567*, 1614–1620. https://doi.org/10.1016/j.scitotenv.2016.06.059.

Kurganskiy, A., Skjøth, C. A., Baklanov, A., Sofiev, M., Saarto, A., Severova, E., et al. (2020). Incorporation of pollen data in source maps is vital for pollen dispersion models. *Atmospheric Chemistry and Physics, 20*(4), 2099–2121. https://doi.org/10.5194/acp-20-2099-2020.

León-Ruiz, E., Alcázar, P., Domínguez-Vilches, E., & Galán, C. (2011). Study of Poaceae phenology in a Mediterranean climate. Which species contribute most to airborne pollen counts? *Aerobiologia, 27*(1), 37–50. https://doi.org/10.1007/s10453-010-9174-y.

Liddle, A. M. J., Budd, C. S. J., & Hutchings, M. J. (1982). Population dynamics and neighbourhood effects in establishing swards of Festuca rubra. *Oikos, 38*(1), 52–59. https://doi.org/10.2307/3544567.

Lindner, R., & Garcia, A. (1997). Geographic distribution and genetic resources of Dactylis in Galicia (northwest Spain).

Genetic Resources and Crop Evolution, 44, 499–507. https://doi.org/10.1023/A:1008690831828.

Lo, F., Bitz, C. M., Battisti, D. S., & Hess, J. J. (2019). Pollen calendars and maps of allergenic pollen in North America. *Aerobiologia, 35*(4), 613–633. https://doi.org/10.1007/s10453-019-09601-2.

Mayer, C. D., Lorent, J., & Horgan, G. W. (2011). Exploratory analysis of multiple omics datasets using the adjusted RV coefficient. *Statistical Applications in Genetics and Molecular Biology, 10*(1), 1–27. https://doi.org/10.2202/1544-6115.1540.

Meier, U., Bleiholder, H., Buhr, L., Feller, C., Hack, H., Heß, M., et al. (2009). The BBCH system to coding the phenological growth stages of plants-history and publications. *Journal für Kulturpflanzen, 61*(2), 41–52. https://doi.org/10.5073/JfK.2009.02.01.

Meier, U. (2018). *Growth stages of mono- and dicotyledonous plants. BBCH Monograph*. Quedlinburg, Germany: Julius Kühn-Institute (JKI). https://doi.org/10.5073/20180906-074619.

Meyn, S. P., & Tweedie, R. L. (1993). *Markov Chains and Stochastic Stability* (1st ed.). London: Springer-Verlag, London.

Mizianty, M. (1986). Biosystematic studies on Dactylis L. 1. Review of the previous studies 1.1. Systematics, variability, ecology, biology and cultivation problems. *Acta Societatis Botanicorum Poloniae, 55*(3), 467–479. https://doi.org/10.5586/asbp.1986.039.

Mizianty, M. (1990). Biosystematic studies on Dactylis L. 1. Review of the previous studies 1.2. Cytology, genetics, experimental studies and evolution. *Acta Societatis Botanicorum Poloniae, 59*(1), 105–118. https://doi.org/10.5586/asbp.1990.011.

Munson, S. M., & Long, A. L. (2017). Climate drives shifts in grass reproductive phenology across the western USA. *New Phytologist, 213*(4), 1945–1955. https://doi.org/10.1111/nph.14327.

Nakaoka, M. (1996). Dynamics of age- and size-structured populations in fluctuating environments: applications of stochastic matrix models to natural populations. *Researches on Population Ecology, 38*(2), 141–152. https://doi.org/10.1007/BF02515722.

Pauling, A., Rotach, M. W., Gehrig, R., Clot, B., Jäger, S., Cerny, M., et al. (2012). A method to derive vegetation distribution maps for pollen dispersion models using birch as an example. *International Journal of Biometeorology, 56*(5), 949–958. https://doi.org/10.1007/s00484-011-0505-7.

Peel, R. G., Ørby, P. V., Skjøth, C. A., Kennedy, R., Schlünssen, V., Smith, M., et al. (2014). Seasonal variation in diurnal atmospheric grass pollen concentration profiles. *Biogeosciences, 11*(3), 821–832. https://doi.org/10.5194/bg-11-821-2014.

Prank, M., Chapman, D. S., Bullock, J. M., Belmonte, J., Berger, U., Dahl, A., et al. (2013). An operational model for forecasting ragweed pollen release and dispersion in Europe. *Agricultural and Forest Meteorology, 182–183,* 43–53. https://doi.org/10.1016/j.agrformet.2013.08.003.

Prieto-Baena, J. C., Hidalgo, P. J., Domínguez, E., & Galán, C. (2003). Pollen production in the Poaceae family. *Grana, 42*(3), 153–160. https://doi.org/10.1080/00173130310011810.

Robert, P., & Escoufier, Y. (1976). A Unifying Tool for Linear Multivariate Statistical Methods: The RV-Coefficient. *Applied Statistics, 25*(3), 257–265. https://doi.org/10.2307/2347233.

Rojo, J., Rivero, R., Romero-Morte, J., Fernández-González, F., & Pérez-Badia, R. (2017). Modeling pollen time series using seasonal-trend decomposition procedure based on LOESS smoothing. *International Journal of Biometeorology, 61*(2), 335–348. https://doi.org/10.1007/s00484-016-1215-y.

Romero-Morte, J., Rojo, J., & Pérez-Badia, R. (2020). Meteorological factors driving airborne grass pollen concentration in central Iberian Peninsula. *Aerobiologia, 36,* 527–540. https://doi.org/10.1007/s10453-020-09647-7.

Romero-Morte, J., Rojo, J., Rivero, R., Fernández-González, F., & Pérez-Badia, R. (2018). Standardised index for measuring atmospheric grass-pollen emission. *Science of the Total Environment, 612,* 180–191. https://doi.org/10.1016/j.scitotenv.2017.08.139.

Rossignol, N., Andueza, D., Carrère, P., Cruz, P., Duru, M., Fiorelli, J. L., et al. (2014). Assessing population maturity of three perennial grass species: Influence of phenology and tiller demography along latitudinal and altitudinal gradients. *Grass and Forage Science, 69*(3), 534–548. https://doi.org/10.1111/gfs.12067.

Rowney, F. M., Brennan, G. L., Skjøth, C. A., Griffith, G. W., McInnes, R. N., Clewlow, et al. (2021). Environmental DNA reveals links between abundance and composition of airborne grass pollen and respiratory health. [In press].

Shapiro, S. S., & Wilk, M. B. (1965). An Analysis of Variance Test for Normality (Complete Samples). *Biometrika, 52*(3), 591–611. https://doi.org/10.2307/2333709.

Šikoparija, B., Skjøth, C. A., Alm Kübler, K., Dahl, A., Sommer, J., Grewling, L., et al. (2013). A mechanism for long distance transport of Ambrosia pollen from the Pannonian Plain. *Agricultural and Forest Meteorology, 180,* 112–117. https://doi.org/10.1016/j.agrformet.2013.05.014.

Siljamo, P., Sofiev, M., Ranta, H., Linkosalo, T., Kubin, E., Ahas, R., et al. (2008). Representativeness of point-wise phenological Betula data collected in different parts of Europe. *Global Ecology and Biogeography, 17*(4), 489–502. https://doi.org/10.1111/j.1466-8238.2008.00383.x.

Silva, J. F., Raventos, J., Caswell, H., & Trevisan, M. C. (1991). Population Responses to Fire in a Tropical Savanna Grass, Andropogon semiberbis: A Matrix Model Approach. *The Journal of Ecology, 79*(2), 345. https://doi.org/10.2307/2260717.

Simoleit, A., Werchan, M., Werchan, B., Mücke, H.-G., Gauger, U., Zuberbier, T., & Bergmann, K.-C. (2017). Birch, grass, and mugwort pollen concentrations and intradiurnal patterns at two different urban sites in Berlin. *Germany. Allergo Journal International, 26*(5), 155–164. https://doi.org/10.1007/s40629-017-0012-4.

Skjøth, C. A., Ørby, P. V., Becker, T., Geels, C., Schlünssen, V., Sigsgaard, T., et al. (2013). Identifying urban sources as cause of elevated grass pollen concentrations using GIS and remote sensing. *Biogeosciences, 10*(1), 541–554. https://doi.org/10.5194/bg-10-541-2013.

Skjøth, C. A., Sommer, J., Stach, A., Smith, M., & Brandt, J. (2007). The long-range transport of birch (Betula) pollen from Poland and Germany causes significant pre-season concentrations in Denmark. *Clinical and Experimental Allergy, 37*(8), 1204–1212. https://doi.org/10.1111/j.1365-2222.2007.02771.x.

Skjøth, C. A., Sun, Y., Karrer, G., Sikoparija, B., Smith, M., Schaffner, U., & Müller-Schärer, H. (2019). Predicting abundances of invasive ragweed across Europe using a "top-down" approach. *Science of the Total Environment, 686,* 212–222. https://doi.org/10.1016/j.scitotenv.2019.05.215.

Smilde, A. K., Kiers, H. A. L., Bijlsma, S., Rubingh, C. M., & Van Erk, M. J. (2009). Matrix correlations for high-dimensional data: The modified RV-coefficient. *Bioinformatics, 25*(3), 401–405. https://doi.org/10.1093/bioinformatics/btn634.

Smith, D. C. (1944). Pollination and seeds formation in grasses. *Journal of Agricultural Research, 68*(2), 79–95.

Sofiev, M., Berger, U., Prank, M., Vira, J., Arteta, J., Belmonte, J., et al. (2015). MACC regional multi-model ensemble simulations of birch pollen dispersion in Europe. *Atmospheric Chemistry and Physics, 15*(14), 8115–8130. https://doi.org/10.5194/acp-15-8115-2015.

Soons, M. B., Heil, G. W., Nathan, R., & Katul, G. G. (2004). Determinants of long-distance seed dispersal by wind in grasslands. *Ecology, 85*(11), 3056–3068. https://doi.org/10.1890/03-0522.

Spearman, C. (1904). The Proof and Measurement of Association Between Two Things. *The American Journal of Psychology 15*(1), 72–101. https://archive.org/details/jstor-4576614

Spedicato, G. A. (2017). Discrete time Markov chains with R. *The R Journal*, *9*(2), 84–104. https://doi.org/10.32614/RJ-2017-036.

Tormo-Molina, R., Maya-Manzano, J. M., Silva-Palacios, I., Fernández-Rodríguez, S., & Gonzalo-Garijo, Á. (2015). Flower production and phenology in Dactylis glomerata. *Aerobiologia, 31*(4), 469–479. https://doi.org/10.1007/s10453-015-9381-7.

Tormo, R., Silva, I., Gonzalo, Á., Moreno, A., Pérez, R., & Fernández, S. (2011). Phenological records as a complement to aerobiological data. *International Journal of Biometeorology, 55*(1), 51–65. https://doi.org/10.1007/s00484-010-0308-2.

Tseng, Y. T., Kawashima, S., Kobayashi, S., Takeuchi, S., & Nakamura, K. (2020). Forecasting the seasonal pollen index by using a hidden Markov model combining meteorological and biological factors. *Science of the Total Environment, 698,* 1–10. https://doi.org/10.1016/j.scitotenv.2019.134246.

Tufto, J., Engen, S., & Hindar, K. (1997). Stochastic dispersal processes in plant populations. *Theoretical Population Biology, 52*(1), 16–26. https://doi.org/10.1006/tpbi.1997.1306.

Watkinson, A. R., & Ormerod, S. J. (2001). Grasslands, grazing and biodiversity: Editors' introduction. *Journal of Applied Ecology, 38*(2), 233–237. https://doi.org/10.1046/j.1365-2664.2001.00621.x.

Werchan, B., Werchan, M., Mücke, H. G., Gauger, U., Simoleit, A., Zuberbier, T., & Bergmann, K. C. (2017). Spatial distribution of allergenic pollen through a large metropolitan area. *Environmental Monitoring and Assessment, 189,* 1–19. https://doi.org/10.1007/s10661-017-5876-8.

Wolfe, T. K. (1925). Observations on the blooming of orchard grass flowers. *Agronomy Journal, 17*(10), 605–618. https://doi.org/10.2134/agronj1925.00021962001700100004x.

Wolfe, T. K., & Kipps, M. S. (1925). Pollination studies with orchard grass. *Agronomy Journal, 17*(11), 748–752. https://doi.org/10.2134/agronj1925.00021962001700110014x.

Wolfe, T. K., & Kipps, M. S. (1926). Further studies of the pollination of orchard grass. *Agronomy Journal, 18*(12), 1121–1127. https://doi.org/10.2134/agronj1926.00021962001800120012x.

Yan, D., Zhao, X., Cheng, Y., Ma, X., Huang, L., & Zhang, X. (2016). Phylogenetic and diversity analysis of Dactylis glomerata subspecies using SSR and IT-ISJ Markers. *Molecules, 21*(12), 1–13. https://doi.org/10.3390/molecules21111459.

Zhang, R., Duhl, T., Salam, M. T., House, J. M., Flagan, R. C., Avol, E. L., et al. (2014). Development of a regional-scale pollen emission and transport modeling framework for investigating the impact of climate change on allergic airway disease. *Biogeosciences, 11*(6), 1461–1478. https://doi.org/10.5194/bg-11-1461-2014.

Zink, K., Pauling, A., Rotach, M. W., Vogel, H., Kaufmann, P., & Clot, B. (2013). EMPOL 1.0: a new parameterization of pollen emission in numerical weather prediction models. *Geoscientific Model Development Discussions, 6*(2), 3137–3178. https://doi.org/10.5194/gmdd-6-3137-2013.

Zink, K., Kaufmann, P., Petitpierre, B., Broennimann, O., Guisan, A., Gentilini, E., & Rotach, M. W. (2017). Numerical ragweed pollen forecasts using different source maps: a comparison for France. *International Journal of Biometeorology, 61*(1), 23–33. https://doi.org/10.1007/s00484-016-1188-x.